



THE HONG KONG
POLYTECHNIC UNIVERSITY

香港理工大學

Pao Yue-kong Library

包玉剛圖書館

Copyright Undertaking

This thesis is protected by copyright, with all rights reserved.

By reading and using the thesis, the reader understands and agrees to the following terms:

1. The reader will abide by the rules and legal ordinances governing copyright regarding the use of the thesis.
2. The reader will use the thesis for the purpose of research or private study only and not for distribution or further reproduction or any other purpose.
3. The reader agrees to indemnify and hold the University harmless from and against any loss, damage, cost, liability or expenses arising from copyright infringement or unauthorized usage.

IMPORTANT

If you have reasons to believe that any materials in this thesis are deemed not suitable to be distributed in this form, or a copyright owner having difficulty with the material being included in our database, please contact lbsys@polyu.edu.hk providing details. The Library will look into your claim and consider taking remedial action upon receipt of the written requests.

**SUSTAINABILITY AND RESILIENCE ASSESSMENT ON
RENEWABLE ENERGY MICROGRID DEDICATED TO UNSDG 7**

RICHARD WANG

PhD

The Hong Kong Polytechnic University

2022

The Hong Kong Polytechnic University

Department of Civil and Environmental Engineering

**Sustainability and Resilience Assessment on Renewable Energy Microgrid Dedicated to
UNSDG 7**

Richard Wang

A thesis submitted in partial fulfilment of the requirements for the degree of Doctor of
Philosophy

December 2021

CERTIFICATE OF ORIGINALITY

I hereby declare that this thesis is my own work and that, to the best of my knowledge and belief, it reproduces no material previously published or written, nor material that has been accepted for the award of any other degree or diploma, except where due acknowledgement has been made in the text.

(Signed)

Richard Wang

(Name of student)

ABSTRACT

“Affordable and Clean Energy” is Goal 7 of the United Nations Sustainable Development Goals (UNSDGs). This goal aims to ensure access to affordable, reliable, sustainable, and modern energy for all. In alignment with this UNSDG, it is critical to carry out a comprehensive assessment of renewable energy microgrids. Scientific evidence based on actual applications is essential for demonstrating the merits of microgrid solutions.

This thesis aims to advance our understanding of renewable energy microgrids by conducting a multi-aspect assessment, covering environmental, economic, technical, resilience, and socio-environmental dimensions. Owing to the multi-aspect nature of the assessment, a wide range of assessment tools are deployed that are specific to each dimension of interest, including life cycle assessment, life cycle costing, building energy modelling, and agent-based modelling.

For environmental performance, a comparative life cycle assessment was carried out via a case study of the Town Island Microgrid. The assessment indicates that the Town Island Microgrid is less impactful in 8 impact categories out of 12, compared to 2 electrification options (diesel generator and grid extension). The system energy payback time was calculated to be 9.2 years, while the energy payback time of the diesel generator and the grid extension is 10.1 and 6.5 times longer.

On the economic side, an evaluation of 24 renewable energy microgrids worldwide was performed, involving life cycle costing, economies of scale, and net present value. Life cycle costing approximated the investment costs to be 2,135 USD/kW and operating costs to be 0.066 USD/kWh, which showed lower price competitiveness against pulverized-coal and natural gas.

Weak savings from economies of scale is expected as the economies of scale factor was close to 0.9. The net present value suggests that a microgrid investment may not be a profitable one.

To address the technical dimension, a modelling framework is proposed for examining photovoltaic rooftops with varying roof availability to achieve peak shaving and carbon reduction. The framework was applied to a 10-storey reference office building with respect to Hong Kong's climate. The study analyzed a series of electricity output data for photovoltaic arrays occupying a minimum of 10%, 30%, and the practical maximum of 50%, to correspond to low, medium, and high photovoltaic potential. Strategies to perform peak shaving are proposed. For instance, if a photovoltaic system covers 50% roofs, the optimum strategy for summer would be 09:00 – 18:00 (595 kg CO₂ per weekday carbon savings), and 09:00 – 12:00 & 14:00 – 18:00, excluding lunch hours for winter (271 kg CO₂ per weekday carbon savings).

Resilience is also an important aspect of effective energy management, especially during a crisis such as COVID-19. To understand the impact of work-from-home arrangements, building energy simulations were conducted in which the increased energy demand for a high-rise public residential building in Hong Kong was quantified to be 9%. The potential contribution to the increased energy demand by photovoltaic roofs, as an alternative to on-site energy generation, was modelled. Among the 4 first work-from-home periods, the photovoltaic system could potentially contribute to 6.8% to 11% of additional energy demand. During the remaining normal work arrangement time periods, the photovoltaic system could contribute to around 1.5% of total residential units' energy demand when air-conditioning was on, and 3-4% when air conditioning was off.

For socio-environmental aspect, an agent-based model (ABM) was developed to analyse post-

pandemic work-from-home behaviours based on social theories. Scenario simulations were carried out to understand the impacts of environment constraints (specifically family and colleague influences), resource constraints, and personal stress tolerance on work-from-home behaviour. Analysis across all four simulated scenarios reveals that improving personal stress tolerance is the most effective means for achieving more significant community level energy reduction. More agents were willing to work-from-home for consecutive days (≥ 3 days) as they overcame personal stress and opted for additional work-from-home days. This resulted in a 42% increase in community level energy reduction owing to the reduction in office and transportation energy consumption.

Overall, the thesis contributes to sustainable energy research by comprehensively assessing renewable energy microgrids using a wide array of analytic tools and case studies. Policy making recommendations are presented to further promote the adoption of renewable energy microgrids.

Publications arising from the thesis

The thesis is based on the following peer-reviewed papers:

- I. Richard Wang, Chor-Man Lam, Shu-Chien Hsu, Jieh-Haur Chen,**
Life cycle assessment and energy payback time of a standalone hybrid renewable energy commercial microgrid: A case study of Town Island in Hong Kong, *Applied Energy*, Volume 250, 2019, Pages 760-775, ISSN 0306-2619,
<https://doi.org/10.1016/j.apenergy.2019.04.183>.

- II. Richard Wang, Shu-Chien Hsu, Saina Zheng, Jieh-Haur Chen, Xuran Ivan Li,**
Renewable energy microgrids: Economic evaluation and decision making for government policies to contribute to affordable and clean energy, *Applied Energy*, Volume 274, 2020, 115287, ISSN 0306-2619,
<https://doi.org/10.1016/j.apenergy.2020.115287>.

- III. Richard Wang, Chor Man Lam, Valeria Alvarado, Shu-Chien Hsu,**
A modeling framework to examine photovoltaic rooftop peak shaving with varying roof availability: A case of office building in Hong Kong, *Journal of Building Engineering*, Volume 44, 2021, 103349, ISSN 2352-7102,
<https://doi.org/10.1016/j.jobbe.2021.103349>.

VI. Richard Wang, Zongnan Ye, Shu-Chien Hsu, Jieh-Haur Chen,

Photovoltaic rooftop's contribution to improve building-level energy resilience during
COVID-19 work-from-home arrangement

Accepted by Energy for Sustainable Development in March 2022

Other content covered in this thesis is under preparation for peer-review:

V. Richard Wang, Zhongnan Ye, Miaoqia Lu, Shu-Chien Hsu

Understanding Post-Pandemic Work-from-home behaviours and community level energy
reduction via agent-based modelling

Submitted to Applied Energy in December 2021

Acknowledgments

I would like to express the deepest gratitude to my chief supervisor, Dr Shu-Chien Hsu. Throughout these six years, he has given me unlimited support and allowed me freedom to manage my research works and other aspects of life. He has taught me to always stay positive and calm in times of difficulties. I am forever thankful for his trust and the lessons he taught me, in and outside office. I would also like to thank my co-supervisors, Prof. Poon Chi Sun and Dr Leu Shao Yuan for their kind advice, especially during my confirmation which helped me steer my research directions.

I am thankful to my research team teammates, Lu Miaoqia, Chor-Man Lam, Saina Zheng, Valeria Isabel Alvarado Román, Ye Zhongnan, and Yuan Ziyue. They have helped me settle well in the team and catch up with on-campus happenings.

After all, it has been a tremendous journey. A part-time doctorate degree alongside a full-time job has not been easy, yet I have not faltered in my aspiration to bridge scientific research and application.

This is only the first step. I am ready to contribute more.

Table of Contents

1.	CHAPTER 1: INTRODUCTION	24
1.1	Research background	24
1.2	Research questions	27
1.2.1	Environmental assessment (Chapter 2).....	27
1.2.2	Economic assessment (Chapter 3)	27
1.2.3	Technical assessment (Chapter 4)	28
1.2.4	Resilience assessment (Chapter 5).....	28
1.2.5	Socio-environmental assessment (Chapter 6).....	29
1.3	Research methodology	30
1.4	Structure of the thesis.....	32
2.	CHAPTER 2: LIFE CYCLE ASSESSMENT AND ENERGY PAYBACK TIME OF A STANDALONE HYBRID RENEWABLE ENERGY COMMERCIAL MICROGRID: A CASE STUDY OF TOWN ISLAND IN HONG KONG	34
2.1	Introduction.....	34
2.2	Literature review	35
2.2.1	Microgrid technology.....	35
2.2.2	Existing environmental studies	36
2.3	Objective and significance	37
2.4	Methodologies.....	38
2.4.1	Case study: Town Island Microgrid	38
2.4.2	Life Cycle Assessment (LCA)	40
2.4.3	Life cycle inventory	43
2.4.4	Life cycle impact categories	51
2.4.5	Energy Payback Time (EPBT).....	53

2.4.6	Energy output and functional unit.....	53
2.5	Results and discussion	55
2.5.1	Life cycle environmental impacts of the Town Island Microgrid.....	55
2.5.2	Life cycle environmental impacts per unit of electrical energy output....	56
2.5.3	Life cycle impact category comparisons by life cycle stages	58
2.5.4	Overall life cycle environmental performance of the Town Island Microgrid compared to other electrification options	71
2.5.5	EPBT of the Town Island Microgrid.....	72
2.5.6	Limitations	73
2.6	Summary	74
3.	CHAPTER 3: RENEWABLE ENERGY MICROGRIDS: ECONOMIC EVALUATION AND DECISION MAKING FOR GOVERNMENT POLICIES TO CONTRIBUTE TO AFFORDABLE AND CLEAN ENERGY	76
3.1	Introduction.....	76
3.2	Literature review	77
3.2.1	Renewable energy application in microgrids.....	77
3.2.2	Existing economic studies.....	79
3.2.3	International government policies on renewable energy and microgrids	80
3.3	Objective and significance	83
3.4	Proposed methodologies	85
3.4.1	Case Study: 24 microgrid projects.....	85
3.4.2	Life Cycle Costing (LCC).....	89
3.4.3	Economies of scale (EOS)	90
3.4.4	Net Present Value (NPV)	91
3.5	Results and Discussion	93

3.5.1	A dilemma between environmental and economic performance.....	93
3.5.2	LCC: Investment cost and operating cost	95
3.5.3	Implications of economies of scale.....	97
3.5.4	Net present value.....	99
3.5.5	Decision making support for government policies	102
3.5.6	Limitations	104
3.6	Summary.....	106
4.	CHAPTER 4: A MODELLING FRAMEWORK TO EXAMINE PHOTOVOLTAIC ROOFTOP PEAK SHAVING WITH VARYING ROOF AVAILABILITY: A CASE OF OFFICE REFERENCE BUILDING IN HONG KONG	108
4.1	Introduction.....	108
4.2	Literature review	109
4.2.1	The urgency to reduce building operational carbon emissions.....	109
4.2.2	Photovoltaic (PV) application in buildings.....	110
4.2.3	Peak shaving by PV in buildings	111
4.3	Objective and significance	112
4.4	Methodologies.....	113
4.4.1	Overview of methodologies	113
4.4.2	Whole building energy modeling.....	115
4.4.3	Photovoltaic (PV) system simulation.....	118
4.4.4	Peak shaving analysis	119
4.5	Results and Discussion	122
4.5.1	Annual building energy use and electric power use profile.....	122
4.5.2	Daily building electric power demand profile	124
4.5.3	Annual solar energy output and hourly average electric power	126

4.5.4	Financial analysis.....	128
4.5.5	Carbon reduction and peak shaving analysis for weekdays.....	129
4.5.6	Carbon reduction and peak shaving analysis for weekend.....	134
4.5.7	Limitations.....	138
4.5.8	Policy recommendations.....	140
4.6	Summary.....	141
5.	CHAPTER 5: PHOTOVOLTAIC ROOFTOP’S CONTRIBUTION TO IMPROVE BUILDING-LEVEL ENERGY RESILIENCE DURING COVID-19 WORK-FROM-HOME ARRANGEMENT.....	144
5.1	Introduction.....	144
5.2	Literature Review.....	146
5.2.1	Energy resilience during the COVID-19 crisis.....	146
5.2.2	Solar energy’s contribution to energy resilience.....	147
5.2.3	Solar energy application in Hong Kong.....	148
5.3	Objective and significance.....	149
5.4	Methodology.....	149
5.4.1	Whole building energy modelling.....	149
5.4.2	Photovoltaic (PV) energy generation simulation.....	160
5.5	Results and Discussion.....	161
5.5.1	Building energy modelling.....	161
5.5.2	Rooftop photovoltaic (PV) system’s contribution to increased energy demand	164
5.5.3	Limitations.....	170
5.6	Summary.....	171
6.	CHAPTER 6 UNDERSTANDING POST-PANDEMIC WORK-FROM-HOME	

BEHAVIOURS AND COMMUNITY LEVEL ENERGY REDUCTION VIA AGENT-BASED MODELLING.....	174
6.1 Introduction.....	174
6.2 Literature review	175
6.2.1 Social theories	175
6.2.2 Consideration factors during decision-making for WFH.....	176
6.2.3 Agent-based modelling (ABM) Applications to COVID 19	178
6.3 Objective and significance	180
6.4 Methodology	180
6.4.1 Agent-based modelling (ABM)	180
6.4.2 Methodology overview	181
6.4.3 Data collection	182
6.4.4 ABM development.....	183
6.4.5 Utility	185
6.4.6 Model validation	187
6.4.7 Scenario simulation.....	188
6.4.8 Energy assessment	190
6.5 Results and discussion	191
6.5.1 Scenario simulation – Family influence	191
6.5.2 Scenario simulation – Colleague influence.....	194
6.5.3 Scenario simulation – Resource constraint	197
6.5.4 Scenario simulation – Personal stress tolerance	200
6.5.5 Model output comparisons with peers	202
6.5.6 Policy implications.....	203
6.5.7 Limitations	204

6.6	Summary.....	205
7.	CONCLUSIONS AND SUGGESTIONS FOR FUTURE WORKS.....	210
7.1	Conclusions.....	210
7.2	Contributions of research.....	213
7.3	Suggestions for future works.....	215
8.	REFERENCES.....	216
9.	APPENDICES.....	260
9.1	Appendix 1.....	260
9.2	Appendix 2.....	269
9.3	Appendix 3.....	277

List of Figures

Figure 1-1 – Methodologies, including assessment tools and case study / application, adopted in this thesis.....	30
Figure 2-1 – Diesel generator used to power Town Island before system upgrade (left) (CLP, 2010) and Town Island Microgrid (right) (CLP, 2019).....	39
Figure 2-2 – Overview of the system boundary of the 3 electrification options	41
Figure 2-3 – Electrical energy output of the Town Island Microgrid PV panels.....	54
Figure 2-4 – Electrical energy output by the wind turbines in Town Island Microgrid.....	54
Figure 2-5 – Life cycle environmental impacts of major components of the Town Island Microgrid	56
Figure 2-6 – Global warming potential / kg CO ₂ eq.....	59
Figure 2-7 – Fossil fuel depletion / kg oil eq.....	60
Figure 2-8 – Particulate matter formation / kg PM ₁₀ eq	61
Figure 2-9 – Terrestrial acidification potential / kg SO ₂ eq	62
Figure 2-10 – Ozone depletion potential / kg CFC-11 eq.....	63
Figure 2-11 – Human toxicity potential / kg 1,4-DB eq	64
Figure 2-12 – Freshwater ecotoxicity potential / kg 1,4-DB eq	66
Figure 2-13 – Marine ecotoxicity potential / kg 1,4-DB eq.....	67
Figure 2-14 – Terrestrial ecotoxicity potential / kg 1,4-DB eq.....	68
Figure 2-15 – Agricultural land occupation / m ² a.....	69
Figure 2-16 – Urban land occupation / m ² a	70
Figure 2-17 – Natural land transformation / m ²	71
Figure 2-18 – Aggregated single score of the three electrification options assessed using endpoint methodology	72

Figure 3-1 – Classification of Renewable Energy Support Schemes	83
Figure 3-2 – Graphical illustratin of the proposed methodology.....	86
Figure 3-3 – Global Price of electricity per kWh in USD (2018) (Statista, 2018)	92
Figure 3-4 – Investment cost per microgrid capacity against time, with a linear trendline.....	94
Figure 3-5 – Investment cost per microgrid capacity against renewable energy adoption, with a linear trendline	94
Figure 3-6 – Capacity of microgrid against investment cost per capacity, with logarithm trendline	98
Figure 3-7 – Natural log graph to deduce the economies of the scale factor, with a linear trendline	99
Figure 4-1 - Flow chart illustration of the proposed modelling framework. This framework is applied on a hypothetical reference office building.....	114
Figure 4-2 - Axonometric view of the simulated office building	116
Figure 4-3 - Layout of the simulated office building.....	116
Figure 4-4 - Graphical illustration of peak shaving strategy options during weekdays and weekends.....	121
Figure 4-5 - Building system energy use breakdown	123
Figure 4-6 – Annual whole building electric power demand.....	123
Figure 4-7 - Daily building electric power demand profile, with electric power as a primary axis (left) and occupancy as a secondary axis (right)	126
Figure 4-8 - Hourly electric power output by PV system (10% roof area) by month	127
Figure 4-9 – Weekday building power demand profiles and peak loads reduction achieved by different peak shaving strategies and PV panel rooftop area availability.	131
Figure 4-10 – Weekday avoided carbon emissions of different peak shaving strategies, and PV panel rooftop availability	132

Figure 4-11 – Weekend building power demand profiles and peak load reductions achieved by different peak shaving strategies and PV panel rooftop availability	136
Figure 4-12 – Weekend avoided carbon emissions of different peak shaving strategies and PV panel rooftop availability	137
Figure 5-1 – Standard typical floor plans of concord-type public residential building provided by the Hong Kong Housing Authority (left), and the geometry built in Design Builder to facilitate the whole building energy simulation (right).....	151
Figure 5-2 – Total electric power demand of all residential flats, results from building energy model.....	162
Figure 5-3 – Pie chart showing major energy consumption sources and their respective percentage contribution.....	162
Figure 5-4 – Energy demand during normal work and work-from-home arrangements, and the PV generation contribution to the increased energy demand.....	166
Figure 6-1 – Workflow of ABM development.....	182
Figure 6-2 – Simulation environment in Netlogo	184
Figure 6-3 – Agent decision-making flow	186
Figure 6-4 – Calibration exercise for finding the best-fit values for maximum family social influence, maximum colleague social influence, utility threshold, and personal stress tolerance threshold.....	188
Figure 6-5 – Number of agents working at the office in the ABM with varying maximum family social influence values.....	192
Figure 6-6 – Segregation of WFH preferences in response to varying maximum family social influence values	193
Figure 6-7 – Energy difference with varying maximum family social influence values.....	194
Figure 6-8 – Percentage of agents working at the office in the ABM with varying mean	

resource constraint values	195
Figure 6-9 – Segregation of WFH preferences with varying maximum colleague social influence values	196
Figure 6-10 – Energy difference with varying maximum colleague social influence values	197
Figure 6-11 – Percentage of agents working at the office in the ABM with varying mean resource constraint values	198
Figure 6-12 – Segregation of WFH preferences with varying mean resource constraint values	199
Figure 6-13 – Energy difference with varying mean resource constraint values.....	199
Figure 6-14 – Percentage of agents working at the office in the ABM with varying personal stress tolerance threshold values	200
Figure 6-15 – Segregation of WFH preference with varying personal stress tolerance thresholds	201
Figure 6-16 – Energy difference with varying personal stress tolerance thresholds	202

List of Tables

Table 2-1 – Life cycle inventory of a 200 W PV panel and a 280 W PV panel.....	46
Table 2-2 – Life cycle inventory of a 6 kW wind turbine.....	47
Table 2-3 – Life cycle inventory of a 960 Ah lead-calcium alloy (assumed to be lead-acid) solar battery.....	48
Table 2-4 – Life cycle inventory of a 65 kW diesel generator.....	49
Table 2-5 – Life cycle inventory of a transformer	51
Table 2-6 – Life cycle inventory of the 6.7km submarine cable	51
Table 2-7 – Life cycle environmental impacts of PV panels and wind turbine, with battery, factored in, based on 1 kWh electrical energy output, compared to microgrid assembly, diesel generator system, and grid extension.....	57
Table 2-8 – Total primary energy demand and energy payback time of the three electrification options.....	73
Table 3-1 – Illustration of how the economic performance indicators can help investor decision making	84
Table 3-2 – Illustration of how the economic performance indicators can help government decision making	85
Table 3-3 – Background information on 24 microgrid projects worldwide, their capacity (total and renewable energy portion), and investment cost.....	87
Table 3-4 – Estimated investment cost and operating cost of renewable energy microgrid and other non-renewable energy power plants (Nalbandian-Sugden, 2016).....	96
Table 3-5 – Projection of renewable energy microgrid investment cost (2020 – 2029).....	96
Table 3-6 – NPV calculation of renewable energy microgrid generating 1kWh (per year) ..	101
Table 3-7 – Sensitivity test for varying ratios of capital cost to operating cost.....	102

Table 4-1 - Key building architectural properties	115
Table 4-2 - Key building system parameters	118
Table 4-3 – Construction cost and revenue estimation of PV rooftop	129
Table 4-4 – Avoided carbon emissions (kg CO ₂ per day) based on average carbon emission factor (0.7 kg CO ₂ /kWh)	139
Table 5-1 – Physical properties of building envelope construction materials (HKGBC, 2010)	152
Table 5-2 – Physical properties of roof construction materials (HKGBC, 2010).....	153
Table 5-3 – Physical properties of window glazing material (HKGBC, 2010)	153
Table 5-4 – Modelling input parameters: Occupancy, lighting power density and equipment load of regularly occupied spaces	154
Table 5-5 – Modelling input parameters: Lighting power density and equipment load of non-regularly occupied spaces	155
Table 5-6 – Time records of government special work arrangement announcement	156
Table 5-7 – Occupancy schedules and operation schedules of master bedroom and bedroom	158
Table 5-8 – Occupancy schedules and operation schedules of living rooms.....	159
Table 5-9 – Simulated monthly hourly generation of the rooftop photovoltaic system	165
Table 6-1 – Factors which affect decision-making to WFH	178
Table 6-2 – Variables and input data which exhibit statistically significant correlation with WFH preference according to Table 8 in the abovementioned previous study	183
Table 6-3 – Four simulated scenarios with varying model inputs and specific objectives....	189
Table 6-4 – Energy use per capita across sectors.....	191
Table 6-5 – Summary of scenario simulations results as key decision-making factors strengthen.....	208

List of Acronyms

ABM	Agent based modelling
ACH	Air change per hour
ALO	Agricultural land occupation
BOS	Balance of system
COP	Coefficient of performance
EOS	Economies of scale
EPBT	Energy payback time
EUI	Energy utilization index
FFD	Fossil fuel depletion
FETP	Freshwater ecotoxicity potential
GWP	Global warming potential
HVAC	Heating, ventilation, and air-conditioning
HTP	Human toxicity potential
LCA	Life cycle assessment
LCC	Life cycle costing
LPD	Lighting power densities
LSRES	Living Spring Renewable Energy Station
METP	Marine ecotoxicity
MCRES	Mount Carmel Renewable Energy Station
NLT	Natural land transformation
NPV	Net present value
ODP	Ozone depletion potential
PMFP	Particulate matter formation potential

PV	Photovoltaic
RE	Renewable energy
TAP	Terrestrial acidification potential
TETP	Terrestrial ecotoxicity potential
UNSDGs	United Nations Sustainable Development Goals
ULO	Urban land occupation
WWR	Window to wall ratio
WFH	Work-from-home

1. CHAPTER 1: INTRODUCTION

1.1 Research background

“Affordable and Clean Energy” is Goal 7 of the United Nations Sustainable Development Goals (UNSDGs). It aims to ensure access to affordable, reliable, sustainable and modern energy for all (United Nations, 2019a). The Goal is supported by 3 sub-targets:

- i. 7.1 By 2030, ensure universal access to affordable, reliable and modern energy services,
- ii. 7.2 By 2030, increase substantially the share of renewable energy in the global energy mix,
- iii. 7.3 By 2030, double the global rate of improvement in energy efficiency.

Microgrids are suggested to be a sustainable solution to serve the ever-growing energy demand (Dawoud, Lin and Okba, 2018). Microgrids are defined as small-scale power systems which consist of distributed generators, a group of loads, energy storage and points of common coupling between the generator (Rao, Vijayapriya and Kowsalya, 2019). Microgrids exhibit ability to integrate renewable energy by reducing the scale of the grid, so that the unpredictable nature of renewable energy sources (eg. wind and solar) can be better coped with (Ustun, Ozansoy and Zayegh, 2011; Wissner, 2011). Harnessing renewable energy has been challenging because of its unstable supply, yet microgrids can be a solution for effectively managing renewable energy generators, reducing pollution, and lowering costs with the aid of energy storage systems and appropriate optimization (Basak *et al.*, 2012).

Aligning with UNSDG 7, the benefits of microgrids can be assessed using the three pillars of sustainability: social, environmental, and economical. For social benefits, microgrids, as a localized electrification solution, can provide electricity to remote areas, enhance energy security, and prevent blackouts (Palizban, Kauhaniemi and Guerrero, 2014). In addition,

microgrids are associated with other long-term social benefits, for instance increasing public awareness of energy saving and greenhouse gas emission reduction, and new research and electrification in underdeveloped areas (Schwaegerl and Tao, 2013). Though given that renewable energy generation is often fluctuating, it may require sophisticated algorithm optimization to maximize the social welfare, (Fu *et al.*, 2016).

Regarding environmental benefits, the current literature offers plenty of life cycle assessment and other environmental analysis of renewable energy generation and microgrids (Guezuraga, Zauner and Pölz, 2012; Gerbinet, Belboom and Léonard, 2014a; Wu *et al.*, 2017; Jani and Rangan, 2018; Tabar, Jirdehi and Hemmati, 2018; Nagapurkar and Smith, 2019). In general, the literature favors the environmental performance of renewable energy microgrids, with findings suggesting that the utilization of natural renewable resources can reduce environmental pollution, but also highlighting a few environmental burdens such as heavy metal emissions.

In the economic arena, with proper planning and management, microgrids can result in enhanced economic efficiency, resulting from reductions in costs such as transmission loss, interruption cost, fuel cost, and emission cost (Basu *et al.*, 2011). On the other hand, it is also suggested that distributed energy and storage systems exhibit high economic costs and therefore hinder the development of their application (Tian *et al.*, 2018). Such findings may be inconsistent because, unlike environmental life cycle assessment, there are no universal ISO standards that can be applied on life cycle costing, and the cost data is often not public due to commercial reasons. Overall, the above three pillars of sustainable development, including in the case of microgrids, are tightly interlinked and multi-disciplinary (Alajdin, Iljas and Darko, 2011).

In addition to the three pillars, renewable energy is closely associated with energy security and resilience. Energy resilience covers a wide range of factors, including reliability, economy, environment (Adefarati and Bansal, 2019b). In particular, the recent COVID-19 crisis has imposed disruption in energy access and distribution, and livelihoods globally. It is reported that in some developing countries, COVID-19 even caused energy poverty to an extent that 220 billion US dollars were lost (Zaman, van Vliet and Posch, 2021). The new normal has caused a redistribution among electricity consumer groups, essentially from commercial to residential due to work-from-home arrangement. In addition, electricity consumption profile on grid level has changed as peak demands and their corresponding instants shifted according to work-from-home occupant behaviors (Bielecki *et al.*, 2021).

Summarising the above, it is important to carry out further investigation in renewable energy microgrids, and provide scientific evidence based on actual applications to document the merits of renewable energy microgrids in order to facilitate UNSDG 7. This thesis aims to provide understanding in renewable energy microgrid by conducting a multi-aspect assessment, covering environment, economic, technical, resilience, and social dimensions. The multi-aspect matrix is defined to include the three traditional pillars of sustainability (environment, economic, and social), technical to ensure practicality, and resilience for the sake of long-term stability. The thesis contributes by assessing renewable energy microgrid comprehensively by leveraging different analytic tools and case studies. In addition, policy making recommendations are presented to further promote the application of renewable energy microgrid.

1.2 Research questions

1.2.1 Environmental assessment (Chapter 2)

Chapter 2 explores the life cycle environmental impacts of a standalone hybrid renewable energy microgrid system and describes the methods and results of tests conducted to assess the system's environmental performance advantage, with comparison against other electrification means. The study explores the case of the Town Island Microgrid, which is the first standalone solar/wind hybrid renewable energy commercial microgrid in Hong Kong, through conducting a life cycle assessment (LCA) on and calculating the energy payback time (EPBT) of the microgrid.

The study addresses the following research questions:

- i. What are the life cycle environmental impacts of the renewable energy microgrid throughout its life cycle?
- ii. How environmentally friendly is the renewable energy microgrid compared to alternative electrification options?

1.2.2 Economic assessment (Chapter 3)

Chapter 3 presents a methodology for evaluating the economics of renewable energy microgrids, using three economic performance indicators. Compared to recently published single case studies, this study provides a more comprehensive approach to assessing microgrid adoption by generalizing 24 microgrid projects worldwide spanning different capacities and different levels of renewable energy adoption. Furthermore, based on the performance indicator results, this study offers suggestions to help government decision making in crafting policies to fund renewable energy efforts.

The study addresses the following research questions:

- i. What is the entry investment cost and the operating cost of renewable energy microgrids over the life cycle?
- ii. What are the possibilities of benefiting from economies of scale by building larger capacity microgrids?
- iii. What is the worthiness of investment considering the net present value over time?

1.2.3 Technical assessment (Chapter 4)

Some existing buildings do not have sufficient roof space for PV panels because on-site renewables may not have been considered in their initial designs. Among these buildings, the roof space availability varies and the potential to utilize these spaces is not well documented. There are few readily available guidelines for new building designers to analyze the relationships between system size, suitable peak shaving strategies, and carbon emission savings. While most studies in the literature have focused on PV systems in small-scale residential buildings, it is believed that with proper design guidance and peak shaving strategies, PV systems for medium- to high-rise office buildings could result in considerable savings.

The study addresses the following research questions:

- i. How does roof availability affect the contribution that PV rooftops can make in reducing reliance on grid electricity?
- ii. How do different management strategies for PV electricity lead to different reduced peaks and avoided carbon emission?

1.2.4 Resilience assessment (Chapter 5)

As it was envisaged that there would be an increase in energy demand when occupants spent more time at home during COVID-19 lockdowns, it would be desirable to consider additional

sources of energy supply for the sake of resilience. While it is currently not a common practice to equip on-site rooftop photovoltaic systems on public residential buildings, this study aims to assess the possibility of leveraging photovoltaic systems as a solution for supplementing the increased energy demand. The potential contribution of photovoltaic systems is evaluated in terms of their ability to utilize their energy output to supplement the additional energy demand.

The study addresses the following research questions:

- i. How much has the electricity consumption in a high-rise residential building increased during work-from-home arrangements?
- ii. How much can a PV rooftop, as an alternative power supply, contribute to meeting the increased electricity demand for the sake of resilience?

1.2.5 Socio-environmental assessment (Chapter 6)


While the COVID-19 outbreak has undoubtedly influenced workers' workplace preferences, to examine and predict the environmental impacts and energy savings that may occur in a post-COVID-19 world resulting from expanded work-from-home (WFH) arrangements. An agent-based model (ABM) is developed to simulate post-pandemic WFH behaviours based on social behaviour theories, specifically, conservation of resources theory and small-world theory. Key decision factors affecting WFH behaviour are identified, including environment constraints (the social influences of family members and colleagues), resource constraints, and personal stress tolerance.

The study addresses the following research questions:

- i. How do these key decision factors affect WFH decision-making and the overall WFH population?
- ii. How much variation in community level energy reduction arises from WFH arrangements?

1.3 Research methodology

Figure 1-1 outlines the methodologies, including the assessment tools and case study / application, adopted in this thesis. Due to the multidimensional nature of the assessment, a wide range of assessment tools are deployed to investigate each dimension of interest.



Multi-aspect assessment of renewable energy microgrid

Aspects	Assessment Tools	Case study / Application
Environmental	Life cycle assessment Energy payback time analysis	Town Island Microgrid, Hong Kong
Economic	Life cycle costing Economies of scale analysis	24 microgrid projects worldwide
Technical	Whole building energy simulation PV generation simulation	Reference office building
Resilience	Whole building energy simulation PV generation simulation	High-rise residential building
Socio- environmental	Agent-based modelling	Post-pandemic community

Figure 1-1 – Methodologies, including assessment tools and case study / application, adopted in this thesis

To address the environmental aspect, a comparative life cycle assessment (LCA) was conducted on the Town Island Microgrid, the first standalone solar/wind hybrid renewable energy commercial microgrid in Hong Kong, compared to other possible electrification options.

The reason to conduct such case study is that before the renewable energy microgrid was built, Town Island was powered non-continuously by a diesel generator, so it is reasonable to develop an alternative diesel generator scenario to relate the past and the present. The energy payback time is also analysed to measure the payback period of the energy system in terms of its input and output energy.

To consider the economic aspect, details on 24 microgrids worldwide were gathered from government and commercial reports. The economic performance of these renewable energy microgrids were evaluated using key performance indicators including life cycle costing, net present value, and economies of scale. Although there are some costing studies on microgrids in the existing literature, they are mostly carried out for a single case study, producing results that are highly specific to that case's grid configuration and therefore of limited application to the planning of future projects. Compare to recently published single case study works, this study contributes to more effectively assessing microgrid adoption by generalizing 24 microgrid projects worldwide spanning different capacities and different levels of renewable energy adoption.

In terms of technicality, it has been observed that existing buildings may not have sufficient roof space for PV installations, given that on-site renewable systems may not have been previously considered. A systematic modelling framework which involves the use of computational software (whole building energy simulation and PV system simulation) is proposed. The methodology framework is illustrated with a 10-storey office reference building. The analysis includes various peak shaving strategies and facilitates decision-making based on their corresponding carbon reductions.

To examine resilience, the potential contribution of a photovoltaic system is evaluated in terms of its ability to utilize its energy output to supplement the additional energy demand during the COVID-19 crisis. Public high-rise residential buildings are specifically targeted for energy modeling in this study as they accommodate about half of the Hong Kong population, and it is not yet a common practice to equip on-site rooftop photovoltaic systems on public residential buildings. Whole building energy and PV system simulations are used to conduct the analysis.

To take into account socio-environmental factors, an agent-based model (ABM) is developed to simulate post-pandemic work-from-home (WFH) behaviours based on social behaviour theories (i.e. conservation of resources theory and small-world theory). Key decision factors affecting WFH behaviour are identified, including environment constraints (the social influences of family members and colleagues), resource constraints, and personal stress tolerance. The model is validated with a previously conducted full-time worker survey which collected almost 2,000 effective responses. Scenario simulations were carried out to understand the impacts of these factors on WFH behaviour.

1.4 Structure of the thesis

Following an overview of the research background, research questions and research methodologies, the remaining chapters are organised as follows. Chapter 2 provides an introduction to environmental assessment, a review of relevant literature, and a case study on the Town Island Microgrid. Chapter 3 presents a review of existing economic studies and contains an economic analysis based on 24 microgrids worldwide. Chapter 4 makes a case for the urgent need to reduce building operational carbon emissions and suggests the application of photovoltaic (PV) rooftops and peak shaving for a reference office building. Chapter 5 provides an assessment of a PV rooftop on a high-rise residential building from a resilience

perspective, in the context of the COVID-19 pandemic. Chapter 6 examines post-pandemic work-from-home behaviours and community level energy reduction based on agent-based modelling. Relevant limitations, policy making implications and future research suggestions are presented in each chapter. The last chapter, Chapter 7, presents the thesis's conclusions and suggests directions for future research.

2. CHAPTER 2: LIFE CYCLE ASSESSMENT AND ENERGY PAYBACK TIME OF A STANDALONE HYBRID RENEWABLE ENERGY COMMERCIAL MICROGRID: A CASE STUDY OF TOWN ISLAND IN HONG KONG

2.1 Introduction

The traditional centralized coal-fired electrical power generation system has generated increased environmental concern in recent years. Microgrids are believed to be a greener and more sustainable solution to serve the ever-growing energy demand (Dawoud, Lin and Okba, 2018). In essence, microgrids are small-scale power systems which consist of distributed generators, a group of loads, energy storage and points of common coupling between the generator (Rao, Vijayapriya and Kowsalya, 2019). The heart of the microgrid concept is to decentralize the power generation system, reducing the need for centralized management and allowing more efficient energy management and a higher degree of control during the generation process (Ustun, Ozansoy and Zayegh, 2011; Su and Wang, 2012). There is no standard definition for microgrids, and different countries implement different types and structures (Nosratabadi, Hooshmand and Gholipour, 2017). The capacity of microgrids can have a very wide range, being able to serve loads with size stretching from small facilities to a large community. One major advantage of a microgrid is the ability to divide a traditional bulky power network into more easily controllable and operable small networks (Mahmoud, Azher Hussain and Abido, 2014; Li, Li and Zhou, 2016).

In addition to these technical advantages, microgrids are thought to be a more environmentally friendly electrification solution due to their higher ability to integrate renewable energy (RE). By reducing the scale of the grid, the unpredictable nature of renewable energy sources (eg. wind and solar) can be better coped with (Ustun, Ozansoy and Zayegh, 2011; Wissner, 2011). By 2015, there are already more than 1,400 microgrid projects undergoing planning,

construction, and operation worldwide (Ali, Li, Hussain, He, Barry WWilliams, *et al.*, 2017). Despite this enthusiastic welcome, some suggest that renewable energy technology should not be perceived as sustainable as the public imagines it to be. Renewable energy technology can be associated with several adverse environmental impacts such as loss of habitat, the release of hazardous pollutants, noise pollution, and forest depletion (Abbasi andAbbasi, 2000). This study investigates the life cycle environmental impacts of a standalone hybrid renewable energy microgrid system and tests its environmental performance advantage by comparing the results against other electrification means.

2.2 Literature review

2.2.1Microgrid technology

Microgrids can operate autonomously, which is known as “island mode”. Under circumstances when a main grid fails, the generators in microgrids can maintain power supply to local users. Such an uninterruptable feature is especially important for critical loads that continuously require electricity, such as equipment in medical facilities or commercial computer systems (Barnes andKorba, 2010). The ability to undergo autonomous operation significantly improves energy security to areas exposed to high risk of blackouts caused by natural disasters, for instance in east California, USA. Microgrids as a supplement to the main grid can enhance reliability by switching to island mode if the main grid collapses. In addition to urban areas, due to their “micro” nature, microgrids can also enhance energy security in remote districts where it is difficult to erect large grid infrastructure. Around 20% of the global population does not have access to electricity and most of them live in rural areas. Also it is not technically easy to erect grid connection to rural areas, and the economies of scale does not favour high investment for usually small population in rural areas (Adefarati andBansal, 2019a). Therefore microgrids offer huge potential to provide these people with steady and secure access to

electricity (Smith et al., 2015).

2.2.2 Existing environmental studies

So far, most studies are focused on operation control, optimization, and technology. An energy system should not be considered to comprise only technologies and infrastructures, it is also made up of environmental concerns, markets, its users and other factors affect how the energy system is developed and operated (Yan *et al.*, 2017a). Currently, apart from technological solutions, the existing literature mainly focuses on optimizing systems cost reduction and carbon dioxide reduction (Yan *et al.*, 2017b). The environmental performance of microgrids is seldom assessed, and there is a lack of case studies to prove that microgrids have superior environmental performance compared to traditional electrification means. As far as LCA and environmental impacts are concerned, most available studies focus on the component or product level, for instance, a photovoltaic (PV) module or a wind turbine. Only a few studies have investigated the environmental impacts of the entire microgrid including hybrid power generation means and battery system. A case study in Northern Italy (Gallo *et al.*, 2016) was conducted to evaluate its greenhouse gas emissions via LCA and to identify the least greenhouse gas intensive option to provide electricity to buildings in that region. It is reported that among 3 options for providing electricity: (1) a national grid, (2) a micro gas turbine, or (3) a hybrid PV microgrid and national grid, the 3rd option emitted the least amount of greenhouse gas. Another study conducted LCA to compare a hybrid diesel generator, PV and wind turbine remote microgrid, with 265 kWh electricity output per day, in Thailand against grid extension and home diesel generators (Smith *et al.*, 2015). Some previous studies also assessed microgrids using energy payback time (EPBT) as a key performance parameter. A grid-connected roof-top multi-crystalline PV system was reported to have an EPBT of 1.5 years, and another grid connected to a ground-mounted polycrystalline PV system was shown to have an EBPT of 2.2 years based on present-day technologies and an irradiation of 1700

kWh/m²/year (Alsema, 2000). Another study, which also did not include assessment of a battery system, reported that a grid-connected polycrystalline PV system for a hospital building in Malaysia has an EPBT of 5 years (Mat Isa, Wei Tan and Yatim, 2017). On the other hand, a study that focused on the EPBT of the storage system reported that a 27 kWp lead-based battery storage system linked with PV panels in India has an EPBT of 1.9 – 2.3 years (Das *et al.*, 2018a). Most studies have only focused on analysing the PV modules (Yue, You and Darling, 2014) and few studies include both PV panels and battery system in their EPBT calculation, not to mention a hybrid microgrid comprised of other renewable energy technologies such as wind turbines. A close reference found considered a decentralised hybrid PV solar-diesel in Nigeria, reporting an EPBT of 9.5 – 10.5 years, depending on the level of solar irradiation (Akinyele, 2017).

2.3 Objective and significance

The aims of this study are to investigate the life cycle environmental impacts of a standalone hybrid renewable energy microgrid system and to test its environmental performance advantage by comparing the results against other electrification means. To achieve these aims, the study explores the case of the Town Island Microgrid, which is the first standalone solar/wind hybrid renewable energy commercial microgrid in Hong Kong, through conducting an LCA on and calculating the EPBT of the microgrid. The LCA applies 12 life cycle impact categories to not only the as-built configuration of the Town Island Microgrid, but also to compare its impacts against two other electrification means, specifically an on-site diesel generator system and a grid extension via a submarine cable. This approach provides extensive coverage on a system level instead of just on a product level. This study represents the first comprehensive LCA study of the first standalone renewable energy commercial microgrid in Hong Kong. The findings will be valuable for future microgrid projects considered by

electricity operators, researchers, and policy makers in Hong Kong and other regions interested in microgrid deployment.

2.4 Methodologies

2.4.1 Case study: Town Island Microgrid

2.4.1.1 Background of Town Island Microgrid

Town Island is situated off the Sai Kung Peninsula. On the island, there is a drug rehabilitation center which serves around 80 people including recovering drug users. In 2008, China Light and Power (CLP), one of the two main electricity operators in Hong Kong, began to build a renewable energy system to provide electricity to Town Island. This became the first standalone commercial renewable energy system in Hong Kong. The implementation was divided into two phases. The first phase was completed in 2010, and in 2012 the second phase marked the completion of the entire renewable energy microgrid project. The Town Island Microgrid project was honored as one of the Hong Kong People Engineering Wonders in the 21st Century (CLP, 2010).

On the technical side, the Town Island Microgrid consists of two energy stations: Mount Carmel Renewable Energy Station (MCRES) and Living Spring Renewable Energy Station (LSRES). MCRES is made up of 96 200-W polycrystalline PV panels, 360 280-W polycrystalline PV panels, and a 6 kW wind turbine, with a capacity of 126 kW. LSRES is composed of 216 280-W polycrystalline PV panels and a 6 kW wind turbine, with a capacity of 66.48 kW. Operations at each renewable energy station are supported by a shared battery system, with a combined capacity of 1,105 kWh containing 576 pieces of lead-calcium alloy solar batteries, along with an inverter system that includes a solar inverter, wind inverter, and bi-directional inverter.

Prior to the installation of the renewable energy microgrid, electricity supplied to residents on Town Island was generated by diesel generators (Figure 2-1). This method was not only costly and time-consuming due to the necessarily frequent transportation of fuel, but it also led to adverse environmental impacts during operations on site.



Figure 2-1 – Diesel generator used to power Town Island before system upgrade (left) (CLP, 2010) and Town Island Microgrid (right) (CLP, 2019)

2.4.1.2 Alternative scenarios

2 other electrification options are examined in this study, including (1) an on-site diesel generator system, and (2) a grid extension, according to the following rationales:

- i. On-site diesel generator system: before the renewable energy microgrid was built, Town Island was powered non-continuously by a diesel generator, so it is reasonable to develop an alternative diesel generator scenario to relate the past and the present. Compared to a microgrid, diesel generators are easier to implement, with low capital costs options available and great ease of installation (Green, Mueller-Stoffels and Whitney, 2017). Although a study in 2003 (Oparaku, 2003) reported that it would take 15 years for PV technology to reach the same cost-effectiveness of a diesel generator, nowadays some remote islands in Hong Kong are still powered by diesel generators due to economic reasons. Overall, many benefits, including low investment

and convenient installation, are harnessed at the early stage of the life cycle of a diesel generator.

- ii. Grid extension: it has been suggested that grid extension to remote areas is a particularly cost-efficient electrification method. Previous studies indicate that, upon proper optimization, grid extension can be comparably environmental friendly as a renewable energy system (Fürsch *et al.*, 2013; López-González, Domenech and Ferrer-Martí, 2018). Some remote areas, although isolated from the main grid, can still benefit from connecting to a main grid via extension (Nouni, Mullick and Kandpal, 2009). Extension construction can be more complicated than setting up a diesel generator, but during the operation stage, grid extension seems to be a more secure and stable option.

2.4.2 Life Cycle Assessment (LCA)

2.4.2.1 Life Cycle Assessment (LCA)

LCA is used to investigate and identify the environmental impacts of products or services throughout their life cycle. This method has earned popularity in evaluating renewable energy systems such as solar energy and wind energy. Although these energy systems are emerging and are generally supported by government bodies and operators, specific scientific confirmation of their environmental performance is often not considered, particularly not through a life cycle approach (Góralczyk, 2003). Nevertheless, LCA has gained momentum as a systematic environmental impacts evaluation tool adopted to study the environmental performance of renewable energy systems in and of themselves and for comparing the environmental performance of different energy systems (Gerbinet, Belboom and Léonard, 2014b; Lamnatou and Chemisana, 2017). ISO standards (ISO 14040 and ISO 14044) were established to provide guidelines on how to conduct an LCA, which include 4 steps: (1) goal and scope definition, (2) life cycle inventory, (3) impacts assessment, and (4) results in

interpretation. This study follows the procedures outlined in these standards.

In the present study comparative LCA was conducted to check whether the as-built configuration of the Town Island Microgrid is superior, from a life cycle environmental perspective, to other possible electrification options.

2.4.2.2 System boundary

This section presents an overview of the system boundary by illustrating the life cycle of each electrification option and highlighting the scope of the LCAs in this study (Figure 2-2). The general assumptions in the LCAs and details on the corresponding electrification option are presented in later sections.

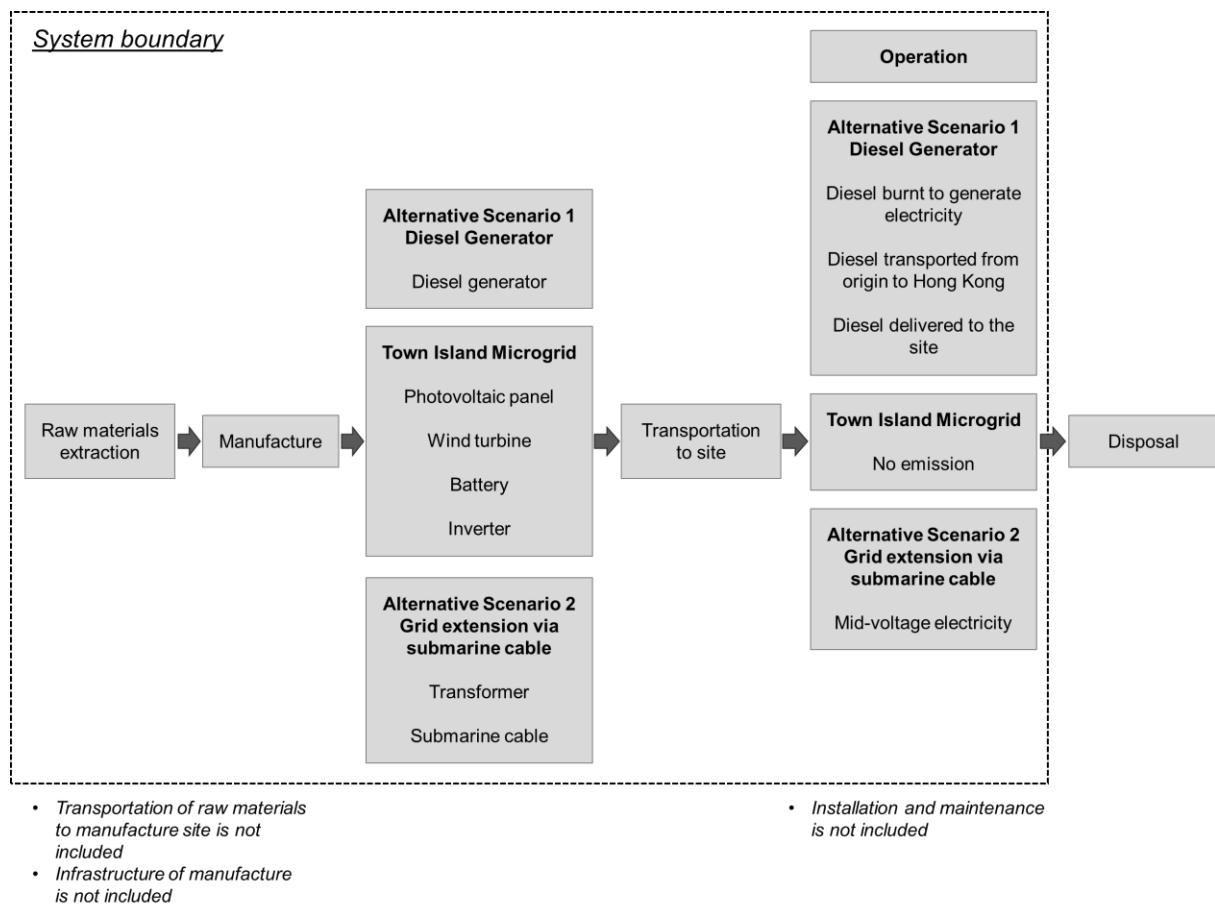


Figure 2-2 – Overview of the system boundary of the 3 electrification options

2.4.2.3 Functional unit

For the sake of a fair and systematic comparison between the above 3 electrification scenarios, the annual electrical energy output of the Town Island Microgrid was estimated, and this electrical energy output was used as the functional unit. The timeframe of the LCA was set to be 20 years.

RETScreen, a clean energy management software developed by the government of Canada (Natural Resources Canada, 2019), is used to estimate the annual energy output by the PV panels. This software underwent validation and is equipped to conduct feasibility studies and energy assessments for renewable energy projects (RETScreen® International Clean Energy Decision Support Centre, 2005). The software can estimate the annual solar energy output of a PV system based on the local solar radiation data. In this case data from the Hong Kong Observatory is referenced.

For a wind turbine, the below formula (Equation 2-1) is used to estimate the annual energy generation, where ρ is air density, A is the swept area that the plane of wind intersected by the generator v is wind speed and C_p is the combined efficiency of energy conversion from kinetic energy to mechanical energy, then to electrical energy. A C_p of 0.41 is used for best design wind turbine (Uddin and Kumar, 2014).

Equation 2-1 – Annual energy generation of wind turbine

$$P = \frac{1}{2} \times \rho \times A \times v^3 \times C_p$$

The wind speed data was obtained from the Hong Kong Observatory Sai Kung station, the closest wind station to Town Island. The daily mean wind data for 2 years (2014 and 2015) was

used and the calculated power was averaged. Since the cut-in speed is 3.5 m/s, when the daily mean wind speed is lower than 3.5 m/s, it is assumed that there is no generation.

2.4.3 Life cycle inventory

2.4.3.1 General assumptions

Conducting LCA requires a very comprehensive set of data throughout the life cycle of the targeted system. The best scenario is that every piece of data is specific to the system, for instance geographically, technically and temporally specific. However, in reality, not every piece of data is readily available. Therefore, to fill in data gaps, combined references of built-in the database in SimaPro, published academic journals, scientific reports, and manufacturer data are used, and adjustments to available data are made. These references will be stated in their corresponding sections.

The below general assumptions are made in the LCA of all 3 electrification options:

- i. On Town Island, the power transmission system from the point of electrical supply to the building is similar for the three scenarios, therefore the transmission system from the supply point to the building, and the transmission system within the building are not considered in this comparison exercise.
- ii. Since combined references are used and each reference has a different depth of detail, in order to avoid over-estimation or under-estimation in any one particular system equipment, a general rule (Vogtländer, 2010) is applied in this study to normalize the depth of inventory data. If a system's equipment consists of less than 20 items on the inventory list, items with less than 1% of the weight of the equipment are neglected. If a system's equipment consists of 20 – 40 items on the inventory list, items with less than 0.5% of the weight of the equipment are neglected.

- iii. A lifespan is allocated for each piece of equipment. After the lifespan is reached, the equipment is replaced.
- iv. The emissions from installation, maintenance, and disposal are not considered. Previous LCA studies of renewable energy systems (Greening and Azapagic, 2013) have found that installation, maintenance, and disposal only contribute to 2%, 1%, and 0.5% of emissions respectively, hence the significance is considered negligible compared to other major stages. For batteries, due to the lack of relevant local data, the disposal is not considered as well. Among existing literature, only a rare amount of LCA study covers the end of life, for instance this study in Kenya (Bilich *et al.*, 2017), due to the lack of data.
- v. The stages within a life cycle that are the focus in this study include: raw materials extraction and preparation; manufacture, transportation of assembled system equipment from the production site to Town Island; and operation.
- vi. For items on the inventory list, the most applicable and relevant information is used. For instance, if the PV panels are assumed to be made in Asia, the inventory data in Asia will be referenced, if available. If data associated with a location is not available, data from other locations will be used.

2.4.3.2 Electrification Option 1: Microgrid (As-built Configuration)

The first LCA was conducted on the as-built microgrid system. The as-built configuration of the microgrid is described in previous section. For the purposes of this LCA, it is assumed that the headquarters of a brand is the origin of equipment production and transportation. The inventory data for the extraction and processing of raw materials and manufacture is considered. Regarding transportation, the transportation of raw materials from the site of extraction to the headquarters is considered negligible; however, transportation from the headquarter to Town

Island is considered.

A previous study (Fu, Liu and Yuan, 2015) carried out an LCA for 1,000 W polycrystalline PV panels in China. This study is believed to be the most applicable available reference, and its LCI results were adopted in the present study. Instead of simply using a linear approach, the below non-linear economy of scale scaling law is applied to better reflect the industry reality. A scale factor of 0.6 is used, as it is often applied to the majority of energy and chemical plants (D. Yogi Goswami, 2015). The same method was adopted by an LCA study on wind turbines (Greening and Azapagic, 2013), which involved scaling down a 30 kW wind turbine to a 6 kW one. In the present study, the LCI of 1,000 W polycrystalline PV panels is scaled down to 280 W and 200 W, respectively.

Equation 2-2 – Non-linear economy of scale scaling law

$$C_2 = C_1 \left(\frac{S_2}{S_1} \right)^n$$

C represents the input into the process, n represents the scaling factor, and S represents the sizes of the process. The subscripts 1 and 2 refer to the respective process. The manufacturing location of the PV panels is in East Asia and it is assumed that they are transported to the final operation site by sea. The lifespan is assumed to be 20 years. The LCI of the PV panels is listed in Table 2-1.

Table 2-1 – Life cycle inventory of a 200 W PV panel and a 280 W PV panel

Input	200 W	280 W
Quartz / kg	13.65	16.70
Calcium oxide / kg	2.48	3.04
Silicon carbide / g	90.5	110.74
Glass / kg	25.03	30.62
Ethylene vinyl acetate copolymer (EVA) / kg	2.86	3.50
Steel / kg	6.51	7.97
Aluminum / kg	4.63	5.66
Polyethylene terephthalate part (PET) / kg	1.24	1.52
Polyvinyl fluoride film (PVF) / kg	1.24	1.52
Electricity / kWh	341.3	417.7

The LCI for 6 kW wind turbines was drawn from a wind turbine LCA study (Greening and Azapagic, 2013). It is assumed that the wind turbines were manufactured in Northwest Europe and were transported to Hong Kong by sea, for which the sailing distance was estimated using online tools (*SEA-DISTANCES.ORG - Distances*, 2019). The turbines' lifespan is assumed to be 20 years. The life cycle inventory list is provided in Table 2-2.

Table 2-2 – Life cycle inventory of a 6 kW wind turbine

Input	
Cast iron / kg	101.96
Fiberglass reinforced plastic / kg	128.84
Low-alloyed steel / kg	5359.32
Stainless steel / kg	681.39
Synthetic rubber / kg	1.2
Aluminum / kg	5.47
Copper / kg	15.22
Epoxy resin / kg	14.00
Polyethylene / kg	10.23
Polyvinylchloride / kg	2.28
Electricity / kWh	219.68

No readily available literature presenting the LCI of lead-calcium alloy batteries has been found by the time of this study is conducted. Instead, the LCI of lead-calcium alloy batteries was derived from an LCA study comparing the environmental impacts of different types of batteries (Unterreiner, Jülch and Reith, 2016) and an LCA study on lead-acid batteries (Liu *et al.*, 2015). The LCI of a lead-acid battery and a lead-calcium battery are considered to be reasonably similar, as the composition of calcium in lead-calcium alloy battery is usually less than 0.1% wt. for anti-corrosion purposes. The batteries are assumed to have been produced in Central Europe and transported to Hong Kong by sea, and their lifespan is assumed to be 20 years. The LCI of a 960 Ah solar battery is listed in Table 2-3.

Table 2-3 – Life cycle inventory of a 960 Ah lead-calcium alloy (assumed to be lead-acid) solar battery

Input	
Lead / kg	17.00
Lead oxides / kg	23.80
Polypropylene / kg	6.80
Sulfuric acid / kg	6.80
Water / kg	10.88
Glass / kg	1.36
Antimony / kg	0.68
Electricity / kWh	345.22

The Balance of System (BOS) associated environmental impacts are considered negligible as the BOS was reported to contribute only a very small amount of emissions compared to the rest of the system. Also, the environmental impacts of maintenance are considered negligible (Fu, Liu and Yuan, 2015).

2.4.3.3 Electrification Option 2: On-site Diesel Generators

Before Town Island was powered by the current renewable energy microgrid, electricity was supplied diesel generators which ran only for a few hours a day. In order to compare the current renewable energy microgrid solution against the previous diesel generator solution, an LCA of the latter is conducted as the first alternative method electrification.

For the sake of a fair comparison, the same capacity as the Town Island Microgrid is assumed for the diesel generator system configuration. Three 65 kW diesel generators, rather than a

single 195 kW power system, are used. This is because the base load of a correctional facility is around one-third of its peak load (Ernest Orlando Lawrence Berkeley National Laboratory, 2010) and therefore this configuration is closer to normal practice. It is assumed that each diesel generator has a 10-year lifespan (Smith *et al.*, 2015). Another assumption made is that the generators were produced in a city in South China and transported to Hong Kong by a lorry. During the operation stage, the diesel consumed by the generators is assumed to have been imported from Southeast Asia and was transported to Hong Kong by sea. Each diesel generator has an assumed combined efficiency of 55%. The LCI of a 65 kW diesel generator is drawn from a previous study (Smith *et al.*, 2015) and is shown in Table 2-4. Unlike the Town Island Microgrid, which is automated during operation, the diesel generators require regular fuel delivery to the area. It is assumed that this refill takes place weekly and is delivered by a boat consuming 2 L/km of diesel.

Table 2-4 – Life cycle inventory of a 65 kW diesel generator

Input	
Steel / kg	558.00
Aluminum / kg	325.50
Copper / kg	18.60
Electricity / kWh	4133
Lubricating oil / kg	872.50

2.4.3.4 Electrification Option 3: Grid Extension

Given that Town Island is a remote area isolated from the main CLP electricity grid, the previously presented options are considered to power the island as on-site standalone systems. In addition to these unconnected systems, it is worthwhile to study whether it is environmental

advantageous to extend the main grid electricity supply to the remote island. Typically extension can take place in two forms: overhead cable or submarine cable. The nearest substation of CLP is located on High Island. Extension via a submarine cable is believed to be a more technically and economically viable means compared to overhead cables. Therefore the second alternative scenario is set to be a grid extension via a submarine cable. The approximated distance from this substation going along the coast of High Island to Town Island is 6.7 km.

In this scenario, several assumptions are adopted. Firstly, no major upgrade is required for the main grid nor the High Island substation. Secondly, the submarine cable starts from the High Island substation, with a distance to Town Island assumed to be 6.7 km. Thirdly, an additional stepdown transformer is installed in Town Island to reduce the voltage from 11 kV to 220 V for end use. Given the power capacity and the voltage of transmission, the current of transmission is worked out and the corresponding cable is chosen from the manufacturer's catalog. It is assumed that the submarine cable was manufactured in South China and was transported to Hong Kong by trucks. The LCI of the transformer and submarine cable are shown in Table 2-5 and Table 2-6, respectively. This LCA adopts a generalized electricity mix in China, for which data is available in SimaPro, to represent the operation stage. The data refers to a country-specific electricity mix including production.

Table 2-5 – Life cycle inventory of a transformer

Input	
Steel / kg	571.33
Aluminum / kg	226.67
Mineral oil / kg	133.20
Electricity / kWh	146.94

Table 2-6 – Life cycle inventory of the 6.7km submarine cable

Input	
Copper / kg	7950.18
Polypropylene / kg	9895.60
Polypropylene fibres / kg	2860.00
Steel / kg	34447.57
Wire drawing of copper / kg	7950.18

2.4.4 Life cycle impact categories

In this study, Simapro was employed to carry out the LCA. It is a professional LCA software program supported by ecoinvent database, which contains a compliant data source for studies and assessments based on ISO 14040 and ISO 14044. The ReCiPe (midpoint) framework, with a hierarchies perspective, was used to express the level of environmental impact for each category (Huijbregts *et al.*, 2017). Following the methodology guidelines on Life Cycle Assessment of Photovoltaic Electricity (Fthenakis *et al.*, 2011), the below impact categories are primarily focused on in this study:

- i. Climate change, measured in kg CO₂ eq: When using a midpoint methodology, climate

change represents the global warming potential (GWP) – the amount of energy absorbed by the greenhouse gases emitted, with CO₂ as a reference. The higher the climate change factor is, the stronger the climate change impacts will be, meaning that the gas warms the Earth more.

- ii. Fossil fuel depletion (FFD), measured in kg oil: This category describes the cumulative energy demand along the life cycle of the object being studied. The default fossil fuel in Simapro is crude oil (42 MJ per kg). With the mass of fossil fuel multiplied by this factor, the cumulative energy demand in energy units can be worked out.
- iii. Particulate matter formation potential (PMFP), measured in kg PM₁₀ eq: This indicator measures the sum of particulate matter directly emitted and objects that transformed into particulate matter in the air.
- iv. Terrestrial acidification potential (TAP), measured in kg SO₂ eq: This indicator measures the change in acidity in soil caused by sulphates, nitrates, and phosphates deposited from the atmosphere.
- v. Ozone depletion potential (ODP), measured in kg CFC-11 eq: This indicator measures the thinning of the stratospheric ozone layer caused by anthropogenic emissions.
- vi. Human toxicity potential (HTP), measured in kg 1,4-DB eq: This category measures the harmful impacts on human health caused by the chemicals that are released and to which humans are exposed via a channel, for instance, inhalation of the chemical in the air. 1,4-dichlorobenzene is used as a reference.
- vii. Ecotoxicity (measured in kg 1,4-DB eq): This indicator measures the impacts on ecosystems, including freshwater ecotoxicity potential (FETP), marine ecotoxicity potential (METP) and terrestrial ecotoxicity potential (TETP).
- viii. Land use and Water use: This category of indicators measures the use of land, including agricultural land occupation (ALO) and urban land occupation (ULO), measured in m²a,

and land transformation (LT), measured in m². However there is insufficient data to accurately reflect the water use of all 3 electrification scenarios, thus water depletion is considered beyond the scope of this study.

In addition to the midpoint methodology, an endpoint methodology was also used to aggregate all impact categories to result in a final single score for each electrification option, enabling an overall comparison to be carried out.

2.4.5 Energy Payback Time (EPBT)

In addition to the above life cycle impact categories, the energy payback time (EPBT) is a commonly used parameter to measure the payback period of a system in terms of its input and output energy. The below formula (Equation 2-3) may be used:

Equation 2-3 – Energy payback time

$$\text{EPBT/year} = \frac{\text{Total primary energy demand}}{\text{Annual energy output}}$$

Based on the FFD results, the total primary energy demand can be deduced. In the energy output section, the estimation of the annual energy output of the Town Island Microgrid will be illustrated. By considering the total primary energy demand and the annual energy output, the resulting EPBT can be interpreted to reflect the efficiency from an energy investment and generation point of view.

2.4.6 Energy output and functional unit

2.4.6.1 Estimated energy output of Town Island Microgrid

RET Screen is used to estimate the annual energy output of the PV system. Figure 2-3 shows the energy output generated by the PV panels in the Town Island Microgrid. The 280 W PV panels in MCRES contribute the most due to their higher capacity and the greater number of

installations. The second-highest output contributor is the 280 W PV system in LSRES, and the third is the 200 W PV panel system in MCRES due to its lower capacity and lower number of installations. Combining the PV panels of both the MCRES and LSRES, the annual electrical energy output of the panels is therefore 204.5 MWh.

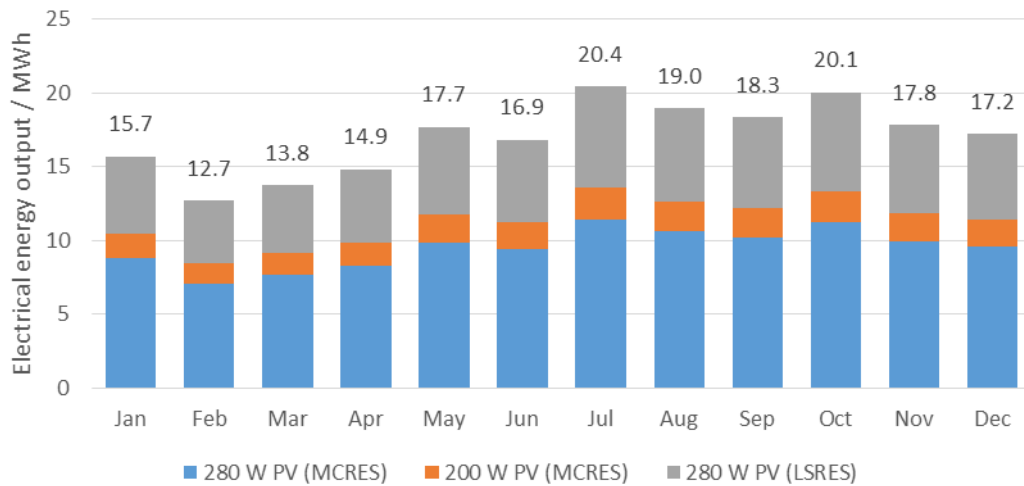


Figure 2-3 – Electrical energy output of the Town Island Microgrid PV panels

The annual electrical energy outputs of the 6 kW wind turbines of the two renewable energy stations are shown in Figure 2-4. The annual electrical energy output is estimated to be 100.2 kWh. The number of windy days (wind speed larger than 3.5 m/s cut-in speed) is also presented.

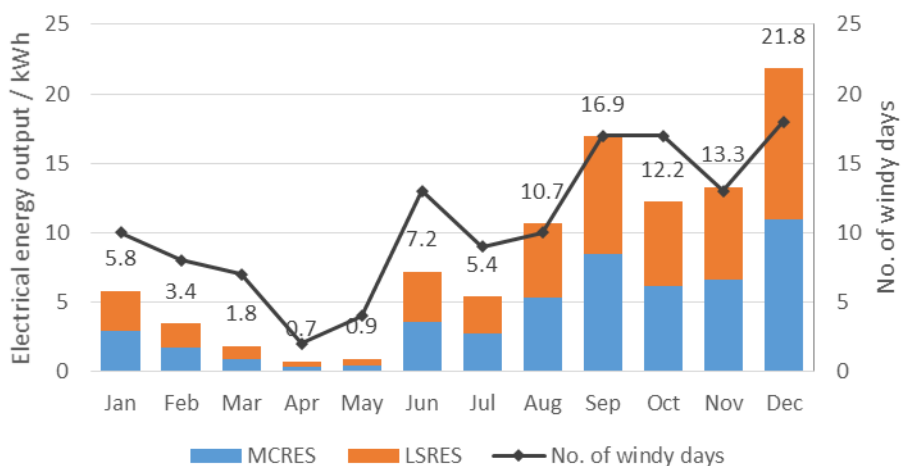


Figure 2-4 – Electrical energy output by the wind turbines in Town Island Microgrid

2.4.6.2 Functional unit

By combining the values in the above two figures, the annual energy output of the entire microgrid system is found to be 204.7 MWh. Thus, the functional unit for this comparative LCA is an annual electrical energy output of 204.7 MWh for 20 years. With the functional unit confirmed, the details of the two alternative electrification options can be further developed. For the on-site diesel generators option, it is assumed that almost 30,000 kg of diesel is required each year to generate the same amount of electrical energy output as the Town Island Microgrid, based on a calorific value of diesel of 40 MJ/kg and a combined efficiency of 55% of a diesel generator. In addition, for the grid extension option, the amount of electrical energy output will be based on medium-voltage electricity generation.

2.5 Results and discussion

2.5.1 Life cycle environmental impacts of the Town Island Microgrid

The life cycle environmental impacts of the major components, including the 200 W and 280 W PV panels, the 6 kW wind turbines, and the 1,105 kWh battery system, are shown in Figure 2-5. The PV panels, 200 W and 280 W combined, contribute to more than 50% in climate change (GWP), fossil fuel depletion (FFD), particulate matter formulation (PMF), terrestrial acidification potential (TAP), ozone depletion potential (ODP), terrestrial ecotoxicity potential (TETP), agricultural land occupation (ALO), urban land occupation (ULO), and natural land transformation (NLT). The battery system also contributed to more than 50% in human toxicity potential (HTP), freshwater ecotoxicity potential (FETP), and marine ecotoxicity (METP). Since only 2 wind turbines were installed on site, their associated environmental impacts are not particularly significant compared to the PV panels and the battery system. The results of these impact categories are further broken down into different stages of the life cycle and are

discussed in the next sections.

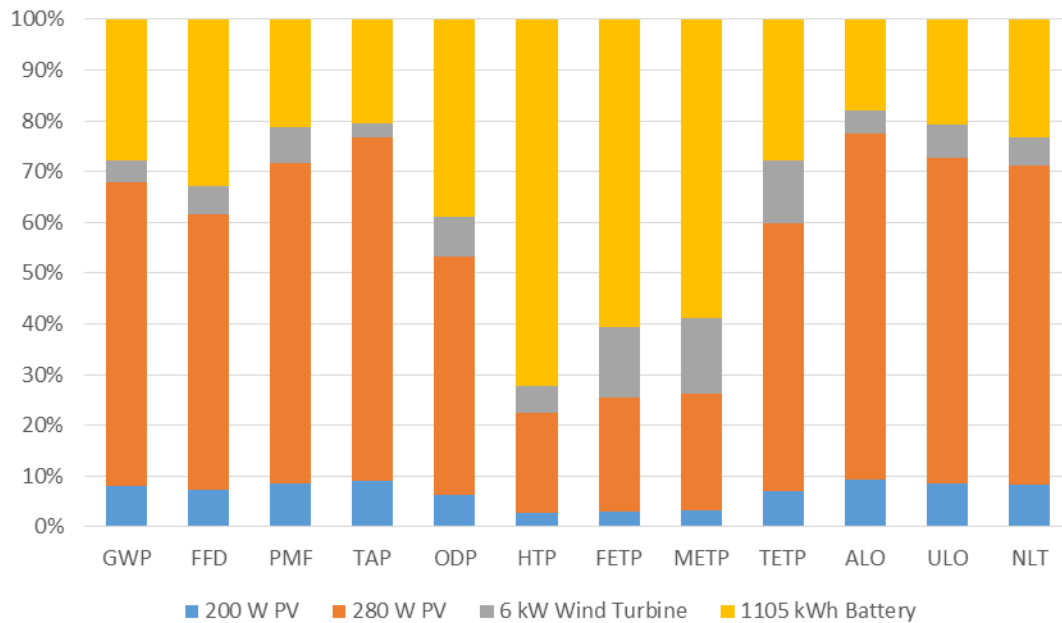


Figure 2-5 – Life cycle environmental impacts of major components of the Town Island Microgrid

2.5.2 Life cycle environmental impacts per unit of electrical energy output

Although the life cycle environmental impacts of the 2 wind turbines may seem small due to their relatively small installed capacity, this does not imply that wind turbine technology has a better environmental performance than PV technology. To further illustrate this, the environmental impacts of 1 kWh of electrical energy output generated by a PV panel (combined 200 W and 280 W) and a wind turbine are calculated. The life cycle environmental impacts of the battery system, which is essential to support the operation of the energy system, are weighted according to the corresponding electrical energy output of the two renewable energy technologies. The life cycle environmental impacts of PV panels and wind turbine are shown in Table 2-7 and the results are compared against each other across impact categories.

It can be reasoned that a wind turbine is not necessarily more environmentally friendly than

PV panels based on Hong Kong climate data. In fact, PV panels demonstrate better environmental performance in all impact categories by a large margin. This is because wind power cannot be fully harnessed from relatively low wind speeds. Mathematically, environmental impact diminishes as the electrical energy output decreases, given the fixed environmental impacts associated with the raw materials stage and manufacturing stage of a PV panel. Hence the lower electrical energy output by a wind turbine leads to a less promising environmental performance compared to PV panels. The aim of this analysis is not to prove that wind energy is not environmentally friendly, but to simply demonstrate that the PV panels on Town Island lead to less life cycle environmental impacts per unit of electrical output compared to the wind turbine. Nevertheless, the two wind turbines only take up a small portion of the installed power capacity in this pilot project. Instead of solely focusing on the life cycle environmental impacts and energy efficiency of the renewable energy microgrid, the wind turbines can serve educational and research purposes, particularly in testing the complementary effect of hybrid renewable energy resources.

Table 2-7 – Life cycle environmental impacts of PV panels and wind turbine, with battery, factored in, based on 1 kWh electrical energy output, compared to microgrid assembly, diesel generator system, and grid extension

Impact Categories	PV Panels	Wind Turbine	Microgrid Assembly	Diesel Generator System	Grid Extension
Global warming potential / kg CO ₂ eq	2.940	282.441	3.077	13.943	24.091
Fossil fuel depletion / kg oil eq	0.746	90.950	0.790	7.995	5.122

Impact Categories	PV Panels	Wind Turbine	Microgrid Assembly	Diesel Generator System	Grid Extension
Particulate matter formation / kg PM ₁₀ eq	0.007	1.050	0.007	0.074	0.067
Terrestrial acidification potential / kg SO ₂ eq	0.204	1.161	0.021	0.132	0.001
Ozone depletion potential / kg CFC-11 eq	0.000	0.000	0.000	0.000	0.000
Human toxicity potential / kg 1,4-DB eq	1.812	215.840	1.917	0.2289	6.454
Freshwater ecotoxicity potential / kg 1,4-DB eq	0.310	10.292	0.036	0.023	0.105
Marine ecotoxicity potential / kg 1,4-DB eq	0.030	10.671	0.035	0.020	0.108
Terrestrial ecotoxicity potential / kg 1,4-DB eq	0.001	0.037	0.000	0.002	0.001
Agricultural land occupation / m ² a	0.066	6.698	0.069	0.018	0.708
Urban land occupation / m ² a	0.020	2.921	0.022	0.037	0.205
Natural land transformation / m ²	0.0003	0.032	0.000	0.011	0.002

2.5.3 Life cycle impact category comparisons by life cycle stages

This section presents the results of the comparative LCA. The results of each electrification

option are broken down into life cycle stages and discussed per impact category.

2.5.3.1 Global Warming Potential (GWP)

The GWP caused by the diesel generator system and the grid extension is 4.3 times and 7.8 times higher, than the GWP caused by the microgrid, respectively (Figure 2-6). This makes the microgrid the least climate-change causing electrification option. For the Town Island Microgrid, the comparatively high GWP during the manufacturing stage is mostly due to multiple energy-intensive treatment processes, including the purification of quartz to generate metallurgical grade silicon and solar grade silicon. These processes can be powered by mainly non-renewable energy resources. On the other hand, the raw materials of the other 2 electrification options are less energy intensive to extract from their original sources and to process during the manufacturing. However, although the earlier stages of these two options contributed relatively less to GWP, both of their operation stages took up 98% of life cycle GWP due to their heavy reliance on fossil fuel.

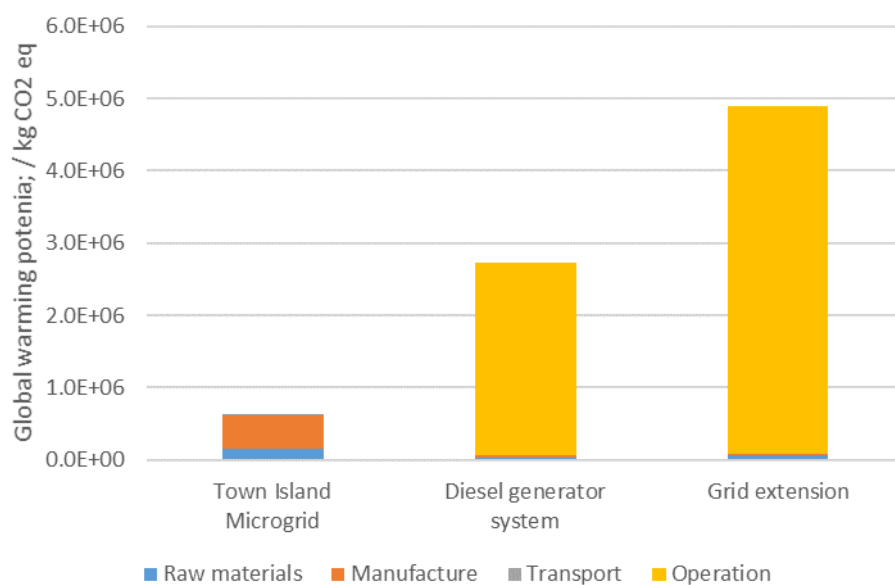


Figure 2-6 – Global warming potential / kg CO₂ eq

2.5.3.2 Fossil Fuel Depletion (FFD)

The FFD caused by the diesel generator system and the grid extension is 10.1 times and 6.4 times greater than the FFD caused by the microgrid, respectively, as shown in Figure 2-7. The microgrid is shown to be the least fossil depleting option out of the three electrification options. As similarly seen in Figure 2-6, the microgrid option shows the least FFD due to its zero emissions during operation. In contrast to the climate change impacts presented above, the FFD of the diesel generators is higher than that of the grid extension. This is because the operation stage of the diesel generator involves two major contributors to FFD: (1) the production of diesel fuel and (2) the burning of diesel fuel to generate electricity on site, both of which are activities that consume a lot of fossil fuel, whereas the operation of the grid extension only involves the generation of medium-voltage electricity. The operation stage carries the highest portion of life cycle FFD, 99% and 96% for the diesel generator and grid extension, respectively.

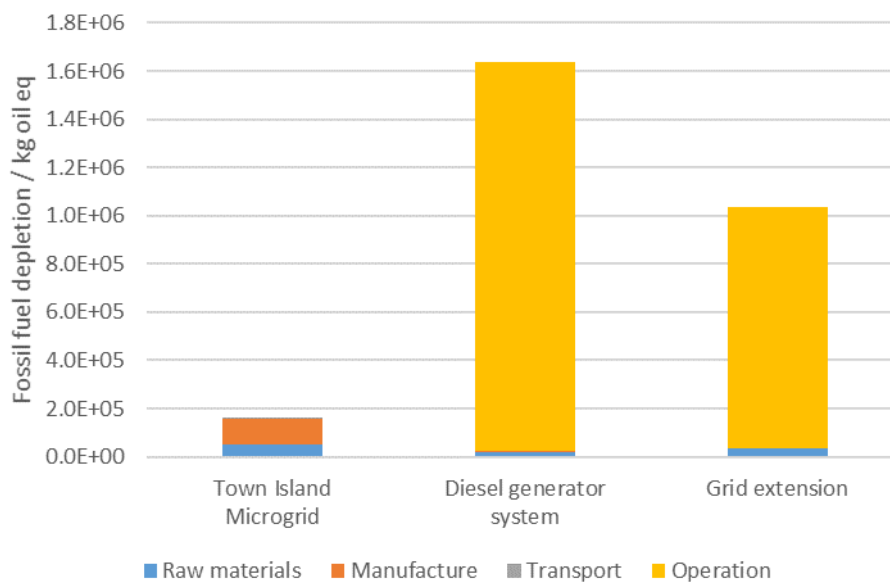


Figure 2-7 – Fossil fuel depletion / kg oil eq

2.5.3.3 Particulate Matter Formation Potential (PMFP)

The PMFP caused by the diesel generator system and the grid extension is 10.1 and 9.0 times

greater than the the PMFP caused by the microgrid, respectively (Figure 2-8). The microgrid generates the least particulate matter among the 3 electrification options. Some degree of correlation is observed between the GWP, FFD, and PMFP in the case of the microgrid, and this is because of the use of fossil fuel during raw materials extraction, treatment, and manufacture. For the other 2 options, it should be apparent that the high particulate matter formation is also due to the combustion of fossil fuel during the operation stage, through which particulate matter is directly emitted into the atmosphere. For the diesel generator system, most of the particulate matter is emitted during the burning of diesel on site. In contrast, the PMFP caused by the grid extension option is not on site and the particulate matter released most likely takes place in a controlled environment with mitigation to reduce emissions into the atmosphere. On the other hand, little control can be imposed when a diesel generator is used and residents on Town Island are more directly exposed to the emissions.

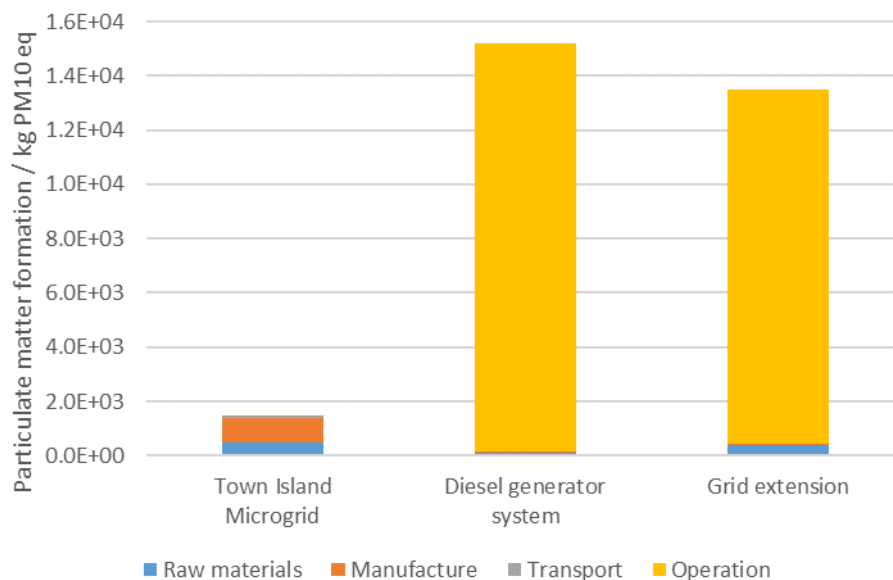


Figure 2-8 – Particulate matter formation / kg PM₁₀ eq

2.5.3.4 Terrestrial Acidification Potential (TAP)

The TAP of the diesel generator system and the grid extension is 7.0 times and 9.9 times greater

than the TAP caused by the microgrid, respectively (Figure 2-9). The microgrid option leads to the lowest level of TAP among the 3 options. The TAP is related to the use of fossil fuels from China, which are particularly rich in sulphur dioxide and nitrogen oxides (Fu, Liu and Yuan, 2015). The lower level of reliance on fossil fuels can help reduce the life cycle TAP of the electrification option.

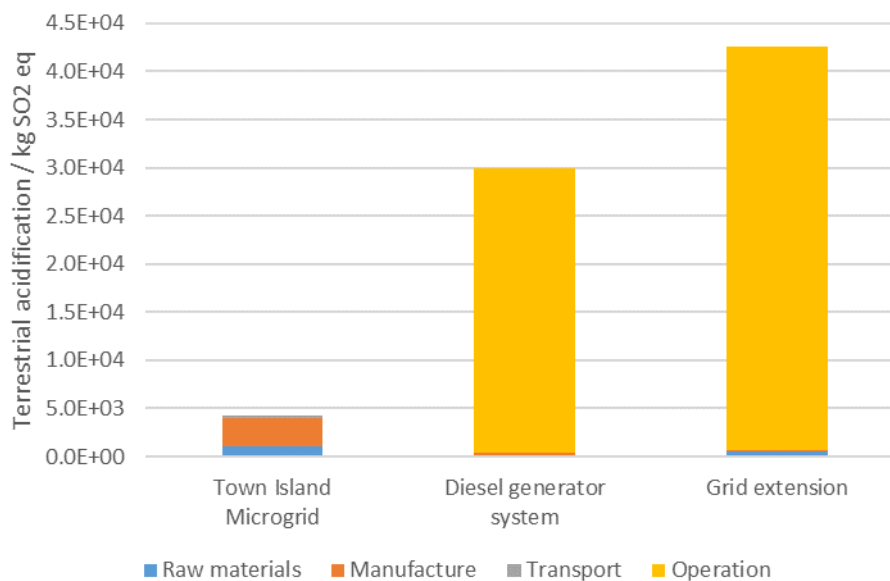


Figure 2-9 – Terrestrial acidification potential / kg SO₂ eq

2.5.3.5 Ozone Depletion Potential (ODP)

The ODP caused by the diesel generator system and the grid extension is 32.4 times and 1.7 times greater than the ODP caused by the microgrid, respectively (Figure 2-10). The microgrid is the least ozone depleting of the 3 electrification options. The ODP resulting from the microgrid may be due to the fuel used to extract raw materials and manufacture. For the diesel generator system, the significant ODP is largely due to the emission of Halon-1301, which is an organic halide. The activities responsible for the Halon-1301 emission during operation include the production of diesel (48.5 %) and burning of diesel (51.5 %). On the other hand, since the major energy resource in China is coal, the grid extension option generates far less

Halon-1301.

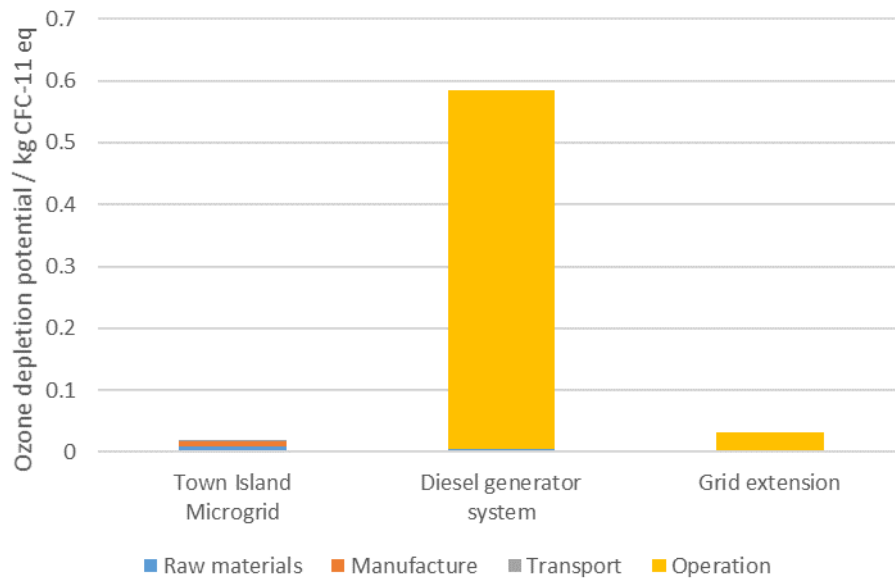


Figure 2-10 – Ozone depletion potential / kg CFC-11 eq

2.5.3.6 Human Toxicity Potential (HTP)

The two major contributors to HTP in a microgrid are the PV panels (200 W and 280 W), contributing 22.3%, and the batteries, contributing 72.2% (Figure 2-11). These are due to the use of heavy metals, such as manganese, arsenic, selenium, barium, cadmium, and lead, during the raw materials extraction and processing stage, and manufacture stage. The heavy metals emissions take place through various paths, including the release of impurities (manganese) in crystalline silicon, the discharge of cadmium through fossil fuel use, and the use of arsenic as a semi-conductor (Fthenakis, Kim and Alsema, 2008). The grid extension option features the highest life cycle HTP, 29.2% of which is caused by the submarine cable and 68.5% of which is caused by electricity generation during operation. Within the HTP associated with the submarine cable, 83.2% is due to the use of copper as a conductor, while copper is toxic to humans upon consumption (National Research Council (U.S.), 2000). The generation of human toxicity during the operation stage, for both the diesel generator system and the grid extension,

is due to the use of fossil fuels. Despite the same electricity output during operation stage, the generation of medium-voltage electricity emits almost 10 times more heavy metals through grid extension compared to the amount emitted when burning diesel therefore exhibiting significantly higher HTP.

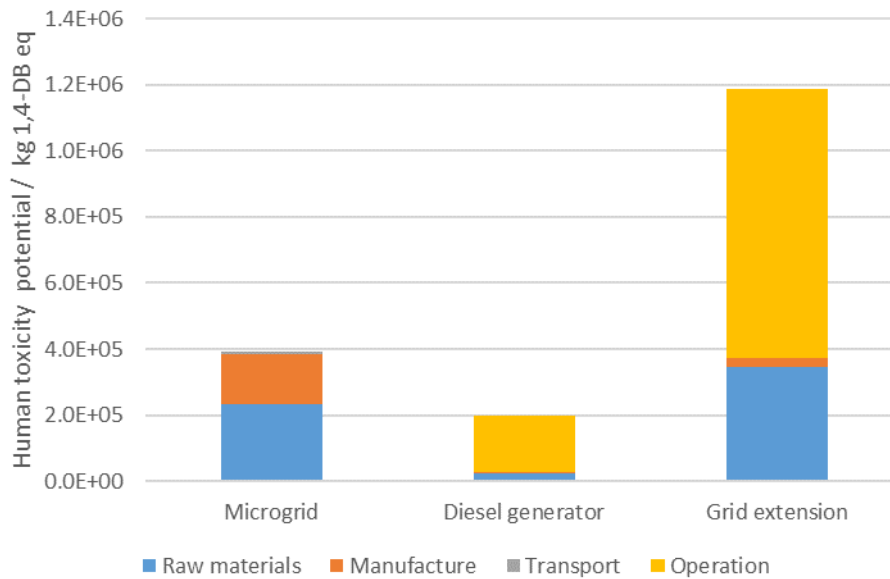


Figure 2-11 – Human toxicity potential / kg 1,4-DB eq

2.5.3.7 Ecotoxicity

The levels of freshwater ecotoxicity potential (FETP) and marine ecotoxicity potential (METP) are shown in Figure 2-12 and Figure 2-13, respectively. The major contributor to the FETP and METP for the Town Island Microgrid is the battery system, contributing 60.7% and 58.9%, respectively. This is primarily due to the use of antimony, despite the small quantity used, which contributed to 43.37% of FETP and 42.06% of METP caused by the battery system. The processing of antimony involves two heavy metals: manganese and zinc. 36.2% of the antimony-associated FETP and 37.1% of the antimony-associated METP are due to the emission of manganese, whereas 27.9% of the antimony-associated FETP and 24.2% of the antimony-associated METP are due to the emission of zinc. Firstly, antimony often naturally

occurs as an antimony compound bound with manganese oxides. When antimony is extracted, manganese is also extracted and released (*Toxicological Profile for Antimony and Compounds*, 2010). Since manganese ions are soluble in water, the release of manganese into the environment will cause harm to both the freshwater environment and marine environment. In freshwater, the affected species include crustaceans, fish, algae and bacteria, while in marine habitats, the affected species include crustaceans, algae and molluscs. The release of manganese is not only harmful to the environment, but also to human life, by playing a role in, for instance, neurotoxicity, hepatotoxicity, and infant mortality (Peters *et al.*, 2010). In addition to the manganese released during antimony refining, zinc is also another major contributor to FETP and METP, which may due to zinc poisoning of wildlife (Irwin *et al.*, 1997). The release of zinc is also due to the extraction of antimony, which in ores is often bound with zinc (Minz *et al.*, 2015). Furthermore, substantial life cycle FETP (48.90%) and METP (50.1%) is emitted during the manufacturing stage. This is associated with nickel released during electricity production (Silva *et al.*, 2013), which affects the survival and reproduction of wildlife including Oligochaeta, Crustacea, and Arthropods (Binet *et al.*, 2018).

For the diesel generator system, the FETP and METP are mainly due to diesel production (43.6% of the operation stage FETP and 54% of the operation stage METP) and diesel burning on site (39.8% of operation stage FETP and 58.2% of operation stage METP). For operation stage FETP, diesel production and burning result in the release of bromine and nickel. Bromine is soluble in water and is harmful to freshwater fish and aquatic invertebrates (United States Environmental Protection Agency, 1993). Nickel, as explained earlier, is released during combustion of fossil fuels. Bromine and nickel account for 38.3% and 26.3% of the diesel fuel production-associated FETP, respectively, whereas bromine and nickel account for 33.1% and 29.2% of the diesel fuel combustion-associated FETP, respectively. The METP generated

during the production of diesel fuel is mainly due to heavy metals including zinc (32.2%) and nickel (22.7%), whereas the METP generated during diesel fuel combustion is mainly due to heavy metals including zinc (24.6%), nickel (21.3%) and copper (16.3%). For grid extension, the major contributor to both raw material stage FETP and METP is the production of copper. During this process, heavy metals including manganese, zinc, and nickel are emitted. For the operation stage, the significantly high FETP and METP values are caused by the emissions of fossil fuel combustion, including the emission of nickel (41.9% of operation stage FETP and 40.3% of operation stage METP) and vanadium (22.6% of operation stage FETP and 22.1% of operation stage METP).

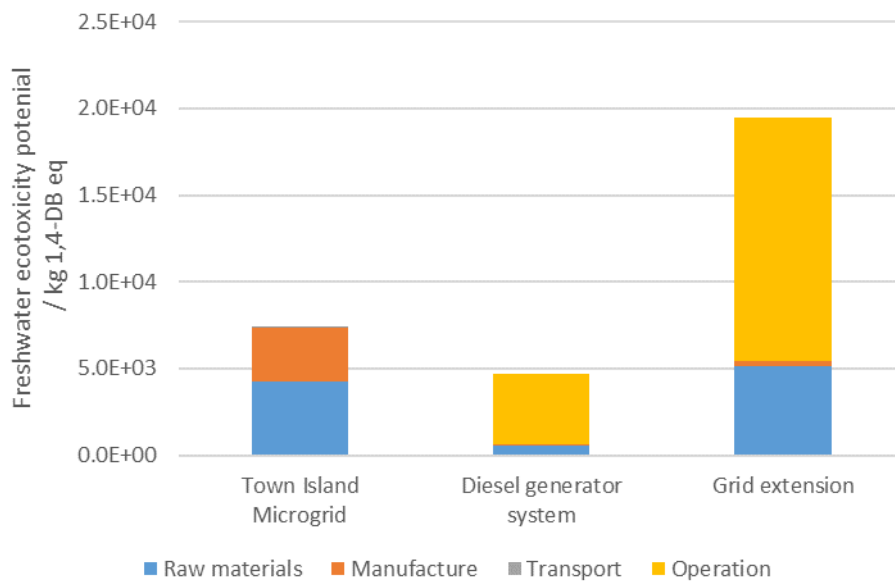


Figure 2-12 – Freshwater ecotoxicity potential / kg 1,4-DB eq

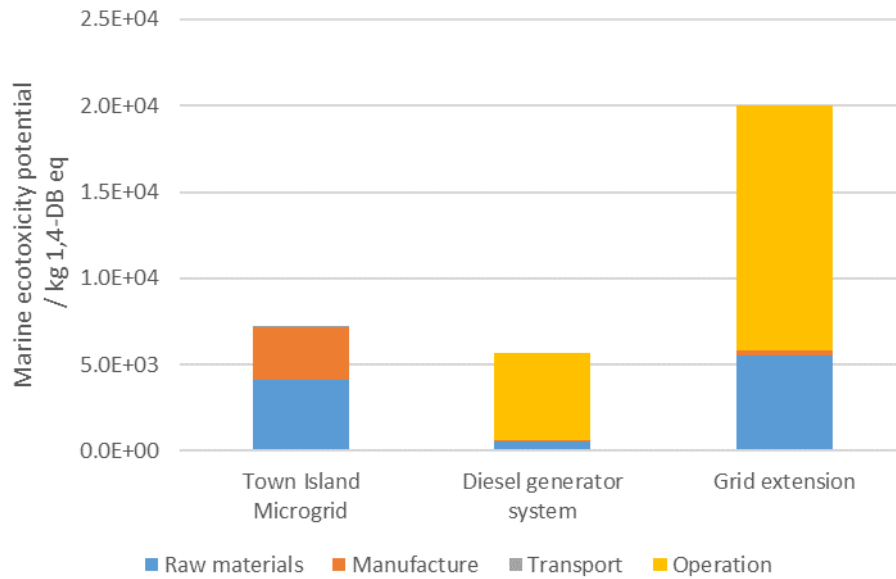


Figure 2-13 – Marine ecotoxicity potential / kg 1,4-DB eq

The terrestrial ecotoxicity potential (TETP) caused by the diesel generator system and the grid extension is 12.0 times and 5.4 times greater than the TETP caused by the Town Island Microgrid, respectively (Figure 2-14). The microgrid solution is the least terrestrial toxic option. The high TETP emitted by the operation of diesel generators is due to the emissions of phosphorus as the exhaust of diesel fuel and fossil fuel combustion (Dallmann *et al.*, 2014). This is similarly the case for the grid extension scenarios. Provided that the operation of the Town Island Microgrid does not rely on fossil fuels, the life cycle TETP is significantly lower than the other two options.

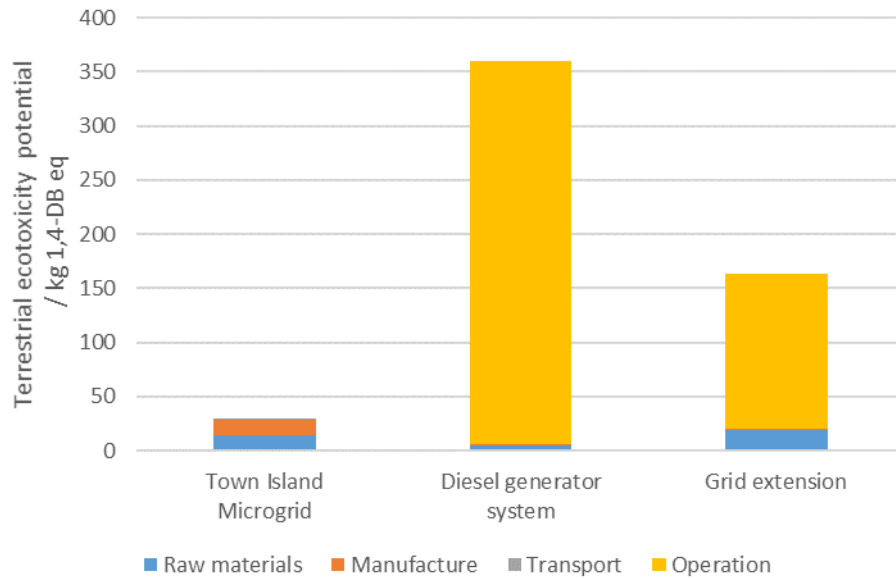


Figure 2-14 – Terrestrial ecotoxicity potential / kg 1,4-DB eq

2.5.3.8 Land use

78.2% of the agricultural land occupation (ALO) associated with the Town Island Microgrid occurs during the manufacturing stage (Figure 2-15). The ALO can be correlated to the consumption of fossil fuels (Repele andBazbauers, 2015). Since the production of microgrid equipment requires more electricity than the diesel generators and the submarine cable, the Town Island Microgrid features higher ALO. Grid extension operation involves off-site electricity generation, with a consequently significant ALO.

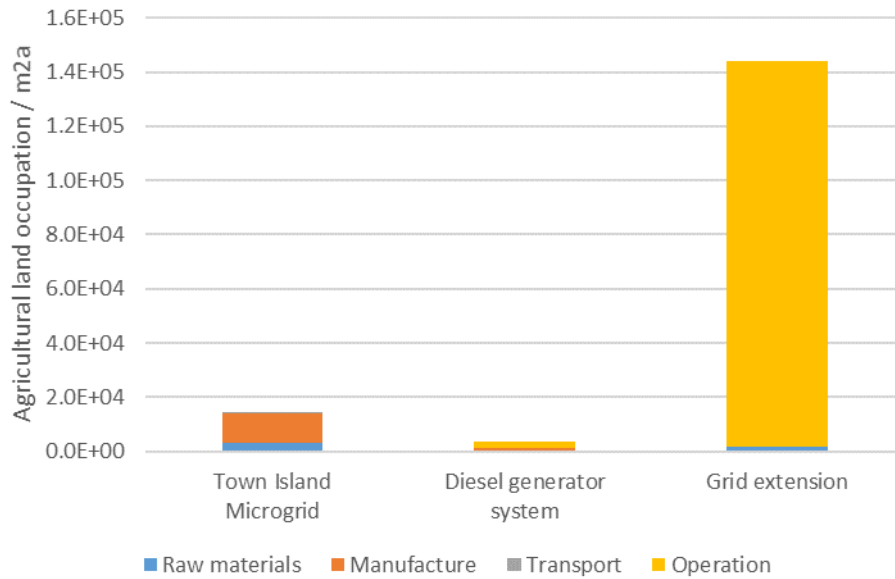


Figure 2-15 – Agricultural land occupation / m²a

The urban land occupation (ULO) required for the diesel generator system and the grid extension is 1.7 times and 9.4 times greater than the ULO caused by the microgrid, respectively (Figure 2-16). The microgrid solution is the least urban land occupying option. For the manufacturing stage of the microgrid and the operation stage of the grid extension scenario, the is mainly a function of the dump site associated with electricity generation. On the other hand, during the operation stage of the diesel generator system, the urban land occupation is needed for diesel production and diesel combustion.

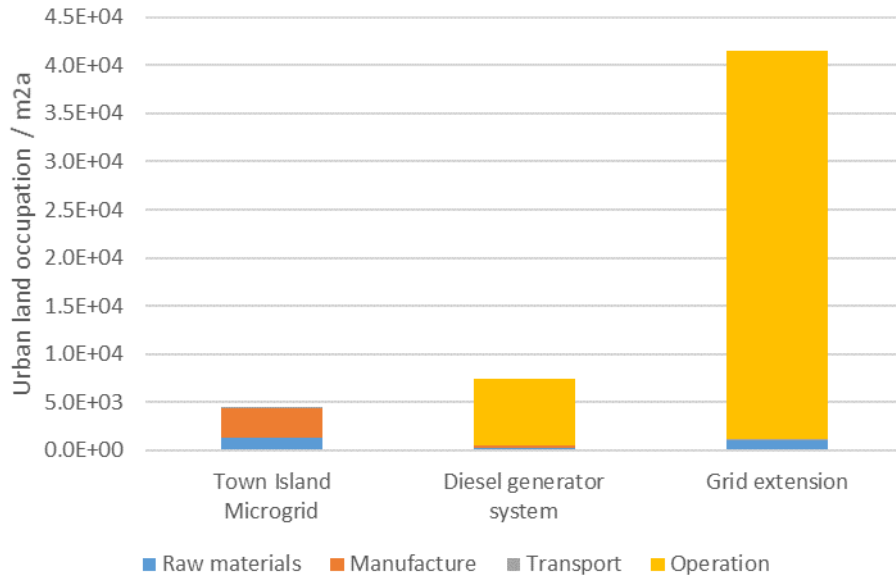


Figure 2-16 – Urban land occupation / m²a

The natural land transformation (NLT) required by the diesel generator system and the grid extension is 40.9 times and 5.7 times greater than the NLT caused by the microgrid respectively (Figure 2-17). The microgrid solution leads to the least amount of natural land transformation. The production and combustion of diesel fuel are the two major contributors to NLT. NLT caused by grid extension involves transforming forest from extensive to intensive.

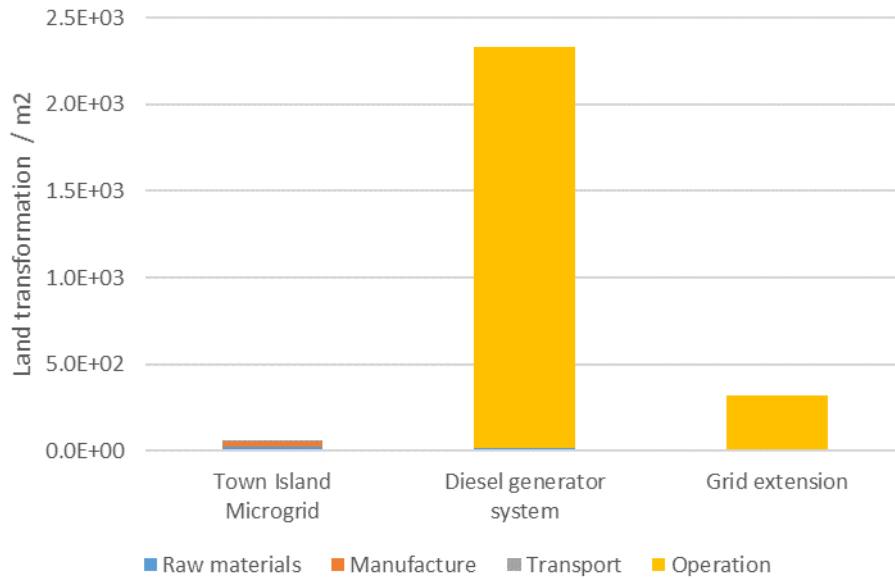


Figure 2-17 – Natural land transformation / m²

2.5.4 Overall life cycle environmental performance of the Town Island Microgrid compared to other electrification options

Summarising the results of the comparative LCA based on midpoint methodology, the Town Island Microgrid is found to be the least impactful in 8 out of the 12 studied impact categories, and for no impact categories is the Town Island Microgrid found to be the poorest performer. In addition, the endpoint methodology is used to aggregate the impact categories to construct a single score to compare the three options (Figure 2-18). The significant impacts on human health include mainly particulate matter formation, global warming potential, and human toxicity, whereas the noticeable impacts on resources involve mainly metal depletions and fossil fuel depletion.

Overall, this study suggests that the microgrid is the most favorable option. This is consistent with previous studies, which have found a microgrid to be a more environmental friendly electrification solution compared to other conventional electrification solutions (Smith *et al.*, 2015). In contrast, the diesel generator system option imposes the most significant

environmental impacts, which can be attributed to the continuous diesel fuel production and emissions from diesel fuel combustion during operation that characterize this system. The grid extension option performs slightly better; however, it still imposes significantly more life cycle environmental impacts than the microgrid solution. The results of this study highlight the importance and merit of using LCA as a comprehensive environmental impact evaluating tool in order to identify under which impact category a solution can be further improved. For instance, as described in earlier sections, the relatively high HTP, FETP, and METP emitted by the microgrid are largely due to heavy metals. Now that these LCA results are published, equipment manufacturers can introduce technological improvements in treating the heavy metals, such as chemical precipitation and ion exchange or absorption (Fu and Wang, 2011).

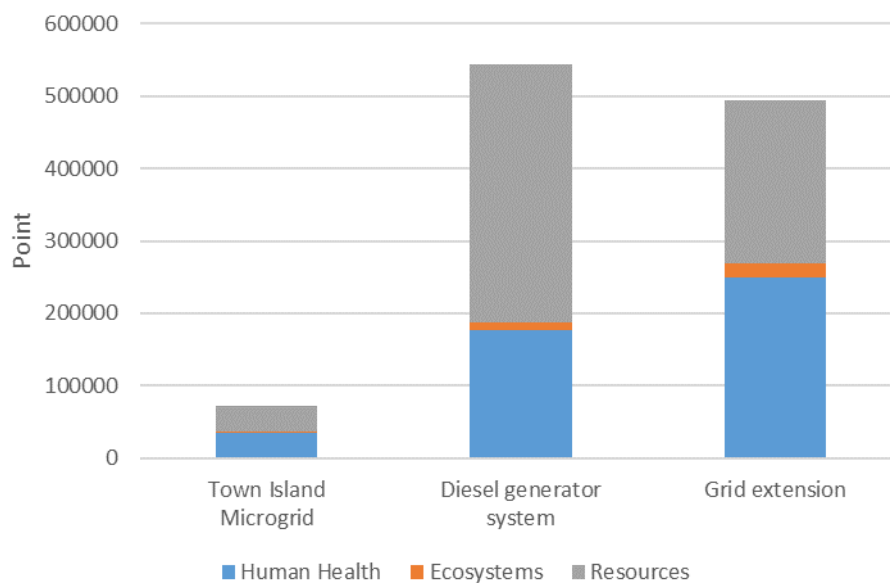


Figure 2-18 – Aggregated single score of the three electrification options assessed using endpoint methodology

2.5.5 EPBT of the Town Island Microgrid

The EPBT values for each of the three scenarios are shown in Table 2-8. It is estimated that the Town Island Microgrid has an EPBT of 9.2 years, meaning that it will take this period of time

for the system to generate enough energy output to compensate for the primary energy required to develop the system. The EPBT of the diesel generator system is about 10 times greater than that of the Town Island Microgrid, and the EBPT of the grid extension option is 6.4 times greater than that of the Town Island Microgrid. As mentioned in the introduction, few studies have considered all the microgrid components, including the renewable energy generators and the battery system. Nevertheless, the EPBT calculated for the Town Island Microgrid in the present study is comparable to the value found in a previous study that suggested it would be 9.5 to 10.5 years (Akinyele, 2017).

Table 2-8 – Total primary energy demand and energy payback time of the three electrification options

Electrification Option	Total Primary Energy Demand	Energy Payback Time
	/ MWh	/ Year
Town Island Microgrid	1886.95	9.2
Diesel generator	19085.76	93.2
Grid extension	12074.62	59.0

2.5.6 Limitations

The concept of sustainability covers environment, economics, and society. In addition to environmental sustainability, the other two aspects of sustainability are equally important. For instance, social sustainability is believed to be significantly enhanced by using microgrid systems because of the improved energy security that they provide. Prior to the microgrid installation, Town Island was powered non-continuously by diesel generators. Emissions and pollutions from the generators negatively impacted the lives of Town Island residents, but with the implementation of the clean renewable energy microgrid, these negative impacts have been

significantly mitigated. Also, the frequent delivery of diesel fuel is costly and time-consuming, and sometimes uncertain if sea traffic conditions are adverse. A study (Moslehi and Reddy, 2019) suggested a framework to evaluate the overall sustainability of an energy system, not only the different aspects have to be considered, they have to be compared against each other in order to effectively identify the tradeoffs. This framework may be applied when more data is available.

2.6 Summary

This study assesses the life cycle environmental impacts of the microgrid. An LCA case study was carried out on the Town Island Microgrid, the first standalone hybrid renewable energy commercial microgrid in Hong Kong. To comprehensively review its environmental performance, 12 LCA impact categories were considered and the system's EPBT was calculated. The PV panel system (composed of both 200 W and 280 W panels) is the major contributor to several impact categories including GWP, FFD, PMF, TAP, ODP, TETP, ALO, ULO, and NLT, whereas the battery system is the major contributor to HTP, FETP, and METP. The system EBPT is calculated to be 9.2 years, which is comparable to previous studies. The environmental performance of the microgrid was further tested against two alternative electrification options, including an on-site diesel generator system and a grid extension via a submarine cable. Among the 12 LCA impact categories, the Town Island Microgrid has been demonstrated to be the least impactful in 8 categories, and for no impact category was the microgrid found to be the most impactful. The EBPT of the diesel generator and the grid extension is 10.1 and 6.5 times greater than the EBPT of the Town Island Microgrid. It can thus be concluded that the case study supported the microgrid as a more environmental friendly solution compared to other common electrification options.

For future works, the scope of study could be expanded by also taking into account the end of life for an energy system. Given that recycling data in Hong Kong is not readily available, it was decided not to include the end of life in the LCA at the current study. Future LCA research could factor in the impacts of recycling and disposal if the data becomes more accessible. In addition, for microgrid projects undergoing the initial planning and design stage, smart grid features such as demand response can be considered for further optimization and to harness benefits from possible enhanced efficiency. The associated environmental performance improvement can then be quantified by LCA.

3. CHAPTER 3: RENEWABLE ENERGY MICROGRIDS: ECONOMIC EVALUATION AND DECISION MAKING FOR GOVERNMENT POLICIES TO CONTRIBUTE TO AFFORDABLE AND CLEAN ENERGY

3.1 Introduction

“Affordable and Clean Energy” is Goal 7 of the United Nations Sustainable Development Goals (UNSDGs) which focuses on universal access to energy, increased energy efficiency and the increased use of renewable energy through new economic and job opportunities by ensuring access to affordable, reliable, sustainable and modern energy (United Nations, 2019a). While this UNSDG formulates the ultimate goal, efforts are paid worldwide but the possible roads reaching the goal seem divergent with different considerations of energy access, and the costs and benefits of energy systems from different stakeholders’ angles (Cash, 2018). To understand the affordability, the economics of clean renewable energy has become more important than ever.

Although fossil fuels continue to dominate the energy market, investment in renewable energy has been catching up, growing from 45 billion USD to 270 billion USD between 2004 and 2014. Among most types of renewable energy technologies, wind (onshore and offshore) received almost 56% of the share of finance, solar energy received around 24%, and biomass, waste, and biofuels received 15.2% (Mazzucato and Semieniuk, 2018). This rise in investment could in part be due to a general perception that new renewable energy generations, backed up by suitable energy management strategies, can outperform traditional generation (Bhowmik *et al.*, 2017). Harnessing renewable energy has been an ongoing challenge because of its unstable supply, yet microgrids have been considered to be a solution for effectively managing renewable energy generators and could also reduce pollution and lower costs with the aid of energy storage systems and appropriate optimization (Basak *et al.*, 2012). Microgrids can

generally comprise 20-25 % of on-site renewable energy in terms of capacity, but given the right demand and supply conditions, a higher renewable energy proportion is also possible (Burr *et al.*, 2014). Owing to its small-scale nature, its application is not limited to specialized operation by professional grid owners, but can be implemented at commercial and residential building sites (Anvari-Moghaddam *et al.*, 2017; Zhang and Jia, 2017), meaning that the public is engaged as stakeholders in the electricity market than ever. Overall, the use of renewable energy microgrids seems to be an effective solution for tackling global warming by acting as a clean energy management scheme. In addition to its technological and environmental advantages, its economic performance equally deserves the public's attention.

This study collects publicly available financial data from 24 microgrid projects worldwide and investigates the economic performance of renewable energy microgrids by evaluating key performance indicators including life cycle costing, net present value, and economies of scale. Furthermore, based on the economic study results, this study provides decision making supports for government policies and to contribute to the UNSDG Goal 7.

3.2 Literature review

3.2.1 Renewable energy application in microgrids

It has been suggested that renewable energy generations should: be unaffected by international political situations, be unarmful to the environment, utilize infinite resources, be accessible to all class and geographies, and be affordable (Rezaie, Esmailzadeh and Dincer, 2011). These criteria lead to consideration of a wide variety of parameters during renewable energy application decision making, including environmental protection, technology, economics, market maturity, an abundance of renewable energy, and reliability (Lupangu and Bansal, 2017; Xu *et al.*, 2018; Zhao *et al.*, 2018). Determining the most appropriate renewable energy

application, with consideration of, for example, energy source types and mixes, depends on how much weight is allocated to each of these parameters. For instance, case studies (Rezaie, Esmailzadeh and Dincer, 2011) have reported that although solar thermal system for providing hot water and space heating in buildings could be the most cost-effective option out of the studied renewable energy technology options, solar energy from PV panels and hybrid renewable energy systems could offer other benefits (higher efficiencies, technological feasibility) that could be similarly important. In other words, renewable energy application is a complicated concept which needs iteration and optimization of multiple factors to result in a fit-for-purpose system.

Microgrids can be seen as a way to connect a number of independent and heterogeneous renewable energy systems together to form a complex and dynamic integrated energy system, essentially a system of systems (Mahmoud, Rahman and Sunni, 2015). The simplified general structure of a microgrid comprises of generators (renewable or non-renewable), storage systems, and loads. It can operate in alternating current, direct current or a mix of both, with their respective pros and cons (Planas *et al.*, 2013). There are a number of applicable standards to microgrids, such as IEEE 1547 Criteria and requirements for interconnection of DERs with the main grid and EN 50160 Voltage characteristics of electricity supplied by public distribution networks. Yet due to its emerging popularity, a wide variety (in terms of generation source, capacity, grid connection, etc.) of microgrids are undergoing development and operating worldwide (Zia, Elbouchikhi and Benbouzid, 2018). Nevertheless, despite the dynamic nature of renewable energy resources, with proper balancing and control, a complex renewable energy microgrid can deliver stable and satisfactory electricity and energy (Gu *et al.*, 2014; Shuai *et al.*, 2016). It was reported that microgrid gained its popularity due to mainly resilience concerns, and also the increasing technological and economic feasibility (Ajaz, 2019).

3.2.2 Existing economic studies

Microgrids have been seen as challenging to commercially evaluate for several reasons. Firstly, a microgrid represents a series of assets and infrastructure that come from different value streams, and during operation, a microgrid may go through several phases (generation, control, independence) but these phases are not distinct and often overlap (Burr *et al.*, 2014). In addition, not all costs and benefits can be taken into account by investors because the costs and benefits may be associated with a broad range of stakeholders. As investors are usually preoccupied with technical benefits and financial returns, they may not consider the part of the costs and benefits which do not have a direct impact on them (Quashie, Bouffard and Joós, 2017; Hirsch, Parag and Guerrero, 2018). Few studies have successfully captured non-financial outcomes of microgrids such as improved air quality, and represent them in economic terms (Byrne *et al.*, 2017). All these factors lead to difficulties in formulating a business case for microgrids.

Despite these hurdles, some studies indicate that microgrids could be a solution to current economic inefficiencies associated with conventional electrical grids (Faber *et al.*, 2014; Yoldaş *et al.*, 2017). However, the literature does not seem to have reached an agreement regarding the investment payback of renewable energy. It has been reported that the payback period of PV panels could be up to 14 years, which is considerably long and primarily due to high equipment cost. This financial hurdle is shared across many emerging green technologies (Baljit, Chan and Sopian, 2016a). A business plan was prepared for a 4kW microgrid in a rural area of Kenya which aimed to generate sufficient revenue to cover the maintenance and replacement of equipment for the grid, in addition to human costs and other operation costs. It was concluded that the microgrid was economically sustainable and would also be profitable after one year of operation (VanAcker *et al.*, 2014). On the other hand, another study (Zachar,

Trifkovic and Daoutidis, 2014) found that it could be difficult for microgrids to be economically attractive when there is an alternative to connect to the main grid. In addition, renewable energy may sometimes suffer from cost fluctuation due to technological breakthroughs, government policies, and changes in feedstock prices (Yu, Song and Bao, 2012). There are some studies attempting to optimize the use of renewable energy based on economics and energy performance. Such techno-economic optimization can be carried out by comprehensively considering load profiles, penetration, energy investment, renewable energy generation, storage capacity. The optimum may be based on a performance index such as energy returned on energy invested, energy payback time, investment payment time and net present value (He *et al.*, 2018; Jo, Aldeman, H. S. Lee, *et al.*, 2018; Jo, Aldeman, H.-S. Lee, *et al.*, 2018). It is apparent that existing studies have different positions on the commercial viability of microgrid solutions.

3.2.3 International government policies on renewable energy and microgrids

Worldwide there are governments supporting the finance of microgrid projects (Mariam, Basu and Conlon, 2016; Ali, Li, Hussain, He, Barry W. Williams, *et al.*, 2017). (Milis, Peremans and Van Passel, 2018) prepared a review of the impacts of government policies on microgrid economics. One of the main objectives of government policies is to help grid owners achieve economic efficiency, such as through minimizing capital costs and/or operating costs. A variety of policies can be implemented to achieve this objective. Taking Australia as an example, a renewable energy fund (\$500 million) was set up on a 1:2 basis, in order to leverage over \$1.5 billion towards having national energy needs met with 20% renewable energy by 2020 (Zahedi, 2010). (Aalto *et al.*, 2012) suggested that support policies can be conceptualized in terms of four dimensions: resource-geographic, financial, institutional and ecological. The study also discussed major constraints in meeting renewable energy goals, such as the lack of interactions

between technical experts and social scientists, and huge investments to promote renewable energy on a national level. Effective policy making also requires consideration of different stakeholders, across disciplines and social demography (Rommel and Sagebiel, 2017). Similarly, (Zhang *et al.*, 2013; Soshinskaya *et al.*, 2014; Gaona, Trujillo and Guacaneme, 2015) point out that the importance of a government exercising caution about the interactions between its policies and industrial development in order to ensure healthy and sustainable growth in the renewable energy sector. As promoting renewable energy is not merely a hardware transition from fossil fuels to alternative energy sources, the promotion requires support from prolonged social empowerment and social equity on a global scale, on this topic some studies suggested the energy democracy movement (Burke and Stephens, 2018; Thombs, 2019). Putting into practice, a previous study (Hazboun *et al.*, 2019) gathered feedbacks from the public regarding their government's policies on renewable energy and concluded general approval, and another study (Arpan *et al.*, 2018) further divided the public's response into individual political orientations, values and norms to learn the correlation in-between. Furthermore, (McGee and Greiner, 2019) suggested that with the aid of mindful government policies on populations who are most exposed to energy poverty geographically and financially, social inequality and emissions can be simultaneously reduced via increasing renewable energy consumption.

Governments can jumpstart conversion to renewable energy use by rolling out policies that support a stable and commercially sizable market, and reduce barriers to entry in terms of costs, infrastructure and information (Huang *et al.*, 2012). (Boute, 2012) reported that renewable energy support can be categorized as either investment-based or production-based schemes (Figure 3-1). Investment-based schemes finance systems with particular consideration of installation capacity, while production-based schemes, including quantity-based approaches (such as purchase obligations and tradable green certificates) and price-based ones (such as

feed-in-tariffs and power purchase agreements), support renewable energy based on the output, and thus are more related to the electricity commodity market. There are also other production-based policies such as levying carbon taxes that may help capture the negative externalities of non-renewable energy and in turn increase the price competitiveness of renewable energy (Tulpule *et al.*, 2013). An on-going debate is still taking place vigorously among existing research literatures on which scheme will have more influence on promoting renewable energy, in particular (Alizada, 2018) attempted to present a review.

The success rates of various support policies differ between countries. For instance, despite the economic potential of renewable energy is very high in Russia and support by its government, the growth of the sector remains low (Lanshina *et al.*, 2018). Besides, it is suggested that Mexico's government has not demonstrated serious engagement in promoting renewable energy deployment as little has been done to improve transport efficiency (Valenzuela and Qi, 2012). In the UK, a series of policies have been implemented to ensure that the wholesale electricity market can accommodate low-carbon generation in the pursuit of meeting the country's renewable targets without compromising supply security (Connor *et al.*, 2014). For oil-producing countries, even more, effort will be required from the government as the current energy generation option is considerably less expensive than the deployment of renewable energy (Mezher, Dawelbait and Abbas, 2012). In contrast, the Chinese government has achieved remarkable gains—the wind turbine installation growth rate has been increasing by 100% each year, and nine out of fifteen PV manufacturers worldwide are located in China (Zhang, Chang and Eric, 2012). Not limited to the renewable energy support schemes, the support form government and institutions, and the level of regulations on innovators are also factors affecting the growth of microgrid market (Sergi *et al.*, 2018). Overall, as suggested by (Monyei *et al.*, 2019), it is important to reduce policy vagueness, and to provide tangible

benchmarks, that are agreed internationally, for governments to quantitatively and qualitatively make their policies.

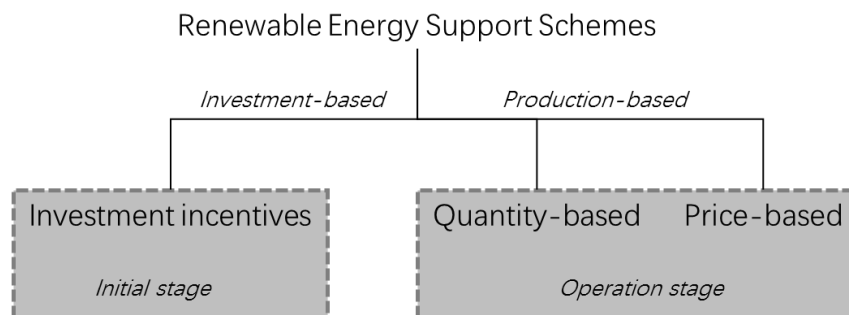


Figure 3-1 – Classification of Renewable Energy Support Schemes

3.3 Objective and significance

This study is considered to be a contribution to “Affordable and Clean Energy”, Goal 7 of United Nations Sustainable Development Goals. Unlike in traditional large-scale electricity generation (primarily coal and natural gas), where only the utility investors have to pay attention to grid economics, with microgrids any individual can be an investor given the small-scale and distributed nature of the technology. Although there are some costing studies on microgrids in the existing literature, they are mostly carried out for a single case study, producing results that are highly specific to that case’s grid configuration and therefore of limited application to the planning of future projects.

The aim of the present study is to evaluate the economics of renewable energy microgrids for the public’s general understanding, using three economic performance indicators (Table 3-1). Compare to recently published single case study works, this study contributes to more effectively assessing microgrid adoption by generalizing 24 microgrid projects worldwide spanning different capacities and different levels of renewable energy adoption. Furthermore, based on the performance indicator results, this study offers suggestions to help government

decision making in crafting policies to fund renewable energy efforts (Table 3-2).

Table 3-1 – Illustration of how the economic performance indicators can help investor decision making

Economic performance indicators	Decision making support for grid investors
Life cycle cost	Quantify the entry investment cost and the operating cost over the lifetime
Economies of scale	Evaluate the possibility of benefiting from savings by building larger capacity microgrids
Net present value	Understand the worthiness of investment considering the cash flow over time

Table 3-2 – Illustration of how the economic performance indicators can help government decision making

Economic performance indicators	Decision making support for government policies		
	Investment incentives	Quantity-based	Price-based
Life cycle cost	<ul style="list-style-type: none"> Determine the level of capital cost support 	<ul style="list-style-type: none"> Determine the level of operating cost support (quantity-based) 	<ul style="list-style-type: none"> Determine the level of operating cost support (price-based)
Economies of scale	<ul style="list-style-type: none"> Differentiate measures to promote low and high capacity microgrid 	<ul style="list-style-type: none"> N/A 	<ul style="list-style-type: none"> N/A
Net present value	<ul style="list-style-type: none"> Determine the level of capital cost support 	<ul style="list-style-type: none"> Consider cash flow revenue support (quantity-based) 	<ul style="list-style-type: none"> Consider cash flow revenue support (price-based)

3.4 Proposed methodologies

3.4.1 Case Study: 24 microgrid projects

Details for 24 microgrids worldwide were gathered from government and commercial reports (Ernest Orlando Lawrence Berkeley National Laboratory, 2010; Siddique, 2016; The World Business Council for Sustainable Development, 2016; Brown, 2018; Microgrids at Berkeley Lab, 2019; Port of Long Beach, 2019; State Government of Victoria, 2019). Background

information on these projects is provided in Table 3-3. In order to generalize the economic performance of renewable energy microgrid projects, the referenced projects must share one common feature which is the use of renewable energy in the grid at any capacity level. For a fair comparison, this study attempts to report results as unit cost, in terms of USD/kW capacity and USD/kWh energy output. Firstly, the background information of the microgrid projects is analyzed to produce generalized economic performance data on them. Secondly, 3 economic methodologies are employed to assess the performance and sustainability of the generalized case. Thirdly, the results are translated to policy making support. The proposed methodology flow is graphically shown in Figure 3-2.

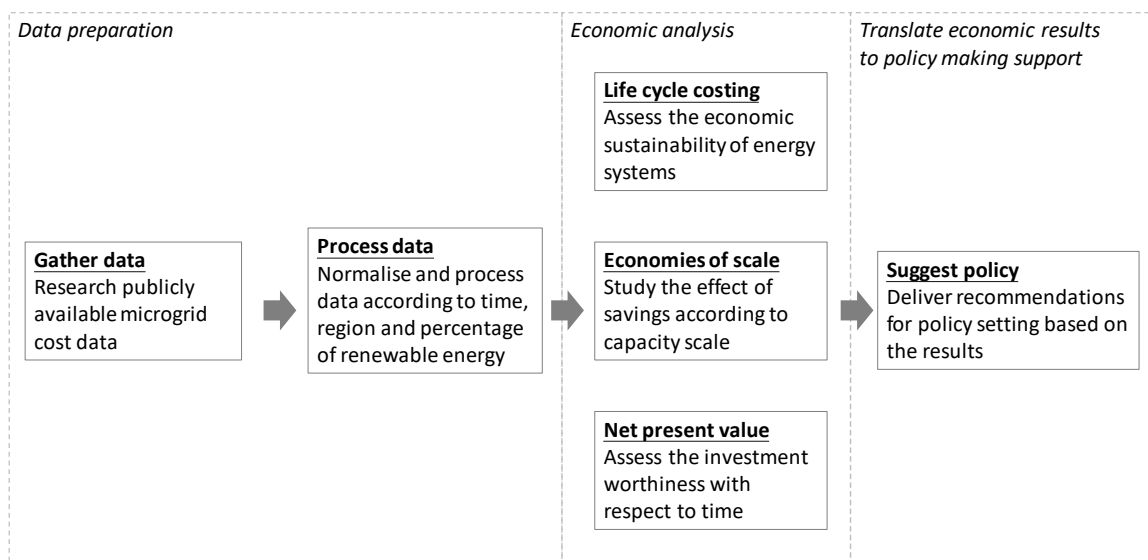


Figure 3-2 – Graphical illustration of the proposed methodology

The limitations of the case study are discussed in the later section, especially the limited data completeness and the inadequate depth of publicly available cost data. The authors pay the best effort to ensure the usefulness of this study to produce results adoptable for future studies and for the public's reference, cautions are paid while making reasonable assumptions, yet not to make conclusions beyond logical justifications.

Table 3-3 – Background information on 24 microgrid projects worldwide, their capacity (total and renewable energy portion), and investment cost

The renewable energy microgrid projects	Location	Year ^a	Capacity / kW	Renewable energy / kW	Investment Cost / USD ^b
Santa Rita Jail Microgrid	Japan	2002	6,848	1,448	14,000,000
Isle of Eigg	UK	2008	266	166	2,124,800
L&T Chennai Campus	India	2009	1,820	138	2,000,000
Marble Bar and Nullagine	Australia	2010	1,580	300	3,577,000
San Diego Zoo Solar-to-EV Project	US	2012	190	190	1,000,000
Eagle Picher Power Pyramid TM	US	2012	1,030	30	2,628,000
Demonstration 2500 R Midtown Development	US	2013	281	77	850,000
Kansas Survival Condo	US	2013	450	100	800,000
Nagoya Landfill Microgrid	Japan	2014	700	500	1,500,000

The renewable energy microgrid projects	Location	Year ^a	Capacity / kW	Renewable energy / kW	Investment Cost / USD ^b
US Marine Corps					
Base Camp	US	2015	202	152	1,035,000
Pendleton					
Alpha Omega Winery	US	2016	500	400	1,100,000
Ameren					
Distribution Microgrid	US	2016	1,475	225	5,000,000
Amtrak Sunnyside Yard microgrid					
Shanghai Microgrid Demonstration	China	2017	206	156	371,400
The Thacher School	US	2017	1,000	1,000	4,330,000
Marcus Garvey Apartments	US	2017	1,100	800	3,000,000
OATI Microgrid Technology Center	US	2017	2,400	174	1,500,000
Peña Station NEXT	US	2017	2,600	1,600	10,300,000
Euroa Microgrid	Australia	2018	989	589	4,380,000
The Port of Long Beach Microgrid	US	2018	1,380	300	7,100,000

The renewable energy microgrid projects	Location	Year ^a	Capacity / kW	Renewable energy / kW	Investment Cost / USD ^b
Singapore					
Renewable Energy Integration Demonstration	Singapore	2018	2,800	300	3,000,000
Miramar Naval Base	US	2018	7,000	1,600	20,000,000
Birchip Cropping Group Microgrid Demonstration	Australia	2019	188	51	232,870
Bornholm Island EcoGrid 2.0	Denmark	2019	112,500	35,500	14,700,000

Remarks:

- a. Year refers to reported commissioned year or the year when the investment cost subject to how the reference is made available.
- b. The investment cost shall be normalized to eliminate the price level change effect for analysis, an annual inflation rate of 2.5% is assumed. Exchange rates at the time of study are adopted (1 AUD:0.73 USD).

3.4.2 Life Cycle Costing (LCC)

Life cycle costing (LCC) has been proven to be an effective tool to assess the economic sustainability of energy systems. LCC addresses a system's economic performance over the entire life cycle, covering capital investment cost and operating costs such as operation,

maintenance, and replacement (Weldu and Assefa, 2017). Successful execution of LCC requires an adequate database and high transparency of cost data (Bornschlegl, Bregulla and Franke, 2016). In this regard, the authors of this study made a diligent effort to gather the information required to perform the included analyses, and while assumptions are necessary, they are stated in relevant sections. Equation 3-1 represents the life cycle costs.

Equation 3-1 – Life cycle costing

$$\text{Life cycle cost} = \text{Capital costs} + \text{Lifetime operating costs}$$

While the investment costs of the renewable energy microgrid projects are already listed in Table 3-3, the operating cost of a microgrid depends on many factors, for instance, its type of generation, operation schedule, location, and level of automation (Siemens, 2016). Given that operating cost information for the projects included in this study is not available, the study alternatively estimates the operating cost as a percentage of capital cost. The previous microgrid LCC case studies report markedly divergent results: with operating costs as low as 1% of capital cost (Jacob, Banerjee and Ghosh, 2018) up to 5-13% of capital cost (Arriaga, Cañizares and Kazerani, 2016; Horhoianu and Horhoianu, 2017; Kyaw, 2017). This study assumes that the operating costs, including operation, maintenance, and replacement, is 10% of the investment cost. In addition, the capacity factor of renewable energy is assumed to be 0.3, and that of non-renewable energy is assumed to be 0.8 (Rubin, Rao and Chen, 2005; Nalbandian-Sugden, 2016).

3.4.3 Economies of scale (EOS)

While making a commercial decision regarding renewable energy microgrid installation, the life cycle cost is not the only concern; whether an installation can benefit from economies of

scale is also critical. The effect of savings due to economies of scale is usually measured by the economies of the scale factor. When the factor is smaller than 1, the cost per capacity keeps reducing as the capacity increases. The lower the factor is, the higher the economies of scale impact will be (DeNeufville and Scholtes, 2011). The economies of scale factor can be represented as shown in Equation 3-2.

Equation 3-2 – Economies of scale factor

$$C_2 = C_1 \left(\frac{S_2}{S_1} \right)^n \quad n = \frac{\ln \left(\frac{C_2}{C_1} \right)}{\ln \left(\frac{S_2}{S_1} \right)}$$

C represents the cost of the plant and S represents the capacity of the plant. The subscripts 1 and 2 refer to the two respective systems to be evaluated. n is the economies of the scale factor. Note that in this particular section of the study, 3 outliers are not considered: the Isle of Eigg (outlier for relatively high investment cost per capacity), the Amtrak Sunnyside Yard microgrid, and the Bornholm Island EcoGrid 2.0 (outliers for relatively high capacity).

3.4.4 Net Present Value (NPV)

The investment worthiness of microgrids can be reflected by their net present value (NPV). NPV represents a discounted cash flow calculation, with the net cash flow discounted by a discount rate (interest rate) at a specific time, typically annually, and throughout the product's lifetime (Mitscher and R  ther, 2011). If the NPV over the lifetime is positive, the system is profitable, implying it is worthy of investment. In contrast, if the NPV is negative, the system is not profitable. Equation 3-3 is a standard formula for calculating NPV.

Equation 3-3 – Net present value

$$NPV = \sum_{t=0}^n \frac{\text{Net cash flow}}{(1 + i)^t}$$

n represents the system’s life, t is the year, and i is the interest rate. To deduce the unit NPV (the NPV to provide 1 kWh each year), the investment costs and the capacities of microgrids are averaged. The net cash flow is the difference between the averaged global electricity price as derived from Figure 3-3 and the operating cost, an assumed 6% interest rate (Dohn, 2011), and an assumed lifespan of 20 years. The NPV formula can be defined as shown below.

Equation 3-4 – Net present value for renewable energy generation, given the assumed electricity price and interest rate

$$NPV_{1 \text{ kWh}} = \text{Investment cost}_{t=0, \text{ capacity to generate 1kWh}}$$

$$+ \sum_{t=1}^{20} \frac{(\text{Electricity price}_{1\text{kWh}} - \text{Operating cost of RE microgrid}_{1\text{kWh}})}{(1 + 0.06)^t}$$

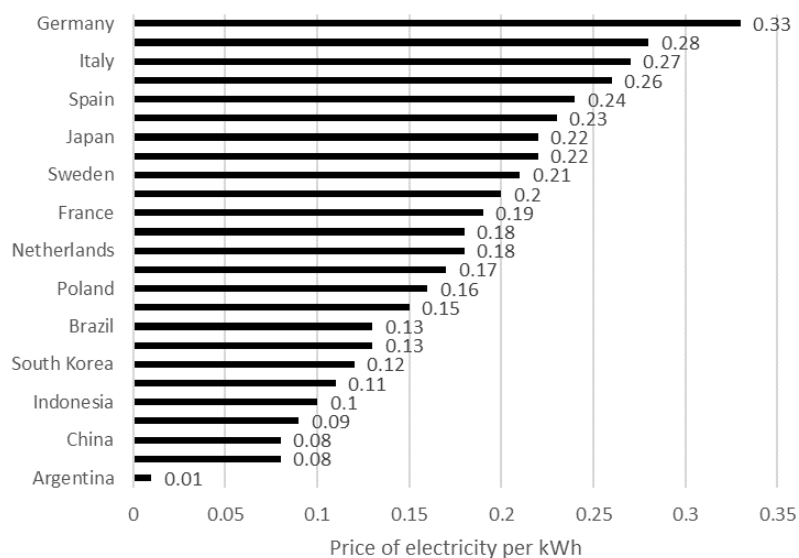


Figure 3-3 – Global Price of electricity per kWh in USD (2018) (Statista, 2018)

3.5 Results and Discussion

3.5.1A dilemma between environmental and economic performance

Figure 3-4 shows the investment cost of a microgrid per installed capacity over their respective time spans of operation. With the cost normalized against inflation to eliminate the impacts of price level change, it can be observed that the investment cost per capacity gradually reduces with time. This could be due to the steady reduction in renewable energy cost in the last decade (International Renewable Energy Agency, 2018). However, the commercial attractiveness of renewable energy microgrid investment cannot be easily determined by one parameter. Figure 3-5 presents the investment cost per capacity against the percentage of renewable energy capacity in a microgrid. The figure shows that the higher the renewable energy percentage is, the higher the investment will be required. It is commonly known that renewable energy is superior to non-renewable energy in terms of environmental performance. The findings in Figure 3-5 imply a dilemma between environmental performance and economic performance which is not often reported in the existing literature. The results of these two graphs indicate that despite the investment barrier shrinking over the past decade, harnessing the environmental benefits of renewable energy microgrids is still hindered by their steep investment costs.

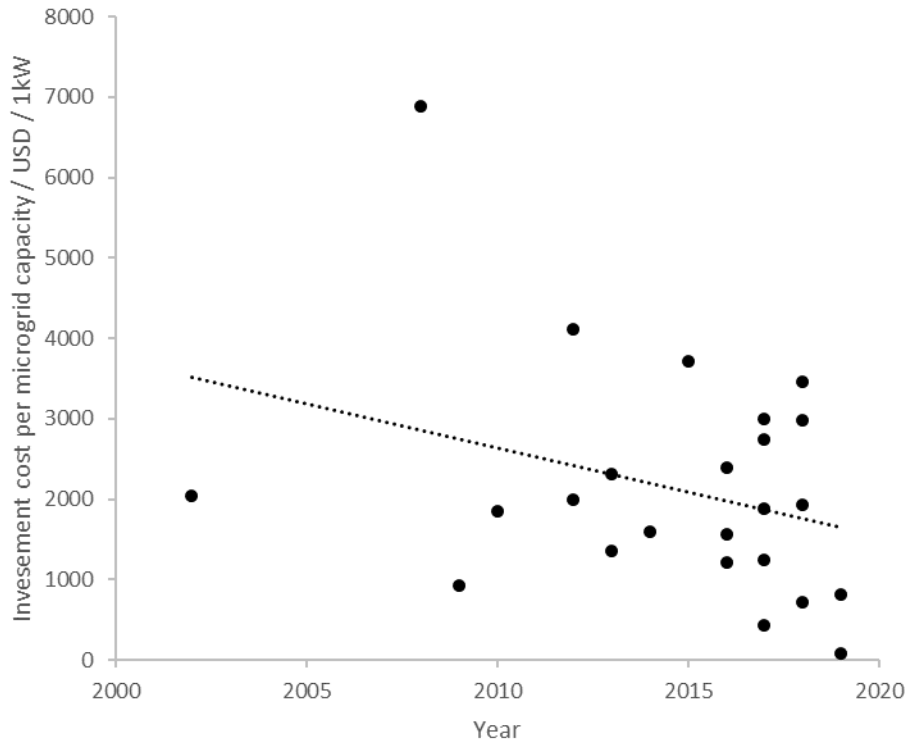


Figure 3-4 – Investment cost per microgrid capacity against time, with a linear trendline

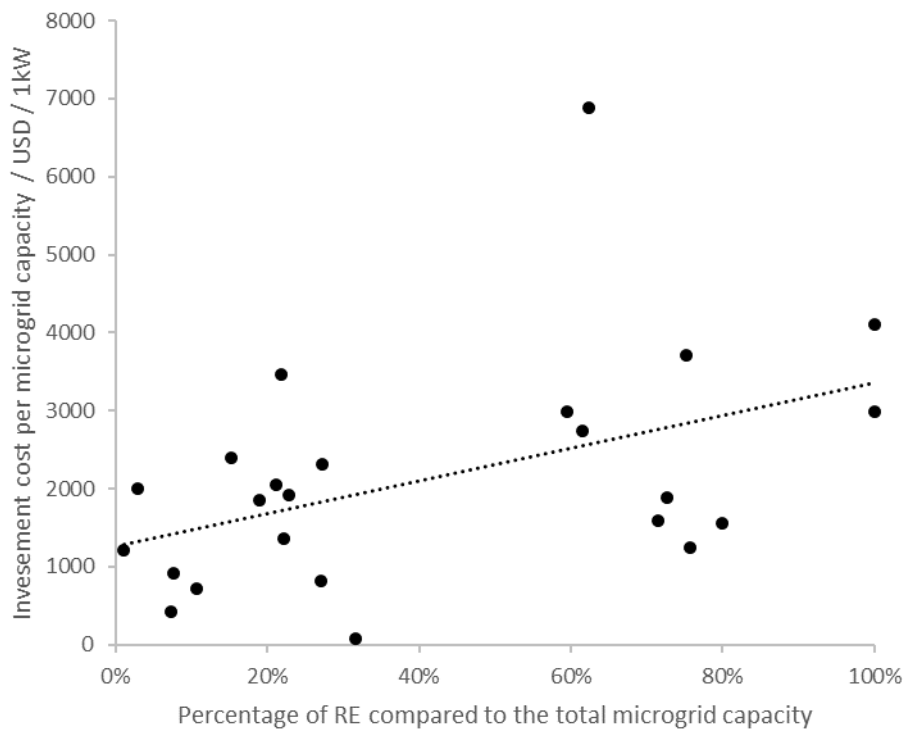


Figure 3-5 – Investment cost per microgrid capacity against renewable energy adoption, with

a linear trendline

3.5.2LCC: Investment cost and operating cost

The life cycle cost of renewable energy microgrids consists of initial investment cost and operating costs. The investment cost is presented in USD/kW, in terms of installed capacity before operation commences. During the operation stage, the cost can be measured in USD/kWh, representing the unit cost of energy output. As a result, the investment cost and operating cost of a renewable energy microgrid are calculated to be 2,135 USD/kW and 0.066 USD/kWh respectively. These cost figures are compared to non-renewable energy power plants (Table 3-4). For investment cost, it is found that the capital needed to set up a renewable energy microgrid is higher than pulverized-coal combustion and natural gas combustion by 98% to 296% and 147% to 370%, respectively. Operating costs for a renewable energy microgrid are 0.55 to 2.3 times greater than for pulverized-coal combustion, though these costs for a renewable energy microgrid are comparable to that for natural gas combustion (34% lower to 65% higher). The distribution system of a microgrid accounts for a small percentage (Giraldez *et al.*, 2018) hence it is considered acceptable to compare the total cost of a microgrid against a power plant. Given the ongoing demand for clean energy and the gradual ruling out of coal combustion, the authors believe that the estimated renewable energy microgrid operating costs are bearable by investors.

Yet the more critical issue remains unsolved, as the investment cost of renewable energy microgrids creates a high market entry barrier and reveals significantly inferior price competitiveness compared to non-renewable energy electricity generation. As mentioned earlier, one of the essential principles of new energy generation is for it to be financially affordable to all parties, including investors and customers. The LCC results, in contrast, reveal

that renewable energy microgrids still have not managed to reach a competitive level in the past decade. With reference to the trendline in Figure 3-4 and projecting the investment cost for another decade, renewable energy microgrids may begin to be price competitive with non-renewable energy generation in 2025, assuming there are no external factors such as significant technological breakthroughs or additional government interventions (Table 3-5). This finding suggests a 5-year delay for renewable energy’s cost to undercut non-renewable energy’s as compared to the suggestion in a renewable energy cost study (International Renewable Energy Agency, 2018) which suggested that renewable energy technologies could fall within the price range of fossil fuels by 2020.

Table 3-4 – Estimated investment cost and operating cost of renewable energy microgrid and other non-renewable energy power plants (Nalbandian-Sugden, 2016)

Technology	Investment cost / USD/kW	Operating cost / USD/kWh
Renewable energy microgrid	2,135	0.066
Pulverised-coal combustion	500 – 1,000	0.02 – 0.04
Natural gas combustion	400 – 800	0.04 – 0.10

Table 3-5 – Projection of renewable energy microgrid investment cost (2020 – 2029)

Year	Investment cost / USD/kW	Year	Investment cost / USD/kW
2020	1560	2025	1010
2021	1450	2026	900
2022	1340	2027	790
2023	1230	2028	680
2024	1120	2029	570

3.5.3 Implications of economies of scale

Graph depicting the economies of scale for the microgrid projects under study are shown in Figure 3-6 and Figure 3-7). Firstly, it can be observed that the investment cost per microgrid capacity non-linearly decreases as the capacity of the microgrid increases (Figure 3-6). This demonstrates some level of economies of scale taking place, meaning that the savings in terms of unit capacity can be enjoyed as the capacity is increased. Next, to quantify such savings, the data is mathematically analyzed with a natural log function. The gradient of the trendline in Figure 3-7 represents the economies of scale factor (EOS factor, n) which is computed to be 0.897 (or 0.9 when rounded to one significant figure). By definition, the closer to 1 the EOS factor is, the weaker the economies of scale will be, yet the product still benefits from related savings. Therefore, it can be interpreted that renewable energy microgrid projects exhibit weak economies of scale. Some literature has reported the EOS factors of various energy systems. It has been suggested that energy and chemical production plants generally have an EOS factor of 0.6 (D. Yogi.Goswami, 2015) and that coal generation features weak economies of scale (Lenzen, 2010). Overall, such high EOS factors (though still lower than 1) can be considered as discouraging to investors to build renewable energy microgrids with considerable capacity. However, these EOS factors do not imply that there is no market potential for renewable energy microgrids at any capacity. For instance, a study on PV systems in Brazil (Mitscher and Rüter, 2011) suggested that the market potential was strong particularly for small scale distributed systems.

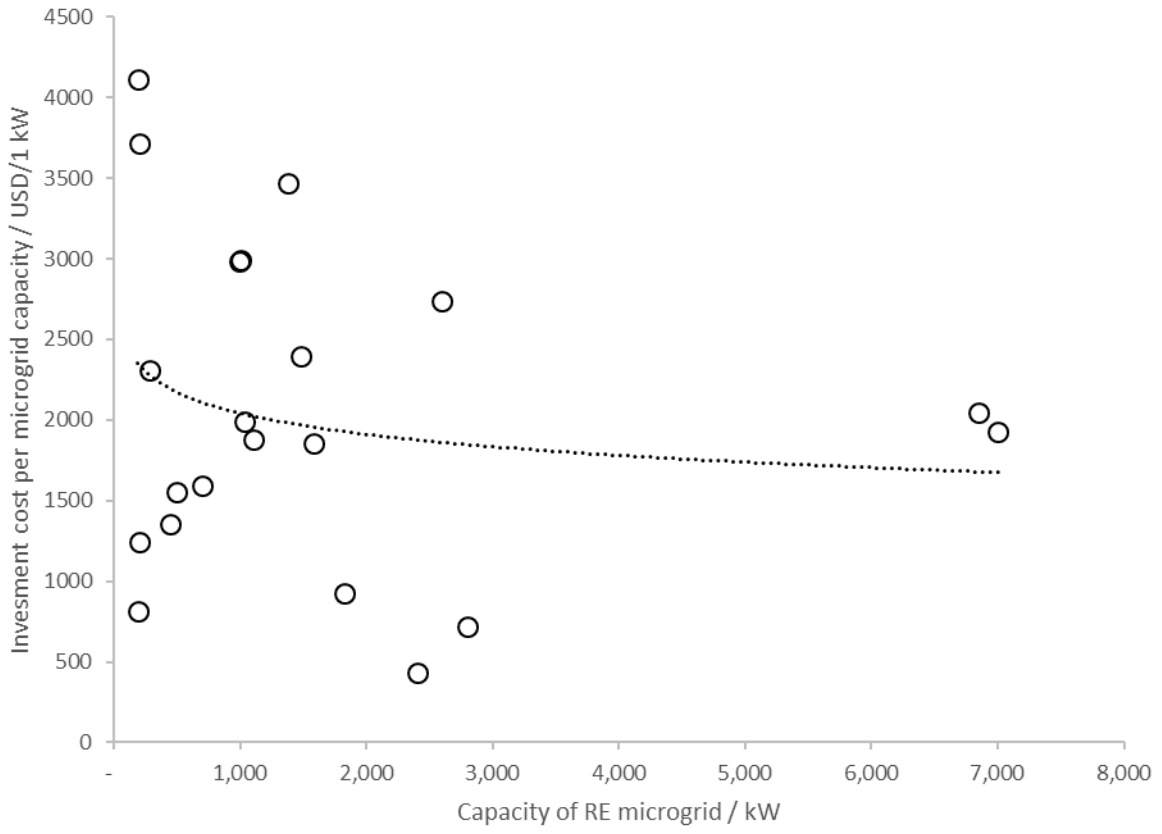


Figure 3-6 – Capacity of microgrid against investment cost per capacity, with logarithm trendline

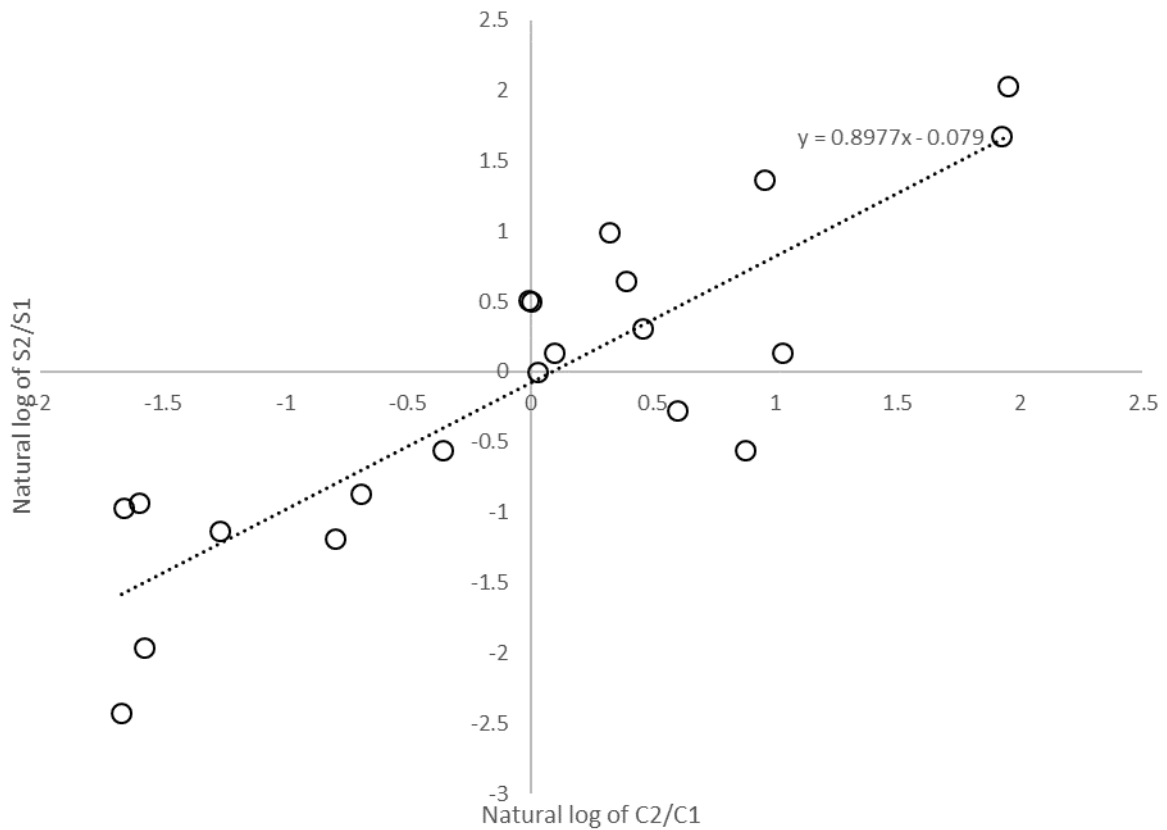


Figure 3-7 – Natural log graph to deduce the economies of the scale factor, with a linear trendline

3.5.4 Net present value

Table 3-6 shows the NPV calculation. The net cash flow is assumed to be the difference between electricity price (0.17 USD) and the operating cost (0.066 USD). From this table, three observations can be made. Firstly, the net cash flow during operation (20 years) is positive despite being discounted by the interest rate. This implies that renewable energy microgrid projects can be profitable during the operation stage. Secondly, as far as the NPV is concerned, the initial investment also has to be taken into account. As a result, the NPV does not become positive, despite the positive net cash flow during operation. Thirdly, by comparing the initial investment cost and the cash flow during operation, the difference in magnitude between the two is significant. It is highly unlikely that the operation revenue can cover the investment cost.

Considering these observations together, the economic sustainability of renewable energy microgrids is not encouraging. However, it is not uncommon to generate pessimistic economic sustainability results for renewable energy systems; two PV systems in the US were also reported to have negative NPV (Sivaraman and Moore, 2012). Another case study in Australia also concluded that the capital cost to run renewable energy is unaffordable and that climate change can only be effectively addressed on the supply side (Trainer, 2013). Yet the electricity price assumed in an NPV calculation can be limited because the electricity price may increase as the supply of fossil fuels faces shortage (Pickard, 2012). However as shown in the NPV calculation, the most apparent barrier to achieving positive NPV lies with the investment cost, and the electricity price charged during service has little impact on the NPV over the 20-year lifetime. Overall, it may be argued that a negative NPV should not be considered decisively disadvantageous, since current non-renewable energy technologies may also face the same problem. The deployment decision should not be based on solely commercial factors as renewable energy microgrids can generate social benefits such as energy security and reliability.

Table 3-6 – NPV calculation of renewable energy microgrid generating 1kWh (per year)

Year	Net cash flow / USD/kWh	Year	Net cash flow / USD/kWh
0 (Investment)	-2135.31	11	0.057
1	0.101	12	0.053
2	0.096	13	0.050
3	0.090	14	0.048
4	0.085	15	0.045
5	0.080	16	0.042
6	0.076	17	0.040
7	0.072	18	0.038
8	0.067	19	0.036
9	0.064	20	0.034
10	0.060	End of life	-2,134.08 (NPV)

As mentioned in previous section, the operating cost can be 5 - 13% of the capital cost, thus a sensitivity test is carried out to reveal the impacts of this ratio on operating cost and net present value (Table 3-7). It is shown that within this ratio range, the impact on NPV is minimal because the net cash flow (electricity price minus operating cost) during operation is insignificant compared to the initial investment cost. This sensitivity test result echoes the previous suggestion that the investment cost is the major reason why microgrid may not be a worthwhile investment.

Table 3-7 – Sensitivity test for varying ratios of capital cost to operating cost

The ratio of capital cost to operating cost	Operating cost / USD/kWh	NPV / USD
1: 0.1	0.066	-2,134.08
1: 0.05	0.033	-2,133.70
1: 0.013	0.086	-2,134.31

3.5.5 Decision making support for government policies

This section provides decision making supports for government policies on renewable energy microgrids based on the three presented economic performance indicators. As mentioned in previous section and illustrated in Figure 3-1, government policies can be classified as investment-based, quantity-based, or price-based. It should be noted that investment-based policies focus on the initial stage, while quantity-based policies concentrate more on the operation stage.

3.5.5.1 Investment subsidy (Initial stage)

Based on the life cycle cost and net present value results, it is shown that the investment cost is significant compared to operating cost, and the investment is not paid back in 20 years. Therefore, it is apparent that the investment cost is the major hurdle for market entry. If a government wishes to encourage investors to participate in the microgrid market, it should deliver policies that can lower the barriers to entry, such as through subsidies. While this study compared the unit investment cost of renewable energy microgrid against traditional fossil fuel generations, it is recommended that a government subsidize the investment cost of a microgrid to a level comparable to these traditional means. Recapping the Australian case (Zahedi, 2010) mentioned in previous section, it is possible that this 1:2 basis may create just enough incentive

for investors to enter the market. This depends on the price competitiveness of renewable energy compared to fossil fuels, where for instance in oil-producing countries greater subsidies for renewable energy is required due to the abundant supply and lower price of oil.

Next, based on the economies of the scale factor, it is shown that renewable energy microgrids of large capacity may not be an attractive option for investors. Thus, it is recommended that if a government wishes to engage the public (any individuals), it may be more effective to first promote small-scale renewable energy installation, for instance, rooftop solar thermal systems or PV systems. Secondly, should a government wish to appoint investors to build large scale showcase renewable energy systems to raise public environmental awareness, it is proposed that the subsidy amount should increase with the capacity of the microgrid because investors may not enjoy economies of scale by building larger grids.

3.5.5.2 Quantity-based & price-based (Operation stage)

During the operation stage, a government can deliver quantity-based policies and price-based policies. Quantity-based policies can mandate electricity users to acquire a certain amount of electricity from renewable energy sources, and to mandate electricity providers to purchase tradable green certificates from renewable energy generators. Overall, quantity-based policies are pursued to help reach the targeted quantity of renewable energy generation. For price-based policies, such as feed-in-tariffs and purchase agreements, they set a price for renewable generations in the electricity market so that the generation becomes more cost-effective, or even profitable.

With reference to the life cycle cost and net present value results, two relevant points regarding operation can be recapped: 1) the operating cost of renewable energy is uncompetitive

compared to coal but comparable to natural gas, 2) due to the high investment cost and little revenue generated, the investment does not pay itself back. While the gap in operating cost between renewable energy and fossil fuels is not as wide as the one in capital cost between the two, if a government wishes to financially support renewable energy operations, production-based policies may not be as effective as investment-based ones, however production-based policies are still necessary to maintain the price competitiveness and economic sustainability of renewable energy.

3.5.5.3 Complementary investment-based and production-based policies

Although it is suggested that investment incentives may be a more effective approach compared to production-based policies, a complementary implementation of the two policy types is essential because a singular focus on investment may lead to a compromise in quality and system efficiency, while a sole focus on production may not generate sufficient interest for investors to enter the market in the first place. Thus to create a welcoming and sustainable market for renewable energy microgrids, it is proposed that a government should first lower the barriers to entry by subsidizing the investment cost, then introduce production-based policies which can further promote the renewable energy microgrid market growth by supporting its commercial practicality.

3.5.6 Limitations

3.5.6.1 Data availability

This study is based on cost data publicly available online which is presented as a total installation cost and no further breakdown is open to public. This poses limitations on further possible analysis on the featured microgrid projects, such as investigating the relationship between configuration complexity and cost performance indicators. To avoid assumptions

based on inadequate data and unjustified reasons, further analysis on the featured microgrids has been constrained. Nevertheless, it is believed that this study has served its purpose by assessing microgrids' economic performance for general use and have contributed to the UNSDGs Goal 7: Affordable and Clean Energy by providing key results to support governments' decision making.

3.5.6.2 Constant electricity pricing in NPV calculation

This study assumes a constant (not time-varying) electricity price in the NPV calculation. Despite the rising popularity of real-time pricing and time-of-use pricing (Milis, Peremans and VanPassel, 2018), such impact on the microgrid's economic performance is outside the scope of this study. It was reported that time-of-day pricing could, but not necessarily, improve the economics of microgrids, depending on whether net metering is allowed (Sesmero, Jung and Tyner, 2016). Another previous study (Darghouth, Barbose and Wiser, 2014) suggested that a high solar energy penetration (i.e., 33%) scenario does not necessarily lead to savings in electricity bills. It also depended on the pricing mechanism (time-of-use / real time) and whether hourly netting or net metering was adopted. The variation in changes in electricity bill was reported to be -25% to +7%. These studies demonstrate noticeable uncertainty remaining in generating savings through renewable energy and smart pricing.

3.5.6.3 Unaccounted externalities

While examining the sustainability of a microgrid, it is best that all costs and benefits that microgrids incur and bring are considered (Khodaei *et al.*, 2017). It has been suggested that investment in a microgrid can result in manifold benefits, such as enhanced energy efficiency and integrated renewable power generation. The benefits may also include greater balancing of supply and demand, cutting-edge security solutions to protect important infrastructure, and

modular and operation-friendly solutions which may allow easy upgrade (Dohn, 2011). Even though these benefits are indeed commendable, not all these benefits can be straightforwardly quantified in economic terms and consequently can be overlooked during microgrid investment considerations. Therefore, non-renewable energy has the advantage of incurring low private costs although it imposes high social costs, while renewable energy suffers from high private costs although it exhibits high social benefits (Byrnes *et al.*, 2013). It is suggested that in future research sustainability net present value (SNPV) (Zore *et al.*, 2018) can be adopted to comprehensively account for the economic, environmental, and social implications of various energy systems. Alternatively, real options' valuation can be considered as it may provide additional insights by taking account of realistic flexibility and choice.

3.6 Summary

To contribute to UNSDGs Goal 7: Affordable and Clean Energy, this study assesses the economic performance and sustainability of renewable energy microgrids, with the aim to assist investors' decision-making. In contrast to traditional electricity generation, anyone can be an investor in renewable energy microgrids due to their small-capacity and distributed nature. It is necessary to inform the public about the economic implications of renewable energy microgrids.

Data for 24 renewable energy microgrids installed worldwide was gathered and generalized to form the basis of this study. It is found that the investment costs of renewable energy microgrids have gradually declined over the last decade. In addition, a dilemma between environmental and economic performance is revealed as the investment cost of renewable energy microgrid increases with the percentage of renewable energy use. This represents difficulties in harnessing the environmental benefits of renewable energy. On the economic side, with the aid

of LCC, the investment cost and operating cost of a renewable energy microgrid are calculated to be 2,135 USD/kW and 0.066 USD/kWh respectively. These cost figures are compared against non-renewable energy generation including pulverized-coal and natural gas, with renewable energy microgrid displaying inferior price competitiveness. In particular, the investment cost of a renewable energy microgrid is significantly higher than both forms of non-renewable energy generation, while the operating cost of a renewable energy microgrid is also significantly higher than coal, but it is comparable to natural gas. It is projected that by 2025 the costs of renewable energy microgrids will begin to be competitive with non-renewable energy generation. The implication of economies of scale is also studied. The EOS factor is calculated to be 0.9, which implies that the economies of scale is weak, but still takes place. Furthermore, the NPV calculation suggests that investment in a renewable energy microgrid is not a profitable one.

This study also provides decision making support for investment-based or production-based government policies based on economic performance indicators. It is suggested that due to the high market entry barriers, investment-based policies may be more effective compared to production-based policies. However, the two can complement each other in order to create a welcoming and sustainable renewable energy microgrid market.

4. CHAPTER 4: A MODELLING FRAMEWORK TO EXAMINE PHOTOVOLTAIC ROOFTOP PEAK SHAVING WITH VARYING ROOF AVAILABILITY: A CASE OF OFFICE REFERENCE BUILDING IN HONG KONG

4.1 Introduction

The United Nations Sustainable Development Goal 7 “Affordable and Clean Energy” aims to ensure access to affordable, reliable, sustainable and modern energy for all. One of the key targets is to increase substantially the share of renewable energy in energy consumption mix (United Nations, 2019b). While buildings contribute significantly to energy consumption, energy-related carbon emissions in buildings have been climbing in recent years. In particular, direct and indirect emissions from electricity consumption in buildings have reached a record high (IEA, 2020). In the face of the global climate emergency, professionals and authorities are calling for the development of sustainable low carbon buildings worldwide. Current actions include design and operation improvements, regulation and framework development, and technology and innovation encouragement (Díaz López *et al.*, 2019). Strategies to reduce building carbon emissions broadly cover energy efficiency enhancement, renewable energy integration, water use reduction, and waste management. Although awareness about low carbon buildings has risen, progress is still impeded by challenges such as the general public’s unfamiliarity with available technologies and a lack of project guidance (Darko *et al.*, 2017). Photovoltaic (PV) roofing has been shown to be an effective means of enabling on-site renewable energy and reducing reliance on grid electricity often generated from fossil fuels (Yau and Lim, 2016). A building-integrated PV system, coupled with a battery system, creates peak shaving opportunities to reduce a building’s peak loads. This can produce environmental benefits not only to the building but also to the wider grid as the demand at peak hours is partially offset (Braun and Rüther, 2010).

Research gaps are identified as existing buildings may not have sufficient roof space for PV installations as on-site renewable systems may not have been previously considered. The potential to utilize these spaces is not well documented. Furthermore, most studies found in the literature focused on PV systems in small-scale residential buildings due to their low energy requirements and higher energy savings, relatively less emphasis has been put on medium- to high-rise office buildings.

To examine PV rooftops with varying roof availability and measure the environmental benefits of peak shaving to be carried out by PV roof, this study proposes a systematic modelling framework which involves the use of computational software (whole building energy simulation and PV system simulation). The methodology framework is illustrated on a reference 10-storey office building. The analysis includes various peak shaving strategies and facilitate decision-making based on their corresponding carbon reductions.

4.2 Literature review

4.2.1 The urgency to reduce building operational carbon emissions

The building sector is one of the most significant contributors to energy use and carbon emissions. There is an urgent need to decarbonize buildings in design and operation (Hossaini, Hewage and Sadiq, 2015). Considerable research and industry efforts have been devoted to low carbon building design and development, including improving energy efficiency, adopting renewable energy, and reducing fossil fuel consumption (Luo *et al.*, 2019). In recent years, the concept has evolved further to achieve zero-energy buildings and zero-carbon buildings, such that a building is designed to be run with renewable energy and result in net-zero carbon emissions (Rey-Hernández *et al.*, 2018). Policies, mandatory and voluntary, have rapidly picked up the pace to assist the building sector reducing its energy use and carbon emissions

(Van derHeijden, 2018). Operational energy could account for 70% to 90% of the whole life cycle energy consumption of a building (Ingrao *et al.*, 2018), meaning that there could be a high potential for decarbonization improvement during the operation stage. Despite the urgency, the carbon emission in the building sector is predicted to continue to increase in the coming decade in rapidly developing countries, like China (Ma *et al.*, 2020). To achieve low carbon building operation, effective building energy management policies and the adoption of renewable energy technologies are immediately required (Mafimisebi *et al.*, 2018). Macroly speaking, government policies, such as mandatory design standards and assessment standard for green buildings, are also crucial (Ma *et al.*, 2019).

4.2.2 Photovoltaic (PV) application in buildings

On-site building-integrated renewable energy production, in particular PV, is suggested to be effective in reducing operational emissions (Lützkendorf *et al.*, 2015). The crystalline silicon module is known as the most common type of PV panel, accounting for the largest global PV market share (Ban-Weiss *et al.*, 2013). Most studies in the literature have focused on the PV systems in small-scale residential buildings. Given that the energy requirements of these buildings are low, relatively significant energy savings generated by the PV systems were revealed (Leadbetter, 2012; Zheng, 2015; Song, 2018). Battery systems are often used to complement the PV system to accommodate the energy production surplus, if any (Kobayakawa and Kandpal, 2015). Furthermore, battery systems could counter the mismatch between PV energy production and consumption to improve grid interaction (Aelenei *et al.*, 2019).

The deployment of solar energy in urban contexts faces some challenges due to the high density of varying rooftop heights and reduced surface area for sunlight exposure. For instance, it was

suggested that shading caused by the surroundings could lead to a 10% loss in energy yield (Melo *et al.*, 2013). In addition, the available rooftop area suitable for PV installation could vary from around 10% to 50% due to other utilities already installed there and irregularity in layout (Melius, Margolis and Ong, 2013; Singh and Banerjee, 2015). On the other hand, rooftop can be used alternatively as green roof for aesthetic and sustainability purposes (Chen *et al.*, 2019). Nevertheless, it is of great importance to investigate the applicability of solar energy because urban areas are major contributors to global greenhouse gas emissions (Anderson, Wulforth and Lang, 2015). Moreover, solar energy is convenient for installation on limited rooftop space due to its uniform, modular nature (Michael, S and Goic, 2015). One practical advantage of solar energy systems is the synchronicity between the peak production of solar energy during the day and the daytime peak electricity demand of commercial buildings, such as air-conditioning loads, thus offering the potential to relieve the burden of the main grid during peak hours (Cellura *et al.*, 2012). Measurable energy saving by urban rooftop solar panel installations has been reported, indicating that the carbon emissions of buildings could be lowered with reasonable financial investment (Wang *et al.*, 2018).

4.2.3 Peak shaving by PV in buildings

Existing literature offers rich references on energy management, control algorithms, and optimization including charging and discharging mechanisms of battery systems (Uddin *et al.*, 2020), multi-objective techno-economic performance assessment (Rezvani *et al.*, 2015), and generation scheduling (Luo *et al.*, 2020). These studies focused on proposing sets of procedures to regulate the system to achieve designated performance benchmarks or to maintain a predefined balance. To maximize the environmental benefits, a high level of renewable penetration in microgrids is desired. However, this increases the uncertainties in electricity generation. Demand response of controllable loads could contribute to reducing the imbalance

between supply and demand of electricity, yet it also requires complex load shifting algorithms (Reihani *et al.*, 2016; Hakimi *et al.*, 2020).

One of the most crucial energy management strategies is peak shaving in the context of building-PV integration. Essentially, peak shaving refers to smoothing the load profile during peak hours (Zheng, Meinrenken and Lackner, 2015). Peak shaving strategies can be categorized into three major types: demand-side management, incorporation of the energy storage system, and integration of electric vehicles (Uddin *et al.*, 2018). The benefits include reducing national grid infrastructure limits, lowering transmission requirements, and savings on costs (García-Plaza *et al.*, 2018). The effectiveness of peak shaving is time-dependent and peak load-dependent because PV electricity generation and its associated battery system target the peak load hours of a building (Jurasz and Campana, 2019a). Furthermore, it has been suggested that PV energy management strategies should consider seasonal change as the building energy demand and PV electricity generation are dependent on outdoor environmental conditions such as heat loads and sunlight (Kapsalis and Karamanis, 2015). While evaluating the environmental consequences of peak shaving by substituting grid electricity, it is important to refer to temporal marginal grid carbon emission because it has been shown to vary with the grid operation (Hawkes, 2010; Graff Zivin, Kotchen and Mansur, 2014).

4.3 Objective and significance

Some existing buildings do not have sufficient roof space for PV panels because on-site renewables may not have been considered in previous designs. Among these buildings, the roof space availability varies and the potential to utilize these spaces is not well documented. Even though building-integrated PV systems and peak shaving have been proven to be environmentally advantageous, there are limited readily available guidelines for new building

designers to analyze the relationships between system size, suitable peak shaving strategies, and carbon emission savings. While most studies in the literature have focused on the PV systems in small-scale residential buildings, the authors believe that with proper design guidance and peak shaving strategies, PV systems for medium- to high-rise office buildings could result in considerable savings.

The key contributions of this study include (1) providing a framework for measuring performance of PV rooftops according to reduced peaks and avoided carbon emission, (2) shedding light on the peak shaving management of PV electricity based on the size of the system, season, and building demand, and (3) recommending policies based on the findings in order to further promote PV integration.

4.4 Methodologies

4.4.1 Overview of methodologies

This study proposes a methodological framework to examine PV rooftops with varying roof availability, in particular carbon reduction and peak shaving opportunities. This involves several computational tools, including a whole building energy simulation modeling tool and a solar energy simulation tool. In this study, Designer Builder, EnergyPlus, and PVsyst were used. These analytic software applications are validated by the respective software developer. The resolutions of these two tools must be matched such that the building power demand and PV electricity can be mapped to the same time interval (hourly in this study). It is also important that these tools are able to generate year-long data to capture seasonal change. This framework should not have geographical constraints given suitable data is available.

As demonstration, the modelling framework was applied on a 10-story reference office

building. A reference building is a model that can approximately represent other buildings of similar function and climatic zone (Schaefer and Ghisi, 2016). This study selected Hong Kong as an experimental test point because of its high urban density and medium- to high-rise environment. By having 10 stories as a base unit, the applicability of peak shaving on medium- to high-rise buildings can be quickly assessed and extrapolated as a reference. A flow chart illustration is presented to offer a process overview (Figure 4-1). The procedures are outlined in detail in the following sub-sections.

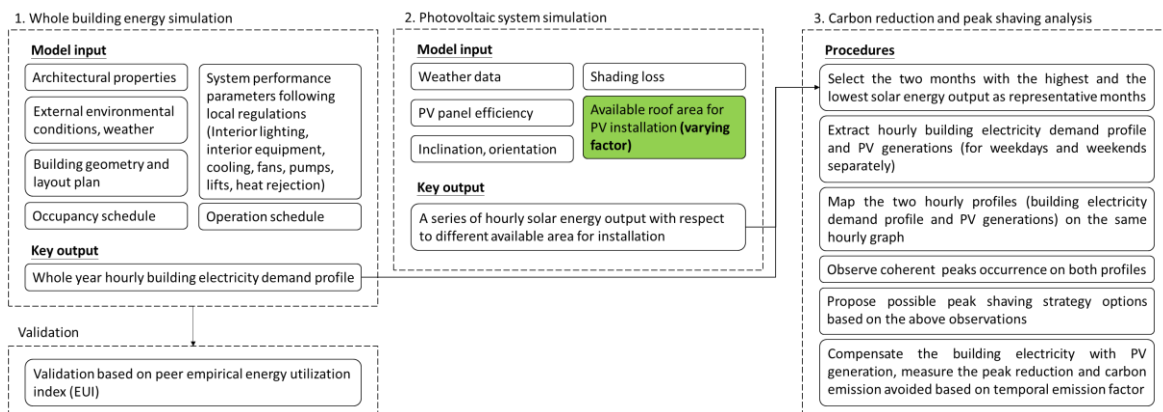


Figure 4-1 - Flow chart illustration of the proposed modelling framework. This framework is applied on a hypothetical reference office building.

To fill the suggested research gaps, the independent variable was set to be rooftop availability (10%, 30%, and 50% of roof area available for PV installation). While the electricity demand of a building and PV generation can change hourly, an array of peak shaving strategies are considered for covering different numbers of peaks and the duration of peak shaving. The performance of PV installation was evaluated with two performance factors: peak loads reduction and the avoided carbon emissions by substituting grid electricity.

4.4.2 Whole building energy modeling

Building energy modeling can generate a whole year energy usage profile of a building for a given building geometry. In the present study, a 3D model of an office building was built using Design Builder, a modeler that is capable of constructing geometry to facilitate further simulations. The reference office building was assumed to have 10 stories with a typical office layout and a curtain wall system (Figure 4-2). The building facades are oriented to face the four cardinal directions. A hypothetical reference building was used to represent the characteristics of a group of similar buildings and to perform a preliminary evaluation for informing further analysis. With 10 stories as a base unit, the applicability of peak shaving on medium- to high-rise buildings could be quickly assessed and extrapolated. The lowest, middle, and top floors were built, and 2 adiabatic component blocks were sandwiched in between as zone multipliers. The office building layout is 50m by 50m, including office space, lifts, toilets, stairs, and plant rooms (Figure 4-3). The key building architectural properties are summarized in Table 4-1.

Table 4-1 - Key building architectural properties

Number of stories	10
Area	2500 m ² per floor
Façade type	Curtain wall
Window to wall ratio (WWR)	80% Glazing: U-value: 0.7, Solar Heat Gain Coefficient: 0.25
Building materials	Concrete wall, U value: 0.35 W/m ² K

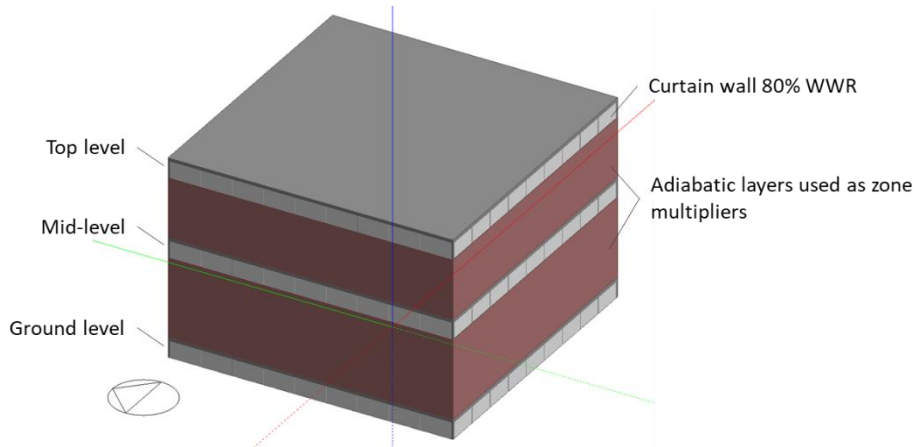


Figure 4-2 - Axonometric view of the simulated office building

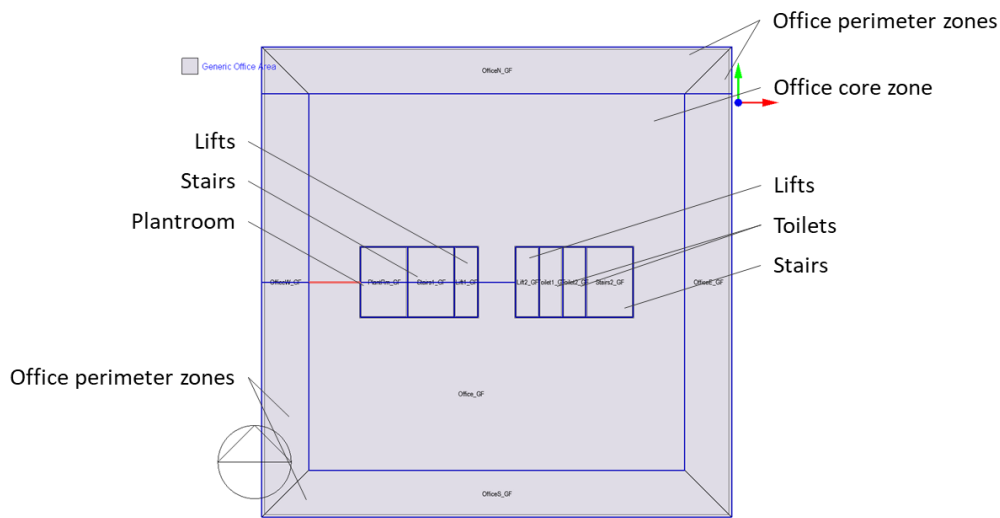


Figure 4-3 - Layout of the simulated office building

The building geometry was output from Design Builder and transferred to EnergyPlus for building energy simulation. EnergyPlus is open-source software funded by the U.S. Department of Energy's (DOE) Building Technologies Office (BTO) and is capable of modeling whole building energy consumption. It is authorized software for performing building energy simulation in compliance with international green building certifications such as Leadership in Energy and Environmental Design (LEED). To initiate energy modeling, it is essential to prepare data on the outdoor weather conditions and the building services system

configurations. Hong Kong weather, based on a statistical analysis of 25 years of weather data, was used to represent the outdoor environmental conditions (Chan *et al.*, 2006a). The simulation output was an hour-by-hour building electric power profile in a complete year (8,760 hours).

The modeling followed the standard procedures as stipulated in ASHARE 90.1. Performance and operating schedules of key building systems, including air conditioning, ventilation, lighting, interior equipment, and lift were assumed and modeled based on local standards (EMSD HK, 2007, 2018). Office space was considered as regularly occupied space, and the number of occupants was assumed based on an occupancy density of 13 m²/person. The occupancy schedule was set according to the abovementioned standards. During weekdays, the number of staff increased from the morning to reach almost full capacity (90%) at 09:00 until lunch at 12:00 – 14:00, then reduced to half during lunch, and resumed to almost full capacity until office hours ended at 18:00. For weekends, the number of staff increased from the morning to 70% of full capacity at 09:00, and office hours were assumed to end at 13:00. For Sundays, it was assumed that the office was unoccupied.

The key building system parameters are summarized in Table 4-2Table 4-1. The fresh air of 8 L/s/person was delivered to the office space to carry away indoor air pollutants, such as carbon dioxide from respiration. The building was designed to be equipped with a centralized air-conditioning system, supported by a centrifugal chiller system with a 6.1 coefficient of performance (COP) (ASHARE 90.1 minimum), to provide cooling to office space. According to ASHARE 90.1 standard, the unmet hours of the model shall be below 300 hours. This was to verify whether the air-conditioning system was sized properly and could meet the cooling setpoint temperature (23.5°C) within the designated zone.

In addition to air-conditioning, other systems were incorporated into the model. Ventilation, in particular toilet exhaust, was assumed to be 20 air change per hour (ACH). For lighting, various lighting power densities (LPD) were assigned to different spaces according to code requirements (EMSD HK, 2018). LPD refers to the power of lighting installation per unit floor area of illuminated space. For interior equipment load, it was assumed to be 10 W/m² and was applied to 70% of the office area. 4 traction drive lifts, each with a rated power of 27.5 kW, were assumed to operate in the building.

Table 4-2 - Key building system parameters

Air conditioning	Occupancy density in office space: 13m ² /person (EMSD HK, 2007) COP of centrifugal chiller: 6.1 (ASHRAE 90.1)
Ventilation	Toilet exhaust: 20 ACH
Lighting, in terms of LPD	Office: 9 W/m ² (EMSD HK, 2018) Stairs: 9 W/m ² (EMSD HK, 2018) Lift: 11 W/m ² (EMSD HK, 2018) Toilet: 11 W/m ² (EMSD HK, 2018) Plantroom: 10 W/m ² (EMSD HK, 2018)
Interior equipment	10 W/m ² (EMSD HK, 2018)
Lift	27.5 kW per lift (traction drive) (EMSD HK, 2018)

4.4.3 Photovoltaic (PV) system simulation

PVsyst was used to obtain the hourly electricity output of the rooftop PV systems, according to different percentages of roof area available for PV panel installation. For general research

applicability purposes, a generic PV panel in PVsyst's built-in library was selected without specifying a brand of PV panel: 250Wp polycrystalline PV panels with 17.25% efficiency. The conventional arrangement for rooftop PV panel installation in Hong Kong is south facing at an inclination of 22° (Fong, Lee and Chow, 2012). A flat roof was considered as a general representation of major roof type in Hong Kong office building (Yu and Chow, 2001). To mimic dense surroundings, 10% of energy loss (Peng *et al.*, 2013a) due to uniform far shadings was accounted for in Hong Kong. It should be noted that the energy yield loss should correspond to the location of the building to be studied. Close shading is not considered as it is highly specific to the building's own layout. It was supposed that electricity was generated by the rooftop PV system, then was stored in a battery bank, and was fed evenly and hourly to the building the next day. To confine the study scope, the interaction between the battery system and the PV system was not considered.

The simulation was conducted to assess the electricity output of the PV array when there were different sizes of areas available for PV installation on the roof. The electricity output of a PV array occupying 10% of the roof area was evaluated, corresponding to a nominal capacity of 36kWp. Subsequently, the electricity output of the PV array occupying more roof area was calculated by multiplying the corresponding percentage with the electricity output. As mentioned in previous section, the rooftop area suitable for PV installation in an urban context generally varies from around 10% to 50%. Thus the present study examined a series of electricity output data of PV arrays occupying 10%, 30%, and the practical maximum of 50%, to represent from low, medium to high PV roof potential.

4.4.4 Peak shaving analysis

The peak shaving analysis studied the relationship between PV system size, peak load reduction,

and carbon emission savings. Since PV electricity was used to substitute grid electricity, more roof space for PV installation enabled higher PV electricity generation and resulted in less reliance on grid electricity. As a result, rooftop availability (10%, 30%, and 50%) for PV installation was set as the independent variable. The PV rooftop performance was evaluated according to two factors: peak loads reduction and avoided carbon emissions.

The temporal pattern of grid electricity carbon emissions is especially important in renewable energy peak shaving. This is because grid electricity carbon emissions vary with time, and is subject to the supply and demand for electricity at that moment. The amount of carbon emitted during given periods of time becomes a decisive factor in determining which hour's peak is to be shaved. It is crucial to consider these two factors holistically as severe peak shaving could result in notable carbon reduction but could also cause an imbalance in the building's power supply system. While hourly grid electricity carbon emissions data in Hong Kong is not readily available in the literature to the authors' knowledge, Singapore's grid is considered a reasonable reference as Hong Kong and Singapore are similar in terms of area and economic activities, as well as in both location's heavy reliance on fossil fuels. Modifications were made on the temporal marginal emission amounts based on a Singapore study (Finenko and Cheah, 2016) for two major reasons. Firstly, the two locations' grid electricity emission factors are different, with Singapore's estimated to be 0.42 kg CO₂/kWh (EMA Singapore, 2019)), while for Hong Kong it is 0.7 kg CO₂/kWh (EPD HK and EMSD HK, 2010)). Secondly, the reference data is in half-hourly resolution, so the corresponding half-hourly and hourly emissions were averaged to better suit this study's resolution. The estimation is carried out based on Equation 4-1.

Equation 4-1 – Estimation of temporal emission factor at any hour (n) using Singapore (SG)

$$\frac{\text{Emission factor}_{n^{th}hour, HK}}{\text{Grid emission factor}_{HK}} = \frac{\text{Emission factor}_{average\ n-0.5^{th} \& n^{th}hour, SG}}{\text{Grid emission factor}_{SG}}$$

As mentioned in previous section, PV energy management strategies should consider seasonal change as building energy demand and PV electricity generation are dependent on outdoor environmental conditions such as heat loads and sunlight. To capture the seasonal impact, the month with the highest PV generation was identified to represent summer, and the month with the lowest PV generation was selected to represent winter. In accordance with the building energy modeling and solar energy simulation, the building electric power demand and solar electricity output were mapped on the same graph, with time on the x-axis and power on the y-axis. 9 strategies were developed to simulate peak shaving performed at different hours and lasting for different durations on weekdays. These options represented various strategies for feeding the stored PV electricity to the building to shave different peaks and different numbers of peaks. The peak shaving strategy options can be categorized into morning only, afternoon, and both morning and afternoon. Figure 4-4 illustrates the peak shaving strategy options during weekdays and weekends. For weekdays, strategies 1 through 3 represents 1 to 3 hours peak shaving in the morning, respectively, and strategies 4 through 7 represent 1 to 4 hours peak shaving in the afternoon. Strategies 8 and 9 represent whole day peak shaving excluding and including lunch hours, respectively. Strategy 9 was evaluated only when lunch hours became peaks in strategy 8. For weekends, given that the building operated for a half-day, strategies 1 through 5 represent 1 to 5 hours peak shaving, respectively.

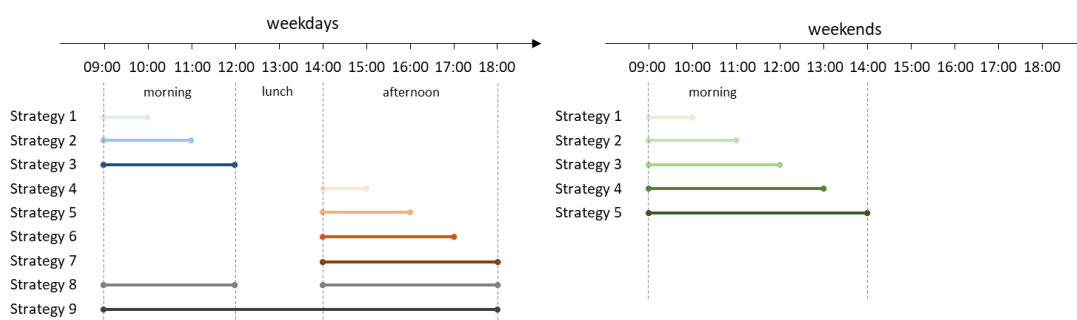


Figure 4-4 - Graphical illustration of peak shaving strategy options during weekdays and

weekends

4.5 Results and Discussion

4.5.1 Annual building energy use and electric power use profile

As mentioned in previous section, performance parameters and operation schedules for key building systems were inputted into the whole building energy simulation. The key results include the annual building energy use, the breakdown of energy use according to major building systems, and an annual building electric power use profile, containing 8,760 hourly data points.

A breakdown of energy use by the building system is presented in Figure 4-5. The three major components in energy use are interior lighting, interior equipment, heating, ventilation, and air-conditioning (HVAC¹). Interior lighting and interior equipment each contributed to 26% of total energy use, whereas HVAC, including cooling (21%), fans (10%), pumps (7%), and heat rejection (4%), contributed to 42% of the total energy use.

¹ In actuality, the simulated building was not equipped with heating due to the climatic conditions. The wording “HVAC” is used merely as general established terminology.

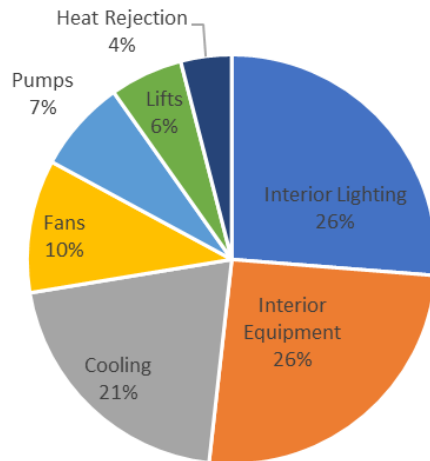


Figure 4-5 - Building system energy use breakdown

Figure 4-6 shows the annual whole-building electric power demand over 8,760 hours. The highest electric power demand (896 kW) was reached on 31 July 08:00. The baseload, which refers to the power of a proportion of equipment and lighting during off-hours, was 47 kW. Over the year, the energy use in summer, from June to October, was higher than in the other months, understandably because of increased air-conditioning.

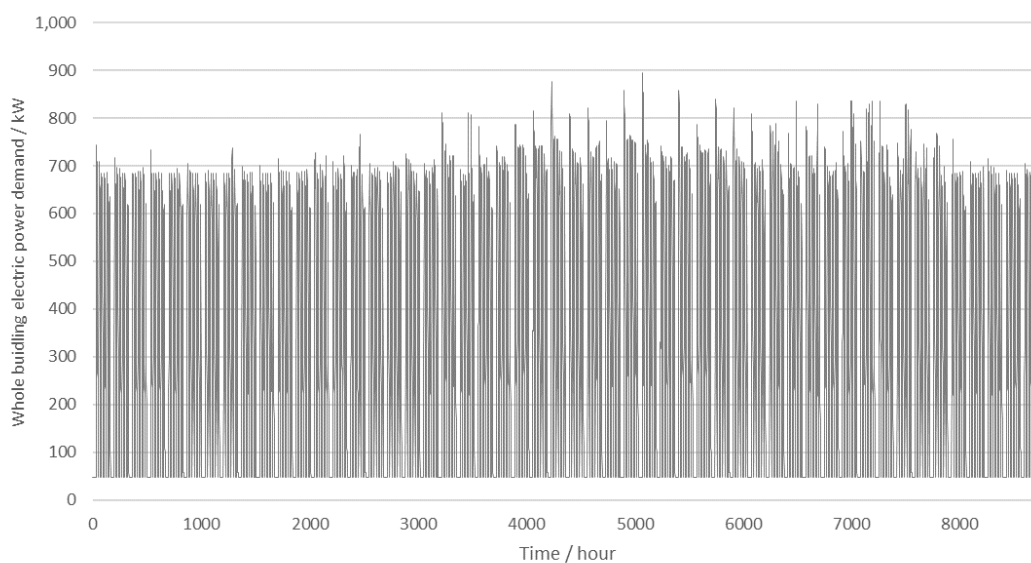


Figure 4-6 – Annual whole building electric power demand

Validation of building energy modelling can be carried out by various methods, including empirical data and peer models (Ryan and Sanquist, 2012a). In order to achieve full realistic validation, ideally one year of empirical data should be collected which covers one heating season, two intermediate seasons, and one cooling season. This makes full validation extremely time and resource intensive (Leal *et al.*, 2013). In addition, the lack of comprehensive data in Hong Kong has been a major barrier to verify the model (Yu *et al.*, 2015a). The building adopted to illustrate the methodology is a theoretical reference building, empirical data of hourly data is not available.

To overcome the above challenges, the model validation is carried out by calculating the energy utilization index (EUI). The simulation estimated that the annual building energy use was 2,902,000 kWh, which translates into an energy utilization index (EUI) as 120 kWh/m². This EUI is compared against the EUI of a typical Hong Kong office building as presented by Hong Kong government department (133 kWh/m²) (EMSD HK, 2020a), and a previous study (Chung and Hui, 2009) of Hong Kong office building (125 kWh/m²). The building energy model EUI is within 10% of peer values, the modelled annual energy consumption is therefore considered reasonable.

4.5.2 Daily building electric power demand profile

This section presents 4 daily building electric power demand profiles (Figure 4-7), specifically for a July weekday, December weekday, July weekend, and December weekend. These profiles are representative of the respective month by taking an average of the power demand on weekdays and weekends in that month accordingly. In comparing the July and December profiles, higher power demand was observed in July (summer), apparently because of the

increased demand for air-conditioning.

In addition to outdoor environmental conditions, it is evident that the profile is also dependent on the occupancy schedule. For weekdays, building systems started operation in the early morning before office hours commence, for instance, the HVAC system started running at 06:00 to pre-cool the office space. The demand gradually increased until 09:00 as the building reached 90% occupancy capacity, then remained relatively steady until noon. The demand dropped during lunch hours (12:00 – 14:00) due to the occupancy reduction from 90% to 50%. The demand again increased after lunch, then dropped while approaching the end of office hours (18:00). Since peak shaving depends on the hourly energy demand, additional validation was carried out on the hourly demand profile. It was observed that the hourly profile exhibited comparable form to previous study on Hong Kong's building air-conditioning energy consumption of various building types, including office building (Yik, Burnett and Prescott, 2001). Moreover, the peak hourly cooling load per floor area in July of this study's model (0.11 kWh/m²) is in range with the literature (0.12 kWh/m²). This provides further evidence that the hourly energy demand was reliable.

The weekend profiles differed from the weekdays mainly because occupants only stayed until 13:00 on the weekends, resulting in a significant drop in demand after 13:00. In addition, the assumed highest occupancy was 70% on weekends, hence the demand was lower compared to weekdays. The profile for Sundays was not included because the building was assumed to be unoccupied, and the demand was essentially the baseload with no peak.

Overall, it was observed that the power demand profile was primarily dependent on office hours, occupancy, and equipment operation, so that the profiles were different on weekdays and

weekends, and in different months. This implies that peak shaving strategies have to be tailored specifically according to the peaks and troughs of electricity demand profiles. While more energy was required in July compared to December, PV generation was also higher in July. Given that peak shaving relies on electricity generated by the PV system, the magnitude of peak shaving will vary in different months. As described in previous section, different strategy options were evaluated to reveal peak shaving taking place at different hours, and the results are presented and discussed in the next section.

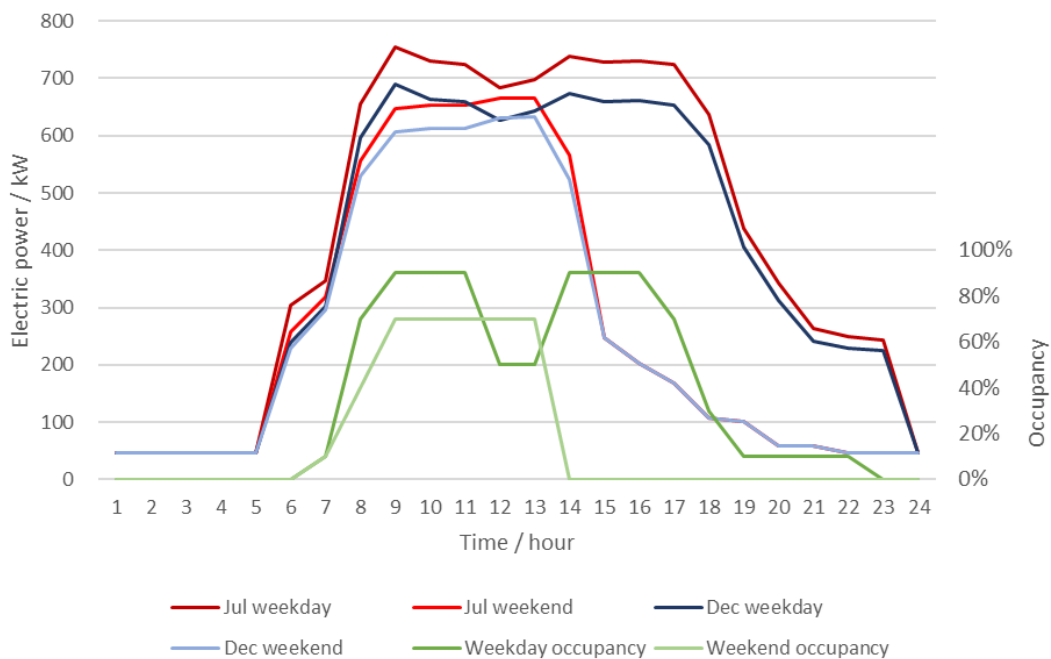


Figure 4-7 - Daily building electric power demand profile, with electric power as a primary axis (left) and occupancy as a secondary axis (right)

4.5.3 Annual solar energy output and hourly average electric power

The key results of the PV system simulation are the annual solar energy generation and the hourly average electric power profile by month. When 10% of the roof area is available for PV system installation, the system could generate 30 MWh annually. In turn, the PV system

contributes to 1% of the annual building energy use, assuming the solar energy generation is fully utilized.

Figure 4-8 shows the hourly electric power output of the PV system given a 10% roof area availability. Across the 12 months, the power output began at around 06:00 and ended at around 19:00. The peak output was generally reached in the afternoon (12:00-13:00). It was observed that the PV system generation takes place mainly during office hours, so that the shape of the output profile corresponded closely with the building demand. This offered an opportunity for the PV system to feed electricity to the building in a real-time manner. The advantage of such a real-time strategy is reduced reliance on battery storage, but this approach requires complex energy management to avoid voltage and power instability. As described previously, energy generated by the PV system is stored in a battery and is discharged evenly depending on the number of hours as determined by the peak shaving strategy.

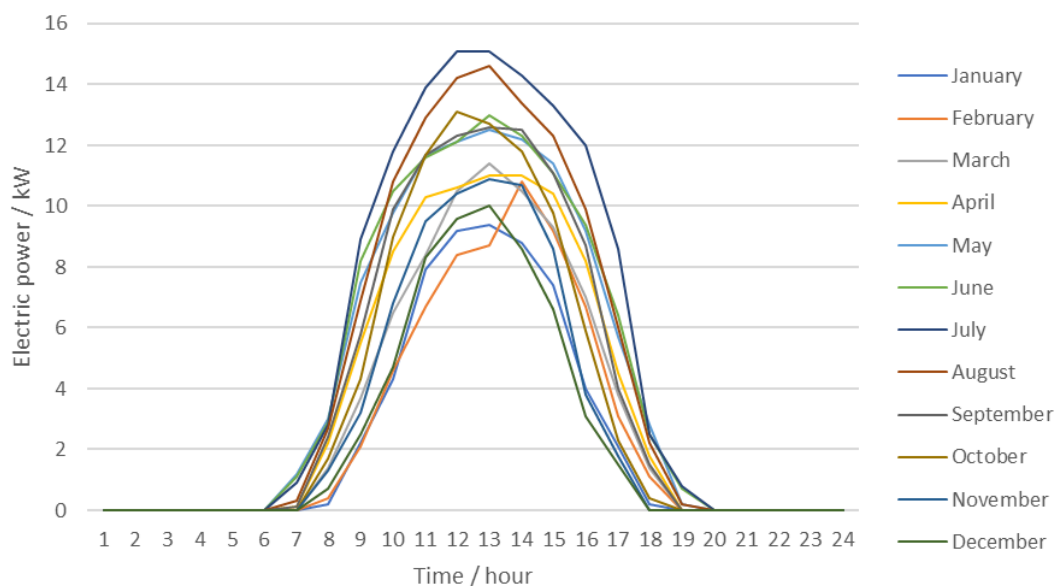


Figure 4-8 - Hourly electric power output by PV system (10% roof area) by month

July had the highest monthly energy output (3.7 MWh), in contrast, December had the lowest monthly output (1.7 MWh). These two months were focused on for the later peak shaving analysis to understand different seasonal cases.

4.5.4 Financial analysis

A financial analysis was carried out to estimate the payback period of the PV rooftop on this reference building. A previous study suggested that the construction cost of PV systems was in the range of 30,000 HKD to 50,000 HKD per kW (Dato, Durmaz and Pommeret, 2021). Based on this range, for 36 kWp PV system (10% roof availability), the construction cost was estimated to be between 1,080,000 HKD to 1,800,000 HKD. The construction cost increased to 3,240,000 HKD to 5,400,000 HKD as the capacity rose to 108 kWp (30% roof availability). As the capacity reached 180 kWp (50% roof availability), the construction cost was approximated to be 5,400,000 HKD to 9,000,000 HKD (Table 4-3).

Given the Feed-in Tariff scheme (FiT) in Hong Kong, the rate is 4 HKD per kWh for a renewable energy system with a capacity between 10k kW to 200 kW. This FiT capacity range was applicable to 10% to 50% roof availability. Based on the annual energy generation, the annual revenue from FiT would be 120,000 HKD, 360,000 HKD, and 600,000 HKD respectively. Referring to the construction cost and the annual revenue, it was estimated that the payback period would be 9 to 15 years. This is in range with the payback period suggested in the same study.

Table 4-3 – Construction cost and revenue estimation of PV rooftop

Roof area with PV	Capacity kWp	Construction cost / HKD	Annual generation / kWh	Revenue from FiT / HKD
10%	36	1,080,000 – 1,800,000	30,000	120,000
30%	108	3,240,000 – 5,400,000	90,000	360,000
50%	180	5,400,000 – 9,000,000	150,000	600,000

4.5.5 Carbon reduction and peak shaving analysis for weekdays

Figure 4-9 shows the weekday building power profile in July and December and the results of peak shaving strategies in accordance with different proportions of roof area available PV panel installation. Peak load reduction and avoided carbon emissions are investigated and critically discussed in this section.

Peak load reduction was evaluated by studying by studying the power demand profiles of the building under different conditions. Given 10% of roof area covered in PV installations, in July strategy 1 resulted in a 16% reduction at 9:00's peak. Strategies 2 and 3, representing morning peak shavings, achieved 8% and 5% average reduction at their corresponding peaks. Strategies 4 to 7, representing afternoon peak shavings, attained 16%, 8%, 5%, 4% average reduction at their respective peaks. Strategy 8 represented full day peak shaving, excluding lunch hours, and achieved a 2% average reduction at peaks. Strategies 1 and 4 demonstrated relatively significant peak reduction, while reductions achieved by the other strategies were comparatively mild. In December, since the PV system only generated limited energy, the peak

shavings for all strategies were relatively mild. For instance, strategy 7 achieved a 2% average peak reduction, while strategy 8 only achieved 1%.

The avoided carbon emissions by replacing grid electricity were also investigated. As mentioned in the peak shaving section, the marginal carbon emissions of grid electricity varies temporally. The reduced peaks by each strategy were mapped against those hours' emission factors, which had been calibrated to fit Hong Kong's grid electricity carbon emissions and then summed to calculate the total emissions avoided per day. The results are shown in Figure 4-10. Strategy 7 managed to avoid the highest amount of emissions (119 kg CO₂ per weekday in July, 54 kg CO₂ per weekday in December). Given the holistic consideration of both peak elimination and carbon emissions avoided, strategy 7 is recommended as the best peak shaving strategy when only 10% of rooftop area is available for PV installation.

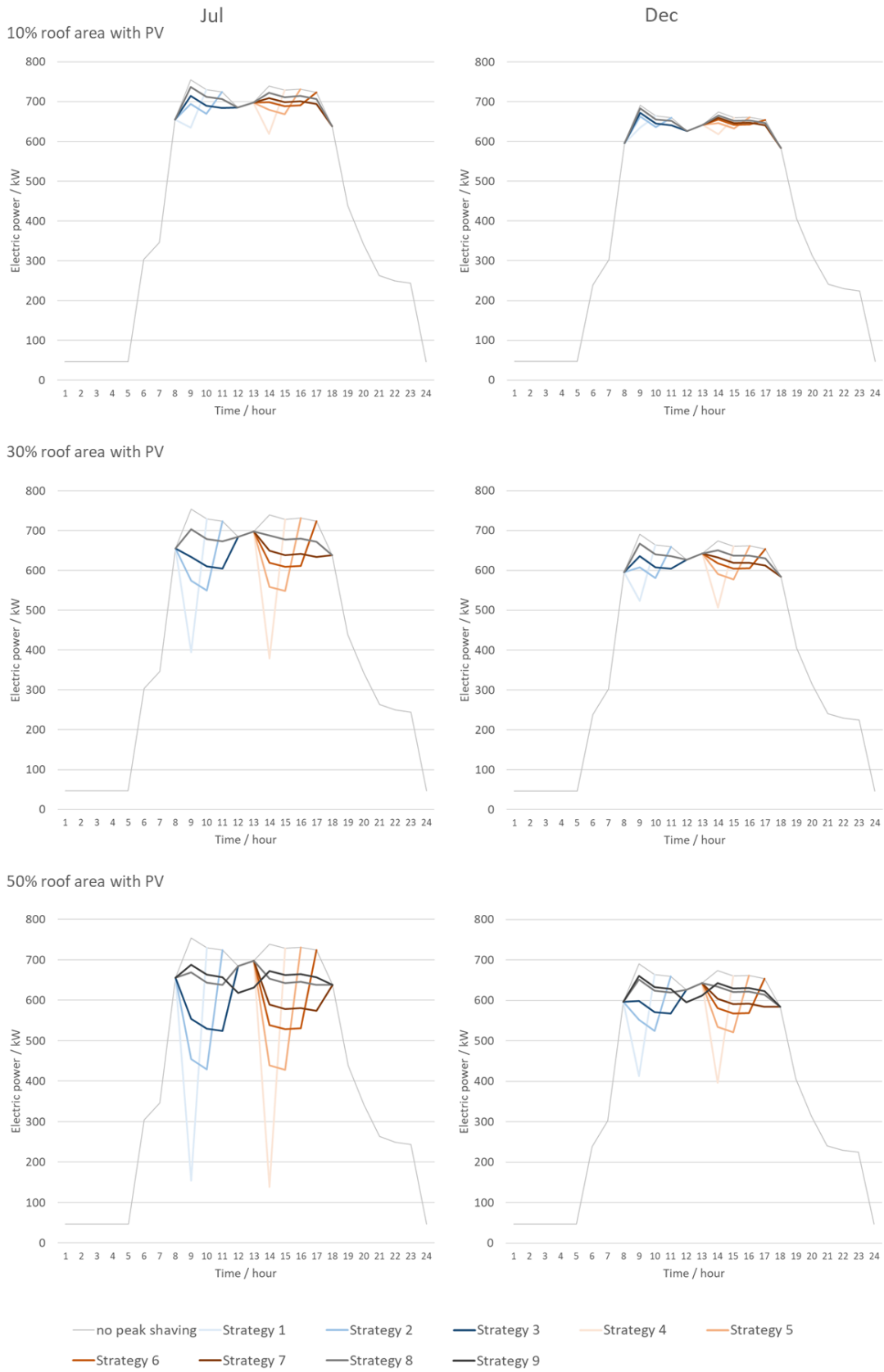


Figure 4-9 – Weekday building power demand profiles and peak loads reduction achieved by

different peak shaving strategies and PV panel rooftop area availability.

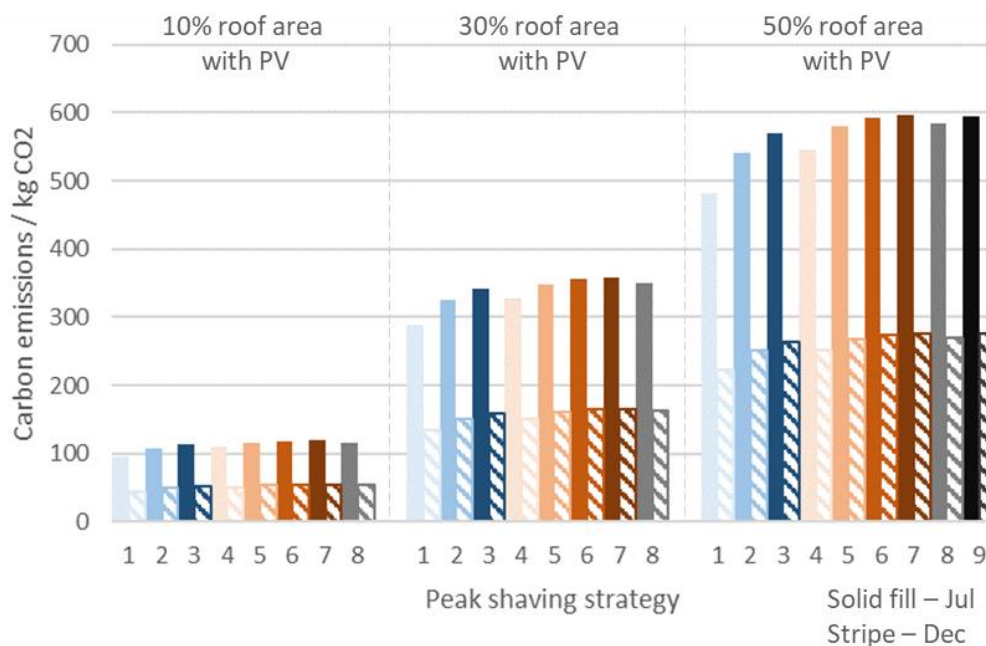


Figure 4-10 – Weekday avoided carbon emissions of different peak shaving strategies, and PV panel rooftop availability

When 30% of rooftop area was available for PV installation, strategies 1 to 3 attained 48%, 24%, and 16% average reductions in July, whereas strategies 4 to 7 achieved 49%, 25%, 16%, and 12% average reduction, at the corresponding peaks. Strategy 8 resulted in 7% reductions at its peaks. In December, the reductions were more significant when the roof area for PV installation increased from 10% to 30%. At their respective peaks, strategies 1 to 3 achieved 24 %, 12%, 8% average reductions, whereas strategies 4 to 7 achieved 25%, 13%, 8%, and 6% average reductions. Strategy 8 resulted in 4% average reductions at its peaks. Although strategy 7 could lead to the highest amount of avoided carbon emission, it was not the most favorable option. This was because the focused shaving in the afternoon could cause an imbalance in the building power supply system and the grid (Nwaigwe, Mutabilwa andDintwa, 2019). It was not desirable for the power supply system to cope with peak times in the morning, and

instantaneously reduce reliance on grid electricity and switch to PV generated electricity. In contrast, strategy 8 featured a rather smooth profile during office hours, so that the peaks before and after lunch became almost within range of the power demand during lunch hours. Moreover, for new buildings that are still undergoing design, strategy 8 could contribute to a power supply equipment sizing reduction because the demand profile is smoothed. Overall, strategy 8 is recommended to be the most appropriate peak shaving strategy, being able to yield carbon emissions reduction of 351 kg CO₂ per weekday in July and 163 kg CO₂ per weekday in December, only 2% less than strategy 7 during both months.

In the case of having 50% of the roof area equipped with PV panels, in July strategies 1 to 3 demonstrated 80%, 40%, and 27% average reductions, and strategies 4 to 7 resulted in 81%, 41%, 27%, and 21% average reductions, at the respective peaks. Attention should be especially paid to strategy 8, which encompassed full-day (excluding lunch hours) peak shaving, as it achieved 12% reductions at its peaks. Interestingly, with peak shaving occurring before and after lunch hours, the lunch hours themselves became spikes in the power demand profile. Hence strategy 9 was developed to further include lunch hours to eliminate the lunch hour spikes. It was estimated that strategy 9 could achieve a 9% average reduction for every hour between 09:00 to 18:00. In December, strategy 8 showed a 6% average reduction, whereas strategy 9 showed a 5% average reduction at their respective peaks. In comparing these two strategies, it was observed that strategy 8 resulted in a flatter profile during office hours, because unlike in July, lunch hours had not turned into spikes. As a result, a hybrid peak shaving strategy is proposed: In summer months when PV generation is high, strategy 9 is recommended (595 kg CO₂ per weekday in July), on the other hand during winter months, strategy 8 is recommended (271 kg CO₂ per weekday in December).

Following the above analysis, the peak shaving performance was compared with peer literature. A previous study reported a 60 kW PV installation served a small office building with an EUI of 160 kWh/m² in Poland. The reduction of peak load was reported to be on average 20% (Jurasz and Campana, 2019b). Another study was conducted on a 3-storey office building located in the Virginia/Maryland, U.S. area. A 104 kW PV system was installed on the building rooftop, allowing the peak demand was decreased by 17% by peak shaving (Sehar, Pipattanasomporn and Rahman, 2016). While the climatic conditions in these regions are different from Hong Kong, it is still reasonable to suggest that the above results show substantial potential for Hong Kong office buildings to deploy photovoltaic rooftops with different levels of roof availability.

4.5.6 Carbon reduction and peak shaving analysis for weekend

The peak shaving strategies during weekends were more straightforward compared to weekdays because the building only operated half-day (09:00 – 13:00). 5 strategies were developed to cover 1 hour to 5 hours of peak shaving (Figure 4-11).

When 10% of the rooftop's area was equipped with PV panels, strategies 1 to 5 reduced the corresponding peaks on average by 19%, 9%, 6%, 5%, and 4% in July. In December, the peak shaving implications were minimal given the limited PV generation. As the area of the PV system was increased to 30%, the reductions were more significant. In July, strategies 1 to 5 resulted in 56%, 28%, 18%, 14%, and 11% on average for their eliminated peaks, whereas in December, the average reductions of the 5 strategies were 27%, 14%, 9%, 7%, and 5%, respectively. Peak shaving was the most significant when 50% of the roof's area was available for PV installation. In July, strategies 1 to 5 reduced their targeted peaks by 93%, 46%, 31%, 23%, and 18% on average, respectively. In December, strategies 1 to 5 were still promising,

achieving average reductions of 46%, 23%, 15%, 11%, and 9%, respectively.

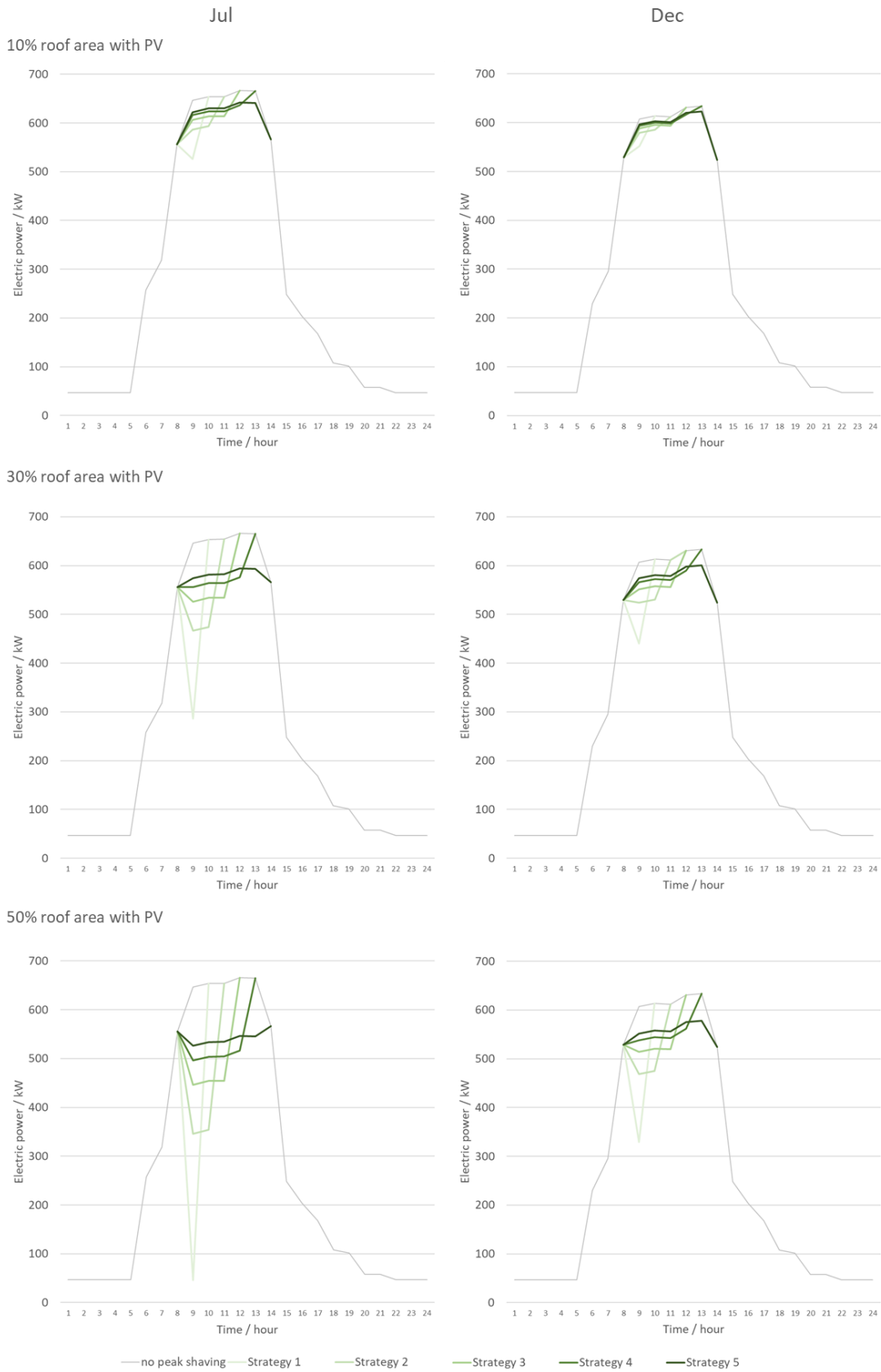


Figure 4-11 – Weekend building power demand profiles and peak load reductions achieved by

different peak shaving strategies and PV panel rooftop availability

For grid electricity substitution, it was calculated that strategy 3 would save the most amount of carbon emissions (Figure 4-12). However, the gap between reduced peaks and the remaining peaks was substantial. As previously discussed, such a gap was not desirable because of the imbalance caused between the building power supply system and the grid. By inclusively considering peak loads reduction and the avoided carbon emissions, strategy 5 is recommended. It was estimated that the PV system could reduce 98 kg CO₂, 293 kg CO₂, and 496 kg CO₂ emissions per weekend in July and 45 kg CO₂, 136 kg CO₂, and 230 kg CO₂ emissions per weekend in December, for 10%, 30%, and 50% of roof area equipped with PV panels, respectively.

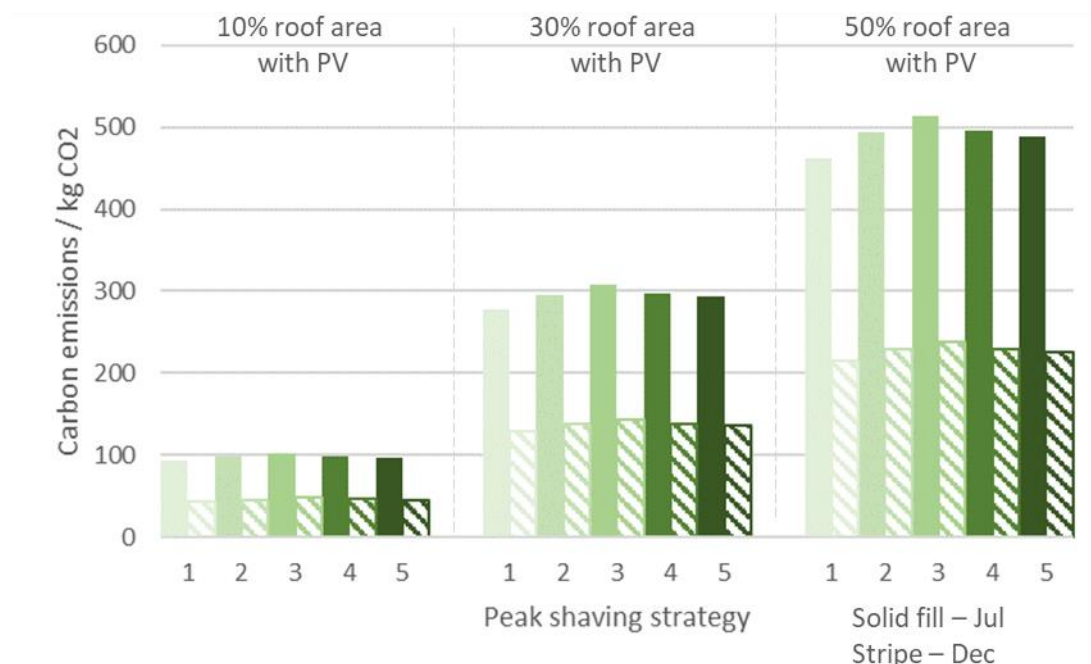


Figure 4-12 – Weekend avoided carbon emissions of different peak shaving strategies and PV panel rooftop availability

4.5.7 Limitations

4.5.7.1 Data resolution

This section discusses two major limitations encountered in this study. The first limitation is the data resolution. The energy modeling output was hourly data, which imposed a constraint on the frequency of applying peak shaving. The implications for estimating building power demand profiles and developing the following peak shaving strategies was, however, considered minimal because the power demand was mainly dependent on the building's occupancy schedule. On the other hand, improving the resolution could result in a more accurate estimation of avoided carbon emissions. It is supposed that grid electricity marginal emission is sensitive to grid operation, which responds to the city's demand in a real-time manner. By improving the data resolution, the environmental performance of each peak shaving strategy could be more precisely reflected. In addition, while the marginal emission performance factor in this study was based on a calibrated data set adopted from a previous study on Singapore's grid (Finenko and Cheah, 2016), building a marginal emission profile for the building location's grid is highly recommended. It is specifically recommended that the marginal emission factor be a yearly data set so that it could capture seasonal changes.

To understand the impact of the assumed temporal emission factor on the peak shaving carbon reduction, a sensitivity analysis is carried out based on the average grid emission factor of 0.7 kg CO₂/kWh without temporal calibration (Table 4-4). While the average emission factor is the same in magnitude across different hours, it should be noted that there should be no difference in carbon emissions reduction among the various hourly dependant peak shaving strategies, nor between weekdays and weekends. The percentage difference in carbon emissions reduction between considering temporal and average ranges from 15% - 41% for weekdays, and 10% - 22% for weekends. This is due to the marginal difference between temporal grid emission

factor and average grid emission factor.

Table 4-4 – Avoided carbon emissions (kg CO₂ per day) based on average carbon emission factor (0.7 kg CO₂/kWh)

Roof area with PV	July	December
10%	84 kg CO ₂ per day	39 kg CO ₂ per day
30%	252 kg CO ₂ per day	117 kg CO ₂ per day
50%	420 kg CO ₂ per day	195 kg CO ₂ per day

4.5.7.2 Energy management

The second limitation relates to the 9 peak shaving strategies for weekdays and 5 strategies for weekends investigated in this study. These strategies assumed the energy collected on the previous day was fed to the building evenly on an hourly basis. This assumption applies to basic on-site PV deployment and does not require a sophisticated energy management system. For more advanced energy management, the PV electricity could react to the building’s power demand in a more timely manner. Matching building power demand and PV generation could be better leveraged. As mentioned previously, advanced energy management would require more vigilant power and voltage stabilization, which would in turn help reduce reliance on battery storage. In addition, the PV panel maintenance, such as regular cleaning, is crucial to maintain optimum efficiency by minimizing soiling loss and operation efficiency loss to fulfil the design intent (Maghami *et al.*, 2016). Also relevant to second limitation, the third limitation is the system boundary of the analysis which is confined to be the photovoltaic roof, echoing with the core objectives. The interaction between the battery system and the PV system was not considered. The impacts on cost and carbon of the battery storage system was not measured as the impacts would differ significantly according to the choice of battery system (Das *et al.*,

2018b).

4.5.8 Policy recommendations

To further promote PV application in buildings, policies could be rolled out to improve PV readiness in both micro and macro environments. On a micro individual building scale, the potential of existing properties could be unleashed and technologies should be embraced in upcoming new building designs. On a macro city-wide urban planning level, policies should create a PV-friendly environment and create synergy among individual buildings to maximize carbon savings for the main grid.

In order to improve both micro and macro environments, three policy-making suggestions are made based on the findings, targeting existing buildings, new buildings, and urban planning. These policies can be applied altogether as they target different area for improvement. For existing buildings, in the results section it is shown that even if only 10% of a roof area is available for PV installation, a 10-story office building could still benefit from 1% yearly energy demand reduction. This creates opportunities for existing medium- to high-rise office buildings with limited available roof space to consider PV deployment. Although these existing buildings could be constrained by their unalterable roof layouts, engagement such as providing commercial incentives is still encouraged. In this era of rapid technological advancement, it is anticipated that the efficiency of PV panels will improve (Sinke, 2019) and yield higher energy savings. For new buildings, this study suggests considerable energy saving potential if roof space is readily available. Given that it is reasonable to extrapolate 5% yearly energy savings by having 50% of a roof area equipped with PV panels, policies that promote PV-ready roofs, such as providing guidance for rooftop layout planning and reserving sufficient space for PV installation, are highly recommended. Furthermore, innovations such as vertical PV installation

should be encouraged to enable higher renewable energy penetration on a building scale.

For urban planning, it is suggested to carefully design building height profiles in developing cities. While this study assumes moderate power loss (10%) due to shading by neighboring buildings, the loss could be reduced by mindfully designing a plain building height profile. If PV roofs are more widely adopted in urban planning, carbon emissions could be reduced on a city level scale.

4.6 Summary

A modelling framework to examine PV rooftops with varying roof availability for carbon reduction and peak shaving was proposed and computational simulations were carried out. As demonstration, the framework was applied on a 10-story reference office building and PV generation simulation based on Hong Kong's climate. Following validation by typical energy utilization index and daily profile in peer literature, the framework was shown to be systemic and reliable. This framework can be applied without geographical constraints given the suitable data and is an effective tool to encourage PV roofs, which promotes renewable energy more extensively and contributes to United Nations Sustainable Development Goal 7 "Affordable and Clean Energy".

To summarize the findings of the framework demonstration, as PV electricity generation increases with available roof area for installation, PV generation from 10%, 30%, and 50% of roof space was estimated. This mimicked the real world situations of having different amounts of available rooftop space for PV installation in buildings. It was shown that a rooftop PV system occupying 10% of the roof area could generate 1% of annual building energy demand. Supported by the Feed-in Tariff scheme in Hong Kong, the payback period was estimated to

be 9 to 15 years. The building power demand and PV generation were mapped on an hourly interval, and the building peak loads were identified as opportunities to perform peak shaving, such that grid electricity could be substituted with PV electricity. To capture seasonal changes, July and December were selected to represent summer and winter conditions, respectively. Since building power demand and PV generation vary hourly, 9 peak shaving strategy options were considered for covering a range of peaks and durations. Peak load reduction and carbon emission saving were evaluated for each peak shaving strategy option.

The results showed that the optimal peak shaving strategy was dependent on the PV system size, so the peak load reduction and carbon emission saving differed as the roof space availability changed. When 10% of the roof area was available for PV installation, afternoon peak shaving (14:00 – 18:00) on weekdays resulted in the most avoided carbon emissions (119 kg CO₂ per weekday in July, 54 kg CO₂ per weekday in December). When the system size was increased to 30% roof area, a full-office-hours strategy (09:00 – 12:00 & 14:00 – 18:00, excluding lunch hours) was proposed. Although other options could achieve higher load reduction percentages and more carbon emission saving, they may cause system imbalance within the building and with the grid, and therefore are not recommended. It was estimated that this strategy could yield a carbon emissions reduction of 351 kg CO₂ per weekday in July and 163 kg CO₂ per weekday in December. When the PV system covered 50% of the roof area, a hybrid peak shaving strategy displayed a superior performance. This is because the high PV generation in summer enables full-office-hours peak shaving to such an extent that lunch hours become peaks compared to other office hours. As a result, a peak shaving strategy (09:00 – 18:00) was proposed for summer that leads to an estimated carbon saving of 595 kg CO₂ per weekday; a peak shaving strategy (09:00 – 12:00 & 14:00 – 18:00, excluding lunch hours) was suggested for winter, resulting in a carbon saving of 271 kg CO₂ per weekday. For weekends,

since the building was assumed to operate half-day, peak shaving from 09:00 – 13:00 was proposed.

Drawing upon the findings, policy-making suggestions to improve PV-readiness in both micro (existing and new individual buildings) and macro (urban planning) environments were provided. On a micro building level, it was suggested that while it could be difficult for existing buildings to alter roof layout, commercial incentives should still be provided to unleash the potential of PV roof systems. For new buildings, guidance should be offered to designers for optimizing roof layouts and reserving sufficient space to achieve appreciable carbon savings in future operations. On a broader city level, mindful urban planning in building height regulations is required to create a PV-friendly environment. In particular, shading by neighboring buildings should be minimized to maintain PV generation performance.

Finally, three directions for future research are suggested. Firstly, the geographical coverage could be expanded to other urban dense cities, potentially providing a more comprehensive picture of the most effective strategies given different climate conditions and grid emissions. Secondly, future studies could assess the temporal marginal carbon emissions of location-specific grid operations, enabling more precise informed decision making. Thirdly, energy management algorithms could be applied to execute more real-time peak shaving strategies.

5. CHAPTER 5: PHOTOVOLTAIC ROOFTOP'S CONTRIBUTION TO IMPROVE BUILDING-LEVEL ENERGY RESILIENCE DURING COVID-19 WORK-FROM-HOME ARRANGEMENT

5.1 Introduction

The COVID-19 pandemic has opened opportunities for more research in resilient cities. With cities experiencing lock-down, city planners and designers are challenged by the ability to rapidly adapt to the more unpredictable future (Lai *et al.*, 2020). COVID-19 imposes disruption in energy access and distribution, and livelihoods globally. Since understanding energy demand is vital for efficient electricity grid planning and operation, it is a common lesson-learnt that work-from-home arrangement during the COVID-19 crisis has imposed severe challenges on grid operators to maintain reliable energy supply (Abdeen *et al.*, 2021; Jiang, Fan andKlemeš, 2021). Therefore, it is essential to understand the impact of work-from-home on residential flat's energy demand. It is envisaged the residential sector energy demand will increase as building occupants spend more time at home, leading to heavier use of household electrical equipment, including air-conditioning, lighting, and household electrical equipment. During the COVID-19 crisis in 2020, the Hong Kong Government announced special work-from-home arrangement four times, in January, March, July, and December respectively. In total, the work-from-home arrangement lasted for 124 working days in the year of 2020, and the normal working arrangement only accounted for 85 working days. Buildings are responsible for more than 90% of total electricity consumption in Hong Kong. In particular, residential buildings are the major source, accountable for one third of the total consumption (Du, Yu andPan, 2020). This implies that residential buildings could have notable impact on the city-scale energy demand. Moving forward, it is even predicted that work-from-home can become a common practice in Hong Kong as the labour force has generally adopted to the arrangement (Vyas andButakhieo, 2021). It is inevitable that energy consumption in residential buildings during

work-from-home arrangement is different compared to normal work arrangement.

High-rise public residential buildings were specifically targeted for energy modeling in this study as they accommodated about half of the Hong Kong population. Land acquisition in Hong Kong has been physically limited by its hilly geography. Shortage of land supply has been a legacy challenge to provide sufficient housing in this highly populated city. To overcome this challenge, the development of high-rise public housing was proposed in the 1980s as a solution to improve land-use efficiency and increase affordable housing supply (Deng, Chan and Poon, 2016). Over the past half-decade, Hong Kong experienced a dramatic increase in housing demand, leading to an immense production of residential buildings (Jaillon and Poon, 2009). Nowadays public housing accommodates about half of the population in Hong Kong, serving over 1.3 million domestic units (Hui and Wong, 2004). Various domestic block designs of public residential buildings were rolled out in the 1990s. One of the leading designs was known as the “Concord” series. Concord-series building can comprise up to 40 storeys with 8 flats per floor, providing 320 flats per block (Chan and Chan, 2011). As it was envisaged that there would be an increase in energy demand when occupants spent more time at home, it would be desirable to consider additional energy supply for the sake of resilience. While currently it has not yet been a common practice to equip on-site rooftop photovoltaic system on public residential buildings, this study also aims to assess the possibility of leverage photovoltaic system as a solution to supplement the increased energy demand. The potential contribution of the photovoltaic system is evaluated in terms of the capability to utilize its generation output to supplement the additional energy demand.

5.2 Literature Review

5.2.1 Energy resilience during the COVID-19 crisis

COVID-19 imposes disruption in energy access and distribution, and livelihoods globally. It is reported that in some developing countries, COVID-19 even caused energy poverty to an extent that 220 billion US dollars were lost (Zaman, van Vliet and Posch, 2021). Besides, in developed countries, there has been a thorough change in work practices from attending offices to work-from-home. For example, a survey suggested almost all employees had changed to work-from-home during lock-down in the UK (Chung *et al.*, 2020). This has caused a redistribution among electricity consumer groups, essentially from commercial to residential due to work-from-home arrangement. In addition, electricity consumption profile on grid level has changed as peak demands and their corresponding instants shifted according to work-from-home occupant behaviors (Bielecki *et al.*, 2021).

Despite work-from-home has become a trending office practice, its implication on social building energy use is still under-researched in the past few years (Hampton, 2017). The influence of work-from-home on energy use has attracted further attention during the COVID-19 pandemic period (Cheshmehzangi, 2020). In the US, it was reported the energy consumption of residential sector increased by 30% during lock down, but the overall electricity demand was lower due to the reduced demand in commercial and manufacturing sectors (Krarti and Aldubyan, 2021). In South Korea, the total energy consumption in most facilities decreased compared to pre-COVID-19 year. In contrast, energy consumption in residential buildings increased during COVID-19 (Kang *et al.*, 2021). The electricity consumption in Spain faced an overall decline of 13%, but some households used 6% more energy compared to pre-lock-down period (Santiago *et al.*, 2021). Overall, it is evident that electricity demand has become more unpredictable compared to normal social situation prior to the COVID-19 pandemic and

has caused technical challenges to the power sector globally (Madurai Elavarasan *et al.*, 2020a).

5.2.2 Solar energy's contribution to energy resilience

Literatures are plentifully available to substantiate that solar energy, as an alternative to fossil fuel, has contributed to enhanced energy efficiency (Li *et al.*, 2020; Al-Shahri *et al.*, 2021). On the other hand, solar energy is closely associated with energy security and resilience. Energy resilience covers a wide range of factors, including reliability, economy, environment (Adefarati and Bansal, 2019b). Communities around the globe have been facing different level of energy security issue. The growing population has led to the pressing to the limit of the planet's carrying capacity with a finite amount of resources. However, energy resilience remains an unpopular topic on the municipal level (Mola, Feofilovs and Romagnoli, 2018).

On-site decentralized renewable energy generation is believed to be advantageous to a city's energy resilience as reliance on external factors such as unreliability in outer supply are reduced (Gómez-Navarro *et al.*, 2021). With the aid of optimal weather conditions, for instance solar irradiance, photovoltaic renewable energy system is capable of delivering reliable performance by maintaining steady output (Acuña, Padilla and Mercado, 2017). The solar energy generation can be further supported by battery energy storage system to supplement electricity supply during severe events (Galvan, Mandal and Sang, 2020). In particular, solar rooftop has a crucial role to play in promoting general adoption of photovoltaic system on a community scale. Various studies are carried out to assess rooftop solar energy potential (Abdullah *et al.*, 2019; Nelson and Grubestic, 2020) to better understand the possibility to produce solar energy in existing infrastructure. In addition, energy management algorithms have been developed to improve energy resilience by controlling roof solar panel output (Prince *et al.*, 2019).

5.2.3 Solar energy application in Hong Kong

Owing to Hong Kong's Climate Action Plan 2030+ and 2050 carbon neutral ambition, the government and the building industry are spending huge efforts in examining technologies in energy efficiency enhancement and building decarbonization (HKSAR Government, 2020). In general, building decarbonization can be achieved via passive design, energy efficient system, on-site renewable energy and user behavioral changes (Qin and Pan, 2020).

The solar potential in Hong Kong is significant. It is estimated that Hong Kong could offer 54 km² suitable rooftop area for potential solar system, making up to 5.97 GWp capacity and capable of potentially producing 5,981 GWh annually (Peng and Lu, 2013). Solar renewable energy is mostly popular in low rise buildings as the energy performance is more promising given the lower energy requirement (Morakinyo *et al.*, 2019). Although building-integrated photovoltaic has earned interest recently, rooftop solar remains to be the mainstream deployment. Despite building-integrated photovoltaic offers additional surface area for energy generation, this technology has not been widely adopted due to its technological limitation and uncertain economic return (Baljit, Chan and Sopian, 2016b). For example, shading on the building façade could significantly hinder the efficiency of building-integrated photovoltaic (Zomer *et al.*, 2020).

The government also offers financial incentives via feed-in tariff scheme. The scheme's objective is to enable renewable energy system owners to recover the installation costs. The feed-in tariff rates are \$5 for ≤ 10 kW; \$4 for > 10 kW to ≤ 200 kW; and \$3 for > 200 kW to ≤ 1 MW (HKSAR Government, 2017). The effectiveness of the feed-in-tariff is widely discussed in terms of its effectiveness in fostering photovoltaic development in Hong Kong (Dato, Durmaz and Pommeret, 2021). Overall, the rate of photovoltaic deployment in Hong Kong is expected

to increase owing to its high solar potential (Wong *et al.*, 2016).

5.3 Objective and significance

The study focuses on the context of high-rise public residential buildings with respect to the fact that public residential buildings accommodate about half of the Hong Kong population. This study has two major objectives. Firstly, building energy modelling is conducted to quantify the increased residential energy demand, followed by validation by comparing with peer models and empirical data. Secondly, while currently it is not a common practice to install photovoltaic system on public residential building rooftops, this study aims to testify the possibility to deploy solar rooftop in these buildings. The potential contribution of the photovoltaic system is estimated by solar energy simulation, and evaluated in terms of the capability to utilize its generation output to supplement the additional energy demand. The findings of this study are believed to be significant in understanding the impact of work-from-home arrangement on residential energy consumption. The contributions are prolonged as work-from-home arrangement is expected to become more common in the long term as the general work force has adopted to this practice during the pandemic. This study's outcomes are valuable to safeguard energy resilience in upcoming grid planning and operation.

5.4 Methodology

5.4.1 Whole building energy modelling

5.4.1.1 Overview of whole building energy modelling

Building energy consumption analysis is a complex task as it considers interactions between the building physical features, HVAC systems, and dynamic outdoor conditions, such as weather. The interactions are modelled using mathematical algorithm and physical principles based on the user's input data (Fumo, Mago and Luck, 2010). The major objective of building

energy simulation is to assist decision-making in building designs, assessing energy consumptions in alternative scenarios, such as different architectural features, HVAC system specifications and occupancy (Zhu *et al.*, 2013; Gao, Koch and Wu, 2019). EnergyPlus is building energy simulation programme developed by the US Department of Energy. EnergyPlus is capable of estimating a building's energy use based on user-configurable modular systems, supported by a heat and mass balance-based zone simulation (Crawley *et al.*, 2001). A complete energy modelling requires the outdoor weather condition, building geometry, construction materials properties, household electrical equipment specifications, and the building's operation schedule.

5.4.1.2 Outdoor weather condition

Outdoor weather condition is a crucial input in building energy modelling as it facilitates the dynamic thermal analysis of the building HVAC system. A typical weather year in Hong Kong was developed as a precise representation of the periodic change in the local weather conditions, based on statistical analysis of 25 years of weather data in Hong Kong (Chan *et al.*, 2006b). The weather file was converted into an open-source EnergyPlus weather format for the building simulation community, including major weather indices covering dry bulb temperature, dew point temperature, wind speed and solar radiation.

5.4.1.3 Building geometry

Standard typical floor plans of public housing buildings are available on the official Hong Kong Housing Authority website (Hong Kong Housing Authority and Housing Department, 2019). One of the leading typical public housing layouts is named as "concord". The building geometry includes a core structure, and four wings extended in 4 directions. Located on these wings are the residential units. Each floor comprises of 8 residential units, each unit including

a master bedroom, 2 bedrooms, 2 toilets, a kitchen, and a living room. The unit floor area is about 60 m², and the entire floor size is about 650 m². The core structure is mainly the common area, consisting of the lobby and building services functions such as lift shaft and ducts. The energy consumption in the common area not considered in this study as it was believed that the energy consumption in common area would not be affected by work-from-home arrangement.

These public housing residential buildings come in high-rise form and usually comprises of 40 storeys (Ting Kwok, Ka-Lun Lau and Yan Yung Ng, 2018; Du, Yu and Pan, 2020). According to previous studies, the building orientation of concord-type public residential buildings in Hong Kong would not significantly influence the building energy consumption due to its self-shading building form (Yu *et al.*, 2020). Therefore, this study adopted a general building orientation for the sake of minimal complication. Design Builder was used to construct the geometry to further facilitate the energy modelling (Figure 5-1).

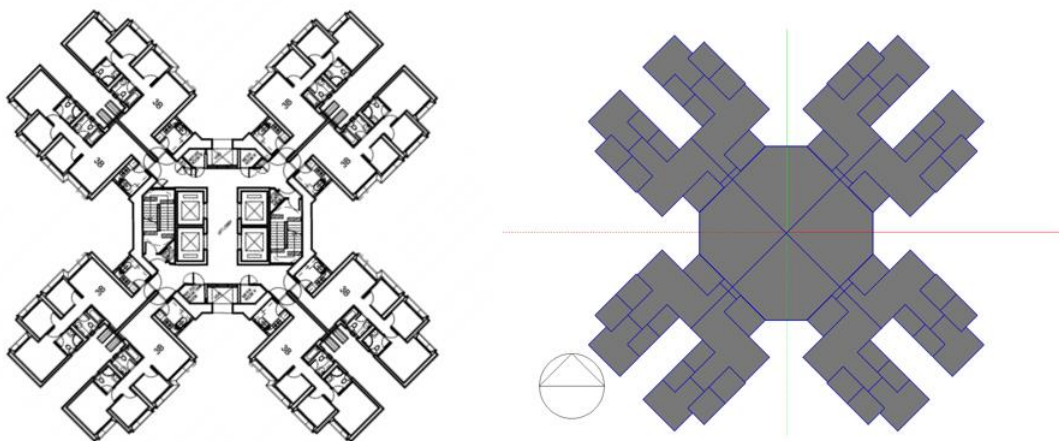


Figure 5-1 – Standard typical floor plans of concord-type public residential building provided by the Hong Kong Housing Authority (left), and the geometry built in Design Builder to facilitate the whole building energy simulation (right)

5.4.1.4 Construction materials properties

Construction material selection of the building envelope is closely associated with building energy use subject to its insulation performance. Suitable envelope material can reduce thermal loss and temperature variation during the day, and hence reduce internal cooling demand (Jeanjean, Olives and Py, 2013). Typical building material properties were made referenced from the Building Environmental Assessment Method (BEAM Plus) (HKGBC, 2010), which is a green building certification scheme administrated by the Hong Kong Green Building Council and the BEAM Society, covering a wide range of building sustainability aspects, including site, energy, water, waste and materials, and indoor environmental quality (Wong and Kuan, 2014). The physical properties of construction materials are summarized in Table 5-1 – Table 5-3. Symbolic abbreviations are used as follow: Thermal conductivity (k), density (ρ), specific heat (C_p), and solar absorptivity of exposed surface (α). The window-to-wall ratio is assumed to be 0.4 (Ting Kwok, Ka-Lun Lau and Yan Yung Ng, 2018).

Table 5-1 – Physical properties of building envelope construction materials (HKGBC, 2010)

External walls	Thickness / m	Material	k / W/mK	ρ / kg/m³	C_p / J/kgK	α
Layer 1	0.005	Mosaic tiles	1.5	2,500	840	0.58
Layer 2	0.01	Cement / Sand plastering	0.72	1,860	840	-
Layer 3	0.1	Heavy concrete	2.16	2,400	840	-
Layer 4	0.01	Gypsum plastering	0.38	1,120	840	0.65

Table 5-2 – Physical properties of roof construction materials (HKGBC, 2010)

External walls	Thickness / m	Material	k / W/mK	ρ / kg/m³	Cp / J/kgK	α
Layer 1	0.025	Concrete tiles	1.1	2,100	920	0.65
Layer 2	0.02	Asphalt	1.15	2,350	1,200	-
Layer 3	0.05	Cement / Sand screed	0.72	1,860	840	-
Layer 4	0.05	Expanded polystyrene	0.034	25	1,380	-
Layer 5	0.15	Heavy concrete	2.16	2,400	840	-
Layer 6	0.01	Gypsum plaster	0.38	1,120	840	0.65

Table 5-3 – Physical properties of window glazing material (HKGBC, 2010)

External walls	Thickness / m	Material	k / W/mK	ρ / kg/m³	Cp / J/kgK	α
Layer 1	0.006	Tinted glass	1.05	2,500	840	0.65

5.4.1.5 Energy consumption sources

Examples of the major energy consumption sources in residential buildings include air-conditioning, lighting, and household electric equipment (Wan and Yik, 2004; Jia and Lee, 2016). Hong Kong's public residential buildings are ventilated both naturally and by air-conditioning. Local exhaust by windows and mechanical extract are provided for specific rooms, such as kitchens and bathrooms, to remove pollutants. In regularly occupied spaces, windows and air-conditioning (window units or split-units) are typically used as general practice (Burnett, 2004). According to the floor plan, it was believed that each residential unit

in the modelled building could house 4 people, with the master bedroom accommodating 2 people, and each bedroom accommodating 1 person. Riding on technology development and improving coefficient of performance (COP) of air-conditioners in newer models (Jia and Lee, 2016), this study's model assumed a Hong Kong Energy Label Grade 1 air-conditioner with COP 3.4 to be used in the living room, master bedroom and bedroom. The air-conditioner was also set to operate only from April to October, while the rooms were ventilated naturally in the remaining months.

Other than air-conditioning, the remaining major energy consumption sources, including lighting and household electric equipment, were modelled. The lighting power density was supposed to be 8 W/m², referencing the dormitory design criteria as stipulated in the Hong Kong Code of Practice for Energy Efficiency of Building Services Installation (EMSD HK, 2018). Furthermore, the equipment load was referred from BEAM Plus guidebook. The equipment load was thought to be 142 W per living room, and 45 W per master bedroom and bedroom (HKGBC, 2010). These model input parameters are summarized in Table 5-4.

Table 5-4 – Modelling input parameters: Occupancy, lighting power density and equipment load of regularly occupied spaces

Space	Maximum occupancy / No. of people	Lighting power density / W/m²	Equipment load / W per room
Living room	4	8	142
Master bedroom	2	8	45
Bedroom	1	8	45

In addition to regularly occupied spaces, lighting was also provided in non-regularly spaces (13 W/m² in kitchen, and 11 W/m² in toilet). The equipment load, mainly made up of refrigerator and wash machine, was assumed to be 3,100 W in kitchen referring to estimated typical electrical appliances input power (HK Electric, 2015). 20 air-change per hour (ACH) was assumed to remove pollutants in these spaces. These model input parameters are summarized in Table 5-5.

Table 5-5 – Modelling input parameters: Lighting power density and equipment load of non-regularly occupied spaces

Space	Lighting power density / W/m²	Equipment load / W per room	Ventilation / ACH
Kitchen	13	3,100	20
Toilet	11	-	20

5.4.1.6 Normal routine and work-from-home occupancy and operation schedules

To facilitate energy modelling in the building design industry, BEAM Plus stipulates a set of universal occupancy schedule and building operation schedule, including air-conditioning, lighting, and household equipment (HKGBC, 2010). These schedules are considered to reflect the building occupants' normal routine and behavior. By coupling the energy consumption sources and their operation schedule, a model was built to represent building energy consumption under normal social circumstances and served as a baseline for further comparison.

In the year of 2020, Hong Kong Government announced special work arrangement 4 times to combat local epidemic situation by reducing the flow of people and social contact. Special work arrangements required government employees to work from home, and private institutions were recommended to follow suit. These announcements were made in January, March, May, and December respectively (Table 5-6). When condition permitted, the Government resumed normal work arrangement. Overall, the work-from-home arrangement accounted for 124 working days, and the normal working arrangement only accounted for 85 working days. Under the influence of the local epidemic, the general public were asked to stay at home, it was envisaged that the energy consumption of residential buildings was severely altered.

Table 5-6 – Time records of government special work arrangement announcement

Date	Government announcement
29 January 2020	Commence special work arrangement
2 March 2020	Resume normal work arrangement
23 March 2020	Commence special work arrangement
4 May 2020	Resume normal work arrangement
20 Jul 2020	Commence special work arrangement
24 Aug 2020	Resume normal work arrangement
2 December 2020	Commence special work arrangement
6 January 2021	Resume normal work arrangement

In order to compute the difference in building energy consumption between normal social circumstances and work-from-home arrangement, an alternative energy model was additionally developed. Despite universal schedules are provided in general guidelines, human

reactions in real world situation may be overlooked in these pre-determined schedules inputted in the simulation (Du and Pan, 2021). Since occupancy is directly correlated to building energy use, it is essential to calibrate traditional modelling assumptions to reflect the non-typical occupant routine under work-from-home arrangement. Occupancy schedules and building operation schedules were modified from normal work arrangement to work-from-home arrangement, including the below adjustments:

- Occupants stayed in their bedrooms to perform office duties during working hours.
- Air-conditioning was turned on when occupants stayed in the bedrooms during working hours.
- Lightings in the bedrooms were kept at a 50% capacity in the morning and were fully turned on in the afternoon.
- Electrical equipment load in the bedrooms was at 100% during working hours.
- Occupants spent more time in the living room during lunch and after working hours.
- Lightings in the living room were kept at 100% capacity after working hours and before bedtime.
- Electrical equipment load in the living room was slightly higher than normal work arrangement.

The occupancy schedules and building operation schedules, under both normal work arrangement and work-from-home arrangement, are shown in Table 5-7 and Table 5-8.

Table 5-7 – Occupancy schedules and operation schedules of master bedroom and bedroom

Hour	Occupant		Air Conditioning		Lighting		Equipment	
	(Fraction)				(Fraction)		(Fraction)	
	Normal	WFH	Normal	WFH	Normal	WFH	Normal	WFH
0	1	1	On	On	0.3	0.3	0.8	0.8
1	1	1	On	On	0	0	0	0
2	1	1	On	On	0	0	0	0
3	1	1	On	On	0	0	0	0
4	1	1	On	On	0	0	0	0
5	1	1	On	On	0	0	0	0
6	1	1	On	On	0.5	0.5	0	0
7	0.25	1	Off	On	0.2	0.2	0	0
8	0	1	Off	On	0.3	0.5	0	1
9	0	1	Off	On	0	0.5	0	1
10	0	1	Off	On	0	0.5	0	1
11	0	0.5	Off	On	0	0.5	0	1
12	0	0.5	Off	On	0	0.5	0	1
13	0.25	1	On	On	1	1	0	1
14	0.25	1	On	On	1	1	0.3	1
15	0.25	1	On	On	1	1	0.3	1
16	0.25	1	On	On	1	1	0.3	1
17	0.25	1	On	On	0	1	0.3	1
18	0.25	0.25	On	On	1	1	0.3	0.5
19	0.25	0.25	On	On	1	1	0.8	0.8
20	0.5	0.5	On	On	1	1	0.8	0.8

Hour	Occupant (Fraction)		Air Conditioning		Lighting (Fraction)		Equipment (Fraction)	
	Normal	WFH	Normal	WFH	Normal	WFH	Normal	WFH
21	0.5	0.5	On	On	1	1	0.8	0.8
22	0.5	0.5	On	On	1	1	0.8	1
23	1	1	On	On	0.6	0.6	1	1

Table 5-8 – Occupancy schedules and operation schedules of living rooms

Hour	Occupant (Fraction)		Air Conditioning		Lighting (Fraction)		Equipment (Fraction)	
	Normal	WFH	Normal	WFH	Normal	WFH	Normal	WFH
0	0	0	Off	Off	0	0	0.2	0.2
1	0	0	Off	Off	0	0	0.2	0.2
2	0	0	Off	Off	0	0	0.2	0.2
3	0	0	Off	Off	0	0	0.2	0.2
4	0	0	Off	Off	0	0	0.2	0.2
5	0	0	Off	Off	0	0	0.2	0.2
6	0	0	Off	Off	0.3	0.3	0.4	0.4
7	0.25	0.25	Off	Off	0.5	0.5	0.5	0.6
8	0.5	0.5	Off	Off	0	0	0.5	0.6
9	0.5	0.5	Off	Off	0	0	0.5	0.6
10	0.5	0.5	Off	Off	0	0	0.5	0.6
11	0.5	0.75	Off	Off	0	0	0.5	0.6
12	0.45	0.75	Off	Off	0	0	0.5	0.6
13	0.5	0.5	On	On	0.5	0.5	0.6	0.7

Hour	Occupant (Fraction)		Air Conditioning		Lighting (Fraction)		Equipment (Fraction)	
	Normal	WFH	Normal	WFH	Normal	WFH	Normal	WFH
14	0.5	0.5	On	On	0	0	0.4	0.5
15	0.5	0.5	On	On	0	0	0.4	0.5
16	0.5	0.5	On	On	0	0	0.4	0.5
17	0.5	0.5	On	On	0	0	0.4	0.5
18	0.5	1	On	On	0.5	1	0.4	0.5
19	0.75	1	On	On	1	1	1	1
20	1	1	On	On	1	1	1	1
21	1	1	On	On	1	1	1	1
22	1	1	Off	Off	1	1	1	1
23	0	0	Off	Off	0.5	0.5	1	1

5.4.2 Photovoltaic (PV) energy generation simulation

Currently it is not a usual practice to install rooftop solar panel on public residential buildings in Hong Kong. Therefore, a photovoltaic simulation was carried out to simulate the annual energy yield of a hypothetical rooftop energy system, and subsequently assess the opportunity for generating on-site solar electricity to supplement the increased energy demand during the work-from-home period. The modeled residential building rooftop had an area of 650 m². It was understood that not 100% of this 650 m² rooftop area would be suitable for photovoltaic installation. To estimate the suitable rooftop area for photovoltaic installation, an architectural suitability factor of 0.7 and a solar suitability factor of 0.55 were applied to the building's rooftop area with reference to a previous solar potential analysis (Peng and Lu, 2013). As a result, 250 m² roof area was approximated to be suitable for photovoltaic, equivalent to a 38.5

kWp system made up of 250W polycrystalline photovoltaic panels, with 16% efficiency. The panels were set to be south facing, with 22° tilt as optimum condition (Jacobson andJadhav, 2018). The photovoltaic simulation was carried out by deploying PVsyst, an effective simulation program used by engineers and researchers to conduct solar energy performance analysis during design (Irwan *et al.*, 2015; Manikandan, Varun andManikandan, 2020). PVsyst was capable to output a profile of monthly solar energy generation, which could be used to compare with the building energy demand during the work-from-home period. The shading effect in dense built environment in Hong Kong, which could cause around 10% photovoltaic generation loss (Peng *et al.*, 2013b), was taken into account in the simulation.

5.5 Results and Discussion

5.5.1 Building energy modelling

5.5.1.1 Building energy consumption under normal work arrangement

The energy model resulted in an annual profile of hourly electricity demand of all residential units. The model suggested the total yearly energy use to be 1,740,000 kWh, made up by air conditioning and ventilation, lighting, and household electrical equipment. The minimum base load was 10 kW in non-air-conditioned months (January – March, and November – December), and increased to 31 kW in air-conditioned months (April to October). On the other hand, the maximum peak load was 200 kW in non-air-conditioned months, and rose to 1,200 kW in air-conditioned months. These variations across the 8,760 hours within a year are shown in Figure 5-2. The major energy consumption sources were modeled, contributed by air-conditioning and ventilation (60%), lighting (20%), and household electrical equipment (20%) (Figure 5-3).

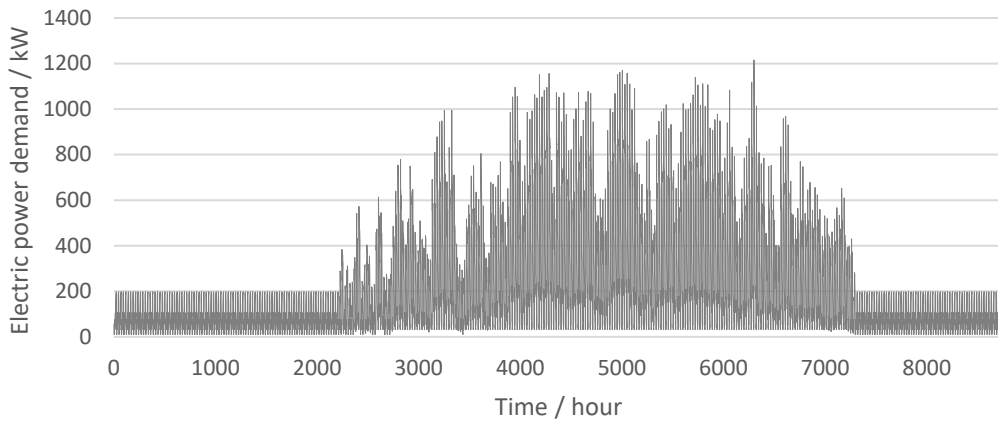


Figure 5-2 – Total electric power demand of all residential flats, results from building energy model

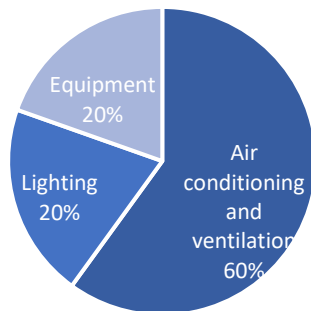


Figure 5-3 – Pie chart showing major energy consumption sources and their respective percentage contribution

5.5.1.2 Validation modelling results under normal work arrangement

It is critical to validate building energy model results to ensure accurate reflection of reality. Validation of computation model can be carried out by comparing the modelling results with empirical data and peer models (Ryan and Sanquist, 2012b). To overcome this difficulty, empirical data in relevant literature and public information are collected to provide evidence to

validate the model. Firstly, according to the Energy Saving Plan For Hong Kong's Built Environment 2015~2025+ (Environment Bureau, 2015), the average household electricity consumption in Hong Kong is about 400 kWh per month. The high-rise residential building simulated in this study consisted of 320 residential units, each residential unit was modeled to consume 450 kWh per month, which is in range with the suggested empirical result. Secondly, a previous study (Wan and Yik, 2004) conducted surveys about actual household energy use, and suggested that residential flats equipped with air-conditioners had an energy intensity of 100 kWh/m². Referring to this study's modelling result, an energy intensity of 91 kWh/m² was estimated, which is also believed to be in range with the suggested surveyed result. Overall, by comparing the energy model results with empirical results provided by literature, it is thought that the model reflecting normal work arrangement provides reliable energy consumption data for further analysis.

5.5.1.3 Building energy consumption under work-from-home arrangement

As mentioned in occupancy and operating schedule section, the occupancy and operation schedules under work-from-home arrangement were adjusted to reflect the difference from normal work arrangement. According to the energy modelling results, the energy consumption during work-from-home arrangement of air conditioning increased by 7%, lighting by 7%, and electrical equipment by 16%. The total consumption was 1,890,000 kWh, the energy intensity was 98 kWh/m², and the energy use per residential unit was 490 kWh/month. The total consumption under work-from-home arrangement increased by 9% as compared to the normal arrangement.

5.5.1.4 Validation of modelling results under work-from-home arrangement

To verify the credibility of the modelling results, actual electricity consumption data was

referenced. Referring to the Hong Kong electricity provider's annual report (CLP Holdings, 2020), the year-on-year change in electricity sales in the residential sector was 9%, comparing 2020 (COVID-19 impact year) and 2019 (pre-COVID-19 year). This figure echoes with the percentage difference in modelling results between normal and work-from-home arrangements, hence it is believed that the occupancy and operation schedules were calibrated appropriately, and the modelling results are close to reality.

5.5.2 Rooftop photovoltaic (PV) system's contribution to increased energy demand

5.5.2.1 Photovoltaic system generation modelling results

A simulation was conducted to estimate the hourly generation of a 38.5 kWp, 250 m² rooftop photovoltaic system. The generation data are summarized in Table 5-9. Generally, the output was mainly during daytime between the 7th to the 18th hour. Across months, the generation was higher in the summer when solar irradiance was more abundant. July had the highest monthly generation of 3,865 kWh and a daily average of 125 kWh, in contrast December had the lowest generation of 1,765 kWh and a daily average of 57 kWh. Aggregating the monthly hourly generation, the annual generation was estimated to be 32,000 kWh.

Table 5-9 – Simulated monthly hourly generation of the rooftop photovoltaic system

Month	Monthly hourly generation / kWh														Monthly total / kWh	Daily average / kWh
	0-6	7	8	9	10	11	12	13	14	15	16	17	18	19-23		
Jan	0	6	71	136	250	292	301	282	237	129	65	7	0	0	1,776	57
Feb	0	11	59	132	194	244	252	313	266	193	88	30	0	0	1,782	64
Mar	0	43	119	207	269	338	366	336	297	225	120	44	0	0	2,364	76
Apr	0	67	171	264	321	329	342	343	323	256	140	56	1	0	2,617	87
May	0	94	242	316	377	388	403	393	366	297	184	90	6	0	3,194	103
Jun	0	89	256	329	361	381	410	386	347	294	200	77	21	0	3,185	106
Jul	0	88	287	379	449	486	487	463	428	387	278	80	26	0	3,865	125
Aug	0	85	221	347	416	457	469	431	397	318	194	70	7	0	3,422	110
Sep	0	73	179	308	365	381	391	389	346	270	124	45	0	0	2,874	96
Oct	0	54	136	287	376	420	407	380	315	189	74	11	0	0	2,649	85
Nov	0	40	98	210	294	322	336	331	266	118	54	1	0	0	2,070	69
Dec	0	20	81	150	264	306	317	272	210	98	46	1	0	0	1,765	57

5.5.2.2 Overview of energy demand and photovoltaic contribution during the four work-from-home periods

This study covered four work-from-home periods, including 29 January to 1 March, 23 March to 3 May, 20 July to 23 August, and 2 December to 31 December. The total building energy consumption under normal and work-from-home arrangements are presented in previous section. In this section and the upcoming sections, the energy demands during these four periods are specifically assessed and discussed.

During work-from-home arrangement, building occupants were expected to stay home which led to increased energy demand consumption. Since it was assumed that air-conditioning was functional from April to October, work-from-home arrangement during these months implied additional use of air-conditioning, lighting, and electrical equipment. For the remaining non-air-conditioned months, the increased energy demand was solely due to the increased use of lighting and electrical equipment.

Echoing with the objective of this study, the potential contribution of the rooftop photovoltaic system is presented in terms of the capability to utilize its generation output to supplement the additional energy demand. As an overview, the results are presented in Figure 5-4. It is shown that the photovoltaic system could contribute 7% to 11% of the additional energy demand in the four periods. The results are critically discussed in-depth in the upcoming sections.

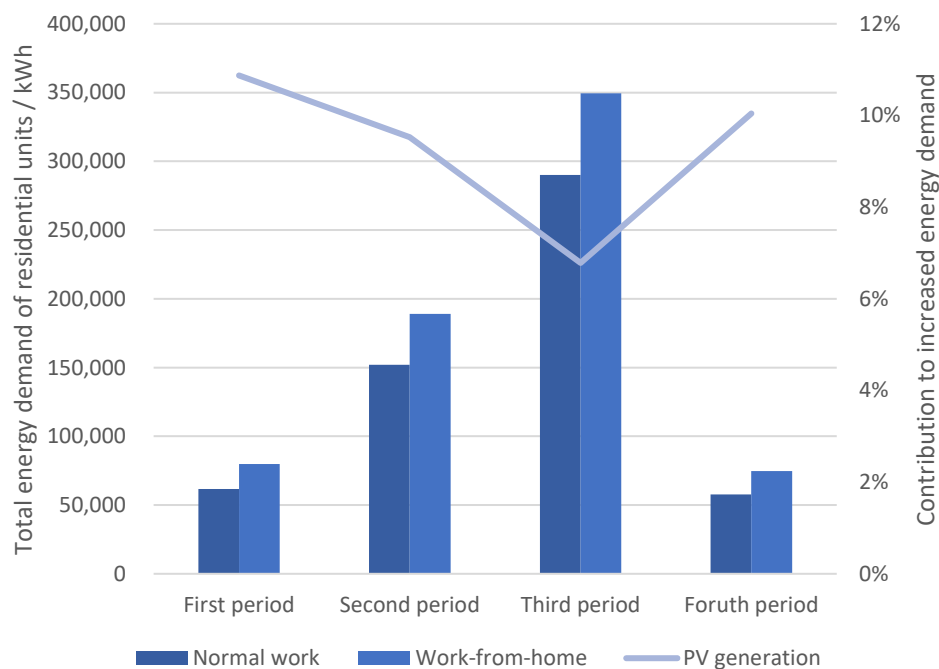


Figure 5-4 – Energy demand during normal work and work-from-home arrangements, and the PV generation contribution to the increased energy demand

5.5.2.3 First work-from-home period

The first work-from-home arrangement was announced on 29 January and lasted until 1 March. Within this period, it was modelled that the total residential units' energy consumption was 79,800 kWh, in which the majority (79,100 kWh) was contribution by non-air-conditioning consumption, and the remaining owing to air-conditioning and ventilation consumption (700 kWh). By comparing with normal work arrangement within the same period, the energy demand was estimated to be 29% higher during work-from-home condition. The percentage difference was mainly due to the higher consumption of lighting and electrical equipment when occupants stayed at home, but was not associated with air-conditioning which was assumed to be turned on during April to October. Simulation suggested that during the first work-from-home period, the rooftop photovoltaic system would have generated 1,970 kWh. This accounted for 2.5% of the total residential units' energy consumption under work-from-home situation, and 11% of the difference between the two work arrangements.

5.5.2.4 Second work-from-home period

The second work-from-home period started on 23 March and finished on 3 May. This period spanned across natural ventilation and air-conditioned periods. From 23 March to 31 March, it was modelled that the residential units consumed 22,400 kWh, 29% higher than normal work situation. Similar to the first work-from-home period, the difference was mainly contributed by non-air-conditioning consumption.

From 1 April to 3 May, the work-from-home energy consumption was simulated to be 166,600 kWh which was 24% higher than normal work condition. Since air-conditioning was functional starting from April, and occupants were assumed to work in their air-conditioned bedroom, the

air-conditioning and ventilation energy demand was modeled to be 19% higher than normal work arrangement, reaching 85,100 kWh. Besides the increased usage of lighting and electrical equipment led to a 30% increment in non-air-conditioning energy demand compared to normal work arrangement, accounting for 81,600 kWh. For the entire period of the second work-from-home situation, the total energy demand was 189,100 kWh, including 103,800 kWh of non-air-conditioning and 85,300 kWh of air-conditioning and ventilation. This was 24% higher in contrast to the energy demand of 152,000 kWh under normal work arrangement. During this period, the rooftop photovoltaic system would have produced 3,500 kWh. In particular, the photovoltaic system could supplement 2.7% of energy demand from 23 March to 31 March (non-air-conditioned period), and 1.8% of energy demand from 1 April to 3 May (air-conditioned period). In total, the photovoltaic system could contribute to 1.9% of the total residential units' demand. Given the 37,100 kWh difference in total energy demand between the two work arrangements, the on-site photovoltaic system could potentially contribute to 9.5% of the additional energy demand.

5.5.2.5 Third work-from-home period

The third work-from-home period was from 20 July to 23 August. It was simulated that the residential units used 349,500 kWh. This represented a 21% increment compared to the energy consumption during normal work arrangement (290,100 kWh). The increment was made up of 18% increase (40,000 kWh) in air-conditioning energy demand and 29% increase (19,500 kWh) in non-air-conditioning energy demand.

It was simulated that the rooftop photovoltaic system could have generated 4,000 kWh during the third work-from-home period. The amount of output was equivalent to 1.2% of the total residential units' energy demand. The percentage contribution was relatively smaller compared

to the first and second work-from-home periods because the flats were air-conditioned during third work-from-home period, despite the higher solar energy generation compared to other months. This was implied that the fact that the building consumed more energy when air-conditioning was used instead of natural ventilation. Nevertheless, the 4,000 kWh photovoltaic output could provide 6.8% of the additional energy demand (59,500 kWh).

5.5.2.6 Fourth work-from-home period

The fourth work-from-home arrangement was announced on 2 December, as normal work was resume in January the next year. The fourth period concerned covered 2 December to 31 December within 2020. Within this period, the flats were not air-conditioned. Since the ventilation operation schedules in toilets and kitchen were the same in both work arrangements, there was no difference in air-conditioning and ventilation consumption. The increased energy demand was modelled to be 17,000 kWh, equivalent to 29% increment from 57,800 kWh (normal work) to 74,800 kWh (work-from-home). This percentage increments in the first and fourth work-from-home periods were the same as the operation schedules were identical. The photovoltaic system was modelled to be capable of producing 1,700 kWh during this period. This amount was adequate to supplement 2.3% of total residential units' energy demand. As of the 17,000 kWh increase in energy demand, the photovoltaic generation could be contributable to 10% additional consumption.

5.5.2.7 Normal work arrangement periods

In addition to the above work-from-home periods, the possible contribution during normal work situation by the photovoltaic system is assessed. The normal work periods include 1 January to 28 January, 2 March – 22 March, 4 May to 19 July, and 24 Aug to 1 December. For these periods which lie within the non-air-conditioned months, the photovoltaic system was

modelled to supplement 3% to 4% of the energy demand of all residential flats. In contrast, when normal work arrangement was applied during air-conditioned months, the photovoltaic system could contribute around 1.5% of the total energy demand.

5.5.3 Limitations

5.5.3.1 Family size

This study made a few critical assumptions which imposed certain limitations on the results. Firstly, the study assumed that all households had a uniform family size of 4 people based on the one master bedroom and two bedrooms floor plan. Referring to the Hong Kong government official population by-census results (Census and Statistics Department, 2016), the average household size was 3.0 in 2006 and 2.8 in 2016. The modelling input may have discrepancy compared to the average household size.

5.5.3.2 Equipment performance specification

Secondly, the equipment performance specification, although was appropriately justified, was to certain level up to the authors' discretion. Performance indicators in residential flats are usually not mandated by government regulations because they are subject to the occupants' own wills. For instance, the lighting power density assumed in the model was based on the reference of mandatory lighting provision in dormitory, which was believed to be a close reference to residential unit. It was almost unavoidable to have some households installing excessive lighting and electrical equipment, or on the other extent using minimal lighting and equipment. The model has not captured such variations which could have been understood by surveying occupants but would have brought another level of complexity to the study. Within the scope of this study, it has not been possible to collect a whole year electricity data of a residential unit due to time constraints. In addition, the lack of suitable data in high rise

buildings has been a common challenge faced by many fellow energy model developers (Yu *et al.*, 2015b). Nevertheless, the modelling results were validated by comparing with peer models and empirical results. It was believed that the modelling results were accurate reflections of reality.

5.5.3.3 Photovoltaic system generation

Thirdly, with regards to the photovoltaic system generation, due to the high-rise nature of public residential flats (40-storeys), it was believed that surround shading would only have a limited impact on the output. Nonetheless, a 10% shading loss was taken into account in the simulation. On the other hand, the availability of roof space was another critical factor determining the generation output. Two factors, including architectural factor and solar suitability factor, were applied to the roof area to deduce the suitable area for photovoltaic installation. These factors could be further subject to the actual architectural roof layout, which could be affected by space irregularity or alternative use of space such as for placing HVAC equipment.

5.6 Summary

A building energy model was developed to estimate the annual energy demand of a 40-storey high-rise public residential building which comprises of 320 units. The modelling inputs were appropriately justified based on local and industrial references, and included major energy consumptions including air-conditioning, ventilation, lighting and household electrical equipment. Energy modelling results suggested an energy intensity of 91 kWh/m² and consumption 450 kWh per month per residential unit under normal work arrangement. These results were validated by comparing against peer models and empirical data, hence the model was believed to be an accurate reflection of the reality.

An alternative building energy model was developed to simulate the energy demand under work-from-home situation by adjusting the occupancy schedule and building operation schedules according to the Government's four announcements of special work arrangement in January, March, July and December 2020 respectively. Modelling results showed that the energy intensity rose to 98 kWh/m², and the energy use per residential unit increased to 490 kWh/month. This quantified a 9% energy demand increment under work-from-home arrangement as compared to normal work arrangement, which was validated to be consistent with the residential electricity sales report according to utility provider's official data. While it has not been a general practice to deploy solar rooftops on public residential buildings, this study testified the possibility to install solar rooftop and generate energy to supplement the increased energy demand. A solar energy simulation was carried out to estimate the annual output of a 250 m², 38.5 kWp rooftop photovoltaic system. The suitable roof area for installation was estimated based on the roof area, adjusted by an architectural factor and a solar suitability factor. The annual generation was estimated to be 32,000 kWh.

The potential contribution was evaluated in terms of the relative capability to utilize its generation output to supplement the additional energy demand. During the first work-from-home period (29 January to 1 March), the photovoltaic system could potentially contribute to 11% of additional energy demand. Moving on the second work-from-home period (23 March to 3 May), the photovoltaic system was modelled to supplement 9.5% of the increased energy consumption. The contribution slightly dropped because air-conditioning started operation in April, leading to an increase in energy consumption. In the third work-from-home period (20 July to 23 August), the solar generation could provide 6.8% of the additional energy demand. The relative percentage contribution dropped further because the flats were air-conditioned for the entire period, despite the higher solar energy generation compared to other months. For the

fourth work-from-home period (2 December to 31 December), the generation was contributable to 10% additional consumption which was similar to the first work-from-home period. In the remaining times of normal work arrangement, the photovoltaic system could contribute to around 1.5% of total residential units' energy demand when air-conditioning was on, and 3-4% when air conditioning was off. The limitations and uncertainties of this study were critically discussed, including the assumed household size, equipment performance specification modelling input, and rooftop spatial availability for photovoltaic installation.

Overall, it is believed that rooftop photovoltaic system could contribute effectively to the increased energy demand during work-from-home arrangement, and it is feasible to improve the buildings' autonomy. In light of future possible crisis, it is recommended to enhance energy resilience on a building level by reviewing the feasibility of on-site generations in existing buildings, and consider to deploy renewable energy microgrids in new buildings under design. The findings are believed to be significant to provide understanding in the impact of work-from-home arrangement on residential energy consumption. The contributions are long-term as work-from-home arrangement may become more common in the future. This study's outcomes are valuable to safeguard energy resilience in upcoming grid planning and operation. Suggested future works are extending the scope to analyze electricity consumptions in other sectors including commercial and industrial to understand the change in total electricity consumption on a city scale. Although the work-from-home arrangement has led to an increase in residential energy demand, the consumption in other sectors is expected to decrease due to restricted business activities. A city-scale analysis can provide an overall insight in COVID-19's impacts on energy resilience.

6. CHAPTER 6 UNDERSTANDING POST-PANDEMIC WORK-FROM-HOME BEHAVIOURS AND COMMUNITY LEVEL ENERGY REDUCTION VIA AGENT-BASED MODELLING

6.1 Introduction

The COVID-19 outbreak has induced drastic changes to traditional workplace practices. Due to social distancing protocols and efforts to mitigate the related risk of diminished productivity, work-from-home (WFH) arrangements have gained in popularity (Zito et al., 2021). It is estimated that over 90% of workers are living in countries that have imposed different degrees of workplace closure (Mehta, 2021). The WFH arrangement has consequently become a worldwide trend. This trend is not limited to developed countries with comparatively resilient IT infrastructure readiness (Mongey, Pilossoph and Weinberg, 2021), but is also occurring in developing countries where even fewer urban jobs are available (Gottlieb et al., 2021). WFH has emerged globally as a countermeasure to the pandemic.

In the United States, the number of employees who were working from home increased from 37% to almost nearly everyone within weeks of the outbreak (Yang et al., 2021). The WFH arrangement has essentially become one of the “new normal” practices triggered by the pandemic and is expected to take over traditional office routines (Carroll and Conboy, 2020). This new arrangement has led to various changes in the social, economic and environmental conditions in societies (Jenkins and Smith, 2021), and has attracted the interest of researchers exploring various topics such as how work is facilitated while social distancing measures are in place, how boundaries are now navigated between work and private life, and how patterns in daily routines are changing (O’Leary, 2020). There is already discussion of transitioning to a new normal and how the workforce will cope with working from home when COVID-19 comes to an end (Jamaludin et al., 2020).

Echoing with the United Nation Sustainable Development Goal 7, the post-pandemic world indicates the need for strategies to energy sustainability (Madurai Elavarasan et al., 2021). Given how the COVID-19 outbreak has undoubtedly influenced workers' workplace preferences, it is important to examine and predict the environmental impacts and energy savings that may occur in a post-COVID-19 world resulting from prolong or permanent WFH (Madurai Elavarasan et al., 2020b). Decision-making processes related to working from home can be very complex, dependent on various factors such as interactions between family members and office co-workers (Athanasiadou and Theriou, 2021). The characteristics of these thought processes make agent-based models (ABM) a powerful tool for simulating the interactions according to certain behaviour rules, thereby generating macroscopic patterns from the bottom-up, and aiding the investigation of topics such as the relationship between post-COVID-19 WFH behaviour and opportunities to reduce environmental impacts.

This study develops an ABM to analyse post-pandemic WFH behaviours. The ABM simulates workers' decision-making processes with the aid of social theories. Different characteristics and attributes are individually assigned to workers (agents in the model) to create heterogeneity among the population. Influences from family and co-workers are also modelled to form social networks between workers. This study aims to investigate the emergent behaviour of post-pandemic WFH arrangements under different scenarios and the associated impact on community level energy consumption.

6.2 Literature review

6.2.1 Social theories

Soon after the COVID-19 outbreak was declared an international public health emergency, most societies worldwide implemented lock-down measures. Employees were either asked or

given the choice to carry out office duties at home to maintain sufficient social distancing. This attracted the attention of social science researchers who then carried out simulations to make predictions on employee decision-making and emotional responses towards WFH arrangements in lieu of burdensome and high cost surveys, given that WFH may become a long term policy in the long run (Min *et al.*, 2021). One key social principle that was adopted in these simulations was conservation of resources (COR) theory. COR theory suggests that individuals are motivated to build and maintain personal resources, such that stress occurs when the resources are threatened or lost (Hobfoll and Ford, 2007). COR theory can be used to explain the human stress and well-being involved in WFH decision making (ten Brummelhuis and Bakker, 2012). This theory has been previously applied to better understand similar family conflicts and strains faced by working mothers (Grandey and Cropanzano, 1999).

In addition to COR theory, small-world theory has demonstrated relevance to informing interventions guidance to lessening the severity of the pandemic (Du, 2021). Small-world theory suggests that every individual is interconnected, hence each individual's decision-making affects each other's due to the high betweenness (Zenk *et al.*, 2020). Within small communities, such as a workplace, small-world theory can model the network between individuals who may have different attributes and interact with each other (Block *et al.*, 2020). It is evident that small-world network models can help explain the relationship between WFH decision-making by predicting movements between home and work, and the spread of the virus (Shaw *et al.*, 2021).

6.2.2 Consideration factors during decision-making for WFH

There are various factors involved in WFH decision making. Making the choice between WFH and working at the office can involve complex thought processes. Since the widespread

adoption of WFH in response to the pandemic, workers have benefited from more flexible work schedules, more time for family and leisure, and reduced time and costs for commuting (Okuyan andBegen, 2021). On the other hand, it is reported that workers began to be affected by stresses from various sources, including work-family boundary challenges, technology related issues, work coordination complications, and workload increases (Shao *et al.*, 2021). It can be difficult for employees to strike a balance between work and family as employees need to overcome high job demands and maintain a healthy work-life balance. In particular, when given a choice between going to the office or WFH on the next day, a worker may consider factors including work-family conflicts, emotional exhaustion, and impacts on company operations (Darouei andPluut, 2021). Min et al. leveraged machine learning by collecting social media tweets to study the public's psychological reactions to WFH orders, finding that immediate emotional benefits were deemed to fade over time as the pandemic situation persisted (Min *et al.*, 2021). Another study showed that technology related stress increased as digital technology and remote work became more dominant during the pandemic (Oksanen *et al.*, 2021), which may support claims that teleworking can be less productive than on-site work (Li, Zhang andWang, 2021). It has been suggested that the effectiveness of WFH strongly depends on the employee's digital orientation and capabilities, and COVID-19 presented an opportunity through time to enhance the readiness of remote workers by improving IT infrastructure and providing training (Afrianty, Artatanaya andBurgess, 2021). In contrast, Rahman et al. suggested that workers found it more productive to WFH rather than at the office (Rahman andZahir Uddin Arif, 2021). To date there has been no conclusive evidence of regarding overall beneficial or adverse impacts of WFH, as the work arrangement practice is still evolving and the general public has yet to fully adapt to it. Table 6-1 summarises a few examples of factors that have been suggested in the literature to be significant in WFH decision-making.

Table 6-1 – Factors which affect decision-making to WFH

Decision-making factors	References
Gender	(Shao <i>et al.</i> , 2021), (Galanti <i>et al.</i> , 2021)
Age	(Shao <i>et al.</i> , 2021), (Galanti <i>et al.</i> , 2021)
Well-being	(Toniolo-Barrios andPitt, 2021)
Space at home	(Russo <i>et al.</i> , 2021)
Communication with colleagues	(Min <i>et al.</i> , 2021)
Disturbance by family members	(Darouei andPluut, 2021)
Availability of office software	(Malecki, 2020)
Availability of office hardware	(Afrianty, Artatanaya andBurgess, 2021)

6.2.3 Agent-based modelling (ABM) Applications to COVID 19

Considered to be a useful tool in social science, agent-based modelling employs mathematical models to describe human decision-making processes (Grimm *et al.*, 2020). During the COVID-19 pandemic, ABM has been applied to investigate several research topics such as projecting epidemic trends and exploring intervention scenarios (Kerr *et al.*, 2021), modelling transmission in a confined indoor environment based on human-to-human interactions (Ying andO’Clery, 2021), and simulating the spread of the virus within a city (Shamil *et al.*, 2021). Humans are modelled as individual agents who operate according to their own behaviours and preferences, for example infection status, contact with others, and mobility. Agents interact and collaborate to produce stochastic results, such as patterns in transmission risk in the context of COVID-19 (Cuevas, 2020).

With the aid of social science theories, ABM is believed to be useful for understanding

emergent behaviours and responses to pandemic social distancing interventions. For example, a previous study employed ABM to model small work networks and investigate the impacts of different population control measures on infection phrase transitions (Braun *et al.*, 2020). A comprehensive literature review (Lorig, Johansson and Davidsson, 2021) was conducted to analyse 126 articles that applied ABM in the context of the COVID-19 pandemic. The review suggested that although ABM could serve as a powerful tool to investigate virus transmission, the full potential of ABM has yet to be fully realized. The review also suggested that most models (about 90%) simplified human behaviours to the extent that decisions were represented to be randomly made with predefined networks. Only a few models included human decision-making that was based on individual needs and utilities.

Following the above literature review, it is observed that limited ABM applications have been demonstrated on interpreting WFH on an individual level. Further research opportunities are identified in the implications of WFH-associated social behaviours on the environmental dimension. This research angle is crucial as it is indicated that WFH has already become mainstream during the pandemic, and will likely grow to be more prevalent in the future new normal (Guler *et al.*, 2021). In addition, flexible work arrangements may be associated with environmental benefits, such as reducing carbon emissions generated by transportation and office activities (Yu, Burke and Raad, 2019). Some countries even experienced a 26% reduction in carbon emissions owing to work restrictions during the pandemic (Yu, Burke and Raad, 2019). In particular, it has been suggested that carbon emissions from transportation, commercial, and residential activities could be considerably impacted by the extension of WFH arrangements (O'Brien and Yazdani Aliabadi, 2020). It is reported that China experienced a 11% nation-wide reduction in carbon emissions due to COVID-19 as people were ordered to stay home and transportation demand dropped dramatically (Han *et al.*, 2021). Besides, a study on a district

in Sweden suggested that there had been no change in overall energy demand comparing normal life and with COVID-19 confined measures (Zhang *et al.*, 2020).

Two previous studies particularly investigated the impacts of flexible work arrangements on carbon emissions prior to the COVID-19 outbreak. One study analysed home office data in the United States in 2003, and suggested flexible work arrangements could reduce transportation emissions, though home-related impacts partially offset the reduction due to additional time at home (Kitou and Horvath, 2003). Another study was conducted in 2017, demonstrating that telework could reduce traffic emissions and office energy consumption but could increase residential consumption. The authors noted in the conclusion that the overall energy implications of telework perhaps remained uncertain (Larson and Zhao, 2017).

6.3 Objective and significance

The research to date has tended to apply ABM in the context of the pandemic primarily to virus transmission and development. This study closes the research gap by demonstrating the effectiveness of ABM as applied to post-pandemic WFH analysis and the corresponding environmental impacts. This study contributes to the understanding of socio-environmental aspect of WFH by 1) advancing our understanding of worker decision-making processes in selecting their workplace based on behaviour theories, and 2) quantifying the variation of community level energy reduction according to various WFH arrangements.

6.4 Methodology

6.4.1 Agent-based modelling (ABM)

This study employs agent-based modelling (ABM) to simulate the work from home (WFH) decision making of the general workforce. As outlined in the literature review, ABM has been proven to be a popular modelling tool, but thus far it has been applied primarily to understand

virus transmission and development. Given its efficacy in predicting emergent macro performances arising from individual behaviours, ABM enables the simulation of the decision-making process of each individual as they choose between WFH and working at the office, based on the individual's consideration factors. With the aid of social science theories that describe interactions between individual agents, the simulation of behavioural patterns for the entire workforce on the macro-level can be modelled more closely to reality.

6.4.2 Methodology overview

The model was developed using NetLogo, a multi-agent programme for complex social system modelling, including studying connections between individuals and emergent patterns resulting from these connections. Figure 6-1 delineates the steps of model development:

- i. Collect data from a historic representative survey
- ii. Develop an ABM to assign individual characteristics and variables to each agent on a micro-level, and allow interactions between agents including influences from family members and co-workers
- iii. Calculate the utility of each agent according to their key decision-making factors to drive individual selection of WFH or work at the office
- iv. Calibrate and validate the model via Monte-Carlo analysis
- v. Carry out scenario simulations by varying the key factors and measure the corresponding environmental performance

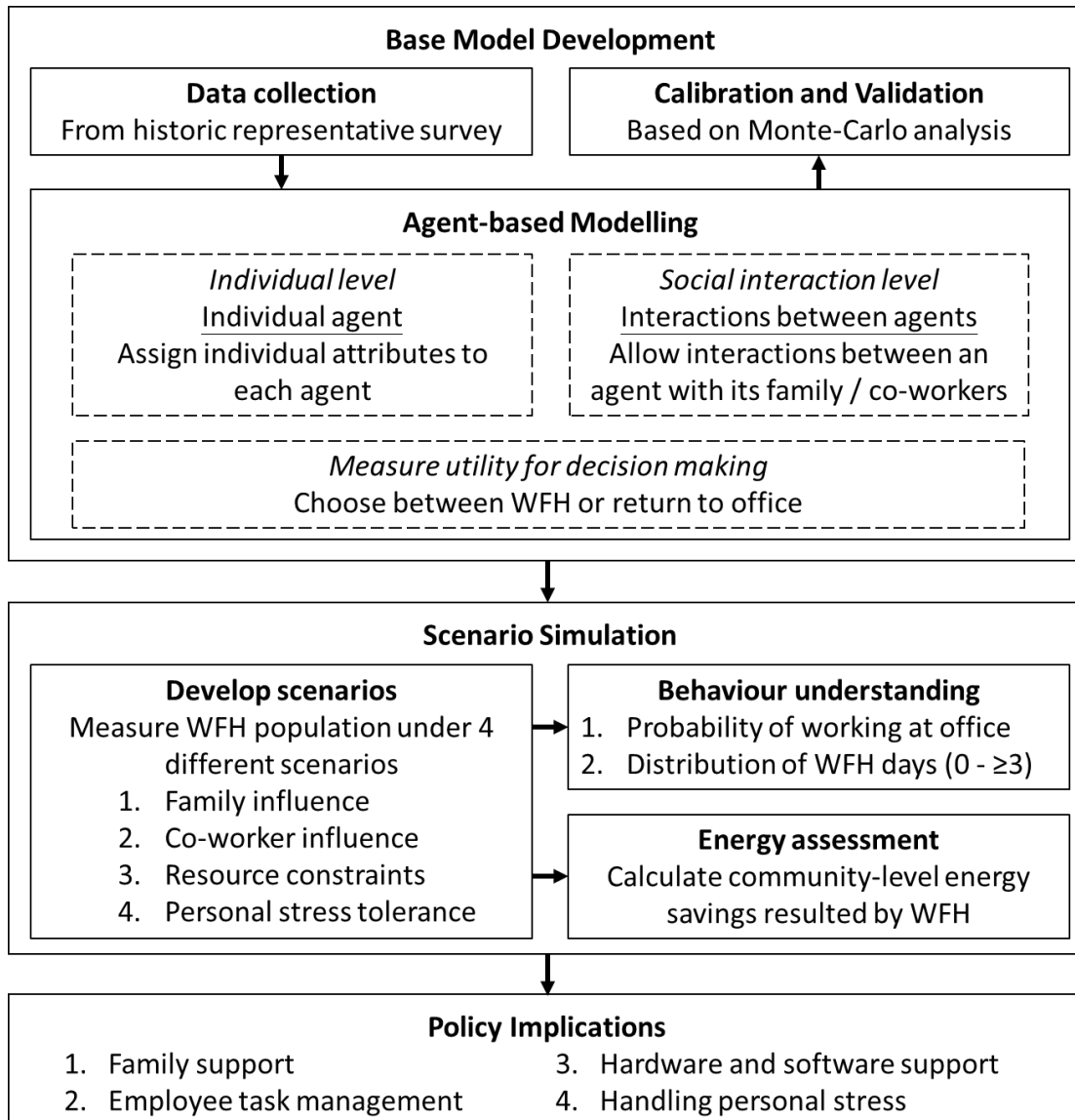


Figure 6-1 – Workflow of ABM development

6.4.3 Data collection

Data was mainly drawn from a local survey (Lingnan University Hong Kong, 2020). The survey involved an online questionnaire issued to full-time Hong Kong workers who had WFH experience during the virus outbreak. The survey was conducted publicly via social media channels in April 2020, and contained questions on preferences regarding WFH after COVID-19, advantages of WFH compared to working at the office, challenges of WFH, and support given to employees by the employers. The survey generally adopted a five-point Likert scale,

where 1 = “strongly disagree” and 5 = “strongly agree”. The survey results were considered to be reliable as almost 2,000 effective responses were received.

Upon regression analysis, one study (Wong, Cheung and Chen, 2021) found various factors to be either positively or negatively correlated to one’s ability to effectively WFH (Table 6-2). These factors include gender, age, well-being, environmental constraints (e.g. lack of work space at home, difficulties in communication with colleagues, presence of distractions from family members), and resource constraints (e.g. lack of office hardware and/or software).

Table 6-2 – Variables and input data which exhibit statistically significant correlation with WFH preference according to Table 8 in the abovementioned previous study

Variable	P Value	Minimum	Maximum	Mean	Standard deviation
Gender	<0.05	1	7	3.56	1.01
Age	<0.01	1	2	1.68	0.47
Well-being	<0.01	1	5	3.55	0.84
Resource constraint	<0.01	3	9	7.08	2.29
Environmental constraint	<0.01	To be defined by social influence (family and colleagues)			

6.4.4 ABM development

The simulation environment contains two zones (Figure 6-2). The white zone on the left represents “home”, and the black zone on the right represents “office”. Agents are allowed to migrate between these two small worlds. This migration is animated and can be regarded as

representing each agent’s choice between working from home or at the office. Agents who choose to WFH are identified in red, and those who choose to work at the office are identified in blue. Agents have social links with each other. An agent who is a family member of another agent is connected with red lines. Agents who are colleagues with each other are connected by blue lines.



Figure 6-2 – Simulation environment in Netlogo

Another critical independent variable is environmental constraint. In the model, agents are associated with their own social networks based on small world theory. An agent’s environmental constraint is derived from a combination of family members’ influence and colleagues’ influence. The model assumes an average family size of 2.8 (C&SD HK, 2020b), and an average work team size of 5 (Wheelan, 2009). According to the same survey, 63% of respondents were disturbed by family members and 56% of respondents experienced difficulties communicating in a timely manner with colleagues when they worked from home. The model relies on these two probabilities to represent the likelihood that a family member and co-worker influences the workplace location decision on a daily basis. Within these two probabilities, these interactions between agents are referred to as the family social influence and colleague social influence, respectively. To allow adjustment of the strength of the influence, two modelling inputs, i.e. maximum “family-social-influence-value” and maximum

“colleague-social-influence-value”, based on a Likert scale of 1 to 5. These inputs, within the set scale, are randomly assigned to agents.

To further characterise the population, each agent was assigned a personal stress tolerance threshold as a reflection of reluctance to WFH. Given that WFH is a new type of work arrangement in contrast to a traditional office work routine, the model assumes that work stress will build up as the agent chooses to WFH, in accordance with COR theory. This will be further elaborated in the Utility section.

6.4.5 Utility

One of the key strengths of ABM is its ability to simulate complex situations based on simple behaviour rules. Drawing upon the statistically significant variables suggested by Wong et al. (Wong, Cheung and Chen, 2021), the model uses the equation below (Equation 6-1) to calculate an agent’s utility, taking into account the weights assigned to each key decision-making factor. The weightings are represented by the corresponding regression coefficient of the statistically significant key decision-making factor determined by the same survey.

Equation 6-1 – Agent utility calculation

$$U = W_a \times D_a + W_g \times D_g + W_{wb} \times D_{wb} + W_{rc} \times D_{rc} + W_{ec} \times (I_{fam} + I_{work})$$

where U = utility; W = Weighting of a key decision-making factor; D = Key decision-making factor; a = age; g = gender; wb = well-being; rc = resource constraint; ec = environmental constraint; I_{fam} = Family social influence value; I_{work} = Colleague social influence value.

The agent decision-making flow is depicted in Figure 6-3. There are two choices available to an agent resulting from the utility calculation: work at the office or WFH. Should the calculated

utility be smaller than a certain utility threshold, the agent will choose to work at the office. Otherwise, the agent will choose to WFH. The simulation cycle is represented as a 5-workday week. Given that working from home is a new type of work arrangement in contrast to traditional office working routines, the model incorporates COR theory, which suggests that work stress will build up as the agent chooses to WFH continuously. When an agent's stress level exceeds its personal stress tolerance threshold, the agent will be programmed to return to the office, and the work stress will reset to 0. The utility and stress tolerance thresholds were determined according to Monte-Carlo analysis during validation to display best-fit with the conducted survey.

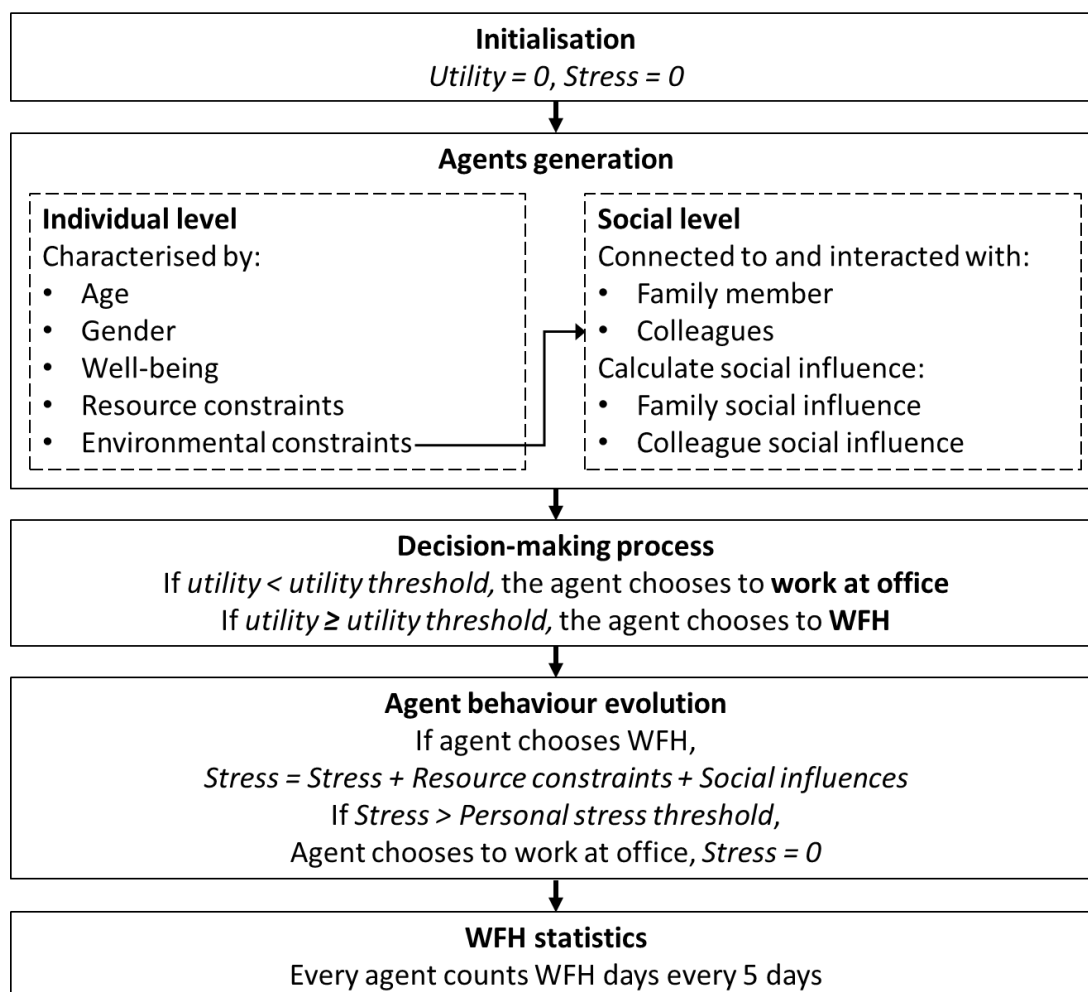


Figure 6-3 – Agent decision-making flow

6.4.6 Model validation

Data was drawn from the survey (Lingnan University Hong Kong, 2020) for calibration and validation to improve the credibility of the model and its results. The survey found that, after the COVID-19 public health crisis subsides, 30% of respondents prefer to WFH once a week, 36% prefer to WFH twice a week, 16% prefer to WFH 3 days or more per week. The remaining (18%) prefer no WFH arrangement at all. The calibration experiment involves finding the best fitting matrix of maximum family social influence value, maximum colleague social influence value, utility threshold, and personal stress tolerance threshold via 100-run Monte-Carlo simulations (Figure 6-4). The dips shown in maximum family social influence value, utility threshold, and personal stress tolerance threshold represent the corresponding values to attain the minimal root mean squared error. Given that there is no dip observed in the set range of maximum colleague social influence values, the value is taken at the lowest root mean squared error based on the Likert scale. As a result, the calibration suggests that the best-fitting model input matrix ought to have a maximum family social influence value of 4, maximum colleague social influence value of 5, a utility threshold at 1.5, and a personal stress tolerance threshold of 8.

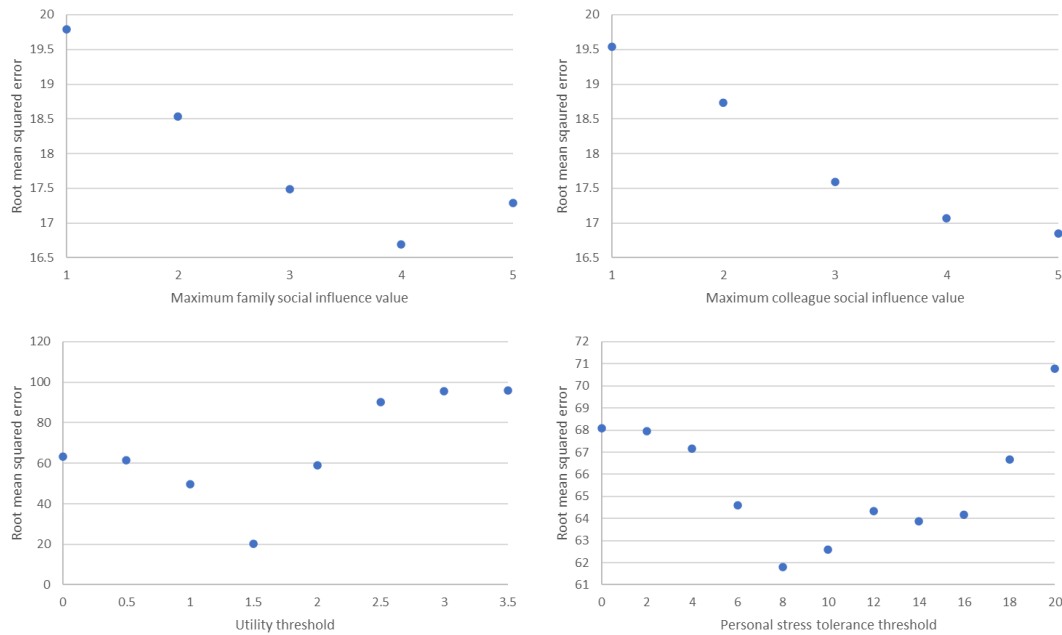


Figure 6-4 – Calibration exercise for finding the best-fit values for maximum family social influence, maximum colleague social influence, utility threshold, and personal stress tolerance threshold

6.4.7 Scenario simulation

The validated model serves as the base case representing post-pandemic circumstances. Following calibration and validation, several scenarios were simulated to study the potential WFH impacts, represented by three sets of results: 1) the proportion of employees choosing to work at the office, 2) the proportion of employees choosing to WFH, and 3) community level energy consumption compared to business-as-usual. All simulation results were generated through 100-run Monte-Carlo simulations.

As suggested by a report published by a reputable global management consultancy company (PricewaterhouseCoopers, PwC) (PwC, 2021), the top 4 widest gaps in perception between employers and employees on the success of a company’s efforts to support WFH are “benefits for family and childcare”, “providing training for managers to lead teams in a remote

environment”, “supporting employee’s mental health”, and “providing mobile experience for work applications”. Echoing these gaps, the scenarios for the present study were developed by varying modelling inputs according to specific investigation objectives (Table 6-3), covering the impacts of environmental constraints (family social influence and colleague social influence), resource constraints, and personal stress tolerance threshold, on WFH decision making.

Three sets of results were generated, including 1) the proportion of employees choosing to work at the office, 2) the proportion of employees choosing to WFH (0 day, 1 day, 2 days, and ≥ 3 days per week), and 3) community level energy reduction compared to business as usual.

Table 6-3 – Four simulated scenarios with varying model inputs and specific objectives

Model input	Objective
Maximum family social influence value	To understand the effects of increasing the influence of family members, such as the agent becoming distracted by household duties during work
Maximum colleague social influence value	To understand the effects of increasing the influence of co-worker(s) such as difficulties in communicating with colleagues
Mean resource constraint	To understand the effects of varying resource support, such as availability of office hardware and software
Personal stress tolerance threshold	To understand the effects of personal stress tolerance across consecutive WFH days

6.4.8 Energy assessment

The COVID-19 pandemic has caused people around the world to change their lifestyle, especially the time they spend at home. This change in occupancy has a direct impact of energy consumption (Rouleau and Gosselin, 2021). The “Hong Kong Energy End-use Data” is a government report that is published annually to provide energy consumption data across different sectors, including residential, commercial, and transport sectors (EMSD HK, 2020b). The yearly data for 2018 was particularly selected to factor out the impact of COVID-19 and represent the business-as-usual case. However, large-scale WFH arrangements were not rolled out until 2020, and that year’s official data has not yet been published by the time of this study. Therefore, to calibrate the energy per capita for the WFH scenario data from a major utility company in Hong Kong was used (CLP, 2020). It is assumed that energy per capita increases in the residential sector due to WFH arrangements and decreases for commercial and transport sectors due to reduced commercial activities. The energy use per capita data that informed the present study’s energy calculations is summarized in Table 6-4. The difference in community level energy used with and without the WFH arrangement was calculated with the equation (Equation 6-2) below:

Equation 6-2 – Community level energy reduction

$$\Delta E = A_{Total}(R_{BAU} + C_{BAU} + T_{BAU}) - A_{Office} \times (R_{BAU} + C_{WFH} + T_{WFH}) - A_{WFH} \times R_{WFH}$$

where ΔE = Difference in community level energy; A = Number of agents; R = Energy per capita in the residential sector; C = Energy per capita in the commercial sector; T = Energy per capita in the transport sector.

Table 6-4 – Energy use per capita across sectors

Sector	Total / TJ (2018 data)	Business as usual (BAU, 2018 data) Energy per capita (GJ / person)	WFH scenario (Calibrated) Energy per capita (GJ / person)
Residential sector	60,793	8.2	8.9
Commercial sector (Office)	13,489	3.4	3.2
Transport sector (Passenger)	59,519	15.0	14.3

Note: For the residential sector, the energy per capita was calculated based on the region’s population. For the commercial and transport sectors, the energy per capita was calculated based on the region’s labour force (C&SD HK, 2020a).

6.5 Results and discussion

6.5.1 Scenario simulation – Family influence

Using the base model as previously described, the first scenario simulated involves altering the maximum family social influence value in order to understand its effect on WFH selection. Family social influence is one of the two contributors to the environmental constraint variable, which in turn impacts an agent’s utility. As described in the Methodology section, the model inputs (maximum “family-social-influence-value” and maximum “colleague-social-influence-value” were given a range of 1 to 5. This first simulated scenario incorporates this range, and the results indicate that stronger family influence can lead to an increased number of agents choosing to work at the office. This can be explained by considering that when an agent faces

distractions caused by the family, the agent will tend to avoid this disturbance and select the office over the home as the workplace. The number of agents (out of 100) choosing to work at the office increases from 69% to 74% (an 8% rise) as the family social influence value increases from its minimum (1) to maximum (5) (Figure 6-5).

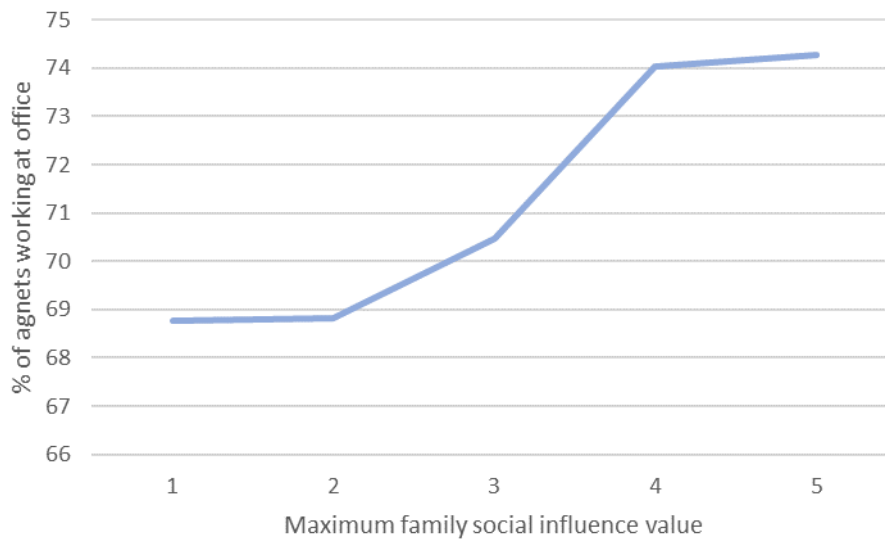


Figure 6-5 – Number of agents working at the office in the ABM with varying maximum family social influence values

Family influence also affects the ratios of preferences (Figure 6-6). For workers who choose to WFH ≥ 3 days a week, the portion changes from 22% when the family influence is at the minimum to 14% when family influence is at the maximum (a 36% reduction). Initially 38% of workers choose to WFH 2 days a week when the family influence is at the minimum and decreases to 35% at the maximum (an 8% reduction). The number of agents who choose to WFH 1 day per week remains relatively steady as family influence varies. The portion of workers who choose to work at the office all week increases from 24% to 31% (a 33% rise) under the elevated pressure of family influence.

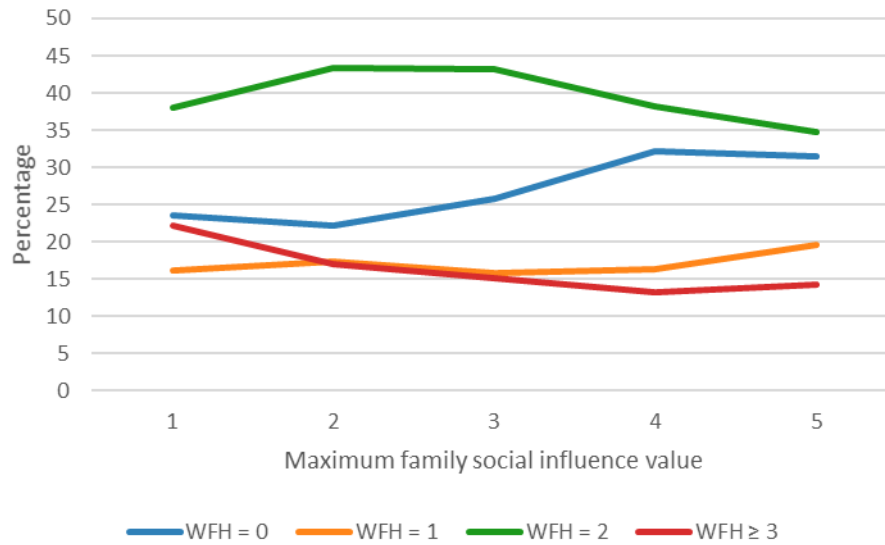


Figure 6-6 – Segregation of WFH preferences in response to varying maximum family social influence values

The community level energy difference with and without WFH arrangements is calculated (Figure 6-7). The energy difference is correlated to the number of agents choosing to work at the office and WFH respectively. The results show that as the family social influence value increases, the energy difference decreases. This implies that as agents face more family influence, they will choose to return to the office, and the number of WFH agents declines. Therefore, the reduced energy consumption associated with working from home diminishes. As the family social influence value increases from its minimum to its maximum, the energy savings decrease from 610 GJ to 510 GJ (a 15% reduction).

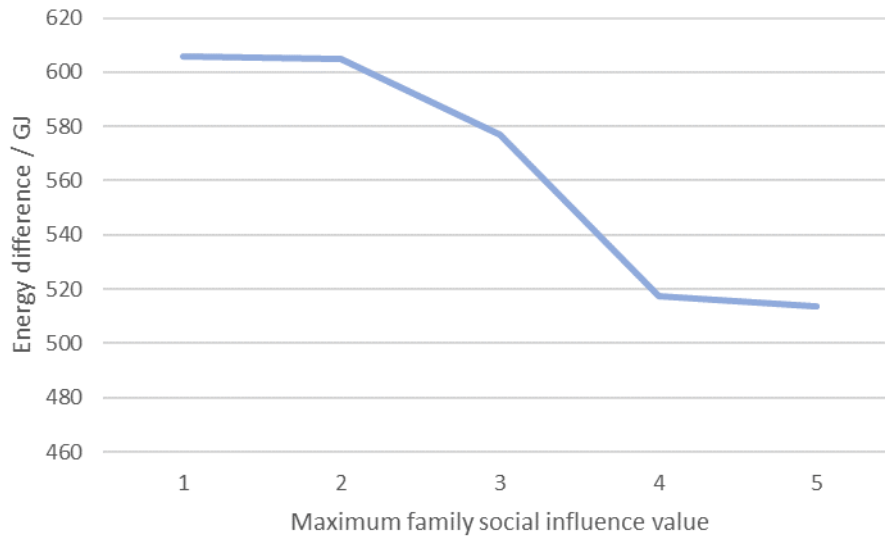


Figure 6-7 – Energy difference with varying maximum family social influence values

6.5.2 Scenario simulation – Colleague influence

The second scenario simulated assesses the impact of varying the maximum colleague social influence value, which is another component of the environment constraint variable (Figure 6-8). The effects are similar to those that occur in the first simulation. As agents face increased difficulties in communicating with colleagues, the tendency to return to the office grows from 68% to 73% (an 8% increase).

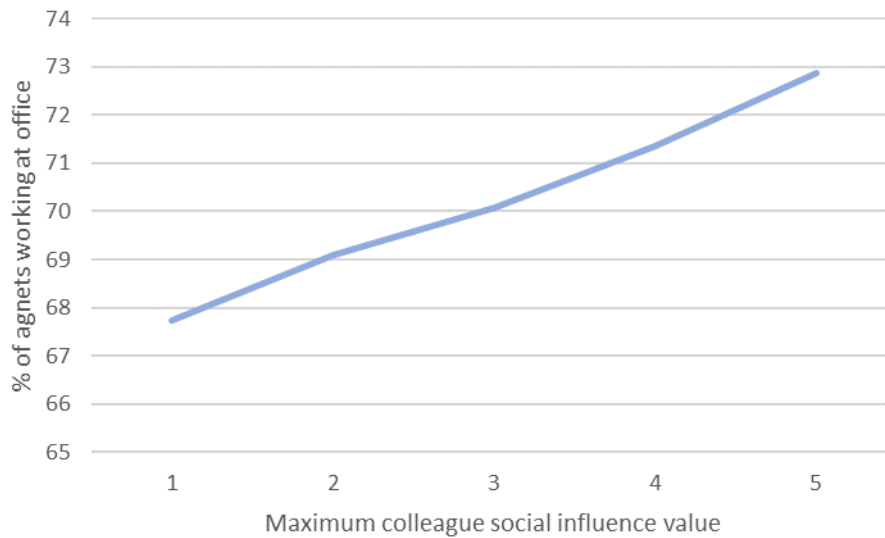


Figure 6-8 – Percentage of agents working at the office in the ABM with varying mean resource constraint values

As the value of colleague social influence climbs (Figure 6-9), more agents choose to work at the office the entire week, and fewer agents choose to WFH 2 days a week (from 44% to 39%, a 13% reduction) or ≥ 3 WFH days a week (from 17% to 12%, a 27% reduction). The percentage of agents who choose to WFH 1 day per week remains relatively stable as colleague influence varies. The group preferring 0 WFH days increases from 22% to 28%, a 28% gain.

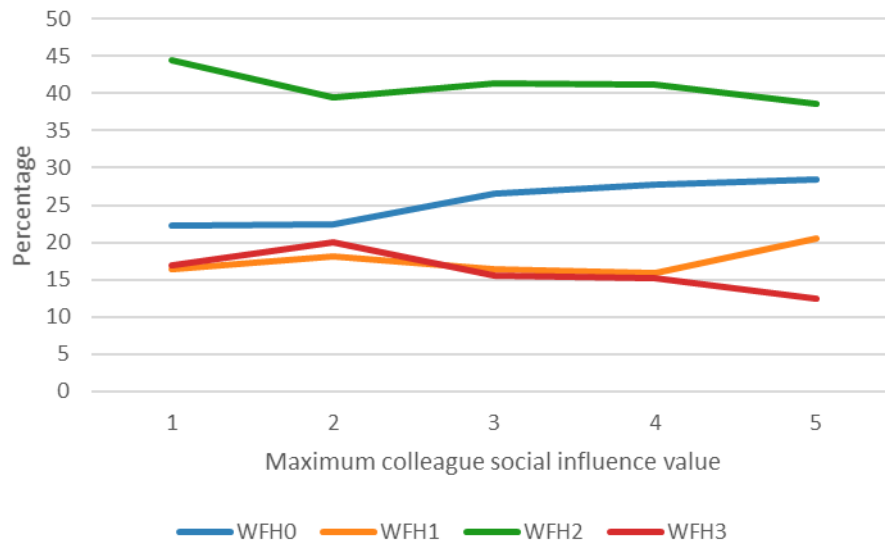


Figure 6-9 – Segregation of WFH preferences with varying maximum colleague social influence values

The impact of varying the maximum colleague social influence value on community level energy consumption was also investigated (Figure 6-10). Energy savings associated with working from home fall from 620 GJ to 540 GJ (a 14% reduction) as more employees work at the office when they face difficulties in communicating with colleagues and in an effective, timely manner. Transportation and office energy consumption increases when more agents return to the office, so that compared to the business-as-usual case, overall community level energy consumption increases.

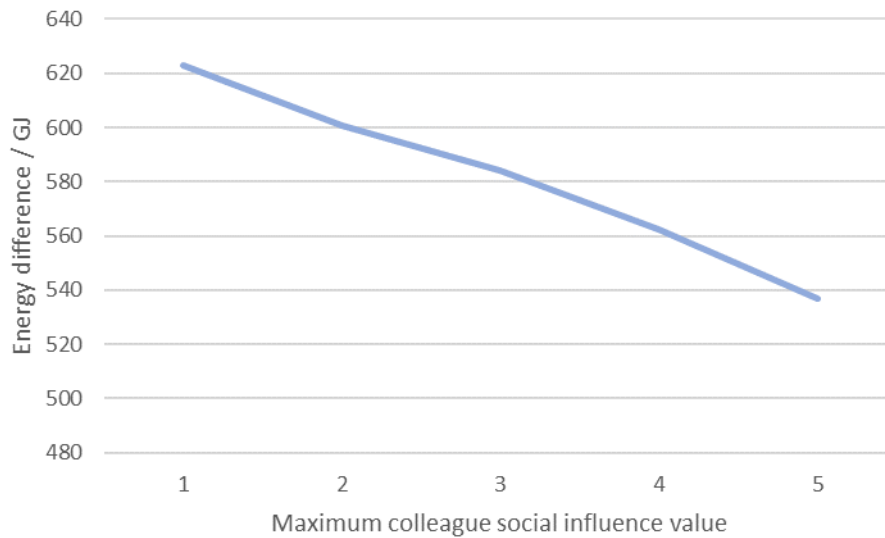


Figure 6-10 – Energy difference with varying maximum colleague social influence values

For both social influences from family and co-workers, the impacts on the number of workers choosing to work at the office can be explained with small world theory. The simulation results indicate that the presence and influence of family members or co-workers will have an impact on the workers’ decisions.

6.5.3 Scenario simulation – Resource constraint

The third scenario simulated in this study focuses on the effects of the resource constraint variable (Figure 6-11). The range of the mean value for this variable is set to be 3 to 9 in order to match the minimum and maximum values of the survey. Increases in the resource constraint value implies a lack of software and/or hardware support. The results of the simulation indicate that as the resource constraint value increases from its minimum to maximum, the percentage of workers at the office increases from 67% to 75% (a 12% rise).

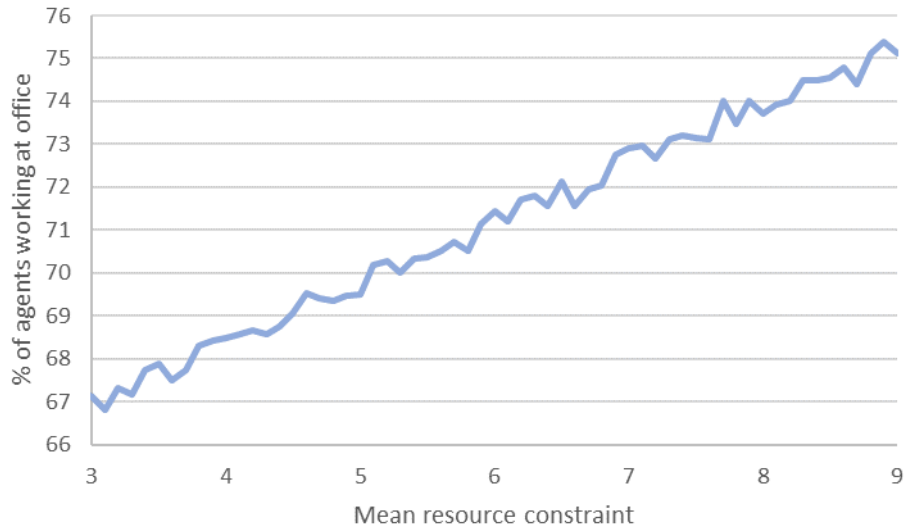


Figure 6-11 – Percentage of agents working at the office in the ABM with varying mean resource constraint values

The proportion of agents choosing to WFH ≥ 3 days a week decreases (from 23% to 11%, a 49% reduction) as the resource constraint value increases (Figure 6-12). Agents choosing 2 WFH days change from 41% to 35%, a 14% reduction. The decrease in these two groups contributes to the increase in groups selecting the other 2 options. The number of agents choosing 1 WFH day a week and to not WFH increases linearly, from 16% to 20% (a 25% increase) and 20% to 33% (a 69% surge), respectively. These results are unsurprising given that resource constraints such as a lack of software and/or hardware support can discourage employees from working from for a prolonged period of time. This can explain why the number of agents who choose to WFH 2 and ≥ 3 days a week decreases, and those preferring to WFH 1 or 0 day a week increases.

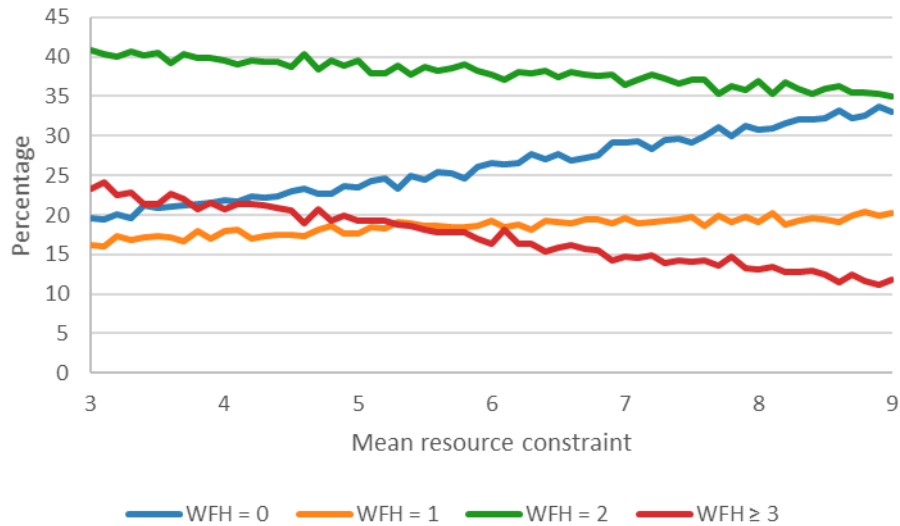


Figure 6-12 – Segregation of WFH preferences with varying mean resource constraint values

When more employees choose to return to the office and fewer employees prefer to WFH 2 and ≥ 3 days a week as the mean resource constraint value increases, the community level energy savings decreases (Figure 6-13). As more employees decide to work at the office, office and transportation related consumption of energy increases. The energy difference decreases from 630 GJ to 500 GJ (a 21% reduction) as the mean resource constraint value shifts from its minimum to its maximum.

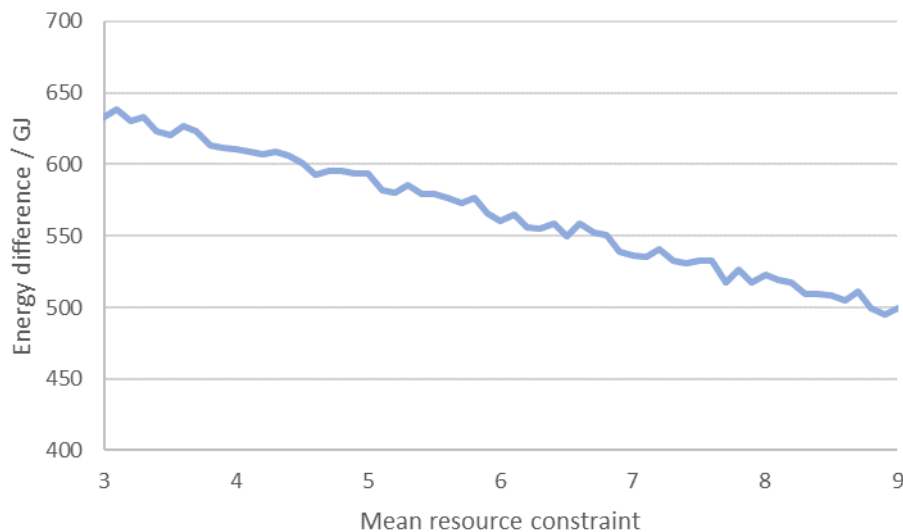


Figure 6-13 – Energy difference with varying mean resource constraint values

6.5.4 Scenario simulation – Personal stress tolerance

The fourth and final simulated scenario covers personal stress tolerance threshold. Based on COR theory, the model assumes that an agent experiences an elevation in stress when working from home in response to the presence of family related distractions and heightened difficulties in communicating with colleagues. When an agent’s personal stress tolerance threshold is exceeded, the agent will choose to return to the office and the stress level resets to 0. The simulation of this scenario investigates the impacts of personal stress tolerance on the WFH population.

As shown in Figure 6-14, when the personal stress tolerance threshold increases, the number of employees working at the office decreases significantly, from 73% to 59% (a 19% reduction). This may be because agents with higher stress tolerance can overcome WFH challenges more effectively and remain out of office.

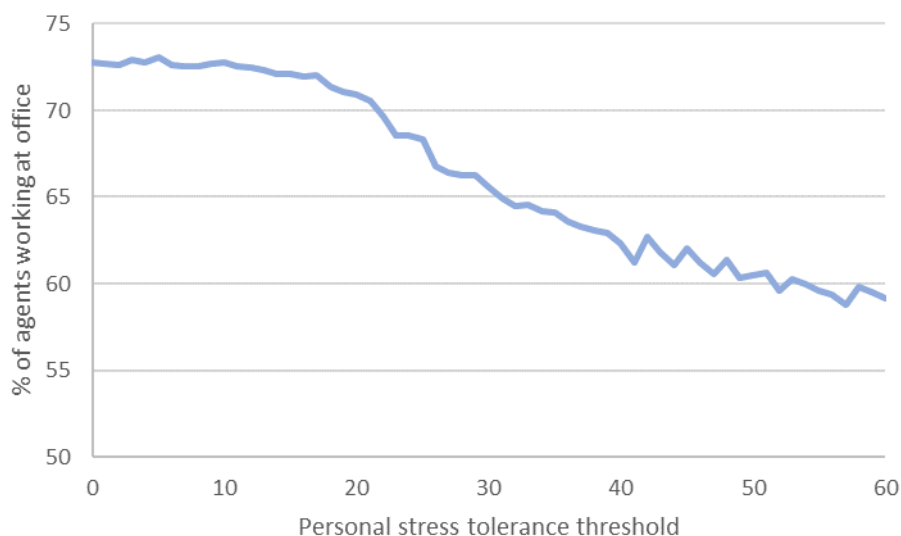


Figure 6-14 – Percentage of agents working at the office in the ABM with varying personal stress tolerance threshold values

A wide range of personal stress tolerance thresholds (0 to 60) is assigned in order to testify and allow the number of workers in each WFH preference group to reach a steady state (Figure 6-15). The number of agents choosing to WFH ≥ 3 days a week increases from 12% to 44% (a 265% surge) while the number of agents choosing to 2 WFH days a week decreases from 40% to 13% (a 67% reduction). This echoes with the COR theory, which was incorporated in the model, in which agents are more willing to WFH when they can withstand higher stress. The number of agents choosing 1 WFH day a week decreases slightly from 19% to 15% (a 24% reduction) owing to the similar reason likely due to the same tendency. Meanwhile the number of agents who opt for 0 WFH days remains relatively steady.

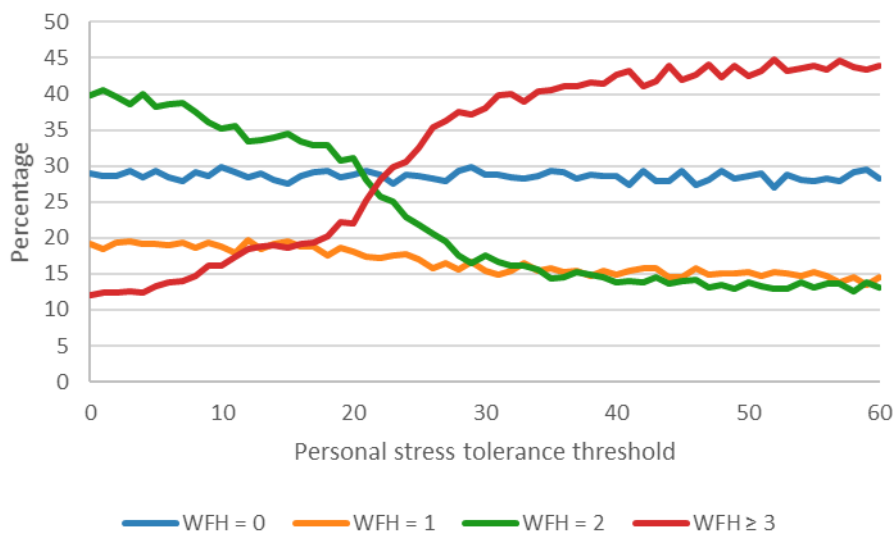


Figure 6-15 – Segregation of WFH preference with varying personal stress tolerance thresholds

Regarding to changes in community level energy consumption with respect to varying personal stress tolerance threshold, energy use further declines as more agents choose to WFH. The energy saving increases from 540 GJ to 770 GJ (a 42% increase), when agents have higher stress tolerance (Figure 6-16). Despite individual level energy consumption leading to higher

average residential energy consumption per capita when an agent chooses to WFH over working at office, the reduced transportation and office energy consumption leads to an overall larger reduction at the community level.

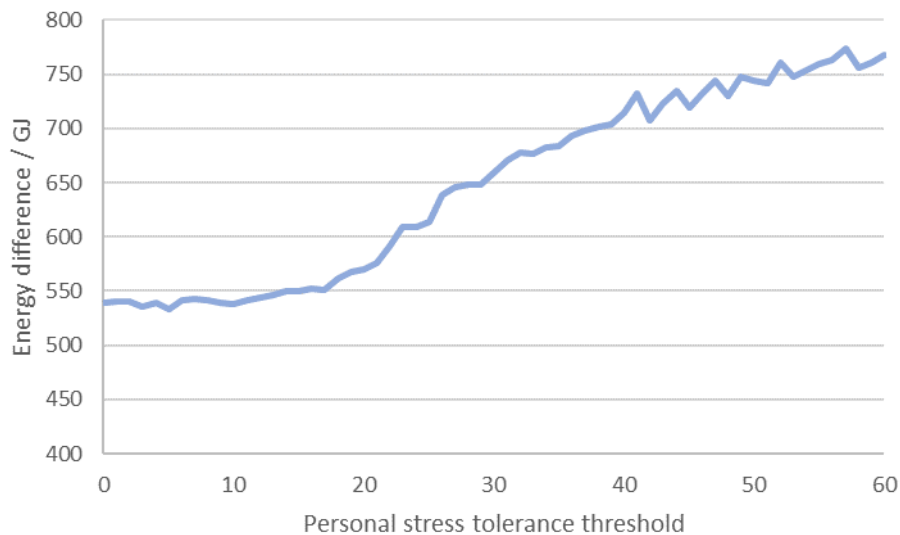


Figure 6-16 – Energy difference with varying personal stress tolerance thresholds

6.5.5 Model output comparisons with peers

We compared the above simulated scenario outputs with peer reports in order to verify the results’ credibility. According to a White Paper published by Randstad’s (global firm in the HR services industry) (Randstad, 2021), employees expect company policies to change after the pandemic. The paper indicates that 58% of employees expressed a desire for more WFH opportunities. This aligns with the results of the fourth scenario simulation examining personal stress thresholds, which show that approximately 60% of agents choose 2 or more WFH days a week as they overcome personal stress caused by the new WFH arrangement.

McKinsey & Company (a global management consulting firm) analysed the WFH potential of 2,000 tasks in more than 800 occupations and discussed the future of working from home

generally (McKinsey & Company, 2021). The analysis suggests that general office administrative and organisational activities could achieve up to 39% remote working as an effective potential with no productivity loss. Furthermore, workers in countries with advanced economies could allocate approximately 30% to 40% of their time to work remotely without compromising productivity. These figures correspond well with the results of all the scenario simulations, in which 30% to 40% of agents are predicted to choose to WFH. In the specific case of Hong Kong, a survey was conducted by the Hong Kong Productivity Council to explore the views of 600 employers and employees regarding the “Future of Work & Skills” (HKPC, 2021). The survey revealed that 72% of respondents stated that they would like their future job to allow hybrid work arrangements in the new normal. Again, this finding aligns with the simulation results.

6.5.6 Policy implications

The impacts of family influence, colleague influence, resource constraints, and personal stress tolerance on the WFH population are explored in the previous section. The simulation results suggest a number of policy implications for leveraging WFH as a soft solution to reduce community-level energy consumption in the post-pandemic era.

The first simulation shows that family distractions can negatively influence a worker’s willingness to WFH. In this regard, childcare and family support is critical to maintain balance within the household. During COVID-19, the caregiver industry faced restrictions in providing services due to social distancing (Christner *et al.*, 2021). However, these restrictions are expected to be lifted after the pandemic, which should be able to help alleviate workers’ family distractions. The second simulation reveals that difficulties in communicating with colleagues can discourage workers from choosing to WFH. Interdependence and task complexity can

affect can considerably impact the effectiveness of communication in virtual settings (Marlow, Lacerenza and Salas, 2017). To overcome this challenge, trainings can be offered to staff to better define work characteristics, including task interdependence and job autonomy (Wang *et al.*, 2021). For work that requires more collaboration, virtual meetings can serve as a platform for employees to communicate with each other and share ideas (Karl, Peluchette and Aghakhani, 2021).

The results of the third simulation indicate that the presence of resource constraints can also discourage workers from choosing to WFH. Both hardware and software are essential for successful WFH deployment, and relevant training should be properly administered to improve employees' skills and adaptiveness (Rachmawati *et al.*, 2021; Schade *et al.*, 2021). Financial subsidies could also be offered to improve workers' digital flexibility. For example, in Singapore, a grant is available for small and medium enterprises to procure laptops for remote working during COVID-19 in order to facilitate online collaboration and virtual meetings (IMDA, 2020). The final simulation suggests that improving personal stress tolerance can help a worker withstand WFH challenges and opt for additional WFH days. This underscores the importance of supporting employee health and well-being when they work at home. The level of employee agreeableness to WFH may differ across age, gender, industries, and job nature. Similarly, the degree of hardship associated with working from home may also vary for different people (Giménez-Nadal, Molina and Velilla, 2020). Supports for working from home should be comprehensive to reduce stress faced by staff, including organisational support, co-worker support, technical support, and boundary management support (Oakman *et al.*, 2020).

6.5.7 Limitations

The ABM runs on a 5-workday cycle. The model considers agent adaptiveness by introducing

a personal stress tolerance threshold. However, the model does not reflect adaptiveness over a longer term. In reality, workers may be able to get used to a new work arrangement in the long run, such that the stress and utility of WFH may wane over time. Or alternatively, employees who WFH may experience emotional benefits at first, and then feel exhaustion over the long term (Min *et al.*, 2021). Another limitation lies in the energy assessment. The assessment is based on an average energy consumption per capita. Ideally, a statistical distribution should be in place to reflect the variability among individuals. For instance, a previous study (Cerqueira *et al.*, 2020) argued that WFH may not necessarily lead to energy reduction as home-based workers may make more trips than non-home-based workers, for both work-related and other purposes such as leisure and social, leading to increased transportation emissions. The model does not capture such non-uniform behaviour and statistical data that is suitable for this study's application in representing such variations does not appear to be available. Given this limitation, the average energy consumption figure is adopted. Thirdly, it is well-acknowledged that there are other dimensions besides the social and environmental ones examined here to consider when evaluating the pros-and-cons of WFH. This study's policy recommendations mainly cover these two aspects as they are based on the ABM results and the objective of reducing environmental impacts. Additional dimensions such as macro-economic (Inoue, Murase and Todo, 2021), work efficiency (Ajjan, Fedorowicz and Owens, 2021), and the quality of parent-child relationships (Martucci, 2021) are not addressed in the present study design, despite their possible impacts on WFH decision-making.

6.6 Summary

An agent-based model (ABM) was developed to analyse post-pandemic WFH behaviours based on social theories. After performing calibration and validation of the base model, this study investigates emergent behaviour under different scenarios and the associated impact on

community level energy consumption. Taking into account the top-listed hurdles to deploying successful arrangements WFH as identified in the literature, scenario simulations were carried out to understand the impacts of social environment constraints (family influence and co-worker influences), resource constraints, and personal stress tolerance on WFH behaviour. The results generated from these simulations include 1) the proportion of employees choosing to work at the office, 2) the proportion of employees choosing to WFH, and 3) community level energy consumption in comparison with the case of business as usual. This study contributes to the understanding of socio-environmental aspect of WFH by 1) advancing our understanding of workers' decision-making processes in selecting their workplace based on behaviour theories, and 2) providing further supporting evidence for a soft solution, i.e. promoting WFH, to reduce the environmental impacts of commercial activities.

Regarding social environment constraints, this study demonstrates that the influence of family and colleague co-workers will discourage employees from working at home, both resulting in 8% more agents choosing the office over home as the workplace. Analysis on the proportion of agents choosing 0 to ≥ 3 WFH days a week shows that more agents tend to reduce their WFH days as they become more affected by social influences. Moreover, as family and colleague influences increase from minimum to maximum, the community level energy savings associated with working from home diminish by 15% and 8%, respectively. The results from the third simulation performed in this study also found that when employees receive less resource support, such as provision of hardware and software, they are more reluctant to WFH. The percentage of agents choosing to work at the office increases by 12% as the mean resource constraint value increases from its minimum to maximum. Fewer agents choose 2 and ≥ 3 WFH days and more agents choose 0 and 1 WFH day as the resource constraint increases. The community level energy savings associated with working from home fall by 21% as the

resource constraint value changes from the minimum to maximum. The final scenario simulation investigates the effect of personal stress tolerance thresholds. When agents become more tolerant to stress arising from WFH, which is deemed to be a new type of work arrangement, fewer agents decide to work at the office (a 19% reduction). More agents are willing to WFH for consecutive days (≥ 3 days) as they overcome personal stress and opt for additional WFH days. This resulted in a 42% increase in community level energy savings due to the reduction in office and transportation energy consumption. Analysis across all four simulated scenarios reveals that improving personal stress tolerance seems to be the most effective means for achieving more significant community level energy reduction. Table 6-5 provides a summary of scenario simulation results.

Table 6-5 – Summary of scenario simulations results as key decision-making factors strengthen

WFH decision-making factors	Changes in number of agents at office	Changes in number of segregation of WFH days	Changes in community level energy saving
Family influence	8% increase	0: 33% increase 1: relatively unaffected 2: 8% decrease ≥3: 36% decrease	15% decrease
Colleague influence	8% increase	0: 28% increase 1: relatively unaffected 2: 13% decrease ≥3: 27% decrease	14% decrease
Resource constraints	12% increase	0: 69% increase 1: 25% increase 2: 14% decrease ≥3: 49% decrease	21% decrease
Personal stress tolerance	19% decrease	0: relatively unaffected 1: 25% decrease 2: 67% decrease ≥3: 265% increase	42% increase

The results of the four scenario simulations are compared with peer reports to evaluate the credibility of the results. In addition, several policy recommendations are made in relation to family support, employee task management, hardware and software support, and personal stress management. The limitations of this study are also critically discussed.

Future research could concentrate on the WFH behaviour of different job types. The feasibility of enacting WFH arrangements may vary across different industries and economies. While this study mainly focuses on office work generally, further research on different jobs and activities would provide a more comprehensive understanding of WFH behaviour. Echoing with suggested limitations, further research can also capture a longer period for prolonged behaviour understanding, and model energy use via personalised profiles subject to individual lifestyle.

7. CONCLUSIONS AND SUGGESTIONS FOR FUTURE WORKS

7.1 Conclusions

This thesis is dedicated to UNSDG 7 “Affordable and Clean Energy”, for it provides a multi-aspect assessment on renewable energy microgrids, covering environmental, economic, technical, resilience and socio-environmental dimensions. The study leverages a wide range of established methodologies, including life cycle assessment, life cycle costing, building energy modelling, and agent-based modelling, in order to comprehensively understand the performance and feasibility of adopting renewable energy microgrids. Based on the results, the following conclusions can be drawn.

For environmental performance, we conducted an LCA case study of the Town Island Microgrid, the first standalone hybrid renewable energy commercial microgrid in Hong Kong, in comparison with 2 electrification options, including an on-site diesel generator system and a grid extension. Our results indicate that the Town Island Microgrid is the least environmentally impactful in the 8 impact categories out of 12. For instance, the global warming potential (GWP) of the diesel generator system and the grid extension are 4.3 times and 7.8 times greater than that caused by the microgrid, respectively. The EPBT found for the microgrid was 9.2 years, while the grid extension and the diesel generator EPBT values were 6.4 and 10.1 times longer than that of the microgrid, respectively. The case study provides substantial evidence that a microgrid solution can deliver a significantly superior life cycle environmental performance than other common electrification options.

In addition, an economic evaluation of renewable energy microgrids was carried out and recommendations for government policy-making are offered. We collected and synthesized publicly available data from 24 renewable energy microgrids worldwide, then present a set of

economic performance indicators including life-cycle cost, economies of scale and net present value. The investment cost and operating cost are calculated to be 2,135 USD/kW and 0.066 USD/kWh respectively, both figures being higher than those for pulverized-coal and natural gas. It is projected that, by 2025, the costs of renewable energy microgrids will begin to be competitive with non-renewable energy generation. The economies of scale factor is 0.9, which means although savings can still be enjoyed, the effect of economies of scale is weak. The net present value calculation reveals that investment in a renewable energy microgrid is not a profitable one. Based on the above results, recommendations for government policy-making are made. It is suggested that investment-based policies administered through government bodies may be more effective than production-based policies, though the two could complement each other in order to form a welcoming and sustainable renewable energy microgrid market.

To address technical factors, a systematic modelling framework is proposed for examining photovoltaic rooftops with varying roof availability and identifying peak shaving strategies for reducing peak load and carbon emissions. The framework incorporates computational simulations to model building power demand and evaluate different peak shaving strategies. By identifying building peak loads, peak shaving offsets part of the loads with photovoltaic electricity. This framework can be applied globally given suitable data, and is demonstrated on a 10-story reference office building with photovoltaic installations occupying 10%, 30%, and 50% of the roof area. In this demonstration, 9 peak shaving strategy options were considered for covering a varying number of peaks that last for different durations on weekdays. The peak load reductions and carbon emission savings of each option are assessed, and optimal peak shaving options are identified according to seasonal changes and area available for photovoltaics. For example, when 50% of a roof's area is available, a full-office-hour strategy

is proposed for the summer, saving approximately 595 kg CO₂ per weekday. In the winter, solar generation is reduced. A strategy proposed in this study that covers a full work day except lunch hours yields an estimated 271 kg in CO₂ savings per weekday. Based on these findings, policies are recommended to encourage utilization of existing rooftops, construct photovoltaic-ready roofs on new buildings, and guide urban planning to avoid excessive shading.

Resilience is as important as the above-mentioned aspects. The COVID-19 pandemic has introduced opportunities for more research in resilience as cities across the globe have experienced lockdowns, causing major divergences from conventional energy consumption patterns, especially in the residential sector. This study quantifies the increased energy demand resulting from work-from-home arrangements, using data on high-rise public residential buildings in Hong Kong, where its government mandated work-from-home arrangements four times in 2020. Building energy consumption was modelled to compare the total energy demand of residential units during normal and work-from-home arrangements, followed by validation against peer models and empirical data. We found a 9% residential energy demand increase, supporting the value of additional energy supply to enhance resilience. This study assesses the possibility of leveraging photovoltaic rooftops to supplement the increased energy demand. The potential contribution of photovoltaics to satisfying energy demand was estimated using solar energy simulation and evaluated in terms of such a photovoltaic system's ability to utilize its energy output to supplement the additional energy demand. The simulations demonstrated that, during the four work-from-home periods, a photovoltaic system could have met 6.8% to 11% of the increased energy demand, depending on the amount of energy consumed through air-conditioning operations and the energy generated through solar power. These findings are valuable for enhancing energy resilience as a component of future grid planning and operation.

In anticipation of a “new normal” in workplace arrangements, an agent-based model (ABM) was developed to analyse post-pandemic WFH behaviours based on social theories. This study investigates emergent behaviour under different scenarios and the associated impact on community level energy consumption. Scenario simulations were carried out to understand the impacts of environment constraints (family and colleague social influences), resource constraints, and personal stress tolerance on WFH behaviour. Analysis across all four simulated scenarios reveals that improving personal stress tolerance is the most effective means for achieving more significant community level energy reduction. When agents become more tolerant of stress arising from working from home, a transition which may inherently induce stress as a change from a previous routine, fewer agents decided to work at the office (a 19% reduction). More agents are willing to WFH for consecutive days (≥ 3 days) as they overcome personal stress and opt for additional WFH days. This resulted in a 42% increase in community level energy savings due to the reduction in office and transportation energy consumption.

7.2 Contributions of research

The major contribution of this research is the multi-aspect analysis (environmental, economic, technical, resilience, and socio-environmental) of renewable energy microgrids, in alignment with UNSDG 7. Owing to the multi-aspect character of the assessment, a wide range of assessment tools were deployed that are specific to each dimension of interest. The key contributions are summarized below.

Environmental

The case of the Town Island Microgrid is studied through conducting an LCA on and calculating the EPBT of the microgrid. This study represents the first comprehensive LCA study of the first standalone renewable energy commercial microgrid in Hong Kong. The findings are valuable for future microgrid projects that may be considered by electricity

operators, researchers, and policy makers in Hong Kong and other regions interested in microgrid deployment.

Economic

Compared to previous single case study research, this study more effectively assesses microgrid adoption by generalizing 24 microgrid projects worldwide spanning different capacities and different levels of renewable energy adoption. Furthermore, based on the performance indicator results, this study offers suggestions to help government decision making in crafting policies to fund renewable energy efforts, such as by determining the level of capital cost support, operating cost support (quantity-based policies), operating cost support (price-based policies), and differentiating measures to promote low and high capacity microgrids.

Technical

Not all existing buildings have sufficient roof space for PV panels because on-site renewables may not have been considered during their initial design. Among these buildings, available roof space varies and the potential to utilize these spaces is not well documented. The key contributions of this study include: the development and validation of a framework for measuring the performance of PV rooftops according to reduced peaks and avoided carbon emission, the identification of peak shaving strategies for PV electricity based on the size of the system, season, and building demand, and policy recommendations based on the findings in order to further promote PV integration.

Resilience

This study advances our understanding of the impact of work-from-home arrangements on residential energy consumption. The contributions are of long-term value as work-from-home

arrangements are expected to persist indefinitely as the general workforce has adapted to this practice during the pandemic. This study's outcomes can be drawn upon to inform efforts to bolster resilience as a component of future grid planning and operation.

Socio-environmental

This study develops an ABM to analyse post-pandemic WFH behaviours, simulating worker decision-making processes with the aid of social theories. This study closes the research gap by demonstrating the utility of ABM deployment in post-pandemic WFH analysis. This study offers some key insights into socio-environmental aspect of WFH, including worker decision-making processes in workplace selection based on behaviour theories, quantifying the variation of community level energy reduction according to various WFH arrangements.

7.3 Suggestions for future works

The thesis presents a multidimensional assessment of renewable energy microgrids. Corresponding future research recommendations are stated in each previous chapter. One additional suggestion for future study would be to apply all the forms of analysis performed in this study to one single renewable energy microgrid project simultaneously. Such a comprehensive analysis has not yet been conducted due to various practical obstacles including limited project availability, data accessibility and time sensitivity. In the future when data is more readily available, an assessment matrix could be developed to carry out a more integrated analysis of renewable energy microgrid performance. Ideally, the scope of such an assessment matrix would be expanded geographically to cover both urban and rural areas, as renewable energy microgrids can support decarbonization in both of these contexts. Weightings of each dimension can be defined on a case-by-case basis, subject to the project's priorities.

8. REFERENCES

- Aalto, P. *et al.* (2012) 'How are Russian energy policies formulated? Linking the actors and structures of energy policy', in *Russia's Energy Policies: National, Interregional and Global Levels*. Edward Elgar Publishing, pp. 20–42. doi: 10.4337/9781781001202.00011.
- Abbasi, S. A. and Abbasi, N. (2000) 'The likely adverse environmental impacts of renewable energy sources', in *Applied Energy*. Elsevier, pp. 121–144. Available at: [https://www-sciencedirect-com.ezproxy.lb.polyu.edu.hk/science/article/pii/S030626199900077X](https://www.sciencedirect.com.ezproxy.lb.polyu.edu.hk/science/article/pii/S030626199900077X) (Accessed: 24 February 2019).
- Abdeen, A. *et al.* (2021) 'The impact of the COVID-19 on households' hourly electricity consumption in Canada', *Energy and Buildings*. Elsevier, 250, p. 111280. doi: 10.1016/J.ENBUILD.2021.111280.
- Abdullah, W. S. W. *et al.* (2019) 'The Potential and Status of Renewable Energy Development in Malaysia', *Energies 2019, Vol. 12, Page 2437*. Multidisciplinary Digital Publishing Institute, 12(12), p. 2437. doi: 10.3390/EN12122437.
- VanAcker, V. *et al.* (2014) 'Survey of energy use and costs in rural Kenya for community microgrid business model development', in *Proceedings of the 4th IEEE Global Humanitarian Technology Conference, GHTC 2014*. IEEE, pp. 166–173. doi: 10.1109/GHTC.2014.6970277.
- Acuña, L. G., Padilla, R. V. and Mercado, A. S. (2017) 'Measuring reliability of hybrid photovoltaic-wind energy systems: A new indicator', *Renewable Energy*. Pergamon, 106, pp. 68–77. doi: 10.1016/J.RENENE.2016.12.089.
- Adefarati, T. and Bansal, R. C. (2019a) 'Economic and environmental analysis of a co-generation power system with the incorporation of renewable energy resources', in *Energy Procedia*. Elsevier, pp. 803–808. doi: 10.1016/j.egypro.2019.01.212.
- Adefarati, T. and Bansal, R. C. (2019b) 'Reliability, economic and environmental analysis of

a microgrid system in the presence of renewable energy resources', *Applied Energy*. Elsevier, 236, pp. 1089–1114. doi: 10.1016/J.APENERGY.2018.12.050.

Aelenei, D. *et al.* (2019) 'Investigating the potential for energy flexibility in an office building with a vertical BIPV and a PV roof system', *Renewable Energy*. Elsevier Ltd, pp. 189–197. doi: 10.1016/j.renene.2018.07.140.

Afrianty, T. W., Artatanaya, I. G. L. S. and Burgess, J. (2021) 'Working from home effectiveness during Covid-19: Evidence from university staff in Indonesia', *Asia Pacific Management Review*. Elsevier. doi: 10.1016/J.APMRV.2021.05.002.

Ajaz, W. (2019) 'Resilience, environmental concern, or energy democracy? A panel data analysis of microgrid adoption in the United States', *Energy Research and Social Science*, 49, pp. 26–35. doi: 10.1016/j.erss.2018.10.027.

Ajjan, S., Fedorowicz, H. and Owens, J. (2021) 'How Working from Home during COVID-19 Affects Academic Productivity', *Communications of the Association for Information Systems*, 48, p. pp-pp. doi: 10.17705/1CAIS.04808.

Akinyele, D. O. (2017) 'Environmental performance evaluation of a grid-independent solar photovoltaic power generation (SPPG) plant', *Energy*. Pergamon, 130, pp. 515–529.

Available at: [https://www.sciencedirect-com.ezproxy.lb.polyu.edu.hk/science/article/pii/S0360544217306928](https://www.sciencedirect.com.ezproxy.lb.polyu.edu.hk/science/article/pii/S0360544217306928) (Accessed: 24February2019).

Al-Shahri, O. A. *et al.* (2021) 'Solar photovoltaic energy optimization methods, challenges and issues: A comprehensive review', *Journal of Cleaner Production*. Elsevier, 284, p. 125465. doi: 10.1016/J.JCLEPRO.2020.125465.

Alajdin, A., Iljas, I. and Darko, S. (2011) 'From A Climate Action Plan (CAP) to a Microgrid: The SEEU Sustainability Concept Including Social Aspects', *Academicus International Scientific Journal*, 4, pp. 42–59. doi: 10.7336/academicus.2011.04.03.

- Ali, A., Li, W., Hussain, R., He, X., Williams, Barry W., *et al.* (2017) ‘Overview of current microgrid policies, incentives and barriers in the European Union, United States and China’, *Sustainability (Switzerland)*. Available at: www.mdpi.com/journal/sustainability (Accessed: 24February2019).
- Ali, A., Li, W., Hussain, R., He, X., Williams, Barry W., *et al.* (2017) ‘Overview of current microgrid policies, incentives and barriers in the European Union, United States and China’, *Sustainability (Switzerland)*, p. 1146. doi: 10.3390/su9071146.
- Alizada, K. (2018) ‘Rethinking the diffusion of renewable energy policies: A global assessment of feed-in tariffs and renewable portfolio standards’, *Energy Research and Social Science*, 44, pp. 346–361. doi: 10.1016/j.erss.2018.05.033.
- Alsema, E. A. (2000) ‘Energy pay-back time and CO₂ emissions of PV systems’, *Progress in Photovoltaics: Research and Applications*. John Wiley & Sons, Ltd, 8(1), pp. 17–25. Available at: <http://doi.wiley.com/10.1002/%28SICI%291099-159X%28200001/02%298%3A1%3C17%3A%3AAID-PIP295%3E3.0.CO%3B2-C> (Accessed: 24February2019).
- Anderson, J. E., Wulforst, G. and Lang, W. (2015) ‘Energy analysis of the built environment - A review and outlook’, *Renewable and Sustainable Energy Reviews*. Elsevier Ltd, pp. 149–158. doi: 10.1016/j.rser.2014.12.027.
- Anvari-Moghaddam, A. *et al.* (2017) ‘A multi-agent based energy management solution for integrated buildings and microgrid system’, *Applied Energy*. Elsevier, 203, pp. 41–56. doi: 10.1016/j.apenergy.2017.06.007.
- Arpan, L. M. *et al.* (2018) ‘Politics, values, and morals: Assessing consumer responses to the framing of residential renewable energy in the United States’, *Energy Research and Social Science*, 46, pp. 321–331. doi: 10.1016/j.erss.2018.08.007.
- Arriaga, M., Cañizares, C. A. and Kazerani, M. (2016) ‘Long-term renewable energy planning

model for remote communities’, *IEEE Transactions on Sustainable Energy*, 7(1), pp. 221–231. doi: 10.1109/TSTE.2015.2483489.

Athanasiadou, C. and Theriou, G. (2021) ‘Telework: systematic literature review and future research agenda’, *Heliyon*. Elsevier, 7(10), p. e08165. doi: 10.1016/j.heliyon.2021.e08165.

Baljit, S. S. S., Chan, H. Y. and Sopian, K. (2016a) ‘Review of building integrated applications of photovoltaic and solar thermal systems’, *Journal of Cleaner Production*, pp. 677–689. doi: 10.1016/j.jclepro.2016.07.150.

Baljit, S. S. S., Chan, H. Y. and Sopian, K. (2016b) ‘Review of building integrated applications of photovoltaic and solar thermal systems’, *Journal of Cleaner Production*. Elsevier, 137, pp. 677–689. doi: 10.1016/J.JCLEPRO.2016.07.150.

Ban-Weiss, G. *et al.* (2013) ‘Electricity production and cooling energy savings from installation of a building-integrated photovoltaic roof on an office building’, *Energy and Buildings*. Elsevier, 56, pp. 210–220. doi: 10.1016/j.enbuild.2012.06.032.

Barnes, M. and Korba, P. (2010) ‘Smartgrids: Microgrid Systems’, *Intelligent Automation & Soft Computing*. Taylor & Francis Group, 16(2), pp. 195–198. Available at: <http://autosoftjournal.net/paperShow.php?paper=10643075> (Accessed: 24 February 2019).

Basak, P. *et al.* (2012) ‘A literature review on integration of distributed energy resources in the perspective of control, protection and stability of microgrid’, *Renewable and Sustainable Energy Reviews*. Pergamon, pp. 5545–5556. doi: 10.1016/j.rser.2012.05.043.

Basu, A. K. *et al.* (2011) ‘Microgrids: Energy management by strategic deployment of DERs - A comprehensive survey’, *Renewable and Sustainable Energy Reviews*. Pergamon, pp. 4348–4356. doi: 10.1016/j.rser.2011.07.116.

Bhowmik, C. *et al.* (2017) ‘Optimal green energy planning for sustainable development: A review’, *Renewable and Sustainable Energy Reviews*, pp. 796–813. doi: 10.1016/j.rser.2016.12.105.

- Bielecki, S. *et al.* (2021) ‘Impact of the lockdown during the covid-19 pandemic on electricity use by residential users’, *Energies*. MDPI AG, 14(4). doi: 10.3390/EN14040980.
- Bilich, A. *et al.* (2017) ‘Life Cycle Assessment of Solar Photovoltaic Microgrid Systems in Off-Grid Communities’, *Environmental Science & Technology*. American Chemical Society, 51(2), pp. 1043–1052. Available at: <http://pubs.acs.org/doi/10.1021/acs.est.6b05455> (Accessed: 24February2019).
- Binet, M. T. *et al.* (2018) ‘Toxicity of nickel to tropical freshwater and sediment biota: A critical literature review and gap analysis’, *Environmental Toxicology and Chemistry*. John Wiley & Sons, Ltd, 37(2), pp. 293–317. Available at: <http://doi.wiley.com/10.1002/etc.3988> (Accessed: 24February2019).
- Block, P. *et al.* (2020) ‘Social network-based distancing strategies to flatten the COVID-19 curve in a post-lockdown world’, *Nature Human Behaviour*. Nature Publishing Group, 4(6), pp. 588–596. doi: 10.1038/s41562-020-0898-6.
- Bornschlegl, M., Bregulla, M. and Franke, J. (2016) ‘Methods-Energy Measurement – An approach for sustainable energy planning of manufacturing technologies’, *Journal of Cleaner Production*, 135, pp. 644–656. doi: 10.1016/j.jclepro.2016.06.059.
- Boute, A. (2012) ‘Promoting renewable energy through capacity markets: An analysis of the Russian support scheme’, *Energy Policy*, 46, pp. 68–77. doi: 10.1016/j.enpol.2012.03.026.
- Braun, B. *et al.* (2020) ‘Simulating phase transitions and control measures for network epidemics caused by infections with presymptomatic, asymptomatic, and symptomatic stages’, *PLoS ONE*. Public Library of Science, 15(9 September), p. e0238412. doi: 10.1371/journal.pone.0238412.
- Braun, P. and Rüter, R. (2010) ‘The role of grid-connected, building-integrated photovoltaic generation in commercial building energy and power loads in a warm and sunny climate’, *Energy Conversion and Management*. Pergamon, 51(12), pp. 2457–2466. doi:

10.1016/j.enconman.2010.04.013.

Brown, E. G. (2018) *Final Project Report California Energy Commission Microgrid Analysis and Case Studies Report California, North America, and Global Case Studies*. Available at: www.energy.ca.gov/research/ (Accessed: 6April2019).

tenBrummelhuis, L. L. and Bakker, A. B. (2012) 'A resource perspective on the work-home interface: The work-home resources model', *American Psychologist*, 67(7), pp. 545–556. doi: 10.1037/A0027974.

Burke, M. J. and Stephens, J. C. (2018) 'Political power and renewable energy futures: A critical review', *Energy Research and Social Science*, 35, pp. 78–93. doi: 10.1016/j.erss.2017.10.018.

Burnett, J. (2004) 'Indoor environments in Hong Kong's high-rise residential buildings', in *International Housing Conference in Hong Kong 2004 - Housing in the 21st Century: Challenges and Commitments, Hong Kong, 2-4 February 2004*. Available at: <http://ira.lib.polyu.edu.hk/handle/10397/42045> (Accessed: 11July2021).

Burr, M. T. *et al.* (2014) 'Emerging models for microgrid finance: Driven by the need to deliver value to end users', *IEEE Electrification Magazine*, 2(1), pp. 30–39. doi: 10.1109/MELE.2013.2297022.

Byrne, J. *et al.* (2017) 'Multivariate analysis of solar city economics: impact of energy prices, policy, finance, and cost on urban photovoltaic power plant implementation', *Wiley Interdisciplinary Reviews: Energy and Environment*, p. e241. doi: 10.1002/wene.241.

Byrnes, L. *et al.* (2013) 'Australian renewable energy policy: Barriers and challenges', *Renewable Energy*, 60, pp. 711–721. doi: 10.1016/j.renene.2013.06.024.

C&SD HK (2020a) *Labour Force, Unemployment and Underemployment*. Available at: https://www.censtatd.gov.hk/en/web_table.html?id=6# (Accessed: 13November2021).

C&SD HK (2020b) *Statistics on Domestic Households*. Available at:

- https://www.censtatd.gov.hk/en/web_table.html?id=5 (Accessed: 21November2021).
- Carroll, N. and Conboy, K. (2020) 'Normalising the "new normal": Changing tech-driven work practices under pandemic time pressure', *International Journal of Information Management*. Pergamon, 55, p. 102186. doi: 10.1016/j.ijinfomgt.2020.102186.
- Cash, D. W. (2018) 'Choices on the road to the clean energy future', *Energy Research and Social Science*, 35, pp. 224–226. doi: 10.1016/j.erSS.2017.10.035.
- Cellura, M. *et al.* (2012) 'Photovoltaic electricity scenario analysis in urban contexts: An Italian case study', *Renewable and Sustainable Energy Reviews*, 16, pp. 2041–2052. doi: 10.1016/j.rser.2012.01.032.
- Census and Statistics Department (2016) *Snapshot of Hong Kong Population | 2016 Population By-census*. Available at: <https://www.byCensus2016.gov.hk/en/Snapshot-04.html> (Accessed: 15August2021).
- Cerqueira, E. D. V. *et al.* (2020) 'Does working from home reduce CO2 emissions? An analysis of travel patterns as dictated by workplaces', *Transportation Research Part D: Transport and Environment*. Pergamon, 83, p. 102338. doi: 10.1016/J.TRD.2020.102338.
- Chan, A. L. S. *et al.* (2006a) 'Generation of a typical meteorological year for Hong Kong', *Energy Conversion and Management*, 47(1), pp. 87–96. doi: 10.1016/j.enconman.2005.02.010.
- Chan, A. L. S. *et al.* (2006b) 'Generation of a typical meteorological year for Hong Kong', *Energy Conversion and Management*. Elsevier Ltd, 47(1), pp. 87–96. doi: 10.1016/J.ENCONMAN.2005.02.010.
- Chan, D. W. M. and Chan, A. P. C. (2011) 'Architectural Science Review Public Housing Construction in Hong Kong: A Review of its Design and Construction Innovations Public Housing Construction in Hong Kong: A Review of its Design and Construction Innovations', *Architectural Science Review*, 45, pp. 349–359. doi: 10.1080/00038628.2002.9696950.

Chen, X. *et al.* (2019) ‘What are the root causes hindering the implementation of green roofs in urban China?’, *Science of the Total Environment*. Elsevier B.V., 654, pp. 742–750. doi: 10.1016/j.scitotenv.2018.11.051.

Cheshmehzangi, A. (2020) ‘COVID-19 and household energy implications: what are the main impacts on energy use?’, *Heliyon*. Elsevier, 6(10), p. e05202. doi: 10.1016/J.HELIYON.2020.E05202.

Christner, N. *et al.* (2021) ‘Children’s psychological well-being and problem behavior during the COVID-19 pandemic: An online study during the lockdown period in Germany’, *PLoS ONE*. Public Library of Science, 16(6 June), p. e0253473. doi: 10.1371/journal.pone.0253473.

Chung, H. *et al.* (2020) *Working from home during the COVID-19 lockdown: Changing preferences and the future of work*.

Chung, W. and Hui, Y.V. (2009) ‘A study of energy efficiency of private office buildings in Hong Kong’, *Energy and Buildings*. Elsevier, 41(6), pp. 696–701. doi: 10.1016/j.enbuild.2009.02.001.

CLP (2010) *CLP’s First Off-grid Commercial RE Supply Project for Dawn Island 2 CLP’s First Off-grid Commercial RE Supply Project for Dawn Island*. Available at: https://www.emsd.gov.hk/minisites/symposium/2011/session/ppt/E1_PPT_Paul Poon.pdf (Accessed: 24February2019).

CLP (2019) *Science and Technology | New Horizons | CLP Group*. Available at: <https://www.clpgroup.com/newhorizons/Pages/article2.aspx?sectionId=TS&articleId=6> (Accessed: 24February2019).

CLP (2020) *2020 Annual Report*.

CLP Holdings (2020) *CLP Holdings 2020 Annual Report*.

Connor, P. M. *et al.* (2014) ‘Policy and regulation for smart grids in the United Kingdom’,

Renewable and Sustainable Energy Reviews, pp. 269–286. doi: 10.1016/j.rser.2014.07.065.

Crawley, D. B. *et al.* (2001) ‘EnergyPlus: creating a new-generation building energy simulation program’, *Energy and Buildings*. Elsevier, 33(4), pp. 319–331. doi: 10.1016/S0378-7788(00)00114-6.

Cuevas, E. (2020) ‘An agent-based model to evaluate the COVID-19 transmission risks in facilities’, *Computers in Biology and Medicine*. Pergamon, 121, p. 103827. doi: 10.1016/J.COMPBIOMED.2020.103827.

Dallmann, T. R. *et al.* (2014) ‘Characterization of particulate matter emissions from on-road gasoline and diesel vehicles using a soot particle aerosol mass spectrometer’, *Atmospheric Chemistry and Physics*, 14(14), pp. 7585–7599. doi: 10.5194/acp-14-7585-2014.

Darghouth, N. R., Barbose, G. and Wiser, R. H. (2014) ‘Customer-economics of residential photovoltaic systems (Part 1): The impact of high renewable energy penetrations on electricity bill savings with net metering’, *Energy Policy*, 67, pp. 290–300. doi: 10.1016/j.enpol.2013.12.042.

Darko, A. *et al.* (2017) ‘Examining issues influencing green building technologies adoption: The United States green building experts’ perspectives’, *Energy and Buildings*. Elsevier Ltd, 144, pp. 320–332. doi: 10.1016/j.enbuild.2017.03.060.

Darouei, M. and Pluut, H. (2021) ‘Work from home today for a better tomorrow! How working from home influences work-family conflict and employees’ start of the next workday’, *Stress and Health*. John Wiley & Sons, Ltd. doi: 10.1002/SMI.3053.

Das, J. *et al.* (2018a) ‘Life cycle energy and carbon footprint analysis of photovoltaic battery microgrid system in India’, *Clean Technologies and Environmental Policy*, 20, pp. 65–80. Available at: <https://doi.org/10.1007/s10098-017-1456-4> (Accessed: 24 February 2019).

Das, J. *et al.* (2018b) ‘Life cycle energy and carbon footprint analysis of photovoltaic battery microgrid system in India’, *Clean Technologies and Environmental Policy*, 20, pp. 65–80.

doi: 10.1007/s10098-017-1456-4.

Dato, P., Durmaz, T. and Pommeret, A. (2021) 'Feed-in tariff policy in Hong Kong: Is it efficient?', *City and Environment Interactions*. Elsevier, 10, p. 100056. doi:

10.1016/J.CACINT.2021.100056.

Dawoud, S. M., Lin, X. and Okba, M. I. (2018) 'Hybrid renewable microgrid optimization techniques: A review', *Renewable and Sustainable Energy Reviews*. Pergamon, pp. 2039–2052. doi: 10.1016/j.rser.2017.08.007.

Deng, Y., Chan, E. H. W. and Poon, S. W. (2016) 'Challenge-driven design for public housing: The case of Hong Kong', *Frontiers of Architectural Research*. Elsevier, 5(2), pp. 213–224. doi: 10.1016/J.FOAR.2016.05.001.

Díaz López, C. *et al.* (2019) 'A comparative analysis of sustainable building assessment methods', *Sustainable Cities and Society*. Elsevier Ltd, 49, p. 101611. doi:

10.1016/j.scs.2019.101611.

Dohn, R. L. (2011) *The business case for microgrids The new face of energy modernization*.

Available at: [https://w3.usa.siemens.com/smartgrid/us/en/microgrid/Documents/The business case for microgrids_Siemens white paper.pdf](https://w3.usa.siemens.com/smartgrid/us/en/microgrid/Documents/The%20business%20case%20for%20microgrids_Siemens%20white%20paper.pdf) (Accessed: 6 April 2019).

Du, J. and Pan, W. (2021) 'Diverse occupant behaviors and energy conservation opportunities for university student residences in Hong Kong', *Building and Environment*. Pergamon, 195, p. 107730. doi: 10.1016/J.BUILDENV.2021.107730.

Du, J., Yu, C. and Pan, W. (2020) 'Multiple influencing factors analysis of household energy consumption in high-rise residential buildings: Evidence from Hong Kong', *Building Simulation*, 13(4), pp. 753–769. doi: 10.1007/s12273-020-0630-5.

Du, M. (2021) 'Mitigating COVID-19 on a small-world network', *Scientific Reports*. Nature Publishing Group, 11(1), pp. 1–9. doi: 10.1038/s41598-021-99607-z.

EMA Singapore (2019) *EMA / Singapore Energy Statistics - Energy Transformation*.

Available at: <https://www.ema.gov.sg/Singapore-Energy-Statistics-2019/Ch02/index2>

(Accessed: 1 August 2020).

EMSD HK (2007) *Guidelines on Performance-based Building Energy Code 2007 Edition*.

EMSD HK (2018) *Code of Practice for Energy Efficiency of Building Services Installation 2018*.

EMSD HK (2020a) *Energy Utilization Index - Commercial Sector*. Available at:

<https://ecib.emsd.gov.hk/index.php/en/energy-utilisation-index-en/commercial-sector-en>

(Accessed: 26 July 2020).

EMSD HK (2020b) *Hong Kong Energy End-use Data 2020*.

Environment Bureau (2015) *Energy Saving Plan For Hong Kong's Built Environment 2015~2025+*.

EPD HK and EMSD HK (2010) *Guidelines to Account for and Report on Greenhouse Gas Emissions and Removals for Buildings (Commercial, Residential or Institutional Purposes) in Hong Kong*.

Ernest Orlando Lawrence Berkeley National Laboratory (2010) 'Methods for Analyzing Electric Load Shape and its Variability', *California Energy Commission*, (May), pp. 1–63.

Available at: <http://eta-publications.lbl.gov/sites/default/files/LBNL-3713E.pdf> (Accessed: 24 February 2019).

Faber, I. *et al.* (2014) 'Micro-energy markets: The role of a consumer preference pricing strategy on microgrid energy investment', *Energy*, 74(C), pp. 567–575. doi:

10.1016/j.energy.2014.07.022.

Finenko, A. and Cheah, L. (2016) 'Temporal CO₂ emissions associated with electricity generation: Case study of Singapore', *Energy Policy*. Elsevier Ltd, 93, pp. 70–79. doi:

10.1016/j.enpol.2016.02.039.

Fong, K. F., Lee, C. K. and Chow, T. T. (2012) 'Comparative study of solar cooling systems

with building-integrated solar collectors for use in sub-tropical regions like Hong Kong', *Applied Energy*. Elsevier Ltd, 90(1), pp. 189–195. doi: 10.1016/j.apenergy.2011.06.013.

Fthenakis, V. *et al.* (2011) *Methodology Guidelines on Life Cycle Assessment of Photovoltaic Electricity*. Available at: http://www.iea-pvps.org/fileadmin/dam/public/report/technical/rep12_11.pdf (Accessed: 24February2019).

Fthenakis, V. M., Kim, H. C. and Alsema, E. (2008) 'Emissions from Photovoltaic Life Cycles', *Environmental Science & Technology*. American Chemical Society, 42(6), pp. 2168–2174. Available at: <http://pubs.acs.org/doi/abs/10.1021/es071763q> (Accessed: 24February2019).

Fu, F. and Wang, Q. (2011) 'Removal of heavy metal ions from wastewaters: A review', *Journal of Environmental Management*. Academic Press, pp. 407–418. Available at: <https://www-sciencedirect-com.ezproxy.lb.polyu.edu.hk/science/article/pii/S0301479710004147> (Accessed: 24February2019).

Fu, Y., Liu, X. and Yuan, Z. (2015) 'Life-cycle assessment of multi-crystalline photovoltaic (PV) systems in China', *Journal of Cleaner Production*. Elsevier, 86, pp. 180–190. Available at: <https://www-sciencedirect-com.ezproxy.lb.polyu.edu.hk/science/article/pii/S0959652614007859> (Accessed: 24February2019).

Fu, Z. *et al.* (2016) 'A distributed continuous time consensus algorithm for maximize social welfare in micro grid', *Journal of the Franklin Institute*, 353(15), pp. 3966–3984. doi: 10.1016/j.jfranklin.2016.07.009.

Fumo, N., Mago, P. and Luck, R. (2010) 'Methodology to estimate building energy consumption using EnergyPlus Benchmark Models', *Energy and Buildings*. Elsevier, 42(12), pp. 2331–2337. doi: 10.1016/J.ENBUILD.2010.07.027.

Fürsch, M. *et al.* (2013) 'The role of grid extensions in a cost-efficient transformation of the European electricity system until 2050', *Applied Energy*. Elsevier, 104, pp. 642–652.

Available at: [https://www.sciencedirect-com.ezproxy.lb.polyu.edu.hk/science/article/pii/S0306261912008537](https://www.sciencedirect.com.ezproxy.lb.polyu.edu.hk/science/article/pii/S0306261912008537) (Accessed: 24February2019).

Galanti, T. *et al.* (2021) 'Work from home during the COVID-19 outbreak: The impact on employees' remote work productivity, engagement, and stress', *Journal of Occupational and Environmental Medicine*. Wolters Kluwer Health, 63(7), pp. E426–E432. doi: 10.1097/JOM.0000000000002236.

Gallo, M. *et al.* (2016) 'Optimal Planning of Sustainable Buildings: Integration of Life Cycle Assessment and Optimization in a Decision Support System (DSS)', *Energies*, 9(7), p. 490. Available at: www.mdpi.com/journal/energies (Accessed: 24February2019).

Galvan, E., Mandal, P. and Sang, Y. (2020) 'Networked microgrids with roof-top solar PV and battery energy storage to improve distribution grids resilience to natural disasters', *International Journal of Electrical Power & Energy Systems*. Elsevier, 123, p. 106239. doi: 10.1016/J.IJEPES.2020.106239.

Gao, H., Koch, C. and Wu, Y. (2019) 'Building information modelling based building energy modelling: A review', *Applied Energy*. Elsevier, 238, pp. 320–343. doi: 10.1016/J.APENERGY.2019.01.032.

Gaona, E. E., Trujillo, C. L. and Guacaneme, J. A. (2015) 'Rural microgrids and its potential application in Colombia', *Renewable and Sustainable Energy Reviews*, pp. 125–137. doi: 10.1016/j.rser.2015.04.176.

García-Plaza, M. *et al.* (2018) 'Peak shaving algorithm with dynamic minimum voltage tracking for battery storage systems in microgrid applications', *Journal of Energy Storage*, 20, pp. 41–48. doi: 10.1016/j.est.2018.08.021.

Gerbinet, S., Belboom, S. and Léonard, A. (2014a) 'Life Cycle Analysis (LCA) of photovoltaic panels: A review', *Renewable and Sustainable Energy Reviews*. Pergamon, pp. 747–753. Available at: <https://www.sciencedirect-com.ezproxy.lb.polyu.edu.hk/science/article/pii/S136403211400495X?via%3Dihub> (Accessed: 13May2019).

Gerbinet, S., Belboom, S. and Léonard, A. (2014b) 'Life Cycle Analysis (LCA) of photovoltaic panels: A review', *Renewable and Sustainable Energy Reviews*. Pergamon, pp. 747–753. Available at: <https://www.sciencedirect-com.ezproxy.lb.polyu.edu.hk/science/article/pii/S136403211400495X> (Accessed: 24February2019).

Giménez-Nadal, J. I., Molina, J. A. and Velilla, J. (2020) 'Work time and well-being for workers at home: evidence from the American Time Use Survey', *International Journal of Manpower*. Emerald Group Holdings Ltd., 41(2), pp. 184–206. doi: 10.1108/IJM-04-2018-0134.

Giraldez, J. *et al.* (2018) *Phase I Microgrid Cost Study: Data Collection and Analysis of Microgrid Costs in the United States*. Available at: <https://www.nrel.gov/docs/fy19osti/67821.pdf>. (Accessed: 13January2020).

Gómez-Navarro, T. *et al.* (2021) 'Analysis of the potential for PV rooftop prosumer production: Technical, economic and environmental assessment for the city of Valencia (Spain)', *Renewable Energy*. Pergamon, 174, pp. 372–381. doi: 10.1016/J.RENENE.2021.04.049.

Góralczyk, M. (2003) 'Life-cycle assessment in the renewable energy sector', *Applied Energy*. Elsevier, 75(3–4), pp. 205–211. Available at: <https://www.sciencedirect-com.ezproxy.lb.polyu.edu.hk/science/article/pii/S0306261903000333> (Accessed: 24February2019).

- Goswami, D. Yogi. (2015) *Principles of solar engineering*. Available at:
https://books.google.nl/books/about/Principles_of_Solar_Engineering_Third_Ed.html?id=sOn-ugAACAAJ&source=kp_book_description&redir_esc=y.
- Goswami, D. Yogi (2015) *Principles of Solar Engineering Third Edition*. CRC Press, Taylor & Francis Group.
- Gottlieb, C. *et al.* (2021) ‘Working from home in developing countries’, *European Economic Review*. North-Holland, 133, p. 103679. doi: 10.1016/J.EUROECOREV.2021.103679.
- Graff Zivin, J. S., Kotchen, M. J. and Mansur, E. T. (2014) ‘Spatial and temporal heterogeneity of marginal emissions: Implications for electric cars and other electricity-shifting policies’, *Journal of Economic Behavior and Organization*. Elsevier, 107(PA), pp. 248–268. doi: 10.1016/j.jebo.2014.03.010.
- Grandey, A. A. and Cropanzano, R. (1999) ‘The Conservation of Resources Model Applied to Work–Family Conflict and Strain’, *Journal of Vocational Behavior*. Academic Press, 54(2), pp. 350–370. doi: 10.1006/JVBE.1998.1666.
- Green, N., Mueller-Stoffels, M. and Whitney, E. (2017) ‘An Alaska case study: Diesel generator technologies’, *Journal of Renewable and Sustainable Energy*. AIP Publishing LLC, 9(6), p. 061701. Available at: <http://aip.scitation.org/doi/10.1063/1.4986585> (Accessed: 24 February 2019).
- Greening, B. and Azapagic, A. (2013) ‘Environmental impacts of micro-wind turbines and their potential to contribute to UK climate change targets’, *Energy*. Pergamon, 59, pp. 454–466. Available at: <https://www.sciencedirect-com.ezproxy.lb.polyu.edu.hk/science/article/pii/S0360544213005355> (Accessed: 24 February 2019).
- Grimm, V. *et al.* (2020) ‘The ODD protocol for describing agent-based and other simulation models: A second update to improve clarity, replication, and structural realism’, *JASSS*,

23(2). doi: 10.18564/jasss.4259.

Gu, W. *et al.* (2014) 'Modeling, planning and optimal energy management of combined cooling, heating and power microgrid: A review', *International Journal of Electrical Power and Energy Systems*. Pergamon, 54, pp. 26–37. doi: 10.1016/j.ijepes.2013.06.028.

Guezuraga, B., Zauner, R. and Pölz, W. (2012) 'Life cycle assessment of two different 2 MW class wind turbines', *Renewable Energy*. Pergamon, 37(1), pp. 37–44. doi: 10.1016/j.renene.2011.05.008.

Guler, M. A. *et al.* (2021) 'Working From Home During a Pandemic', *Journal of Occupational & Environmental Medicine*. Ovid Technologies (Wolters Kluwer Health), 63(9), pp. 731–741. doi: 10.1097/JOM.0000000000002277.

Hakimi, S. M. *et al.* (2020) 'Demand response method for smart microgrids considering high renewable energies penetration', *Sustainable Energy, Grids and Networks*. Elsevier Ltd, 21, p. 100325. doi: 10.1016/j.segan.2020.100325.

Hampton, S. (2017) 'An ethnography of energy demand and working from home: Exploring the affective dimensions of social practice in the United Kingdom', *Energy Research & Social Science*. Elsevier, 28, pp. 1–10. doi: 10.1016/J.ERSS.2017.03.012.

Han, P. *et al.* (2021) 'Assessing the recent impact of COVID-19 on carbon emissions from China using domestic economic data', *Science of The Total Environment*. Elsevier, 750, p. 141688. doi: 10.1016/J.SCITOTENV.2020.141688.

Hawkes, A. D. (2010) 'Estimating marginal CO₂ emissions rates for national electricity systems', *Energy Policy*. Elsevier Ltd, 38(10), pp. 5977–5987. doi: 10.1016/j.enpol.2010.05.053.

Hazboun, S. O. *et al.* (2019) 'Keep quiet on climate: Assessing public response to seven renewable energy frames in the Western United States', *Energy Research and Social Science*, 57. doi: 10.1016/j.erss.2019.101243.

He, L. *et al.* (2018) ‘Techno-economic potential of a renewable energy-based microgrid system for a sustainable large-scale residential community in Beijing, China’, *Renewable and Sustainable Energy Reviews*, pp. 631–641. doi: 10.1016/j.rser.2018.05.053.

Van derHeijden, J. (2018) ‘The limits of voluntary programs for low-carbon buildings for staying under 1.5 °C’, *Current Opinion in Environmental Sustainability*. Elsevier B.V., pp. 59–66. doi: 10.1016/j.cosust.2018.03.006.

Hirsch, A., Parag, Y. and Guerrero, J. (2018) ‘Microgrids: A review of technologies, key drivers, and outstanding issues’, *Renewable and Sustainable Energy Reviews*, pp. 402–411. doi: 10.1016/j.rser.2018.03.040.

HK Electric (2015) *Estimated Electricity Cost of Common Appliances*. Available at: <https://www.hkelectric.com/en/customer-services/billing-payment-electricity-tariffs/know-more-about-electricity-consumption/estimated-electricity-cost-of-common-appliances> (Accessed: 7 August 2021).

HKGBC (2010) *BEAM Plus New Buildings*.

HKPC (2021) *2021 Future of Work & Skills Report*. Available at: <https://www.gartner.com/en/newsroom/press-releases/2020-04-03-gartner-cfo-surey-reveals-74-percent-of-organizations-to-shift-som> (Accessed: 28 November 2021).

HKSAR Government (2017) *GovHK: Feed-in Tariff*. Available at: <https://www.gov.hk/en/residents/environment/renewable/feedintariff.htm> (Accessed: 11 July 2021).

HKSAR Government (2020) *The Chief Executive’s 2020 Policy Address - Policy Address*. Available at: <https://www.policyaddress.gov.hk/2020/eng/p125.html> (Accessed: 11 July 2021).

Hobfoll, S. E. and Ford, J. S. (2007) ‘Conservation of Resources Theory’, *Encyclopedia of Stress*. Academic Press, pp. 562–567. doi: 10.1016/B978-012373947-6.00093-3.

Hong Kong Housing Authority and Housing Department (2019) *Standard Block Typical*

Floor Plans / Hong Kong Housing Authority and Housing Department. Available at: <https://www.housingauthority.gov.hk/en/global-elements/estate-locator/standard-block-typical-floor-plans/> (Accessed: 11 July 2021).

Horhoianu, H. and Horhoianu, A. (2017) 'Evaluation of an industrial microgrid using HOMER software', *UPB Scientific Bulletin, Series C: Electrical Engineering and Computer Science*, 79(4), pp. 193–210. Available at: https://julac.hosted.exlibrisgroup.com/primo-explore/fulldisplay?docid=TN_scopus2-s2.0-85036652203&context=PC&vid=HKPU&lang=en_US&search_scope=All&adaptor=primo_central_multiple_fe&tab=default_tab&query=any,contains,Evaluation of an industrial microgrid u (Accessed: 6 April 2019).

Hossaini, N., Hewage, K. and Sadiq, R. (2015) 'Spatial life cycle sustainability assessment: A conceptual framework for net-zero buildings', *Clean Technologies and Environmental Policy*, 17(8), pp. 2243–2253. doi: 10.1007/s10098-015-0959-0.

Huang, C. *et al.* (2012) 'Government funded renewable energy innovation in China', *Energy Policy*, 51, pp. 121–127. doi: 10.1016/j.enpol.2011.08.069.

Hui, E. C. M. and Wong, F. K. W. (2004) 'The Hong Kong Housing Authority and its Financial Arrangement over the Past 50 Years', in *International Housing Conference in Hong Kong 2004 - Housing in the 21st Century: Challenges and Commitments, Hong Kong, 2-4 February 2004*. Available at: <https://www.housingauthority.gov.hk/hdw/ihc/pdf/thkhafa.pdf> (Accessed: 11 July 2021).

Huijbregts, M. A. J. *et al.* (2017) 'ReCiPe2016: a harmonised life cycle impact assessment method at midpoint and endpoint level', *International Journal of Life Cycle Assessment*, 22(2), pp. 138–147. doi: 10.1007/s11367-016-1246-y.

IEA (2020) *Tracking Buildings 2020*. IEA, Paris. Available at: <https://www.iea.org/reports/tracking-buildings-2020>.

IMDA (2020) *More Subsidised Solutions To Support Working From Home For Businesses - Infocomm Media Development Authority*. Available at: <https://www.imda.gov.sg/news-and-events/Media-Room/Media-Releases/2020/More-Subsidised-Solutions-To-Support--Working-From-Home-For-Businesses> (Accessed: 23November2021).

Ingrao, C. *et al.* (2018) 'How can life cycle thinking support sustainability of buildings? Investigating life cycle assessment applications for energy efficiency and environmental performance', *Journal of Cleaner Production*, pp. 556–569. doi: 10.1016/j.jclepro.2018.08.080.

Inoue, H., Murase, Y. and Todo, Y. (2021) 'Do economic effects of the anti-COVID-19 lockdowns in different regions interact through supply chains?', *PLoS ONE*. Public Library of Science, 16(7 July), p. e0255031. doi: 10.1371/journal.pone.0255031.

International Renewable Energy Agency (2018) *Renewable Power Generation Costs in 2017*. Available at: www.irena.org (Accessed: 6April2019).

Irwan, Y. M. *et al.* (2015) 'Stand-Alone Photovoltaic (SAPV) System Assessment using PVSYST Software', in *Energy Procedia*, pp. 596–603. doi: 10.1016/j.egypro.2015.11.539.

Irwin, R. J. *et al.* (1997) *Environmental Contaminants Encyclopedia*.

Jacob, A. S., Banerjee, R. and Ghosh, P. C. (2018) 'Sizing of hybrid energy storage system for a PV based microgrid through design space approach', *Applied Energy*, 212, pp. 640–653. doi: 10.1016/j.apenergy.2017.12.040.

Jacobson, M. Z. and Jadhav, V. (2018) 'World estimates of PV optimal tilt angles and ratios of sunlight incident upon tilted and tracked PV panels relative to horizontal panels', *Solar Energy*. Pergamon, 169, pp. 55–66. doi: 10.1016/J.SOLENER.2018.04.030.

Jaillon, L. and Poon, C. S. (2009) 'The evolution of prefabricated residential building systems in Hong Kong: A review of the public and the private sector', *Automation in Construction*. Elsevier, 18(3), pp. 239–248. doi: 10.1016/J.AUTCON.2008.09.002.

- Jamaludin, S. *et al.* (2020) 'COVID-19 exit strategy: Transitioning towards a new normal', *Annals of Medicine and Surgery*. Elsevier, 59, pp. 165–170. doi: 10.1016/J.AMSU.2020.09.046.
- Jani, D. and Rangan, B. (2018) 'Life cycle energy and carbon footprint analysis of large MW scale grid connected wind power systems in India', in *E3S Web of Conferences*, pp. 65–80. doi: 10.1051/e3sconf/20186408002.
- Jeanjean, A., Olives, R. and Py, X. (2013) 'Selection criteria of thermal mass materials for low-energy building construction applied to conventional and alternative materials', *Energy and Buildings*. Elsevier, 63, pp. 36–48. doi: 10.1016/J.ENBUILD.2013.03.047.
- Jenkins, F. and Smith, J. (2021) 'Work-from-home during COVID-19: Accounting for the care economy to build back better', *Economic and Labour Relations Review*. SAGE Publications Sage UK: London, England, 32(1), pp. 22–38. doi: 10.1177/1035304620983608.
- Jia, J. and Lee, W. L. (2016) 'Drivers of moderate increase in cooling energy use in residential buildings in Hong Kong', *Energy and Buildings*. Elsevier, 125, pp. 19–26. doi: 10.1016/J.ENBUILD.2016.04.064.
- Jiang, P., Fan, Y. Van and Klemeš, J. J. (2021) 'Impacts of COVID-19 on energy demand and consumption: Challenges, lessons and emerging opportunities', *Applied Energy*. Elsevier, 285, p. 116441. doi: 10.1016/J.APENERGY.2021.116441.
- Jo, J. H., Aldeman, M., Lee, H. S., *et al.* (2018) 'Parametric analysis for cost-optimal renewable energy integration into residential buildings: Techno-economic model', *Renewable Energy*, 125, pp. 907–914. doi: 10.1016/j.renene.2018.03.025.
- Jo, J. H., Aldeman, M., Lee, H.-S., *et al.* (2018) 'Parametric analysis for cost-optimal renewable energy integration into residential buildings: Techno-economic model', *Renewable Energy*, 125, pp. 907–914. Available at: <https://linkinghub.elsevier.com/retrieve/pii/S0960148118303306> (Accessed: 6 April 2019).

- Jurasz, J. and Campana, P. E. (2019a) 'The potential of photovoltaic systems to reduce energy costs for office buildings in time-dependent and peak-load-dependent tariffs', *Sustainable Cities and Society*. Elsevier Ltd, 44, pp. 871–879. doi: 10.1016/j.scs.2018.10.048.
- Jurasz, J. and Campana, P. E. (2019b) 'The potential of photovoltaic systems to reduce energy costs for office buildings in time-dependent and peak-load-dependent tariffs', *Sustainable Cities and Society*, 44, pp. 871–879. doi: 10.1016/j.scs.2018.10.048.
- Kang, H. *et al.* (2021) 'Changes in energy consumption according to building use type under COVID-19 pandemic in South Korea', *Renewable and Sustainable Energy Reviews*. Pergamon, 148, p. 111294. doi: 10.1016/J.RSER.2021.111294.
- Kapsalis, V. and Karamanis, D. (2015) 'On the effect of roof added photovoltaics on building's energy demand', *Energy and Buildings*. Elsevier Ltd, 108, pp. 195–204. doi: 10.1016/j.enbuild.2015.09.016.
- Karl, K. A., Peluchette, J.V. and Aghakhani, N. (2021) 'Virtual Work Meetings During the COVID-19 Pandemic: The Good, Bad, and Ugly', *Small Group Research*. SAGE Publications Sage CA: Los Angeles, CA. doi: 10.1177/10464964211015286.
- Kerr, C. C. *et al.* (2021) 'Covasim: An agent-based model of COVID-19 dynamics and interventions', *PLoS Computational Biology*. Public Library of Science, 17(7). doi: 10.1371/JOURNAL.PCBI.1009149.
- Khodaei, A. *et al.* (2017) 'Microgrid Economic Viability Assessment: An introduction to MG-REVALUE', *Electricity Journal*, 30(4), pp. 7–11. doi: 10.1016/j.tej.2017.03.009.
- Kitou, E. and Horvath, A. (2003) 'Energy-related emissions from telework', *Environmental Science and Technology*, pp. 3467–3475. doi: 10.1021/es025849p.
- Kobayakawa, T. and Kandpal, T. C. (2015) 'Analysis of electricity consumption under a photovoltaic micro-grid system in India', *Solar Energy*, 116, pp. 177–183. doi: 10.1016/j.solener.2015.04.001.

- Krarti, M. and Aldubyan, M. (2021) 'Review analysis of COVID-19 impact on electricity demand for residential buildings', *Renewable and Sustainable Energy Reviews*. Pergamon, 143, p. 110888. doi: 10.1016/J.RSER.2021.110888.
- Kyaw, W. W. (2017) *Optimum Design of Islanded Microgrid Based on Life Cycle Cost for Office Building in Myanmar, Peer-Reviewed, Refereed, Indexed Journal with IC*. Available at: <https://www.ijirmf.com/wp-content/uploads/201710012.pdf> (Accessed: 6 April 2019).
- Lai, K. Y. *et al.* (2020) 'The nature of cities and the Covid-19 pandemic', *Current Opinion in Environmental Sustainability*. Elsevier, 46, pp. 27–31. doi: 10.1016/J.COSUST.2020.08.008.
- Lamnatou, C. and Chemisana, D. (2017) 'Concentrating solar systems: Life Cycle Assessment (LCA) and environmental issues', *Renewable and Sustainable Energy Reviews*. Pergamon, pp. 916–932. Available at: <https://www.sciencedirect.com.ezproxy.lb.polyu.edu.hk/science/article/pii/S1364032117305749> (Accessed: 24 February 2019).
- Lanshina, T. A. *et al.* (2018) 'The slow expansion of renewable energy in Russia: Competitiveness and regulation issues', *Energy Policy*, 120, pp. 600–609. doi: 10.1016/j.enpol.2018.05.052.
- Larson, W. and Zhao, W. (2017) 'Telework: Urban form, energy consumption, and greenhouse gas implications', *Economic Inquiry*. Blackwell Publishing Inc., 55(2), pp. 714–735. doi: 10.1111/ecin.12399.
- Leadbetter, J. (2012) 'Battery storage system for residential electricity peak demand shaving', *Energy and buildings*, 55, pp. 685–692.
- Leal, S. *et al.* (2013) 'Case study of a simplified building energy modeling for performance simulation', in *Proceedings of BS 2013: 13th Conference of the International Building Performance Simulation Association*, pp. 331–336.
- Lenzen, M. (2010) 'Current state of development of electricity-generating technologies: A

- literature review', *Energies*, pp. 462–591. doi: 10.3390/en3030462.
- Li, F., Li, R. and Zhou, F. (2016) *Microgrid Technology and Engineering Application*, *Microgrid Technology and Engineering Application*.
- Li, L. *et al.* (2020) 'Review and outlook on the international renewable energy development', *Energy and Built Environment*. Elsevier. doi: 10.1016/J.ENBENV.2020.12.002.
- Li, Y., Zhang, W. and Wang, P. (2021) 'Working online or offline: Which is more effective?', *Research in International Business and Finance*. Elsevier, 58, p. 101456. doi: 10.1016/J.RIBAF.2021.101456.
- Lingnan University Hong Kong (2020) *Survey Findings on Working from Home under COVID19*. Available at: <https://www.ln.edu.hk/sgs/news/survey-findings-on-working-from-home-under-covid19> (Accessed: 20 November 2021).
- Liu, W. *et al.* (2015) 'Life cycle assessment of lead-acid batteries used in electric bicycles in China', *Journal of Cleaner Production*. Elsevier, 108, pp. 1149–1156. Available at: [https://www.sciencedirect-com.ezproxy.lb.polyu.edu.hk/science/article/pii/S0959652615009063](https://www.sciencedirect.com.ezproxy.lb.polyu.edu.hk/science/article/pii/S0959652615009063) (Accessed: 24 February 2019).
- López-González, A., Domenech, B. and Ferrer-Martí, L. (2018) 'Lifetime, cost and fuel efficiency in diesel projects for rural electrification in Venezuela', *Energy Policy*. Elsevier, 121, pp. 152–161. Available at: <https://www.sciencedirect-com.ezproxy.lb.polyu.edu.hk/science/article/pii/S0301421518304105> (Accessed: 24 February 2019).
- Lorig, F., Johansson, E. and Davidsson, P. (2021) 'Agent-based social simulation of the covid-19 pandemic: A systematic review', *JASSS*. JASSS, 24(3). doi: 10.18564/jasss.4601.
- Luo, L. *et al.* (2020) 'Optimal scheduling of a renewable based microgrid considering photovoltaic system and battery energy storage under uncertainty', *Journal of Energy*

Storage, 28. doi: 10.1016/j.est.2020.101306.

Luo, T. *et al.* (2019) 'Mapping the knowledge roadmap of low carbon building: A scientometric analysis', *Energy and Buildings*. Elsevier Ltd, pp. 163–176. doi: 10.1016/j.enbuild.2019.03.050.

Lupangu, C. and Bansal, R. C. (2017) 'A review of technical issues on the development of solar photovoltaic systems', *Renewable and Sustainable Energy Reviews*, pp. 950–965. doi: 10.1016/j.rser.2017.02.003.

Lützkendorf, T. *et al.* (2015) 'Net-zero buildings: incorporating embodied impacts', *Building Research & Information*. Routledge, 43(1), pp. 62–81. doi: 10.1080/09613218.2014.935575.

Ma, M. *et al.* (2019) 'Carbon-dioxide mitigation in the residential building sector: A household scale-based assessment', *Energy Conversion and Management*. Elsevier Ltd, 198, p. 111915. doi: 10.1016/j.enconman.2019.111915.

Ma, M. *et al.* (2020) 'Low carbon roadmap of residential building sector in China: Historical mitigation and prospective peak', *Applied Energy*. Elsevier Ltd, 273, p. 115247. doi: 10.1016/j.apenergy.2020.115247.

Madurai Elavarasan, R. *et al.* (2020a) 'COVID-19: Impact analysis and recommendations for power sector operation', *Applied Energy*. Elsevier Ltd, 279. doi: 10.1016/J.APENERGY.2020.115739.

Madurai Elavarasan, R. *et al.* (2020b) 'COVID-19: Impact analysis and recommendations for power sector operation', *Applied Energy*. Elsevier, 279, p. 115739. doi: 10.1016/J.APENERGY.2020.115739.

Madurai Elavarasan, R. *et al.* (2021) 'Envisioning the UN Sustainable Development Goals (SDGs) through the lens of energy sustainability (SDG 7) in the post-COVID-19 world', *Applied Energy*, 292. doi: 10.1016/j.apenergy.2021.116665.

Mafimisebi, I. B. *et al.* (2018) 'A validated low carbon office building intervention model

based on structural equation modelling’, *Journal of Cleaner Production*. Elsevier Ltd, 200, pp. 478–489. doi: 10.1016/j.jclepro.2018.07.249.

Maghami, M. R. *et al.* (2016) ‘Power loss due to soiling on solar panel: A review’, *Renewable and Sustainable Energy Reviews*. Pergamon, 59, pp. 1307–1316. doi: 10.1016/J.RSER.2016.01.044.

Mahmoud, M. S., Azher Hussain, S. and Abido, M. A. (2014) ‘Modeling and control of microgrid: An overview’, *Journal of the Franklin Institute*, 351(5), pp. 2822–2859. Available at: <https://linkinghub.elsevier.com/retrieve/pii/S0016003214000180> (Accessed: 24 February 2019).

Mahmoud, M. S., Rahman, M. S. U. and Sunni, F. M. A. L. (2015) ‘Review of microgrid architectures - A system of systems perspective’, *IET Renewable Power Generation*, pp. 1064–1078. doi: 10.1049/iet-rpg.2014.0171.

Malecki, F. (2020) ‘Overcoming the security risks of remote working’, *Computer Fraud & Security*. Elsevier, 2020(7), p. 10. doi: 10.1016/S1361-3723(20)30074-9.

Manikandan, S., Varun, M. and Manikandan, S. (2020) ‘Performance Evaluation of Bifacial and Monofacial modules in vertical and latitude mounting at South India using PVsyst’, in *IOP Conference Series: Materials Science and Engineering*. IOP Publishing Ltd. doi: 10.1088/1757-899X/912/4/042066.

Mariam, L., Basu, M. and Conlon, M. F. (2016) ‘Microgrid: Architecture, policy and future trends’, *Renewable and Sustainable Energy Reviews*, pp. 477–489. doi: 10.1016/j.rser.2016.06.037.

Marlow, S. L., Lacerenza, C. N. and Salas, E. (2017) ‘Communication in virtual teams: a conceptual framework and research agenda’, *Human Resource Management Review*. JAI, 27(4), pp. 575–589. doi: 10.1016/J.HRMR.2016.12.005.

Martucci, S. (2021) ‘He’s Working from Home and I’m at Home Trying to Work:

Experiences of Childcare and the Work–Family Balance Among Mothers During COVID-19’, *Journal of Family Issues*. SAGE PublicationsSage CA: Los Angeles, CA, 0(0), pp. 1–24. doi: 10.1177/0192513X211048476.

Mat Isa, N., Wei Tan, C. andYatim, A. H. M. (2017) ‘A techno-economic assessment of grid connected photovoltaic system for hospital building in Malaysia’, in *IOP Conference Series: Materials Science and Engineering*. IOP Publishing. Available at: <http://stacks.iop.org/1757-899X/217/i=1/a=012016?key=crossref.bc00bb0cd1d5ab5168aab5bfba969bdf> (Accessed: 24February2019).

Mazzucato, M. andSemieniuk, G. (2018) ‘Financing renewable energy: Who is financing what and why it matters’, *Technological Forecasting and Social Change*, 127, pp. 8–22. doi: 10.1016/j.techfore.2017.05.021.

McGee, J. A. andGreiner, P. T. (2019) ‘Renewable energy injustice: The socio-environmental implications of renewable energy consumption’, *Energy Research and Social Science*. doi: 10.1016/j.erss.2019.05.024.

McKinsey & Company (2021) *The future of remote work: An analysis of 2,000 tasks, 800 jobs, and 9 countries*. Available at: <https://www.mckinsey.com/featured-insights/future-of-work/whats-next-for-remote-work-an-analysis-of-2000-tasks-800-jobs-and-nine-countries> (Accessed: 23November2021).

Mehta, P. (2021) ‘Work from home—Work engagement amid COVID-19 lockdown and employee happiness’, *Journal of Public Affairs*. John Wiley & Sons, Ltd, p. e2709. doi: 10.1002/pa.2709.

Melius, J., Margolis, R. andOng, S. (2013) *Estimating Rooftop Suitability for PV: A Review of Methods, Patents, and Validation Techniques*, NREL Technical Report. Golden, CO (United States). doi: 10.2172/1117057.

Melo, E. G. *et al.* (2013) ‘Using a shading matrix to estimate the shading factor and the

irradiation in a three-dimensional model of a receiving surface in an urban environment’, *Solar Energy*. Pergamon, 92, pp. 15–25. doi: 10.1016/j.solener.2013.02.015.

Mezher, T., Dawelbait, G. and Abbas, Z. (2012) ‘Renewable energy policy options for Abu Dhabi: Drivers and barriers’, *Energy Policy*, 42, pp. 315–328. doi: 10.1016/j.enpol.2011.11.089.

Michael, J. J., S, I. and Goic, R. (2015) ‘Flat plate solar photovoltaic-thermal (PV/T) systems: A reference guide’, *Renewable and Sustainable Energy Reviews*. Elsevier Ltd, pp. 62–88. doi: 10.1016/j.rser.2015.06.022.

Microgrids at Berkeley Lab (2019) *Examples of Microgrids | Building Microgrid*. Available at: <https://building-microgrid.lbl.gov/examples-microgrids> (Accessed: 6 April 2019).

Milis, K., Peremans, H. and Van Passel, S. (2018) ‘The impact of policy on microgrid economics: A review’, *Renewable and Sustainable Energy Reviews*, pp. 3111–3119. doi: 10.1016/j.rser.2017.08.091.

Min, H. *et al.* (2021) ‘Using machine learning to investigate the public’s emotional responses to work from home during the COVID-19 pandemic’, *The Journal of applied psychology*. NLM (Medline), 106(2), pp. 214–229. doi: 10.1037/APL0000886.

Minz, F. E. *et al.* (2015) ‘Distribution of Sb minerals in the Cu and Zn flotation of Rockliden massive sulphide ore in north-central Sweden’, *Minerals Engineering*. Pergamon, 82, pp. 125–135. Available at: [https://www.sciencedirect-com.ezproxy.lb.polyu.edu.hk/science/article/pii/S0892687515000977](https://www.sciencedirect.com.ezproxy.lb.polyu.edu.hk/science/article/pii/S0892687515000977) (Accessed: 24 February 2019).

Mitscher, M. and Rüter, R. (2011) ‘An economic assessment of grid-connected residential solar photovoltaic systems in Brazil’, in *30th ISES Biennial Solar World Congress 2011, SWC 2011*, pp. 4255–4265. doi: 10.18086/swc.2011.27.14.

Mola, M., Feofilovs, M. and Romagnoli, F. (2018) ‘Energy resilience: research trends at

urban, municipal and country levels’, *Energy Procedia*. Elsevier, 147, pp. 104–113. doi: 10.1016/J.EGYPRO.2018.07.039.

Mongey, S., Pilossoph, L. and Weinberg, A. (2021) ‘Which workers bear the burden of social distancing?’, *Journal of Economic Inequality*. Springer, 19(3), pp. 509–526. doi: 10.1007/S10888-021-09487-6.

Monyei, C. G. *et al.* (2019) ‘Benchmarks for energy access: Policy vagueness and incoherence as barriers to sustainable electrification of the global south’, *Energy Research and Social Science*, pp. 113–116. doi: 10.1016/j.erss.2019.04.005.

Morakinyo, T. E. *et al.* (2019) ‘Estimates of the impact of extreme heat events on cooling energy demand in Hong Kong’, *Renewable Energy*, 142, pp. 73–84. doi: 10.1016/j.renene.2019.04.077.

Moslehi, S. and Reddy, T. A. (2019) ‘A new quantitative life cycle sustainability assessment framework: Application to integrated energy systems’, *Applied Energy*. Elsevier, 239, pp. 482–493. doi: 10.1016/j.apenergy.2019.01.237.

Nagapurkar, P. and Smith, J. D. (2019) ‘Techno-economic optimization and environmental Life Cycle Assessment (LCA) of microgrids located in the US using genetic algorithm’, *Energy Conversion and Management*, 181, pp. 272–291. doi: 10.1016/j.enconman.2018.11.072.

Nalbandian-Sugden, H. (2016) *Operating ratio and cost of coal power generation*. Available at: www.iea-coal.org (Accessed: 6 April 2019).

National Research Council (U.S.) (2000) *Copper in drinking water*. National Academy Press.

Natural Resources Canada (2019) *RETSscreen*. Available at: <https://www.nrcan.gc.ca/energy/software-tools/7465> (Accessed: 24 February 2019).

Nelson, J. R. and Grubestic, T. H. (2020) ‘The use of LiDAR versus unmanned aerial systems (UAS) to assess rooftop solar energy potential’, *Sustainable Cities and Society*. Elsevier, 61,

p. 102353. doi: 10.1016/J.SCS.2020.102353.

DeNeufville, R. and Scholtes, S. (2011) *Flexibility in engineering design*. MIT Press.

Available at: <https://mitpress.mit.edu/books/flexibility-engineering-design> (Accessed: 6 April 2019).

Nosratabadi, S. M., Hooshmand, R. A. and Gholipour, E. (2017) 'A comprehensive review on microgrid and virtual power plant concepts employed for distributed energy resources scheduling in power systems', *Renewable and Sustainable Energy Reviews*. Pergamon, pp. 341–363. doi: 10.1016/j.rser.2016.09.025.

Nouni, M. R., Mullick, S. C. and Kandpal, T. C. (2009) 'Providing electricity access to remote areas in India: Niche areas for decentralized electricity supply', *Renewable Energy*. Pergamon, 34(2), pp. 430–434. Available at: [https://www.sciencedirect-com.ezproxy.lb.polyu.edu.hk/science/article/pii/S0960148108002127](https://www.sciencedirect.com.ezproxy.lb.polyu.edu.hk/science/article/pii/S0960148108002127) (Accessed: 24 February 2019).

Nwaigwe, K. N., Mutabilwa, P. and Dintwa, E. (2019) 'An overview of solar power (PV systems) integration into electricity grids', *Materials Science for Energy Technologies*. Elsevier BV, 2(3), pp. 629–633. doi: 10.1016/j.mset.2019.07.002.

O'Brien, W. and Yazdani Aliabadi, F. (2020) 'Does telecommuting save energy? A critical review of quantitative studies and their research methods', *Energy and Buildings*. Elsevier, 225, p. 110298. doi: 10.1016/J.ENBUILD.2020.110298.

O'Leary, D. E. (2020) 'Evolving Information Systems and Technology Research Issues for COVID-19 and Other Pandemics', *Journal of Organizational Computing and Electronic Commerce*. Taylor & Francis, 30(1), pp. 1–8. doi: 10.1080/10919392.2020.1755790.

Oakman, J. *et al.* (2020) 'A rapid review of mental and physical health effects of working at home: how do we optimise health?', *BMC Public Health*. BioMed Central Ltd, 20(1), pp. 1–13. doi: 10.1186/S12889-020-09875-Z/TABLES/5.

Oksanen, A. *et al.* (2021) 'COVID-19 crisis and digital stressors at work: A longitudinal study on the Finnish working population', *Computers in Human Behavior*. Pergamon, 122, p. 106853. doi: 10.1016/J.CHB.2021.106853.

Okuyan, C. B. and Begen, M. A. (2021) 'Working from home during the COVID-19 pandemic, its effects on health, and recommendations: The pandemic and beyond', *Perspectives in Psychiatric Care*. John Wiley & Sons, Ltd. doi: 10.1111/PPC.12847.

Oparaku, O. U. (2003) 'Rural area power supply in Nigeria: A cost comparison of the photovoltaic, diesel/gasoline generator and grid utility options', *Renewable Energy*. Pergamon, 28(13), pp. 2089–2098. Available at: [https://www.sciencedirect-com.ezproxy.lb.polyu.edu.hk/science/article/pii/S0960148103000090](https://www.sciencedirect.com.ezproxy.lb.polyu.edu.hk/science/article/pii/S0960148103000090) (Accessed: 24February2019).

Palizban, O., Kauhaniemi, K. and Guerrero, J. M. (2014) 'Microgrids in active network management - Part I: Hierarchical control, energy storage, virtual power plants, and market participation', *Renewable and Sustainable Energy Reviews*. Pergamon, pp. 428–439. doi: 10.1016/j.rser.2014.01.016.

Peng, J. *et al.* (2013a) 'Experimentally diagnosing the shading impact on the power performance of a PV system in Hong Kong', in *2013 World Congress on Sustainable Technologies, WCST 2013*. IEEE Computer Society, pp. 18–22. doi: 10.1109/WCST.2013.6750397.

Peng, J. *et al.* (2013b) 'Experimentally diagnosing the shading impact on the power performance of a PV system in Hong Kong', *2013 World Congress on Sustainable Technologies, WCST 2013*. IEEE Computer Society, pp. 18–22. doi: 10.1109/WCST.2013.6750397.

Peng, J. and Lu, L. (2013) 'Investigation on the development potential of rooftop PV system in Hong Kong and its environmental benefits', *Renewable and Sustainable Energy Reviews*.

Pergamon, 27, pp. 149–162. doi: 10.1016/J.RSER.2013.06.030.

Peters, A. *et al.* (2010) *Proposed EQS for Water Framework Directive Annex VIII substances: manganese (bioavailable) (For Consultation) by Water Framework Directive-United Kingdom Technical Advisory Group (WFD-UKTAG)*.

Pickard, W. F. (2012) ‘Where renewable electricity is concerned, how costly is “too costly”?’’, *Energy Policy*, 49, pp. 346–354. doi: 10.1016/j.enpol.2012.06.036.

Planas, E. *et al.* (2013) ‘General aspects, hierarchical controls and droop methods in microgrids: A review’, *Renewable and Sustainable Energy Reviews*. Pergamon, pp. 147–159. doi: 10.1016/j.rser.2012.09.032.

Port of Long Beach (2019) *Port of Long Beach - News Details*. Available at:

<http://www.polb.com/news/displaynews.asp?NewsID=1772> (Accessed: 6April2019).

Prince, J. J. A. *et al.* (2019) ‘Resilience in energy management system: A study case’, *IFAC-PapersOnLine*. Elsevier, 52(4), pp. 395–400. doi: 10.1016/J.IFACOL.2019.08.242.

PwC (2021) *PwC’s US Remote Work Survey*. Available at:

<https://www.pwc.com/us/en/library/covid-19/us-remote-work-survey.html> (Accessed: 28November2021).

Qin, H. andPan, W. (2020) ‘Energy use of subtropical high-rise public residential buildings and impacts of energy saving measures’, *Journal of Cleaner Production*. Elsevier Ltd, 254. doi: 10.1016/J.JCLEPRO.2020.120041.

Quashie, M., Bouffard, F. andJoós, G. (2017) ‘Business cases for isolated and grid connected microgrids: Methodology and applications’, *Applied Energy*, 205, pp. 105–115. doi: 10.1016/j.apenergy.2017.07.112.

Rachmawati, R. *et al.* (2021) ‘Work from home and the use of ict during the covid-19 pandemic in indonesia and its impact on cities in the future’, *Sustainability (Switzerland)*. Multidisciplinary Digital Publishing Institute, 13(12), p. 6760. doi: 10.3390/su13126760.

- Rahman, K. T. and Zahir Uddin Arif, M. (2021) 'Working from Home during the COVID-19 Pandemic: Satisfaction, Challenges, and Productivity of Employees', *International Journal of Trade and Commerce-IIARTC*. Society for Global Studies and Research, 9(2). doi: 10.46333/IJTC/9/2/3.
- Randstad (2021) *The Future of Work is Remote: White Paper 2021*. Available at: <https://www.randstad.com.hk/hr-trends/workforce-trends/the-future-of-work-is-remote-white-paper-2021/> (Accessed: 23 November 2021).
- Rao, A. N., Vijayapriya, P. and Kowsalya, M. (2019) 'State-of-the-art research on micro grid stability: A review', *International Journal of Ambient Energy*. Taylor & Francis, 40(5), pp. 554–561. doi: 10.1080/01430750.2017.1412351.
- Reihani, E. *et al.* (2016) 'Load peak shaving and power smoothing of a distribution grid with high renewable energy penetration', *Renewable Energy*. Elsevier Ltd, 86, pp. 1372–1379. doi: 10.1016/j.renene.2015.09.050.
- Repele, M. and Bazbauers, G. (2015) 'Life Cycle Assessment of Renewable Energy Alternatives for Replacement of Natural Gas in Building Material Industry', in *Energy Procedia*. Elsevier, pp. 127–134. Available at: <https://www.sciencedirect.com.ezproxy.lb.polyu.edu.hk/science/article/pii/S1876610215007080> (Accessed: 24 February 2019).
- RETScreen® International Clean Energy Decision Support Centre (2005) *Clean Energy Project Analysis RETScreen® Engineering Cases Textbook Third Edition*.
- Rey-Hernández, J. M. *et al.* (2018) 'Modelling the long-term effect of climate change on a zero energy and carbon dioxide building through energy efficiency and renewables', *Energy and Buildings*. Elsevier Ltd, 174, pp. 85–96. doi: 10.1016/j.enbuild.2018.06.006.
- Rezaie, B., Esmailzadeh, E. and Dincer, I. (2011) 'Renewable energy options for buildings: Case studies', *Energy and Buildings*, 43(1), pp. 56–65. doi: 10.1016/j.enbuild.2010.08.013.

- Rezvani, A. *et al.* (2015) 'Environmental/economic scheduling of a micro-grid with renewable energy resources', *Journal of Cleaner Production*, 87(1), pp. 216–226. doi: 10.1016/j.jclepro.2014.09.088.
- Rommel, K. and Sagebiel, J. (2017) 'Preferences for micro-cogeneration in Germany: Policy implications for grid expansion from a discrete choice experiment', *Applied Energy*, 206, pp. 612–622. doi: 10.1016/j.apenergy.2017.08.216.
- Rouleau, J. and Gosselin, L. (2021) 'Impacts of the COVID-19 lockdown on energy consumption in a Canadian social housing building', *Applied Energy*. Elsevier, 287, p. 116565. doi: 10.1016/J.APENERGY.2021.116565.
- Rubin, E. S., Rao, A. B. and Chen, C. (2005) 'Comparative assessments of fossil fuel power plants with CO₂ capture and storage', in *Greenhouse Gas Control Technologies*, pp. 285–293. doi: 10.1016/B978-008044704-9/50029-X.
- Russo, D. *et al.* (2021) 'Predictors of well-being and productivity among software professionals during the COVID-19 pandemic – a longitudinal study', *Empirical Software Engineering*. Springer, 26(4). doi: 10.1007/s10664-021-09945-9.
- Ryan, E. M. and Sanquist, T. F. (2012a) 'Validation of building energy modeling tools under idealized and realistic conditions', *Energy and Buildings*. Elsevier, 47, pp. 375–382. doi: 10.1016/j.enbuild.2011.12.020.
- Ryan, E. M. and Sanquist, T. F. (2012b) 'Validation of building energy modeling tools under idealized and realistic conditions', *Energy and Buildings*. Elsevier, 47, pp. 375–382. doi: 10.1016/J.ENBUILD.2011.12.020.
- Santiago, I. *et al.* (2021) 'Electricity demand during pandemic times: The case of the COVID-19 in Spain', *Energy Policy*. Elsevier Ltd, 148. doi: 10.1016/J.ENPOL.2020.111964.
- Schade, H. M. *et al.* (2021) 'Having to work from home: Basic needs, well-being, and motivation', *International Journal of Environmental Research and Public Health*.

Multidisciplinary Digital Publishing Institute, 18(10), p. 5149. doi: 10.3390/ijerph18105149.

Schaefer, A. and Ghisi, E. (2016) 'Method for obtaining reference buildings', *Energy and Buildings*. Elsevier Ltd, 128, pp. 660–672. doi: 10.1016/j.enbuild.2016.07.001.

Schwaegerl, C. and Tao, L. (2013) 'Quantification of Technical, Economic, Environmental and Social Benefits of Microgrid Operation', in *Microgrids*. Chichester, United Kingdom: John Wiley and Sons Ltd, pp. 275–313. Available at:

<http://doi.wiley.com/10.1002/9781118720677.ch07> (Accessed: 13 May 2019).

SEA-DISTANCES.ORG - Distances (2019). Available at: <https://sea-distances.org/> (Accessed: 24 February 2019).

Sehar, F., Pipattanasomporn, M. and Rahman, S. (2016) 'An energy management model to study energy and peak power savings from PV and storage in demand responsive buildings', *Applied Energy*. Elsevier, 173, pp. 406–417. doi: 10.1016/J.APENERGY.2016.04.039.

Sergi, B. *et al.* (2018) 'Institutional influence on power sector investments: A case study of on- and off-grid energy in Kenya and Tanzania', *Energy Research and Social Science*, 41, pp. 59–70. doi: 10.1016/j.erss.2018.04.011.

Sesmero, J., Jung, J. and Tyner, W. (2016) 'The effect of current and prospective policies on photovoltaic system economics: An application to the US Midwest', *Energy Policy*, 93, pp. 80–95. doi: 10.1016/j.enpol.2016.02.042.

Shamil, M. S. *et al.* (2021) 'An Agent-Based Modeling of COVID-19: Validation, Analysis, and Recommendations', *Cognitive Computation*. doi: 10.1007/s12559-020-09801-w.

Shao, Y. *et al.* (2021) 'Making daily decisions to work from home or to work in the office: The impacts of daily work- and COVID-related stressors on next-day work location.', *Journal of Applied Psychology*. American Psychological Association, 106(6), pp. 825–838. doi: 10.1037/APL0000929.

Shaw, A. K. *et al.* (2021) 'Lessons from movement ecology for the return to work: Modeling

contacts and the spread of COVID-19’, *PLoS ONE*. Public Library of Science, 16(1 January), p. e0242955. doi: 10.1371/journal.pone.0242955.

Shuai, Z. *et al.* (2016) ‘Microgrid stability: Classification and a review’, *Renewable and Sustainable Energy Reviews*. Pergamon, pp. 167–179. doi: 10.1016/j.rser.2015.12.201.

Siddique, J. (2016) *Industry Report Strategic Research (New York) MUFG Union Bank*. Available at: <https://www.bk.mufg.jp/report/indexpt2016/Microgrids.pdf> (Accessed: 6April2019).

Siemens (2016) *How Microgrids Can Achieve Maximum Return on Investment (ROI) The Role of the Advanced Microgrid Controller How Microgrids Can Achieve Maximum Return on Investment (ROI)*. Available at:

https://w3.usa.siemens.com/smartgrid/us/en/microgrid/documents/mgk_guide_to_how_microgrids_achieve_roi_v5.pdf (Accessed: 6April2019).

Silva, L. F. O. *et al.* (2013) ‘Vanadium and Nickel Speciation in Pulverized Coal and Petroleum Coke Co-combustion’, *Energy & Fuels*. American Chemical Society, 27(3), pp. 1194–1203. Available at: <http://pubs.acs.org/doi/10.1021/ef4000038> (Accessed: 24February2019).

Singh, R. and Banerjee, R. (2015) ‘Estimation of rooftop solar photovoltaic potential of a city’, *Solar Energy*. Elsevier Ltd, 115, pp. 589–602. doi: 10.1016/j.solener.2015.03.016.

Sinke, W. C. (2019) ‘Development of photovoltaic technologies for global impact’, *Renewable Energy*. Elsevier Ltd, 138, pp. 911–914. doi: 10.1016/j.renene.2019.02.030.

Sivaraman, D. and Moore, M. R. (2012) ‘Economic performance of grid-connected photovoltaics in California and Texas (United States): The influence of renewable energy and climate policies’, *Energy Policy*, 49, pp. 274–287. doi: 10.1016/j.enpol.2012.06.019.

Smith, C. *et al.* (2015) ‘Comparative Life Cycle Assessment of a Thai Island’s diesel/PV/wind hybrid microgrid’, *Renewable Energy*. Elsevier, 80(7), pp. 85–100. Available

at: <https://www.sciencedirect-com.ezproxy.lb.polyu.edu.hk/science/article/pii/S0306261911000602> (Accessed: 24February2019).

Song, C. (2018) ‘Energy consumption analysis of residential swimming pools for peak load shaving’, *Applied energy*, 220, pp. 176–191.

Soshinskaya, M. *et al.* (2014) ‘Microgrids: Experiences, barriers and success factors’, *Renewable and Sustainable Energy Reviews*, pp. 659–672. doi: 10.1016/j.rser.2014.07.198.

State Government of Victoria (2019) *Microgrids*. Available at: <https://www.energy.vic.gov.au/microgrids> (Accessed: 6April2019).

Statista (2018) *Electricity prices around the world 2018 | Statista*. Available at: <https://www.statista.com/statistics/263492/electricity-prices-in-selected-countries/> (Accessed: 6April2019).

Su, W. and Wang, J. (2012) ‘Energy Management Systems in Microgrid Operations’, *Electricity Journal*. Elsevier, 25(8), pp. 45–60. Available at: <https://www.sciencedirect-com.ezproxy.lb.polyu.edu.hk/science/article/pii/S104061901200214X> (Accessed: 24February2019).

Tabar, V. S., Jirdehi, M. A. and Hemmati, R. (2018) ‘Sustainable planning of hybrid microgrid towards minimizing environmental pollution, operational cost and frequency fluctuations’, *Journal of Cleaner Production*. Elsevier, 203, pp. 1187–1200. doi: 10.1016/j.jclepro.2018.05.059.

The World Business Council for Sustainable Development (2016) *Business case for Low-Carbon Microgrids*.

Thombs, R. P. (2019) ‘When democracy meets energy transitions: A typology of social power and energy system scale’, *Energy Research and Social Science*, 52, pp. 159–168. doi: 10.1016/j.erss.2019.02.020.

Tian, Y. *et al.* (2018) ‘Optimal capacity allocation of multiple energy storage considering microgrid cost’, in *Journal of Physics: Conference Series*, p. 12126. doi: 10.1088/1742-6596/1074/1/012126.

Ting Kwok, Y., Ka-Lun Lau, K. and Yan Yung Ng, E. (2018) ‘The influence of building envelope design on the thermal comfort of high-rise residential buildings in Hong Kong’, in *Windsor Conference Rethinking Comfort*.

Toniolo-Barrios, M. and Pitt, L. (2021) ‘Mindfulness and the challenges of working from home in times of crisis’, *Business Horizons*. Elsevier, pp. 189–197. doi: 10.1016/j.bushor.2020.09.004.

Toxicological Profile for Antimony and Compounds (2010) *ATSDR’s Toxicological Profiles*. Agency for Toxic Substances and Disease Registry, U.S. Public Health Service. Available at: <http://hdl.handle.net/2027/mdp.39015028868779> (Accessed: 24 February 2019).

Trainer, T. (2013) ‘Can Europe run on renewable energy? A negative case’, *Energy Policy*, 63, pp. 845–850. doi: 10.1016/j.enpol.2013.09.027.

Tulpule, P. J. *et al.* (2013) ‘Economic and environmental impacts of a PV powered workplace parking garage charging station’, *Applied Energy*, 108, pp. 323–332. Available at: <https://linkinghub.elsevier.com/retrieve/pii/S0306261913001876> (Accessed: 6 April 2019).

Uddin, M. *et al.* (2018) ‘A review on peak load shaving strategies’, *Renewable and Sustainable Energy Reviews*. Elsevier Ltd, pp. 3323–3332. doi: 10.1016/j.rser.2017.10.056.

Uddin, M. *et al.* (2020) ‘A novel peak shaving algorithm for islanded microgrid using battery energy storage system’, *Energy*, 196. doi: 10.1016/j.energy.2020.117084.

Uddin, M. S. and Kumar, S. (2014) ‘Energy, emissions and environmental impact analysis of wind turbine using life cycle assessment technique’, *Journal of Cleaner Production*. Elsevier, 69, pp. 153–164. Available at: [https://www.sciencedirect-com.ezproxy.lb.polyu.edu.hk/science/article/pii/S0959652614000973](https://www.sciencedirect.com.ezproxy.lb.polyu.edu.hk/science/article/pii/S0959652614000973) (Accessed:

24February2019).

United Nations (2019a) *Energy - United Nations Sustainable Development*. Available at: <https://www.un.org/sustainabledevelopment/energy/> (Accessed: 23November2019).

United Nations (2019b) *Goal 7 | Department of Economic and Social Affairs*. Available at: <https://sdgs.un.org/goals/goal7> (Accessed: 8May2021).

United States Environmental Protection Agency (1993) *Bromine: Reregistration Eligibility Decision (RED) Fact Sheet*.

Unterreiner, L., Jülch, V. and Reith, S. (2016) 'Recycling of Battery Technologies - Ecological Impact Analysis Using Life Cycle Assessment (LCA)', in *Energy Procedia*. Elsevier, pp. 229–234. Available at: <https://www-sciencedirect-com.ezproxy.lb.polyu.edu.hk/science/article/pii/S1876610216310748> (Accessed: 24February2019).

Ustun, T. S., Ozansoy, C. and Zayegh, A. (2011) 'Recent developments in microgrids and example cases around the world - A review', *Renewable and Sustainable Energy Reviews*. Pergamon, pp. 4030–4041. Available at: <https://www-sciencedirect-com.ezproxy.lb.polyu.edu.hk/science/article/pii/S1364032111002735> (Accessed: 24February2019).

Valenzuela, J. M. and Qi, Y. (2012) 'Framing energy efficiency and renewable energy policies: An international comparison between Mexico and China', *Energy Policy*, 51, pp. 128–137. doi: 10.1016/j.enpol.2012.03.083.

Vogtländer, J. G. (Joost G. (2010) *A practical guide to LCA for students, designers and business managers : cradle-to-grave and cradle-to-cradle*. VSSD.

Vyas, L. and Butakhieo, N. (2021) 'The impact of working from home during COVID-19 on work and life domains: an exploratory study on Hong Kong', *Policy Design and Practice*. Routledge, 4(1), pp. 59–76. doi: 10.1080/25741292.2020.1863560.

- Wan, K. S. Y. and Yik, F. H. W. (2004) 'Representative building design and internal load patterns for modelling energy use in residential buildings in Hong Kong', *Applied Energy*, 77(1), pp. 69–85. doi: 10.1016/S0306-2619(03)00104-1.
- Wang, B. *et al.* (2021) 'Achieving Effective Remote Working During the COVID-19 Pandemic: A Work Design Perspective', in *Applied Psychology*. Wiley-Blackwell, pp. 16–59. doi: 10.1111/apps.12290.
- Wang, M. *et al.* (2018) 'Potential of carbon emission reduction and financial feasibility of urban rooftop photovoltaic power generation in Beijing', *Journal of Cleaner Production*, 203, pp. 1119–1131. doi: 10.1016/j.jclepro.2018.08.350.
- Weldu, Y. W. and Assefa, G. (2017) 'The search for most cost-effective way of achieving environmental sustainability status in electricity generation: Environmental life cycle cost analysis of energy scenarios', *Journal of Cleaner Production*, 142, pp. 2296–2304. doi: 10.1016/j.jclepro.2016.11.047.
- Wheelan, S. A. (2009) 'Group size, group development, and group productivity', *Small Group Research*. SAGE Publications Sage CA: Los Angeles, CA, 40(2), pp. 247–262. doi: 10.1177/1046496408328703.
- Wissner, M. (2011) 'The Smart Grid - A saucerful of secrets?', *Applied Energy*. Elsevier, 88(7), pp. 2509–2518. Available at: [https://www.sciencedirect-com.ezproxy.lb.polyu.edu.hk/science/article/pii/S0306261911000602](https://www.sciencedirect.com.ezproxy.lb.polyu.edu.hk/science/article/pii/S0306261911000602) (Accessed: 24February2019).
- Wong, A. H. K., Cheung, J. O. and Chen, Z. (2021) 'Promoting effectiveness of “working from home”': findings from Hong Kong working population under COVID-19', *Asian Education and Development Studies*. Emerald Publishing Limited, 10(2), pp. 210–228. doi: 10.1108/AEDS-06-2020-0139.
- Wong, J. K. W. and Kuan, K. L. (2014) 'Implementing “BEAM Plus” for BIM-based

- sustainability analysis', *Automation in Construction*, 44, pp. 163–175. doi: 10.1016/j.autcon.2014.04.003.
- Wong, M. S. *et al.* (2016) 'Estimation of Hong Kong's solar energy potential using GIS and remote sensing technologies', *Renewable Energy*. Pergamon, 99, pp. 325–335. doi: 10.1016/J.RENENE.2016.07.003.
- Wu, P. *et al.* (2017) 'Review on Life Cycle Assessment of Energy Payback of Solar Photovoltaic Systems and a Case Study', in *Energy Procedia*. Elsevier, pp. 68–74. doi: 10.1016/j.egypro.2017.03.281.
- Xu, Z. *et al.* (2018) 'Analysis on the organization and Development of multi-microgrids', *Renewable and Sustainable Energy Reviews*, pp. 2204–2216. doi: 10.1016/j.rser.2017.06.032.
- Yan, J. *et al.* (2017a) 'Clean, affordable and reliable energy systems for low carbon city transition', *Applied Energy*, 15May, pp. 305–309. Available at: <https://www-sciencedirect-com.ezproxy.lb.polyu.edu.hk/science/article/pii/S0306261917302982> (Accessed: 25February2019).
- Yan, J. *et al.* (2017b) 'Clean, affordable and reliable energy systems for low carbon city transition', *Applied Energy*, 1November, pp. 305–309. doi: 10.1016/j.apenergy.2017.03.066.
- Yang, L. *et al.* (2021) 'The effects of remote work on collaboration among information workers', *Nature Human Behaviour*. doi: 10.1038/s41562-021-01196-4.
- Yau, Y. H. and Lim, K. S. (2016) 'Energy analysis of green office buildings in the tropics - Photovoltaic system', *Energy and Buildings*. Elsevier Ltd, 126, pp. 177–193. doi: 10.1016/j.enbuild.2016.05.010.
- Yik, F. W. H., Burnett, J. and Prescott, I. (2001) 'Predicting air-conditioning energy consumption of a group of buildings using different heat rejection methods', *Energy and Buildings*. Elsevier Sequoia SA, 33(2), pp. 151–166. doi: 10.1016/S0378-7788(00)00094-3.
- Ying, F. and O'Clery, N. (2021) 'Modelling COVID-19 transmission in supermarkets using

an agent-based model', *PLoS ONE*. Public Library of Science, 16(4 April), p. e0249821. doi: 10.1371/journal.pone.0249821.

Yoldaş, Y. *et al.* (2017) 'Enhancing smart grid with microgrids: Challenges and opportunities', *Renewable and Sustainable Energy Reviews*, pp. 205–214. doi: 10.1016/j.rser.2017.01.064.

Yu, C.-R. *et al.* (2020) 'Revealing the Impacts of Passive Cooling Techniques on Building Energy Performance: A Residential Case in Hong Kong', *Applied Sciences* 2020, Vol. 10, Page 4188. Multidisciplinary Digital Publishing Institute, 10(12), p. 4188. doi: 10.3390/AP10124188.

Yu, C. *et al.* (2015a) 'Challenges for Modeling Energy Use in High-rise Office Buildings in Hong Kong', in *Procedia Engineering*. Elsevier Ltd, pp. 513–520. doi: 10.1016/j.proeng.2015.08.1100.

Yu, C. *et al.* (2015b) 'Challenges for Modeling Energy Use in High-rise Office Buildings in Hong Kong', *Procedia Engineering*. Elsevier Ltd, 121, pp. 513–520. doi: 10.1016/J.PROENG.2015.08.1100.

Yu, P. C. H. and Chow, W. K. (2001) 'Energy use in commercial buildings in Hong Kong', *Applied Energy*. Elsevier, 69(4), pp. 243–255. doi: 10.1016/S0306-2619(01)00011-3.

Yu, R., Burke, M. and Raad, N. (2019) 'Exploring impact of future flexible working model evolution on urban environment, economy and planning', *Journal of Urban Management*. Elsevier, 8(3), pp. 447–457. doi: 10.1016/J.JUM.2019.05.002.

Yu, Y., Song, Y. and Bao, H. (2012) 'Why did the price of solar PV Si feedstock fluctuate so wildly in 2004-2009?', *Energy Policy*, 49, pp. 572–585. doi: 10.1016/j.enpol.2012.06.059.

Yue, D., You, F. and Darling, S. B. (2014) 'Domestic and overseas manufacturing scenarios of silicon-based photovoltaics: Life cycle energy and environmental comparative analysis', *Solar Energy*. Pergamon, 105, pp. 669–678. Available at: <https://www.sciencedirect->

com.ezproxy.lb.polyu.edu.hk/science/article/pii/S0360544217306928 (Accessed: 24February2019).

Zachar, M., Trifkovic, M. and Daoutidis, P. (2014) 'Policy effects on microgrid economics, technology selection, and environmental impact', *Computers and Chemical Engineering*, 81, pp. 364–375. doi: 10.1016/j.compchemeng.2015.03.012.

Zahedi, A. (2010) 'Australian renewable energy progress', *Renewable and Sustainable Energy Reviews*, pp. 2208–2213. doi: 10.1016/j.rser.2010.03.026.

Zaman, R., van Vliet, O. and Posch, A. (2021) 'Energy access and pandemic-resilient livelihoods: The role of solar energy safety nets', *Energy Research & Social Science*. Elsevier, 71, p. 101805. doi: 10.1016/J.ERSS.2020.101805.

Zenk, L. *et al.* (2020) 'Fast response to superspreading: Uncertainty and complexity in the context of COVID-19', *International Journal of Environmental Research and Public Health*. Multidisciplinary Digital Publishing Institute, 17(21), pp. 1–13. doi: 10.3390/ijerph17217884.

Zhang, S. *et al.* (2013) 'Interactions between renewable energy policy and renewable energy industrial policy: A critical analysis of china's policy approach to renewable energies', *Energy Policy*, 62, pp. 342–353. doi: 10.1016/j.enpol.2013.07.063.

Zhang, X. *et al.* (2020) 'A preliminary simulation study about the impact of COVID-19 crisis on energy demand of a building mix at a district in Sweden', *Applied Energy*. Elsevier, 280, p. 115954. doi: 10.1016/J.APENERGY.2020.115954.

Zhang, X., Chang, S. and Eric, M. (2012) 'Renewable energy in China: An integrated technology and policy perspective', *Energy Policy*, pp. 1–6. doi: 10.1016/j.enpol.2012.09.071.

Zhang, Y. and Jia, Q. S. (2017) 'Operational Optimization for Microgrid of Buildings with Distributed Solar Power and Battery', *Asian Journal of Control*. John Wiley & Sons, Ltd,

19(3), pp. 996–1008. doi: 10.1002/asjc.1424.

Zhao, B. *et al.* (2018) ‘Three representative island microgrids in the East China Sea: Key technologies and experiences’, *Renewable and Sustainable Energy Reviews*, pp. 262–274. doi: 10.1016/j.rser.2018.07.051.

Zheng, M. (2015) ‘Smart households: Dispatch strategies and economic analysis of distributed energy storage for residential peak shaving’, *Applied Energy*, 147, pp. 246–257.

Zheng, M., Meinrenken, C. J. and Lackner, K. S. (2015) ‘Smart households: Dispatch strategies and economic analysis of distributed energy storage for residential peak shaving’, *Applied Energy*, 147, pp. 246–257. doi: 10.1016/j.apenergy.2015.02.039.

Zhu, D. *et al.* (2013) ‘A detailed loads comparison of three building energy modeling programs: EnergyPlus, DeST and DOE-2.1E’, *Building Simulation 2013* 6:3. Springer, 6(3), pp. 323–335. doi: 10.1007/S12273-013-0126-7.

Zia, M. F., Elbouchikhi, E. and Benbouzid, M. (2018) ‘Microgrids energy management systems: A critical review on methods, solutions, and prospects’, *Applied Energy*. Elsevier, pp. 1033–1055. doi: 10.1016/j.apenergy.2018.04.103.

Zito, M. *et al.* (2021) ‘Does the end justify the means? The role of organizational communication among work-from-home employees during the covid-19 pandemic’, *International Journal of Environmental Research and Public Health*. MDPI AG, 18(8). doi: 10.3390/IJERPH18083933.

Zomer, C. *et al.* (2020) ‘Performance assessment of partially shaded building-integrated photovoltaic (BIPV) systems in a positive-energy solar energy laboratory building: Architecture perspectives’, *Solar Energy*. Pergamon, 211, pp. 879–896. doi: 10.1016/J.SOLENER.2020.10.026.

Zore, Ž. *et al.* (2018) ‘Maximizing the sustainability net present value of renewable energy supply networks’, *Chemical Engineering Research and Design*, 131, pp. 245–265. doi:

10.1016/j.cherd.2018.01.035.

9. APPENDICES

9.1 Appendix 1

Part 1: Life cycle assessment of Microgrid

200W PV Panel system

Impact Category	Raw materials	Manufacture	Transport
Climate change / kg CO ₂ eq	12858.38	37610.46	552.1042
Ozone depletion / kg CFC-11 eq	0.000827	0.000214	8.65E-05
Human toxicity / kg 1,4-DB eq	4315.185	6113.631	60.88026
Particulate matter formation / kg PM ₁₀ eq	25.62532	102.5316	0.724301
Terrestrial acidification / kg SO ₂ eq	62.69982	328.6602	1.627336
Freshwater eutrophication / kg 1,4-DB eq	4.434905	4.773482	0.046636
Terrestrial ecotoxicity / kg 1,4-DB eq	0.987305	1.037941	0.098137
Marine ecotoxicity / kg 1,4-DB eq	117.1759	108.0643	1.670819
Agricultural land occupation / m ² a	197.8284	1114.15	2.010058
Urban land occupation / m ² a	60.21136	315.7439	8.322601
Natural land transformation / m ²	2.176429	2.430539	0.200553
Fossil depletion / kg oil eq	3855.621	7831.607	201.2007

280W PV Panel system

Impact Category	Raw materials	Manufacture	Transport
Climate change / kg CO ₂ eq	94409.13	276177.3	5327.086
Ozone depletion / kg CFC-11 eq	0.006075	0.001572	0.000835
Human toxicity / kg 1,4-DB eq	31677.68	44893.01	587.4151
Particulate matter formation / kg PM ₁₀ eq	188.1242	752.8995	6.988561
Terrestrial acidification / kg SO ₂ eq	460.3608	2413.385	15.70167
Freshwater eutrophication / kg 1,4-DB eq	32.5568	35.05216	0.449975
Terrestrial ecotoxicity / kg 1,4-DB eq	7.247377	7.621703	0.946895
Marine ecotoxicity / kg 1,4-DB eq	860.1615	793.5266	16.12122
Agricultural land occupation / m ² a	1452.389	8181.313	19.39443
Urban land occupation / m ² a	442.0536	2318.539	80.30225
Natural land transformation / m ²	15.97649	17.84769	1.935073
Fossil depletion / kg oil eq	28311.07	57508.27	1941.324

Battery system

Impact Category	Raw materials	Manufacture	Transport
Climate change / kg CO ₂ eq	29339.55	131871.7	13238.16
Ozone depletion / kg CFC-11 eq	0.001461	0.005576	4.94E-07
Human toxicity / kg 1,4-DB eq	176642.6	99769.9	6675.51
Particulate matter formation / kg PM ₁₀ eq	170.9153	58.75847	88.42914
Terrestrial acidification / kg SO ₂ eq	491.5068	160.9131	228.7749
Freshwater eutrophication / kg 1,4-DB eq	106.2568	163.5732	0
Terrestrial ecotoxicity / kg 1,4-DB eq	2.561041	5.801921	0.015343
Marine ecotoxicity / kg 1,4-DB eq	2074.117	2126.744	44.58582
Agricultural land occupation / m ² a	752.6241	1780.619	0
Urban land occupation / m ² a	501.5582	416.7393	0
Natural land transformation / m ²	5.030906	8.261293	0
Fossil depletion / kg oil eq	12938.97	35817.81	4245.525

Wind turbines system

Impact Category	Raw materials	Manufacture	Transport
Climate change / kg CO ₂ eq	27566.02	256.7327	392.3814
Ozone depletion / kg CFC-11 eq	0.001375	6.46E-06	1.46E-08
Human toxicity / kg 1,4-DB eq	21237.2	53.47823	197.8632
Particulate matter formation / kg PM ₁₀ eq	102.1432	0.258459	2.621055
Terrestrial acidification / kg SO ₂ eq	108.3399	0.801059	6.780928
Freshwater eutrophication / kg 1,4-DB eq	16.02731	0.072865	0
Terrestrial ecotoxicity / kg 1,4-DB eq	3.681038	0.01774	0.000455
Marine ecotoxicity / kg 1,4-DB eq	1064.644	1.188045	1.321531
Agricultural land occupation / m ² a	665.1804	4.717496	0
Urban land occupation / m ² a	291.1477	1.112523	0
Natural land transformation / m ²	3.115211	0.050802	0
Fossil depletion / kg oil eq	8881.532	79.87389	125.8381

Part 2 Life cycle assessment of diesel generator

Diesel generator

Impact Category	Raw materials	Manufacture	Transport
Climate change / kg CO ₂ eq	35341.94	28465.43	750.5802
Ozone depletion / kg CFC-11 eq	0.005111	0.000162	0.000118
Human toxicity / kg 1,4-DB eq	22515.25	4627.095	82.76611
Particulate matter formation / kg PM ₁₀ eq	85.35795	77.60089	0.98468
Terrestrial acidification / kg SO ₂ eq	168.5349	248.7461	2.212347
Freshwater eutrophication / kg 1,4-DB eq	19.30292	3.612804	0.063401
Terrestrial ecotoxicity / kg 1,4-DB eq	5.29224	0.785564	0.133416
Marine ecotoxicity / kg 1,4-DB eq	566.4791	81.7883	2.271462
Agricultural land occupation / m ² a	477.4515	843.2429	2.732653
Urban land occupation / m ² a	237.4974	238.9704	11.31449
Natural land transformation / m ²	18.2731	1.839551	0.27265
Fossil depletion / kg oil eq	17412.7	5927.342	273.5303

Diesel generator (diesel combustion and diesel delivery)

Impact Category	Operation	Operation
Climate change / kg CO ₂ eq	2650767.654	17027.31759
Ozone depletion / kg CFC-11 eq	0.564923997	0.014649497
Human toxicity / kg 1,4-DB eq	166541.1628	4222.335771
Particulate matter formation / kg PM ₁₀ eq	14997.00436	55.74037581
Terrestrial acidification / kg SO ₂ eq	29277.02587	191.5414451
Freshwater eutrophication / kg 1,4-DB eq	117.256295	2.658104821
Terrestrial ecotoxicity / kg 1,4-DB eq	345.3197743	8.716486754
Marine ecotoxicity / kg 1,4-DB eq	4890.103515	109.4592365
Agricultural land occupation / m ² a	2294.336837	45.67301589
Urban land occupation / m ² a	6833.117611	152.2502107
Natural land transformation / m ²	2255.080418	58.23655531
Fossil depletion / kg oil eq	1571340.43	40968.63224

Part 3 Life cycle assessment of grid extension

Grid extension (transformer)

Impact Category	Raw materials	Manufacture	Transport
Climate change / kg CO ₂ eq	3073.443	167.5922	21.97039
Ozone depletion / kg CFC-11 eq	0.000142	9.54E-07	3.44E-06
Human toxicity / kg 1,4-DB eq	2115.875	27.24235	2.422664
Particulate matter formation / kg PM ₁₀ eq	7.754342	0.456881	0.028823
Terrestrial acidification / kg SO ₂ eq	13.82942	1.464511	0.064758
Freshwater eutrophication / kg 1,4-DB eq	1.33647	0.021271	0.001856
Terrestrial ecotoxicity / kg 1,4-DB eq	0.287199	0.004625	0.003905
Marine ecotoxicity / kg 1,4-DB eq	51.66084	0.481534	0.066488
Agricultural land occupation / m ² a	40.80548	4.964653	0.079988
Urban land occupation / m ² a	17.62188	1.406955	0.331189
Natural land transformation / m ²	0.412215	0.01083	0.007981
Fossil depletion / kg oil eq	1173.007	34.89765	8.006563

Grid extension (submarine cable)

Impact Category	Raw materials	Manufacture	Transport
Climate change / kg CO ₂ eq	73333.9	2801.086	1978.509
Ozone depletion / kg CFC-11 eq	0.003148	0.000229	0.000301
Human toxicity / kg 1,4-DB eq	343767.7	26745.8	286.1904
Particulate matter formation / kg PM ₁₀ eq	392.7042	13.04251	4.254504
Terrestrial acidification / kg SO ₂ eq	563.1459	35.95491	9.142294
Freshwater eutrophication / kg 1,4-DB eq	194.6521	13.60527	0.216991
Terrestrial ecotoxicity / kg 1,4-DB eq	18.67787	1.467938	0.46046
Marine ecotoxicity / kg 1,4-DB eq	5465.245	320.9847	7.872153
Agricultural land occupation / m ² a	1512.726	65.73149	9.771632
Urban land occupation / m ² a	1047.263	43.49814	43.62892
Natural land transformation / m ²	9.947061	0.761649	0.709459
Fossil depletion / kg oil eq	33486.29	911.9081	714.889

Grid extension (electricity)

Impact Category	Operation
Climate change / kg CO ₂ eq	4818664
Ozone depletion / kg CFC-11 eq	0.027498
Human toxicity / kg 1,4-DB eq	812349.6
Particulate matter formation / kg PM ₁₀ eq	13080.93
Terrestrial acidification / kg SO ₂ eq	41910.23
Freshwater eutrophication / kg 1,4-DB eq	624.7563
Terrestrial ecotoxicity / kg 1,4-DB eq	142.0988
Marine ecotoxicity / kg 1,4-DB eq	14171.07
Agricultural land occupation / m ² a	142626.4
Urban land occupation / m ² a	40362.95
Natural land transformation / m ²	311.3247
Fossil depletion / kg oil eq	998638.7

9.2 Appendix 2

Sample of whole building energy simulation hourly electricity demand output (reference office building), result in July

Electric			Electric			Electric		
Date/Time	Time	Demand	Date/Time	Time	Demand	Date/Time	Time	Demand
		[W]			[W]			[W]
3/7/1995	0:00:00	46,838.20	12/7/1995	0:00:00	46,838.20	21/7/1995	0:00:00	46,838.20
3/7/1995	1:00:00	46,838.20	12/7/1995	1:00:00	46,838.20	21/7/1995	1:00:00	46,838.20
3/7/1995	2:00:00	46,838.20	12/7/1995	2:00:00	46,838.20	21/7/1995	2:00:00	46,838.20
3/7/1995	3:00:00	46,838.20	12/7/1995	3:00:00	46,838.20	21/7/1995	3:00:00	46,838.20
3/7/1995	4:00:00	46,838.20	12/7/1995	4:00:00	46,838.20	21/7/1995	4:00:00	46,838.20
3/7/1995	5:00:00	410,384	12/7/1995	5:00:00	274,863	21/7/1995	5:00:00	246,037
3/7/1995	6:00:00	430,197	12/7/1995	6:00:00	319,531	21/7/1995	6:00:00	309,984
3/7/1995	7:00:00	749,281	12/7/1995	7:00:00	618,077	21/7/1995	7:00:00	601,880
3/7/1995	8:00:00	804,737	12/7/1995	8:00:00	719,857	21/7/1995	8:00:00	704,595
3/7/1995	9:00:00	798,884	12/7/1995	9:00:00	693,773	21/7/1995	9:00:00	675,487
3/7/1995	10:00:00	809,074	12/7/1995	10:00:00	695,806	21/7/1995	10:00:00	674,022
3/7/1995	11:00:00	769,937	12/7/1995	11:00:00	660,567	21/7/1995	11:00:00	624,288
3/7/1995	12:00:00	776,019	12/7/1995	12:00:00	676,363	21/7/1995	12:00:00	638,820
3/7/1995	13:00:00	801,780	12/7/1995	13:00:00	716,466	21/7/1995	13:00:00	703,751
3/7/1995	14:00:00	795,821	12/7/1995	14:00:00	711,476	21/7/1995	14:00:00	671,800
3/7/1995	15:00:00	800,756	12/7/1995	15:00:00	707,842	21/7/1995	15:00:00	667,929
3/7/1995	16:00:00	803,837	12/7/1995	16:00:00	702,445	21/7/1995	16:00:00	648,373
3/7/1995	17:00:00	703,058	12/7/1995	17:00:00	609,728	21/7/1995	17:00:00	588,845
3/7/1995	18:00:00	465,491	12/7/1995	18:00:00	445,712	21/7/1995	18:00:00	423,803

Electric			Electric			Electric		
Date/Time	Time	Demand	Date/Time	Time	Demand	Date/Time	Time	Demand
		[W]			[W]			[W]
3/7/1995	19:00:00	343,297	12/7/1995	19:00:00	340,038	21/7/1995	19:00:00	327,275
3/7/1995	20:00:00	255,074	12/7/1995	20:00:00	262,970	21/7/1995	20:00:00	255,675
3/7/1995	21:00:00	239,544	12/7/1995	21:00:00	248,266	21/7/1995	21:00:00	244,782
3/7/1995	22:00:00	249,539	12/7/1995	22:00:00	239,100	21/7/1995	22:00:00	240,742
3/7/1995	23:00:00	46,838.20	12/7/1995	23:00:00	46,838.20	21/7/1995	23:00:00	46,838.20
4/7/1995	0:00:00	46,838.20	13/7/1995	0:00:00	46,838.20	24/7/1995	0:00:00	46,838.20
4/7/1995	1:00:00	46,838.20	13/7/1995	1:00:00	46,838.20	24/7/1995	1:00:00	46,838.20
4/7/1995	2:00:00	46,838.20	13/7/1995	2:00:00	46,838.20	24/7/1995	2:00:00	46,838.20
4/7/1995	3:00:00	46,838.20	13/7/1995	3:00:00	46,838.20	24/7/1995	3:00:00	46,838.20
4/7/1995	4:00:00	46,838.20	13/7/1995	4:00:00	46,838.20	24/7/1995	4:00:00	46,838.20
4/7/1995	5:00:00	284,432	13/7/1995	5:00:00	266,277	24/7/1995	5:00:00	399,475
4/7/1995	6:00:00	324,991	13/7/1995	6:00:00	315,993	24/7/1995	6:00:00	427,432
4/7/1995	7:00:00	630,639	13/7/1995	7:00:00	616,456	24/7/1995	7:00:00	769,693
4/7/1995	8:00:00	736,336	13/7/1995	8:00:00	736,782	24/7/1995	8:00:00	857,825
4/7/1995	9:00:00	713,542	13/7/1995	9:00:00	711,265	24/7/1995	9:00:00	827,834
4/7/1995	10:00:00	707,793	13/7/1995	10:00:00	699,758	24/7/1995	10:00:00	803,605
4/7/1995	11:00:00	680,355	13/7/1995	11:00:00	663,740	24/7/1995	11:00:00	761,503
4/7/1995	12:00:00	698,806	13/7/1995	12:00:00	682,059	24/7/1995	12:00:00	760,599
4/7/1995	13:00:00	733,036	13/7/1995	13:00:00	725,284	24/7/1995	13:00:00	780,520
4/7/1995	14:00:00	722,511	13/7/1995	14:00:00	720,010	24/7/1995	14:00:00	791,143
4/7/1995	15:00:00	728,772	13/7/1995	15:00:00	733,894	24/7/1995	15:00:00	794,610
4/7/1995	16:00:00	723,163	13/7/1995	16:00:00	742,306	24/7/1995	16:00:00	791,755

Electric			Electric			Electric		
Date/Time	Time	Demand	Date/Time	Time	Demand	Date/Time	Time	Demand
		[W]			[W]			[W]
4/7/1995	17:00:00	665,134	13/7/1995	17:00:00	622,894	24/7/1995	17:00:00	704,947
4/7/1995	18:00:00	446,434	13/7/1995	18:00:00	440,626	24/7/1995	18:00:00	470,293
4/7/1995	19:00:00	353,284	13/7/1995	19:00:00	354,547	24/7/1995	19:00:00	348,360
4/7/1995	20:00:00	273,650	13/7/1995	20:00:00	271,055	24/7/1995	20:00:00	259,442
4/7/1995	21:00:00	256,607	13/7/1995	21:00:00	255,521	24/7/1995	21:00:00	242,087
4/7/1995	22:00:00	247,325	13/7/1995	22:00:00	246,527	24/7/1995	22:00:00	233,383
4/7/1995	23:00:00	46,838.20	13/7/1995	23:00:00	46,838.20	24/7/1995	23:00:00	46,838.20
5/7/1995	0:00:00	46,838.20	14/7/1995	0:00:00	46,838.20	25/7/1995	0:00:00	46,838.20
5/7/1995	1:00:00	46,838.20	14/7/1995	1:00:00	46,838.20	25/7/1995	1:00:00	46,838.20
5/7/1995	2:00:00	46,838.20	14/7/1995	2:00:00	46,838.20	25/7/1995	2:00:00	46,838.20
5/7/1995	3:00:00	46,838.20	14/7/1995	3:00:00	46,838.20	25/7/1995	3:00:00	46,838.20
5/7/1995	4:00:00	46,838.20	14/7/1995	4:00:00	46,838.20	25/7/1995	4:00:00	46,838.20
5/7/1995	5:00:00	275,766	14/7/1995	5:00:00	270,332	25/7/1995	5:00:00	313,465
5/7/1995	6:00:00	324,327	14/7/1995	6:00:00	325,038	25/7/1995	6:00:00	340,430
5/7/1995	7:00:00	623,993	14/7/1995	7:00:00	628,484	25/7/1995	7:00:00	661,732
5/7/1995	8:00:00	728,031	14/7/1995	8:00:00	733,709	25/7/1995	8:00:00	753,335
5/7/1995	9:00:00	702,885	14/7/1995	9:00:00	715,218	25/7/1995	9:00:00	735,754
5/7/1995	10:00:00	697,509	14/7/1995	10:00:00	705,043	25/7/1995	10:00:00	727,585
5/7/1995	11:00:00	662,588	14/7/1995	11:00:00	673,973	25/7/1995	11:00:00	688,966
5/7/1995	12:00:00	679,961	14/7/1995	12:00:00	693,449	25/7/1995	12:00:00	702,189
5/7/1995	13:00:00	714,330	14/7/1995	13:00:00	733,773	25/7/1995	13:00:00	741,837
5/7/1995	14:00:00	700,826	14/7/1995	14:00:00	727,439	25/7/1995	14:00:00	735,712

Electric			Electric			Electric		
Date/Time	Time	Demand	Date/Time	Time	Demand	Date/Time	Time	Demand
		[W]			[W]			[W]
5/7/1995	15:00:00	703,330	14/7/1995	15:00:00	741,382	25/7/1995	15:00:00	751,631
5/7/1995	16:00:00	707,102	14/7/1995	16:00:00	751,757	25/7/1995	16:00:00	755,656
5/7/1995	17:00:00	642,303	14/7/1995	17:00:00	631,224	25/7/1995	17:00:00	655,589
5/7/1995	18:00:00	449,513	14/7/1995	18:00:00	421,767	25/7/1995	18:00:00	438,215
5/7/1995	19:00:00	341,250	14/7/1995	19:00:00	357,541	25/7/1995	19:00:00	339,136
5/7/1995	20:00:00	265,536	14/7/1995	20:00:00	276,672	25/7/1995	20:00:00	259,601
5/7/1995	21:00:00	251,952	14/7/1995	21:00:00	258,121	25/7/1995	21:00:00	266,091
5/7/1995	22:00:00	241,506	14/7/1995	22:00:00	247,835	25/7/1995	22:00:00	255,873
5/7/1995	23:00:00	46,838.20	14/7/1995	23:00:00	46,838.20	25/7/1995	23:00:00	46,838.20
6/7/1995	0:00:00	46,838.20	17/7/1995	0:00:00	46,838.20	26/7/1995	0:00:00	46,838.20
6/7/1995	1:00:00	46,838.20	17/7/1995	1:00:00	46,838.20	26/7/1995	1:00:00	46,838.20
6/7/1995	2:00:00	46,838.20	17/7/1995	2:00:00	46,838.20	26/7/1995	2:00:00	46,838.20
6/7/1995	3:00:00	46,838.20	17/7/1995	3:00:00	46,838.20	26/7/1995	3:00:00	46,838.20
6/7/1995	4:00:00	46,838.20	17/7/1995	4:00:00	46,838.20	26/7/1995	4:00:00	46,838.20
6/7/1995	5:00:00	251,074	17/7/1995	5:00:00	385,119	26/7/1995	5:00:00	284,340
6/7/1995	6:00:00	304,810	17/7/1995	6:00:00	394,298	26/7/1995	6:00:00	335,914
6/7/1995	7:00:00	599,282	17/7/1995	7:00:00	721,292	26/7/1995	7:00:00	649,781
6/7/1995	8:00:00	706,546	17/7/1995	8:00:00	794,536	26/7/1995	8:00:00	758,649
6/7/1995	9:00:00	682,869	17/7/1995	9:00:00	756,534	26/7/1995	9:00:00	736,280
6/7/1995	10:00:00	680,133	17/7/1995	10:00:00	746,425	26/7/1995	10:00:00	732,167
6/7/1995	11:00:00	644,524	17/7/1995	11:00:00	715,385	26/7/1995	11:00:00	686,664
6/7/1995	12:00:00	660,241	17/7/1995	12:00:00	726,017	26/7/1995	12:00:00	707,023

Electric			Electric			Electric		
Date/Time	Time	Demand	Date/Time	Time	Demand	Date/Time	Time	Demand
		[W]			[W]			[W]
6/7/1995	13:00:00	705,839	17/7/1995	13:00:00	744,771	26/7/1995	13:00:00	758,272
6/7/1995	14:00:00	692,327	17/7/1995	14:00:00	721,767	26/7/1995	14:00:00	754,201
6/7/1995	15:00:00	687,656	17/7/1995	15:00:00	714,362	26/7/1995	15:00:00	763,723
6/7/1995	16:00:00	673,223	17/7/1995	16:00:00	705,951	26/7/1995	16:00:00	759,319
6/7/1995	17:00:00	615,702	17/7/1995	17:00:00	624,139	26/7/1995	17:00:00	655,803
6/7/1995	18:00:00	431,044	17/7/1995	18:00:00	449,431	26/7/1995	18:00:00	433,982
6/7/1995	19:00:00	327,732	17/7/1995	19:00:00	346,500	26/7/1995	19:00:00	360,249
6/7/1995	20:00:00	253,921	17/7/1995	20:00:00	265,680	26/7/1995	20:00:00	282,598
6/7/1995	21:00:00	240,612	17/7/1995	21:00:00	251,710	26/7/1995	21:00:00	265,112
6/7/1995	22:00:00	233,044	17/7/1995	22:00:00	242,618	26/7/1995	22:00:00	254,726
6/7/1995	23:00:00	46,838.20	17/7/1995	23:00:00	46,838.20	26/7/1995	23:00:00	46,838.20
7/7/1995	0:00:00	46,838.20	18/7/1995	0:00:00	46,838.20	27/7/1995	0:00:00	46,838.20
7/7/1995	1:00:00	46,838.20	18/7/1995	1:00:00	46,838.20	27/7/1995	1:00:00	46,838.20
7/7/1995	2:00:00	46,838.20	18/7/1995	2:00:00	46,838.20	27/7/1995	2:00:00	46,838.20
7/7/1995	3:00:00	46,838.20	18/7/1995	3:00:00	46,838.20	27/7/1995	3:00:00	46,838.20
7/7/1995	4:00:00	46,838.20	18/7/1995	4:00:00	46,838.20	27/7/1995	4:00:00	46,838.20
7/7/1995	5:00:00	263,359	18/7/1995	5:00:00	277,066	27/7/1995	5:00:00	286,236
7/7/1995	6:00:00	308,906	18/7/1995	6:00:00	319,682	27/7/1995	6:00:00	333,642
7/7/1995	7:00:00	604,966	18/7/1995	7:00:00	613,437	27/7/1995	7:00:00	643,662
7/7/1995	8:00:00	717,012	18/7/1995	8:00:00	715,345	27/7/1995	8:00:00	754,094
7/7/1995	9:00:00	686,991	18/7/1995	9:00:00	685,657	27/7/1995	9:00:00	731,064
7/7/1995	10:00:00	682,807	18/7/1995	10:00:00	671,691	27/7/1995	10:00:00	730,673

Electric			Electric			Electric		
Date/Time	Time	Demand	Date/Time	Time	Demand	Date/Time	Time	Demand
		[W]			[W]			[W]
7/7/1995	11:00:00	649,073	18/7/1995	11:00:00	618,227	27/7/1995	11:00:00	687,715
7/7/1995	12:00:00	660,363	18/7/1995	12:00:00	632,492	27/7/1995	12:00:00	705,906
7/7/1995	13:00:00	709,818	18/7/1995	13:00:00	692,860	27/7/1995	13:00:00	754,781
7/7/1995	14:00:00	691,840	18/7/1995	14:00:00	677,341	27/7/1995	14:00:00	750,522
7/7/1995	15:00:00	697,246	18/7/1995	15:00:00	679,203	27/7/1995	15:00:00	748,311
7/7/1995	16:00:00	677,692	18/7/1995	16:00:00	653,384	27/7/1995	16:00:00	741,658
7/7/1995	17:00:00	588,892	18/7/1995	17:00:00	605,998	27/7/1995	17:00:00	631,559
7/7/1995	18:00:00	435,668	18/7/1995	18:00:00	416,714	27/7/1995	18:00:00	423,790
7/7/1995	19:00:00	332,219	18/7/1995	19:00:00	318,185	27/7/1995	19:00:00	357,452
7/7/1995	20:00:00	254,678	18/7/1995	20:00:00	243,773	27/7/1995	20:00:00	277,906
7/7/1995	21:00:00	240,235	18/7/1995	21:00:00	246,148	27/7/1995	21:00:00	260,691
7/7/1995	22:00:00	232,895	18/7/1995	22:00:00	244,417	27/7/1995	22:00:00	251,117
7/7/1995	23:00:00	46,838.20	18/7/1995	23:00:00	46,838.20	27/7/1995	23:00:00	46,838.20
10/7/1995	0:00:00	46,838.20	19/7/1995	0:00:00	46,838.20	28/7/1995	0:00:00	46,838.20
10/7/1995	1:00:00	46,838.20	19/7/1995	1:00:00	46,838.20	28/7/1995	1:00:00	46,838.20
10/7/1995	2:00:00	46,838.20	19/7/1995	2:00:00	46,838.20	28/7/1995	2:00:00	46,838.20
10/7/1995	3:00:00	46,838.20	19/7/1995	3:00:00	46,838.20	28/7/1995	3:00:00	46,838.20
10/7/1995	4:00:00	46,838.20	19/7/1995	4:00:00	46,838.20	28/7/1995	4:00:00	46,838.20
10/7/1995	5:00:00	380,293	19/7/1995	5:00:00	252,272	28/7/1995	5:00:00	277,081
10/7/1995	6:00:00	393,490	19/7/1995	6:00:00	313,433	28/7/1995	6:00:00	331,032
10/7/1995	7:00:00	740,055	19/7/1995	7:00:00	605,742	28/7/1995	7:00:00	643,166
10/7/1995	8:00:00	821,924	19/7/1995	8:00:00	716,948	28/7/1995	8:00:00	750,770

Electric			Electric			Electric		
Date/Time	Time	Demand	Date/Time	Time	Demand	Date/Time	Time	Demand
		[W]			[W]			[W]
10/7/1995	9:00:00	796,754	19/7/1995	9:00:00	688,658	28/7/1995	9:00:00	729,181
10/7/1995	10:00:00	792,892	19/7/1995	10:00:00	681,372	28/7/1995	10:00:00	717,497
10/7/1995	11:00:00	765,854	19/7/1995	11:00:00	623,150	28/7/1995	11:00:00	678,061
10/7/1995	12:00:00	773,552	19/7/1995	12:00:00	629,374	28/7/1995	12:00:00	696,928
10/7/1995	13:00:00	798,524	19/7/1995	13:00:00	693,206	28/7/1995	13:00:00	740,750
10/7/1995	14:00:00	792,903	19/7/1995	14:00:00	679,566	28/7/1995	14:00:00	735,634
10/7/1995	15:00:00	795,702	19/7/1995	15:00:00	680,880	28/7/1995	15:00:00	740,112
10/7/1995	16:00:00	794,022	19/7/1995	16:00:00	658,760	28/7/1995	16:00:00	748,298
10/7/1995	17:00:00	694,504	19/7/1995	17:00:00	600,284	28/7/1995	17:00:00	644,600
10/7/1995	18:00:00	456,506	19/7/1995	18:00:00	413,129	28/7/1995	18:00:00	431,237
10/7/1995	19:00:00	335,894	19/7/1995	19:00:00	328,127	28/7/1995	19:00:00	358,897
10/7/1995	20:00:00	252,862	19/7/1995	20:00:00	256,153	28/7/1995	20:00:00	279,591
10/7/1995	21:00:00	238,101	19/7/1995	21:00:00	237,940	28/7/1995	21:00:00	264,842
10/7/1995	22:00:00	247,125	19/7/1995	22:00:00	239,174	28/7/1995	22:00:00	252,871
10/7/1995	23:00:00	46,838.20	19/7/1995	23:00:00	46,838.20	28/7/1995	23:00:00	46,838.20
11/7/1995	0:00:00	46,838.20	20/7/1995	0:00:00	46,838.20	31/7/1995	0:00:00	46,838.20
11/7/1995	1:00:00	46,838.20	20/7/1995	1:00:00	46,838.20	31/7/1995	1:00:00	46,838.20
11/7/1995	2:00:00	46,838.20	20/7/1995	2:00:00	46,838.20	31/7/1995	2:00:00	46,838.20
11/7/1995	3:00:00	46,838.20	20/7/1995	3:00:00	46,838.20	31/7/1995	3:00:00	46,838.20
11/7/1995	4:00:00	46,838.20	20/7/1995	4:00:00	46,838.20	31/7/1995	4:00:00	46,838.20
11/7/1995	5:00:00	295,106	20/7/1995	5:00:00	240,770	31/7/1995	5:00:00	451,990
11/7/1995	6:00:00	334,077	20/7/1995	6:00:00	304,783	31/7/1995	6:00:00	472,774

Electric			Electric			Electric		
Date/Time	Time	Demand	Date/Time	Time	Demand	Date/Time	Time	Demand
		[W]			[W]			[W]
11/7/1995	7:00:00	628,525	20/7/1995	7:00:00	598,157	31/7/1995	7:00:00	815,226
11/7/1995	8:00:00	724,112	20/7/1995	8:00:00	709,999	31/7/1995	8:00:00	895,714
11/7/1995	9:00:00	701,408	20/7/1995	9:00:00	685,991	31/7/1995	9:00:00	867,497
11/7/1995	10:00:00	705,419	20/7/1995	10:00:00	682,497	31/7/1995	10:00:00	861,814
11/7/1995	11:00:00	673,638	20/7/1995	11:00:00	619,538	31/7/1995	11:00:00	831,366
11/7/1995	12:00:00	691,112	20/7/1995	12:00:00	628,028	31/7/1995	12:00:00	839,572
11/7/1995	13:00:00	729,251	20/7/1995	13:00:00	686,935	31/7/1995	13:00:00	853,605
11/7/1995	14:00:00	712,852	20/7/1995	14:00:00	667,282	31/7/1995	14:00:00	847,496
11/7/1995	15:00:00	719,113	20/7/1995	15:00:00	666,529	31/7/1995	15:00:00	830,348
11/7/1995	16:00:00	715,456	20/7/1995	16:00:00	645,658	31/7/1995	16:00:00	801,028
11/7/1995	17:00:00	615,341	20/7/1995	17:00:00	589,491	31/7/1995	17:00:00	703,333
11/7/1995	18:00:00	423,928	20/7/1995	18:00:00	423,070	31/7/1995	18:00:00	463,172
11/7/1995	19:00:00	344,525	20/7/1995	19:00:00	326,583	31/7/1995	19:00:00	343,459
11/7/1995	20:00:00	266,505	20/7/1995	20:00:00	255,885	31/7/1995	20:00:00	256,421
11/7/1995	21:00:00	251,192	20/7/1995	21:00:00	243,762	31/7/1995	21:00:00	239,893
11/7/1995	22:00:00	242,886	20/7/1995	22:00:00	237,972	31/7/1995	22:00:00	242,462
11/7/1995	23:00:00	46,838.20	20/7/1995	23:00:00	46,838.20	31/7/1995	23:00:00	46,838.20

9.3 Appendix 3

Agent-based modelling code

directed-link-breed [red-links red-link]

directed-link-breed [blue-links blue-link]

globals [

num-home

num-office

num-no

num-oneday

num-twoday

num-threeday

WFH0

WFH1

WFH2

WFH3

num-home-sum

num-office-sum

energy

previous-energy

sum-energy

num-fconnect

num-cconnect

energy-saving

]

turtles-own [

age

gender

wb ;well-being

;enco ;environmental constraint

reco ;resource constraint

Wwb

Wenco

Wreco

Wgender

Wage

fsocial-influence

csocial-influence

rconnected?

bconnected?

num-family

num-colleagues

week-home

week-office

hUi

stress

choice ;home=0 office=1

ex-choice

personal-stress-threshold

]

to setup

ca

ct

;ask links [hide-link]

set num-home 0

set num-office 0


```

set num-home-sum 0

set num-office-sum 0

set energy 0

set previous-energy 0

set sum-energy 0

setup-home-office

setup-employee

ask red-links [set color red]

ask blue-links [set color blue]

;output-1

reset-ticks

end

to setup-home-office
  ask patches with [pxcor < 0]
  [set pcolor white] ;represent the home
end

to setup-employee
  crt floor (num-total * 0.32);632 / 1976

```

```
[
  set shape "person"
  set size 1
  set color grey
  move-to one-of patches with [(pcolor = white)]; and (not any? turtles-on self)
  set choice random 2
  set age random-normal 3.56 1.01
  set gender 1 ;male
]
```

```
crt floor (num-total * 0.68);1344 / 1976
```

```
[
  set shape "person"
  set size 1
  set color grey
  move-to one-of patches with [(pcolor = white)]; and (not any? turtles-on self)
  set choice random 2
  set age random-normal 3.56 1.01
  set gender 2 ;female
]
```

```
ask turtles
```

```
[
  set fsocial-influence 0
  set csocial-influence 0
```

```

set rconnected? false

set bconnected? false

set wb random-normal 3.55 0.84

;set enco random-normal 3.41 1.00

set reco random-normal mean-reco 2.29 ;7.08 2.29

set Wwb random-normal 0.38 0.03

set Wenco random-normal -0.06 0.02

set Wreco random-normal -0.03 0.01

set Wgender random-normal 0.08 0.04

set Wage random-normal -0.08 0.02

;everyone has different stress thresholds

set personal-stress-threshold random-normal stress-threshold 1

;data from references

set num-family random 3 ;2.66

set num-colleagues random 5

if rconnected? = false [find-family-member]

if bconnected? = false [find-colleagues]

]

initilization

```

end

to find-family-member

if count turtles with [rconnected? = false] > num-family

[

create-red-links-to n-of num-family other turtles with [rconnected? = false]

ask red-link-neighbors [set rconnected? true]

set rconnected? true

]

end

to find-colleagues

if count turtles with [bconnected? = false] > num-colleagues

[

create-blue-links-to n-of num-colleagues other turtles with [bconnected? = false]

ask blue-link-neighbors [set bconnected? true]

set bconnected? true

]

end

to initialization

ask turtles

[

set hUi 0

set stress 0

```
]
end
```

```
to output-1
```

```
  if (file-exists? "TestOutput-WHF.csv") [carefully [file-delete "TestOutput-WHF.csv"] [print
error-message]]
```

```
  file-open "TestOutput-WHF.csv"
```

```
    file-type "tick,"
```

```
    file-type "ID,"
```

```
    file-type "num-home,"
```

```
    file-type "num-office,"
```

```
    file-type "choice,"
```

```
    file-type "wb,"
```

```
    file-type "reco,"
```

```
    file-type "fsocial-influence,"
```

```
    file-type "csocial-influence,"
```

```
    file-type "rconnected,"
```

```
    file-type "bconnected,"
```

```
    file-type "week-home,"
```

```
    file-type "week-office,"
```

```
    file-type "num-no WFH,"
```

```
    file-type "num-WFH1,"
```

```
    file-type "num-WFH2,"
```

```
    file-type "num-WFH3,"
```

```

    file-type "red-link-neighbors,"
    file-type "blue-link-neighbors,"
    file-type "stress,"
    file-print "hUi"
  file-close
end

to go
  if ticks > 100 [stop]
  set num-home 0
  set num-office 0

  ask turtles
  [
    set reco max (list (random-normal mean-reco 2.29) 0) ;7.08 2.29
    calculate-social-influence
    cognitive-process
    change-color
    move
    week-record
  ]

  count-WFH
  count-social-network
  calculate-energy

```

```

;output-2

tick

end

to calculate-social-influence

  if count red-links > 0 ;

  [if random 100 < 63 [set fsocial-influence ((random fsocial-value) + 1)] ]

  if count blue-links > 0 ;

  [if random 100 < 56 [set csocial-influence ((random csocial-value) + 1)] ]

end

to cognitive-process

  set hUi (Wwb * wb + Wenco * (fsocial-influence + csocial-influence) + Wreco * reco +
Wgender * gender + Wage * age) + (random-normal 0.83 0.18)

  ifelse hUi < hUi-threshold [set choice 1][set choice 0]

  if choice = 0 [set stress (stress + reco + csocial-influence + fsocial-influence)]

  if stress > personal-stress-threshold and ex-choice = 0 [

    set choice 1

    set stress 0

  ]

  set ex-choice choice

```

end

to change-color

if choice = 0 [set color red]

if choice = 1 [set color blue]

end

to move

if choice = 0 [move-to one-of patches with [(pcolor = white)]]

if choice = 1 [move-to one-of patches with [(pcolor = black)]]

end

to week-record

if choice = 0 [set week-home (week-home + 1)]

if choice = 1 [set week-office (week-office + 1)]

if ticks mod 5 = 1 [

set num-no 0

set num-oneday 0

set num-twoday 0

set num-threeday 0

]

if ticks mod 5 = 0 [

if week-home = 0 [set num-no (num-no + 1)]


```

if week-home = 1 [set num-oneday (num-oneday + 1)]
if week-home = 2 [set num-twoday (num-twoday + 1)]
if week-home >= 3 [set num-threeday (num-threeday + 1)]

; if week-office = 5 [set num-no (num-no + 1)]
; if week-office = 4 [set num-oneday (num-oneday + 1)]
; if week-office = 3 [set num-twoday (num-twoday + 1)]
; if week-office <= 2 [set num-threeday (num-threeday + 1)]

set WFH0 num-no
set WFH1 num-oneday
set WFH2 num-twoday
set WFH3 num-threeday

set week-home 0
set week-office 0

]
end

```

```

to count-WFH

```

```

set num-home count turtles with [choice = 0]
set num-office count turtles with [choice = 1]

```

```

set num-home-sum num-home-sum + num-home
set num-office-sum num-office-sum + num-office
end

to count-social-network
  set num-fconnect count turtles with [rconnected? = true]
  set num-cconnect count turtles with [bconnected? = true]
end

to calculate-energy
  set previous-energy ((15.0 + 3.4 + 8.2) * num-total)
  set energy ((14.3 + 3.2 + 8.2) * num-office + 8.9 * num-home)
  set sum-energy (sum-energy + energy)
  if ticks > 0 [set energy-saving (previous-energy - sum-energy / ticks)]
end

to output-2
  file-open "TestOutput-WHF.csv"
  ask turtles
  [
    file-type ticks           file-type ","
    file-type who             file-type ","
    file-type num-home       file-type ","
    file-type num-office     file-type ","
    file-type choice         file-type ","
  ]
end

```

```

file-type wb                file-type ","
file-type reco              file-type ","
file-type fsocial-influence file-type ","
file-type csocial-influence file-type ","
file-type rconnected?       file-type ","
file-type bconnected?       file-type ","
file-type week-home         file-type ","
file-type week-office       file-type ","

file-type WFH0              file-type ","
file-type WFH1              file-type ","
file-type WFH2              file-type ","
file-type WFH3              file-type ","
file-type red-link-neighbors file-type ","
file-type blue-link-neighbors file-type ","
file-type stress            file-type ","
file-print hUi

]
file-close
end

```